GEOLOGY AROUND THE MARGINS OF THE EASTERN SAN BERNARDINO MOUNTAINS

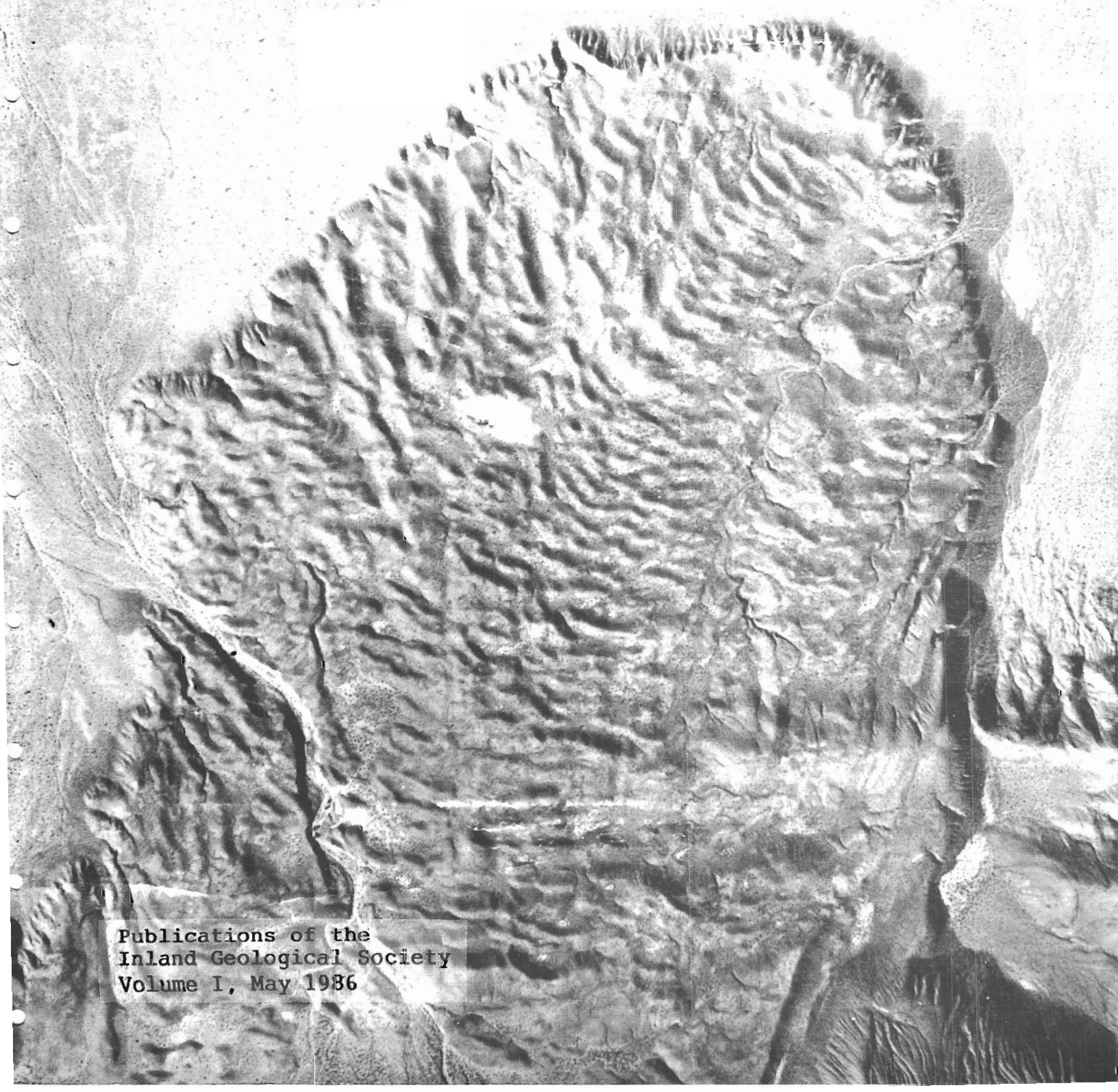

Publications of the
Inland Geological Society
Volume I, May 1986

Front Cover:
The Blackhawk landslide.
Air photo from the collections of the Department of Earth Sciences, University of California, Riverside.

GEOLOGY AROUND THE MARGINS

OF THE EASTERN SAN BERNARDINO MOUNTAINS

Marilyn A. Kooser and Robert E. Reynolds

Editors

Publications of the

Inland Geological Society

Volume I

2024 Orange Tree Lane
Redlands, California 92374

May 1986

Printed with the support of the
Friends Gift Shop of the San Bernardino County Museum
2024 Orange Tree Lane, Redlands, California 92374
and the Board of Supervisors of San Bernardino County
Robert Hammock, Chairman, Fifth District; John Joyner, First District;
Cal McElwain, Second District; Barbara Cram Riordan, Third District;
Gus James Skropos, Fourth District

TABLE OF CONTENTS

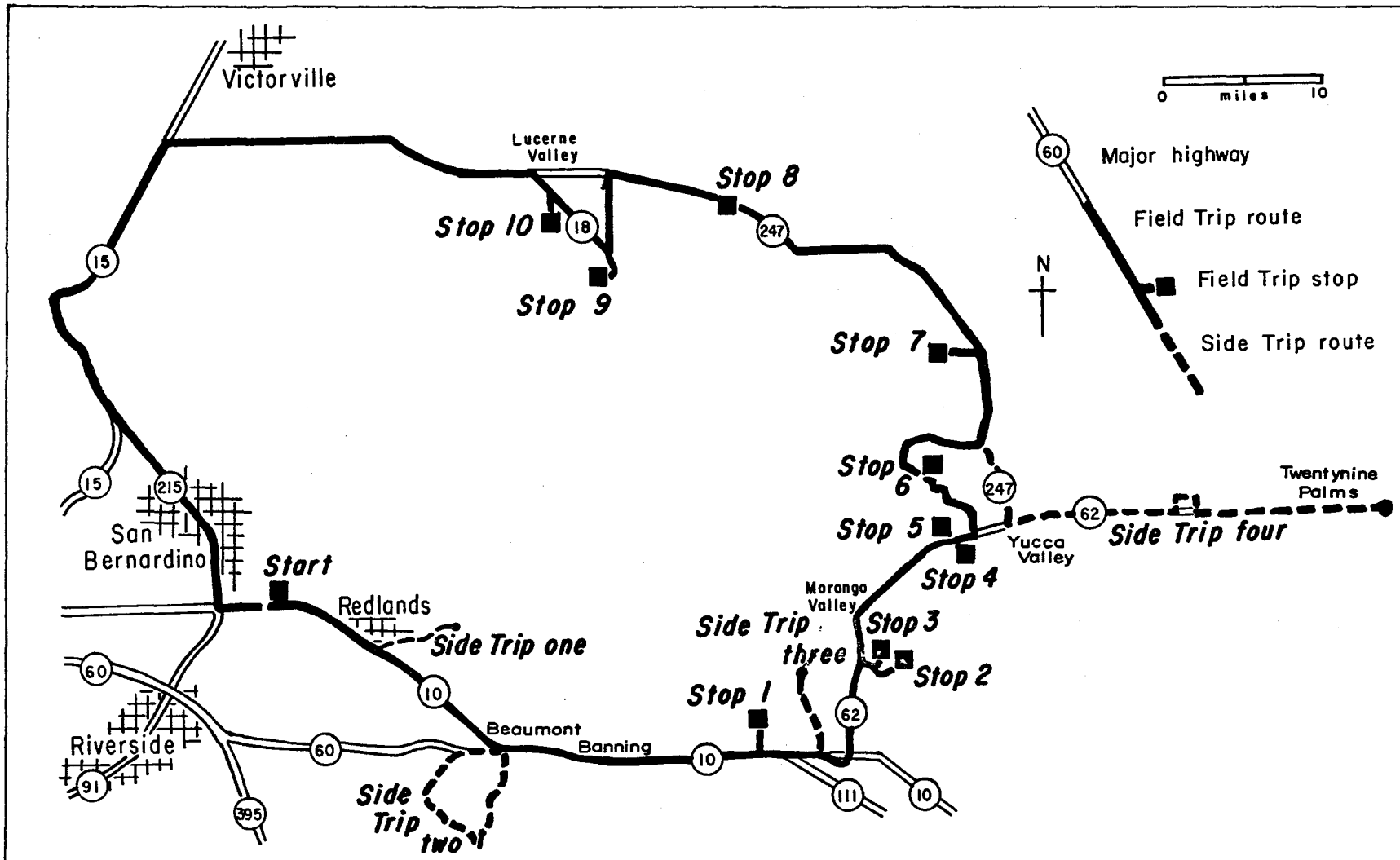

GEOLOGY AROUND THE MARGINS

OF THE EASTERN SAN BERNARDINO MOUNTAINS

Figure 1. Route of the Inland Geological Society 1986 Annual Spring Field Trip around the margins of the eastern San Bernardino Mountains, showing stops and side trips described in the Field Trip Road Log.

GEOLOGY AROUND THE MARGINS OF THE EASTERN SAN BERNARDINO MOUNTAINS: FIELD TRIP ROAD LOG

Robert E. Reynolds and Marilyn A. Kooser
Inland Geological Society
2024 Orange Tree Lane, Redlands, California 92374

START at the San Bernardino County Museum parking lot, 2024 Orange Tree Lane, Redlands, California, at the California Street offramp of Interstate 10. The Museum is a County-owned facility specializing in Earth Sciences, Natural Sciences, History and Anthropology. In addition to active research and education programs and extensive reference collections, three floors of exhibits in mineralogy, paleontology, ornithology, mammals, archaeology, history, fine arts and photography are open to the public. Museum hours are 9 a.m. to 5 p.m. Tuesday through Saturday and 1 to 5 p.m. Sunday; admission is free. The Inland Geological Society holds its regular meetings at the Museum on the third Thursday of every month at 7:30 pm.

The road log was compiled with the assistance, suggestions and shared knowledge of many people. In particular, we would like to thank Doug Morton, Wes Reeder, Jerry Grimes, Scott Neville, John Matti, Peter Sadler, and Jennifer Reynolds.

A map of the road log route is shown as figure 1. Cumulative mileage begins at the Museum parking lot; interval mileage follows in brackets. Side trips, which are described following the field trip log, are optional. They will add to the enjoyment and understanding of the local geology, but because of their interest will be time-consuming. The road log compilers were blessed with clear skies and majestic views during the compilation of this guide: may yours be the same.

LEG 1

0.0 (0.0) TURN RIGHT from parking lot entrance onto Orange Tree Lane, proceed to California Street.

0.2 (0.2) TURN LEFT at the stop sign onto California Street.

0.4 (0.2) TURN LEFT onto Interstate 10 East onramp going east toward Yucaipa and Palm Springs. Ahead you can see Yucaipa Ridge and San Bernardino Peak (elevation 10,524 feet). Yucaipa Ridge sits between the north branch (Mill Creek strand) and south branch (San Bernardino strand) of the San Andreas fault.

Basement rocks similar to those found in the San Gabriel Mountains are overlain by the Mill Creek Formation where it is

exposed on Yucaipa Ridge south of the mountain front. The Mill Creek Formation is a series of nonmarine Tertiary sediments deposited in a pull-apart basin (Demirer, 1985; Sadler and Demirer, 1986). The formation contains fossils which suggest an early Pliocene age (Axelrod, p.c. 1985) but which may be as old as late Miocene or as young as middle Pliocene (Gibson, 1971). The Wilson Creek fault (Matti and others, 1983 and 1985) crosses Yucaipa Ridge and separates the San Gabriel basement from basement rocks typical of the San Bernardino Mountains.

San Bernardino Peak and Mt. San Gorgonio are part of a complex of Precambrian biotite gneiss and schist, and granitoid gneiss intruded by Mesozoic quartz monzonite and granodiorite (Morton and others, 1980b). The massif was glaciated during the Pleistocene (Sharp and others, 1959; Dibblee, 1964).

2.1 (1.7) Holocene alluvium is on both sides of the freeway; to the right at about 2:00 Smiley Heights is on a Pleistocene alluvial surface with a Pleistocene soil (Reynolds and Reeder, 1986). This Pleistocene surface will be encountered repeatedly throughout the Yucaipa/Banning area.

2.6 (0.5) Terraced Pleistocene sediments are encountered near the Orange Street overpass.

3.8 (1.2) At University Street the freeway crosses the zanja, California State Historical Landmark 43. The first irrigation project in the county, the zanja was constructed in 1819 and 1820 by Serrano and Cahuilla Indians under the guidance of Franciscan fathers from the Mission San Gabriel to develop agriculture at Guachama, the Indian rancheria near the site of the Asistencia mission branch in Old San Bernardino (Redlands) (Quinn, 1980).

4.3 (0.5) Cypress overpass. You are now driving on Pleistocene alluvium (Qoa of Morton, 1978a).

4.8 (0.5) Cross the Redlands fault, a normal fault which elevated Pleistocene alluvium on its southeast side. The trace runs southwest along Crescent Avenue across San Timoteo Canyon to join the San Jacinto fault zone.

5.2 (0.4) Ford Street offramp. Return to the Pleistocene surface and soil, visible to the left at 10:00. Based on the degree of soil development, the surface is estimated to be of late but not terminal Pleistocene age.

5.9 (0.7) Reservoir Canyon. Cross the trace of the Crafton fault (Reservoir Canyon fault) offsetting Quaternary alluvium and uplifting Precambrian metamorphic and igneous basement rocks (Rogers, 1967). The Crafton Hills are a faulted complex of upper and lower plate rocks divided by the Vincent Thrust. Octavius Decatur Gass located gold-bearing quartz veins on the Yucaipa side of these hills in 1884. By 1889 the "Gold Bar Company" had developed a 60-foot tunnel and in 1890 the

water-powered Yucaipa Quartz Mill had been constructed to process gold ore. The mine property was located in the canyon north of the Crafton Hills College water tank; the mill site was in Dunlap Acres near 10th Street (Archer, 1976).

6.4 (0.5) Upper plate gneissic quartz diorite, exposed in these road cuts, is separated from lower plate Pelona Schist by the Vincent Thrust. On the left these exposures of the upper plate gneisses include Permo-Triassic Lowe Granodiorite and cataclasites. Pelona Schist is exposed in the road cuts to the left near the top of Reservoir Canyon.

Marked by trees and bushes to the right, Crystal Springs comes to the surface at the fault trace. These springs supported a small bottled water industry in the past. Reservoir Canyon was named from the municipal water reservoir constructed for the Redlands Colony in 1881 (Archer, 1976).

Much of the Yucaipa area was drained through Reservoir Canyon in late Pleistocene times; the drainage was later captured through Live Oak Canyon (Dutcher and Burnham, 1960). Reservoir Canyon was the site of Maria Armenta Bermudez' pioneering farming activities in the area in 1836, when she raised vegetables for the Los Angeles Market. Her crops were irrigated by a ditch dug from the zanja near present-day Crafton (Beattie and Beattie, 1951).

7.4 (1.0) [[SIDE TRIP #1 to the Crafton Hills. EXIT at the Yucaipa Boulevard exit on the right and see Side Trip section following the road log.]]

You are crossing from the upper plate rocks of gneissic quartz diorite into Pleistocene alluvium.

8.1 (0.7) Cross the Western Heights fault cutting Pleistocene alluvium. This fault, which bounds the Crafton Hills on the southeast, is subparallel to the Redlands fault.

8.4 (0.3) Mount San Jacinto is seen ahead at 12:00; Pisgah Peak (elevation 5480 feet) is at 10:30. Pisgah Peak is south of the south branch of the San Andreas fault and consists of upper plate granitic and granitoid gneissic rocks overlying the Vincent Thrust.

9.0 (0.6) Cross Live Oak Canyon Holocene alluvium.

9.7 (0.7) To the right is deep dissection in the Holocene alluvium of Live Oak Canyon.

10.0 (0.4) At County Line Road offramp you have returned to the Pleistocene surface. Fossiliferous Pleistocene sediments of the San Timoteo Formation beneath the Pleistocene surface are located between this offramp and Calimesa Blvd. offramp (Dibblee, 1981; Reynolds and Reeder, 1986).

11.0 (0.9) Calimesa Boulevard offramp.

11.6 (0.6) Cross tributary canyon of San Timoteo drainage on flat surface of Holocene alluvium.

11.8 (0.2) Terraces to the right are developed on Pleistocene and Holocene alluvium The badlands topography is developed in the Plio-Pleistocene San Timoteo Formation. Side Trip #2 through the badlands starts at Milepost 17.8, and see Reynolds and Reeder, 1986.

13.3 (1.5) Cherry Valley offramp. On the left are Pleistocene sediments. At 9:00 the terraces have been developed at a lower elevation than the badlands topography. The northeast-striking valleys toward the skyline on the left are controlled by a branch of the Mission Creek fault and the Vincent Thrust. These faults run northeasterly between the south branch of the San Andreas fault (San Bernardino strand) and the Raywood Flat area on the skyline to the left (Matti and others, 1983).

14.0 (0.7) Return to the Pleistocene surface.

15.5 (1.5) The San Timoteo Canyon Road offramp enters San Timoteo Canyon. The freeway leaves the Pleistocene surface and traverses badlands topography and valley fill, regaining the Pleistocene surface near the junction of Highway 60.

16.6 (1.1) CONTINUE on Interstate 10. Offramp to Interstate 60 West is on the right; Side Trip #2 to the San Timoteo Badlands rejoins main trip route here.

17.8 (0.9) [[SIDE TRIP #2 through the San Timoteo Badlands. EXIT to right at Highway 79 (Beaumont Avenue) and turn to Side Trip guide following road log.]]

If side trip is not taken, continue along Interstate 10 East.

18.0 (0.2) San Gorgonio Pass is the lowest topographic break in southern California through the mountains to the inland deserts, separating Mt. San Gorgonio (elevation 11,502 feet) and Mt. San Jacinto (elevation 10,786 feet), the two highest mountains in southern California. The crest of the pass, although broad and ill-defined, is the complicated junction of three major drainage basins (fig. 2): the interior-draining Whitewater River-Salton Trough to the east via Smith Creek; the generally interior-draining San Jacinto basin to the south via Potrero Creek; and the Santa Ana basin to the west via San Timoteo Canyon. The junction of these three basins is on the crest of an alluvial fan complex 2.5 miles north of Interstate 10 between Noble Creek on the west and Smith Creek on the east.

18.2 (0.2) Leave the Santa Ana basin and cross eastward to the San Jacinto basin.

19.2 (1.0) Through rapid headward erosion Potrero Creek has progressed

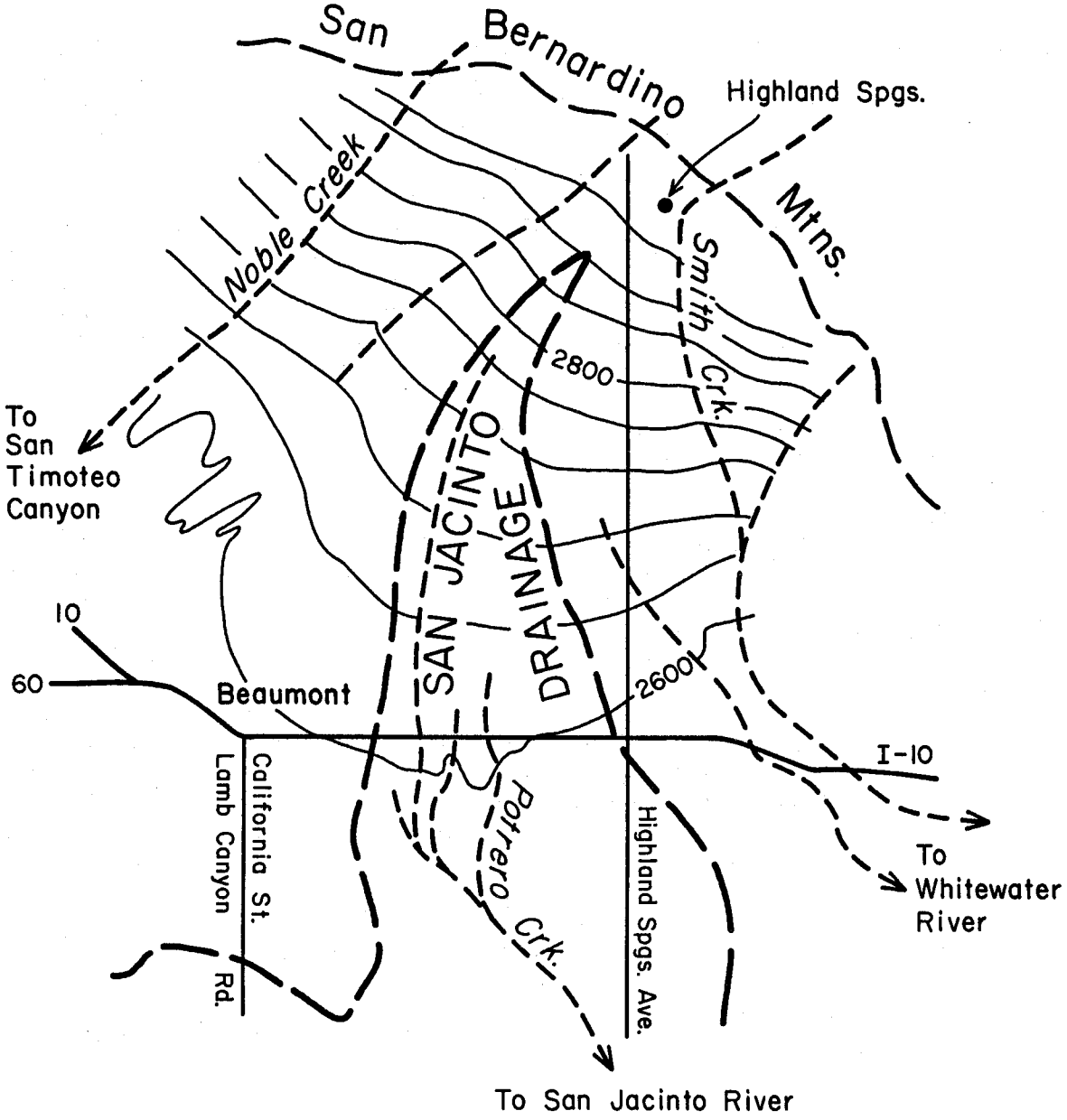

Figure 2. San Gorgonio Pass, showing division into the Santa Ana drainage basin (west), the San Jacinto drainage basin (center) and the Whitewater--Salton Trough drainage basin (east). See Milepost 18.0 in road log.

northward, extending the northward limit of the San Jacinto basin along the crest of the alluvial fan complex essentially to Highland Springs, 2.5 miles north of Interstate 10. At Highland Springs Avenue we are leaving the San Jacinto basin, crossing eastward into the Whitewater River drainage.

21.5 (2.3) To the left is the Banning Bench, bounded on the south by an unnamed thrust fault, and capped by the Heights Fanglomerate of Allen (1957). The deposit is dominated by deeply weathered clasts of gray migmatitic gneiss and greenschist (Pelona Schist) which is probably derived from the upper San Gorgonio River area near the juncture of the Mission Creek and San Bernardino strands of the San Andreas fault. Bison remains have been recovered from the Heights Fanglomerate (Jefferson, 1986) indicating that it is less than 500,000 ybp (Savage and Russell, 1983). The Heights Fanglomerate unconformably overlies sediments similar in appearance to the San Timoteo Formation, which coarsens north of the Banning fault.

From this point eastward to Whitewater you enter an area dominated by compressional features.

24.5 (3.0) The housing area straight ahead is cut by dissected thrust fault scarps. In the hills to the left, the Banning fault has thrust basement rocks over non-marine sandstones, siltstones and conglomerates of the Hathaway Formation. In Lion Canyon, the Hathaway Formation is conformably overlain by the marine Imperial Formation which is in turn conformably overlain by the nonmarine Painted Hill Formation. Elsewhere, the Hathaway Formation is directly overlain by the Painted Hill Formation (Allen 1957). These three formations, Pliocene in age, are caught up between thrust faults along the base of the mountain front from this point to Stubbe Canyon (Allen, 1957; Dibblee, 1982). Allen (1957) divided the Hathaway Formation into two members, a sandstone-dominated lower member and a conglomerate-dominated upper member distinguished by clasts of flaser gneiss derived from an area north of the Banning fault between Cottonwood and San Gorgonio Canyons. He also mentions rare clasts of silicified limestone without speculating upon their possible source. Access to this area is extremely difficult because of private land owners and the Morongo Indian Reservation.

The San Gorgonio Igneous-Metamorphic Complex in this area is predominantly migmatitic gneiss with intrusions of quartz monzonite (Morton and others, 1980b).

25.0 (0.5) The lower hills straight ahead are Cabezon Fanglomerate which has been anticlinally folded and cut by thrust faults. The Quaternary Cabezon Fanglomerate includes gravels from a variety of sources.

26.7 (1.7) To the left, beneath the house trailer, is the most youthful thrust fault scarp in this area related to compression associated with activity along the Banning fault. At this point the

scarp changes orientation from a northwest strike to a northeast strike.

26.9 (0.2) To the right, the steep escarpment of the San Jacinto Mountains is interpreted to be the result of uplift on the postulated South Pass fault (Allen, 1957).

27.3 (0.4) To the right at 1:00 is the north portal of the San Jacinto Tunnel, a part of the Colorado River Aqueduct system. It cuts through the Paleozoic? metasediments (quartzofeldspathic gneiss and schist, phyllite, quartzite and marble) intruded by quartz diorite of Mt. San Jacinto (Morton and others, 1980a).

27.8 (0.5) To the left is Millard Canyon; a fault scarp crosses the alluvial fan near the canycn mouth. The debris of the Millard Canyon fan overwhelms debris from Mount San Jacinto. Drainage to the base of Mt. San Jacinto is thus forced eastward from this point to the Whitewater River.

30.0 (2.2) Good exposures of the Cabezon Fanglomerate are to the left. Hathaway, Imperial, and Painted Hill sediments are thrust over the Cabezon Fanglomerate and are in turn overthrust by the San Gabriel Igenous-Metamorphic complex. Landslides are common at the noses of the ridges.

30.7 (0.7) To the left at 11:00, Lion Canyon is bounded on the east by a large landslide. The upper "boundary" of this landslide is in the Cabezon Fanglomerate and as shown by Allen (1957) is convex and points to the south. Because this is opposite in nature to a landslide headscarp and because pressure ridges are apparent within the landslide, this suggests that the feature is the result of "bulldozing" by a larger mass to the north and not simply a slope failure.

A thrust in the basement rocks to the left at Stubbe Canyon is seen where pink piemontite-bearing rocks are thrust over green epidote-bearing rocks. The distinctive piemontite-bearing gneisses are found as clasts in sediments north and south of the Banning fault. Since the source area is of limited extent, this has proven useful in estimating fault offset as well as identifying source areas and transport directions (Allen, 1957).

32.7 (2.0) Based on geophysical evidence, the ridge of metamorphic rocks (ahead at 12:00 extending from Mt. San Jacinto) continues beneath the alluvium to a point north of the freeway and northward of the southernmost thrusts characteristic of the San Bernardino Mountains side of the pass. This ridge reduces the energy of the strong winds which are regularly funneled through San Gorgonio Pass, and dune sands are deposited against it.

34.3 (1.6) EXIT RIGHT onto Verbenia heading into Cottonwood Creek Canyon.

34.5 (0.2) TURN LEFT at stop sign and proceed north across Interstate 10

toward the mouth of Cottonwood Canyon to observe thrusts of the Banning fault. Proceed past Tamarack and past Sage, curving left.

36.1 (0.6) TURN RIGHT onto Amethyst Drive, curve right and head easterly.

36.4 (0.3) TURN LEFT onto Desert View, a graded dirt road.

36.5 (0.1) BEAR RIGHT just past Jacaranda. Desert View branches; take easterly branch right and go north to top of flood control dike along the west side of Cottonwood Wash. Red Pleistocene alluvium to the right is offset Whitewater River gravels (Matti, p.c. 1985). To the left of the road and straight ahead near the base of the mountains, buff colored exposures are nonmarine coarse clastics of the Quaternary Cabezon Fanglomerate in thrust or landslide (Rasmussen and Reeder, 1986) contact with overlying gneissic basement. The large flattened topographic areas above and beyond the fanglomerate are the remains of a composite landslide domain. Easily visible on the bare face to the right of the landslide is a thrust complex in basement rock. The most obvious of the thrusts is at the color change from the lower olive-colored to the higher gray-colored basement. Orange-colored basement rocks to the right of the road are sericitic and tourmalinized, similar to those at Painted Hill, east of Whitewater Canyon.

36.7 (0.2) The dike on which we are traveling crosses the Metropolitan Water District Colorado River Aqueduct; its trench can be seen to the right.

37.7 (1.0) STOP 1. Park at turn around area. Cottonwood Spring is directly north of the turn-around area. Looking east, the canyon running east is developed along the Banning fault where it is relatively simple, dipping north 45 to 65 degrees. The sense of movement along this steep angle fault is right lateral. North, along Cottonwood Canyon, the fault splays into a complex of shallow, north-dipping thrusts involving a wide variety of rock types. West of Cottonwood Creek the Banning fault shows characteristics of low angle overthrusting. The hill to the west is a complex of thrusts and landslide structres (fig. 3). A trench N 50^{o} W of the stop exposed the low angle fault contacts.

A well-developed soil horizon overlying "Whitewater Gravels" is present on "Windmill Ridge" to the east. These gravels may have originated as alluvium from Whitewater Creek and moved right laterally to their present position. Windmill Ridge is underlain by deformed Cabezon Fanglomerate gravels from the Whitewater River drainage. The Banning fault is to the left of the windmills, juxtaposing basement against alluvium.

The view south to Mt. San Jacinto shows Falls Creek at 11:00 and the Snow Creek fan at 12:00. Boulders on the fan reach house-size. Left of Falls Creek is a chaotic avalanche

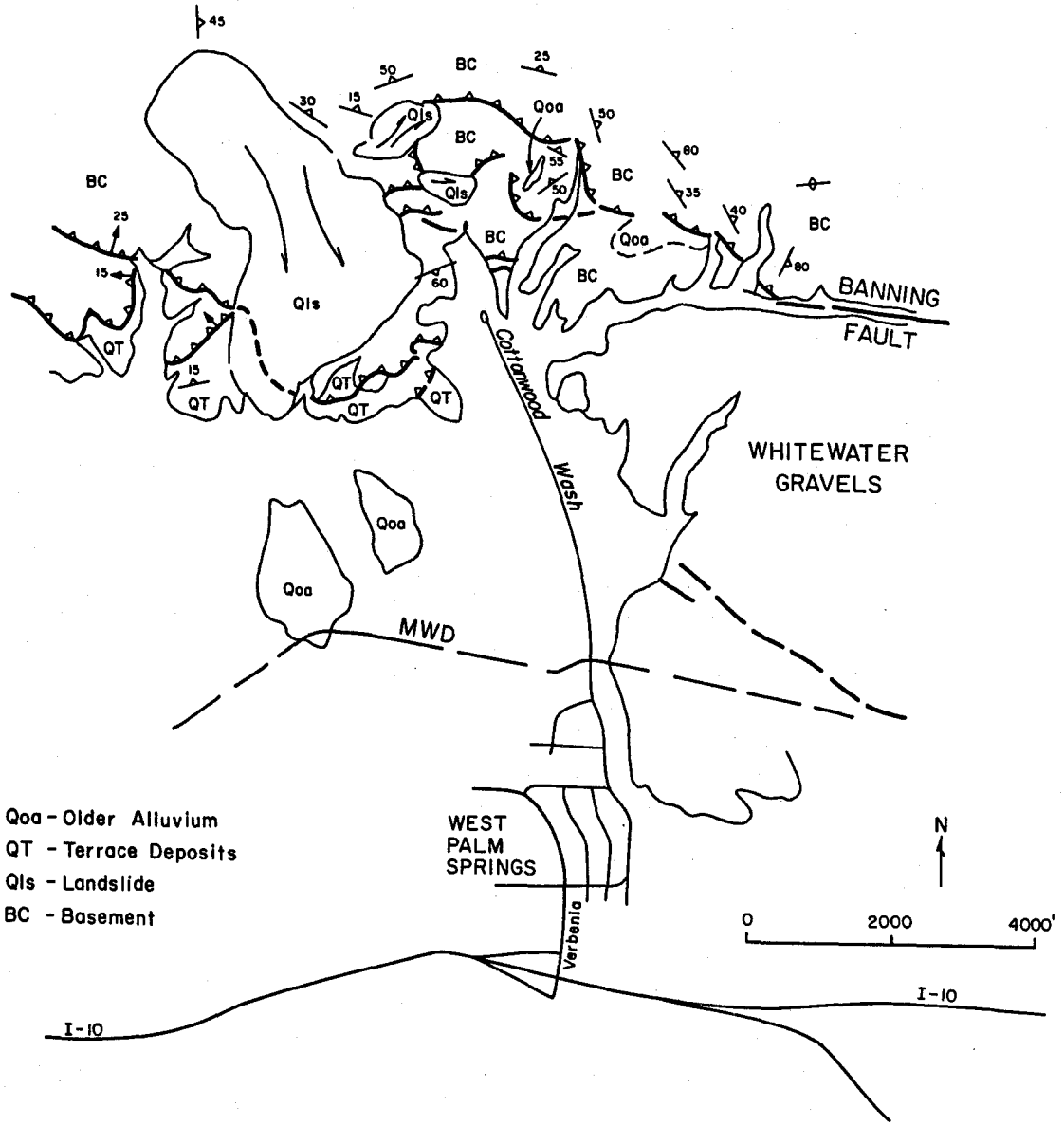

Figure 3. Cottonwood Canyon, showing complex of faults and landslides. See road log Stop #1.

deposit. Lobate structures in the drainage south of Snow Creek are Pleistocene alluvial terraces.

LEAVE turn-around area on road to right, heading southerly.

38.3 (0.6) Rejoin pavement at Cottonwood, going south and passing water tank and high-standing dissected alluvial fans with deeply weathered soil horizons.

39.1 (0.8) TURN LEFT at stop onto Tamarack Street.

39.3 (0.2) TURN RIGHT after stop onto Verbenia Street.

39.4 (0.1) ENTER freeway onramp; go east toward Palm Springs.

42.1 (0.7) Whitewater Gravels of the Cabezon Fanglomerate are to the left (Whitewater Hill). The gravels are capped by a Pleistocene soil.

43.0 (0.9) A large landslide is to the left. To the south of the Interstate large cottonwood trees and building ruins, most of which have disappeared, marked the site of the Whitewater Ranch headquarters. Pauline Weaver and Isaac Williams were the first Anglos to own land in the San Gorgonio Pass; their San Gorgonio Rancho, granted in 1845, encompassed the entire pass area. Weaver sold a portion of the rancho to Isaac Smith in 1853; this purchase, which included the land from Beaumont to Palm Springs, was to develop into the Whitewater Ranch. The riparian water rights from the Whitewater River granted in 1850 passed with the ranch to successive owners and allowed ranching to continue. The site was also a regular freight and stage stop along the Butterfield route (Stocker, 1973).

43.9 (0.9) Highway 111 to Palm Springs passes through the old Whitewater Ranch property; do not exit.

44.5 (0.6) To the left, the Garnet Hill fault disrupts alluvium 2/3 of the way from the freeway to the base of the hills. The fault runs across the mouth of Whitewater Canyon where it is visible at 9:00. The fault trace is exposed only to the west of Whitewater River. Based on recent trenching between Cottonwood and Whitewater Canyons, there is no evidence for Holocene activity on the Garnet Hill fault (Reeder, p.c. 1986). The Garnet Hill fault displaces Pleistocene-age Whitewater gravels of Windmill Hill (Allen, 1957). To the east its trace is covered by alluvium and the main evidence for its existence within the Coachella Valley is a strong gravity anomaly. Gravity low contours define a trough which is almost as well delineated as the gravity troughs associated with the Banning and Mission Creek faults (Proctor, 1968). Proctor suggests that the Garnet Hill fault may be an ancestral branch of the San Andreas fault.

44.8 (0.3) [[SIDE TRIP #3 to Whitewater Canyon, EXIT at Whitewater Road and turn to Side Trip guide following the road log.]]

If side trip is not taken, or after side trip, CONTINUE on Interstate 10.

45.4 (0.6) Beneath the small metal shed to the left is the reverse fault scarp of the Garnet Hill fault.

45.7 (0.3) Cross the Whitewater River.

46.3 (0.6) The north side of the freeway runs along the trace of the Garnet Hill fault next to Beacon Hill. To the left are Pleistocene fan sediments of the Cabezon Fanglomerate separated from the Imperial and Painted Hill Formations (see Murphy, 1986) by the Banning fault. The Cabezon Fanglomerate of Whitewater Hill includes a lens of limestone breccia believed to have been derived from the San Jacinto block (Allen, 1957). Proctor (1968) notes that Whitewater Hill has been uplifted so recently that relict drainages exposed on its surface do not conform to its current topography.

47.1 (0.8) EXIT RIGHT onto the Yucca Valley--29 Palms offramp, following Highway 62 northward over the freeway.

47.5 (0.4) View down the axis of the Salton Trough to the south. The Garnet Hill fault trace is on the south side of the low hills (Garnet Hill).

48.9 (1.4) Red exposures at the Whitewater Rock Quarry are visible to the left at 9:00.

49.4 (0.5) At 1:00 to the right, the trace of the Banning fault is expressed as shutter ridges between the powerline and windmills. Devers Hill protrudes through the alluvium to the right.

49.7 (0.3) Cross the Banning fault over the next 0.1 mile.

51.4 (1.7) Mt. San Gorgonio is viewed to the left; to the right are the Little San Bernardino Mountains.

53.2 (1.8) Mission Creek Road crosses Highway 62. To the left are dissected Mission Creek alluvial deposits cut by northeast-striking faults with the east side down. To the right at 2:00 is a fault-bounded prism of pinkish sediments against the mountain front which is bounded by the Mission Creek strand of the San Andreas fault system.

54.5 (1.3) TURN RIGHT off Highway 62 at Indian Avenue; proceed on pavement southeast. Desert Hot Springs is straight ahead; the Indio Hills are visible at 1:00.

55.4 (0.9) TURN LEFT past "Dip" sign onto the graded dirt California Aqueduct road trending northeasterly.

55.8 (0.4) TURN LEFT onto graded dirt road, the second of two parallel

roads running up "Standpipe Hill". Both of these roads lead to Stop #2; the southerly is less steep. Proceed to top of hill.

56.1 (0.3) STOP 2. Park at top of Standpipe Hill. You are stopped near the southwestern margin of the Little San Bernardino Mountains, which are predominantly Precambrian gneiss and Mesozoic plutonic rocks. Pleistocene nonmarine sediments of the Coachella Fanglomerate (Peterson, 1975) occur sparingly at the southwest foot of the mountains. The Dillon Shear Zone runs through the mountains subparallel to the San Andreas fault zone.

OVERVIEW SOUTH shows the Coachella Valley area through which the southern branch of the San Andreas fault can be traced as far south as the Indio Hills, to the southeast at 11:00. Pleistocene Lake Coahuilla filled this basin, the southern part of which now holds the Salton Sea. The Palm Canyon fault runs north-south along the face of the San Jacinto Mountains at 2:00; the community of Palm Springs can be seen at the foot of the mountain at the northern end of the Palm Springs fault. The south and north branches of the San Andreas fault system, the Banning fault and the Mission Creek fault, respectively, merge in the vicinity of the Indio Hills (Clark, 1984; Dibblee, 1981; Proctor, 1968). Michael Reimer of the U.S. Geological Survey and Kerry Sieh of the California Institute of Technology are currently investigating the late Pleistocene and Holocene history of the southern San Andreas fault in this area.

Return to northerly of two dirt roads and RETRACE ROUTE down Standpipe Hill, heading westerly.

56.3 (0.2) TURN RIGHT at base of hill, heading west-northwest. Prepare for immediate turn.

56.4 (0.1) TURN RIGHT at break in piles of dirt onto dirt track running north-northwesterly into Big Morongo Canyon.

56.9 (0.5) Proceed into Big Morongo Canyon along sandy wash bottom, which drains the Morongo Valley. The scarp of the Mission Creek branch of the San Andreas fault system forms the southwest face of the Little San Bernardino Mountains, into which we are penetrating. Follow existing vehicle tracks and avoid vegetation as you proceed up the wash.

57.3 (0.4) STOP 3. Park at S-bend in canyon to view gneissic basement rocks thrust over Tertiary conglomerate (Dibblee, 1967a) (fig. 4). The thrust fault is known as the Morongo reverse fault (Proctor, 1968) and it may be a western extension of the Dillon shear zone. Proctor (1968) indicates that the Morongo reverse fault is inactive, but this has yet to be clearly demonstrated (Reeder and Rasmussen, 1986). Watch for broken glass from local shootists. Watch for local shootists!

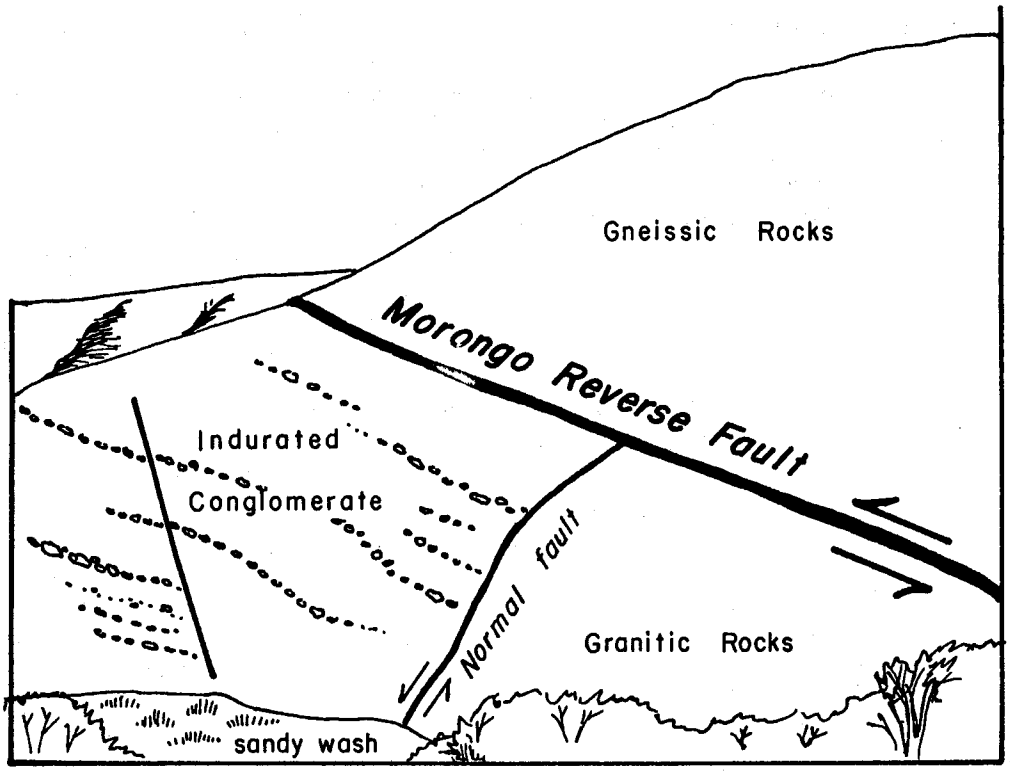

Figure 4. Morongo reverse fault. Sketch of cliff face viewed to the east at Stop #3 in lower Morongo Canyon, showing gneissic rocks thrust over granitic rocks in fault contact with Tertiary conglomerate.

RETRACE ROUTE along wash bottom out of Big Morongo Canyon to Indian Avenue.

58.2 (0.9) TURN RIGHT onto paved Indian Avenue; proceed westerly. Ahead is a good view of Mt. San Gorgonio and of the dissected Pleistocene alluvial fan of Mission Creek.

59.2 (1.0) TURN RIGHT onto Highway 62 heading north toward Morongo Valley.

60.1 (0.2) Cross the Mission Creek branch of the San Andreas fault as you head up Dry Morongo Canyon, entering Mesozoic deformed pluton and Precambrian gneiss.

61.9 (1.8) Gravels to the right were deposited on steeply-dipping basement and cemented by secondary calcium carbonate deposits.

62.4 (0.5) Cross the trace of the Morongo Valley fault.

62.6 (0.2) To the left is perched alluvium. The highway enters fault-bounded Morongo Valley.

62.9 (0.3) View to the right at 12:30 shows fault-terminated ridges east of Big Morongo Canyon.

64.0 (1.1) Covington Park and the Big Morongo Wildlife Refuge are to the right via East Street. The nature reserve is jointly owned and operated by Nature Conservancy, the County of San Bernardino and the Bureau of Land Management. It is unique in the area as a habitat for more than 240 species of resident and migrant birds as well as a sanctuary for mammals including big horn sheep. Permanent water, brought to the surface at springs along the Morongo Valley fault, supports a lush riparian community. Continue on Highway 62.

65.5 (1.5) The Pinto Mountain fault runs on the north side of the valley north of the highway. The Pinto Mountain fault is a major left lateral fault which represents the southern structural boundary of the Mojave block. The Mojave Desert is characterized by a series of active northwest-trending right lateral faults. These faults apparently terminate at or are truncated by the Pinto Mountain fault.

68.0 2.5 Ole Street, to the right, leads south to the trace of the Morongo Valley fault via Oskar Lane and Loma Alta Street. The en echelon fault trace is on private property.

68.2 (0.2) To the right, an en echelon section of the Morongo Valley fault separates the ridge of Pleistocene fanglomerate from the bedrock further south. Start ascent of Morongo Grade.

68.5 (0.3) Light gray granitic bedrock to left is separated from overlying brownish granitic bedrock by low angle faults and shears.

71.1 (0.7) The leveled pad at 3:00 on the right exposes vertically dipping braided stream deposits.

71.6 (0.5) TURN RIGHT off Highway 62 onto Pinon Street; proceed up hill.

71.8 (0.2) TURN RIGHT on Navajo, proceed to end.

72.1 (0.3) STOP 4. Park at end of cul de sac; do not enter private property. From this vantage point, note the sediments to the north, which contain clasts of basalts with ultramafic inclusions (kaersutite). This fanglomerate overlies and is in fault contact with the quartzite fanglomerate which composes the relatively flat surfaces to the south. The basin between us and these surfaces contains finer-grained arkosic sediments which dip steeply to the north. The arkose is a fault-bounded wedge unconformably overlain by the capping quartzite fanglomerate (see Grimes, 1986). Return to Highway 62, preparing to turn west (left).

72.3 (0.2) TURN LEFT onto Highway 62, get into right lane and prepare to turn right.

72.9 (0.6) TURN RIGHT onto Fairway Street, prepare to turn left.

73.0 (0.1) TURN LEFT onto Rockaway Street, go up hill to dirt road on

left.

73.2 (0.2) TURN LEFT before reaching water tank. Turn onto dirt road leading south to leveled pad parking area.

73.3 (0.1) STOP 5. Park on leveled dirt pad. The highway is to the south. The pass through which the highway runs is a geomorphic and geologic boundary between the San Bernardino Mountains and the Little San Bernardino Mountains. A major change in bedrock occurs at the highway between granitic rocks to the north and metamorphic rocks to the south, and high- and low-angle structures converge in the area. The shattered granitic bedrock on which we are parked is associated with a low angle fault system along the south flank of the granitic terrain. This low angle fault system converges with the Pinto Mountain fault in this area.

The near-vertical cut south of the highway exposes a braided stream deposit containing quartzite clasts. These vertical beds are interpreted to be more distal facies of the fanglomerate characterized by quartzite clasts that we observed at the last stop. Between 1:00 and 2:00 escarpments for echelons of the Morongo Valley fault can be seen. Looking down valley at 2:00 to 3:00, the Pinto Mountain fault is buried by alluvium until it enters Big Morongo Canyon.

RETRACE ROUTE along dirt road to Rockaway Street to Fairway Street to Highway 62.

74.0 (0.7) TURN LEFT onto Highway 62, continue northerly.

75.7 (1.7) TURN LEFT on Pioneertown Road, just past flashing yellow pedestrian crossing lights. To the right, this road is called "Deer Trail".

75.8 (0.1) Stop sign at Yucca Trail. Proceed ahead on Pioneertown Road.

76.3 (0.5) Cross the most northern suspected trace of the Pinto Mountain fault as mapped by Dibblee (1967a).

78.3 (2.0) Water Canyon fault. Past Water Canyon, fluviatile deposits are exposed below the terrace on the left. The fault in this canyon has not disturbed these sediments.

79.2 (0.9) During the Tertiary, granitic basement rocks were deeply weathered along joint sets. Recent weathering has exposed this boulder terrain in the Sawtooths (Oberlander, 1972).

80.0 (0.8) Pioneertown Basalts, to the right, cover an area of approximately 22 square kilometers and may reach a thickness of 60 meters. The pile is made up of individual flow units three to seven meters thick, each capped by a terminal vesiculated or amygdoloidal top. Eight or nine individual flow units have been observed in the the thickest portion of the pile. These basalts are alkali olivine in composition

(Neville, 1983); potassium/argon dates for similar flows range from 6.9 ma to 9.3 ma (Morton, p.c. 1985; Peterson, 1976; Oberlander, 1972). The basalts overlie and are interbedded with Tertiary arkose deposits and overlie granitic basement. In some places Tertiary granitic soil horizons are preserved beneath the flows (Oberlander, 1972). The basalts are correlative, in terms of time and petrogenesis, with other alkaline volcanics found throughout the Mojave Desert (e.g. Cima Dome, Amboy Crater, Dish Hill, Pisgah Crater) (see Neville, 1983; Neville and others, 1985).

80.3 (0.3) Pioneertown was originally built as a set for western movies. It was named by Dick Curtis, an actor, on Labor Day 1947 (Gudde, 1974).

80.7 (0.4) Pavement turns right 90 degrees to northeast; continue along Pioneertown Road. Chaparrosa Springs is in bedrock to the left.

81.0 (0.3) Cross Chaparrosa Wash.

81.3 (0.3) View Tertiary sediments underlying basalt flows.

81.7 (0.4) Leaving wash, proceed along road to top of terrace; prepare to turn right.

81.9 (0.2) TURN RIGHT onto dirt road marked with rock gate structure and wooden post. Take roads to left, watching for vehicle-size ruts.

82.2 (0.3) STOP 6. Park within view of Pioneertown Basalts overlying and interfingered with Tertiary arkose. Walk ahead about 0.2 miles to road cuts exposing faulted sediments. In the cut you can see, from lowest: (1) low energy deposition of brown silty sands and paleosols; (2) higher energy deposition of arkosic sands; (3) vertical faults offsetting the sedimentary section downward, to the east; (4) a possible erosional surface and soil which may have formed prior to basalt flows; and (5) 6.9 - 9.3 ma basalts laid down on undulating topography and interfingering with arkose.

The Tertiary sediments have been referred to as the Old Woman Sandstone by Dibblee (1967b) but the difference in clast lithologies and the age of the overlying basalts indicate that their age and source differ significantly from the Old Woman Sandstone. Similarly, lithology and stratigraphy distinguish this arkose from the Santa Ana Sandstone (Sadler, p.c. 1986). Fragmentary vertebrate fossils appear to corroborate an age greater than 7 ma for the lower silty sediments (SBCM collections).

RETRACE ROUTE along ruts to pavement.

82.5 (0.3) TURN RIGHT onto Pioneertown Road, resume route northwest.

The basalts appear to have flowed over a gently undulating surface and are thickest to the southeast. The apparent flow direction was roughly northeast to east. The location of the source vent for these volcanics is not known, although Vaughn (1922) speculated that a volcanic neck was in bedrock to the south.

84.1 (1.6) Pipes Wash.

84.3 (0.2) TURN RIGHT onto Pipes Canyon Road; proceed northwest.

84.8 (0.5) View ahead of mesas of the Pioneertown basalt flow including Flat Top Mountain to the northwest and Black Hill to the south. At 12:00, water rises to the surface of Pipes Wash as a result of the shallow bedrock between the volcanic tablelands.

87.3 (2.5) Note the crude columnar jointing in overlying basalts to the right at 1:30.

88.6 (1.3) Arkose underlying basalt is visible in the road cut to left at 9:00. Approximately 8 individual flow units make up the basalt pile to the left.

89.0 (0.4) Red sediments underlying basalts at 11:00 halfway up slope may be paleosols or a baked contact.

89.3 (0.3) Coarse Pleistocene gravels are deposited against Tertiary arkose to the south at 2:00 in the bank of Pipes Wash.

90.5 (1.2) Quaternary stream deposits of Pipes Wash are exposed to the left and in road cuts.

90.6 (0.1) [[SIDE TRIP #4 through Copper Basin and 29 Palms to Campbell Hill, TURN RIGHT onto Highway 247, Old Woman Springs Road, toward Yucca Valley, and turn to side trip guide following road log.]]

If side trip is bypassed, TURN LEFT from Pipes Canyon Road onto Old Woman Springs Road and proceed northerly. Note the bedded Pleistocene alluvium and terraces.

92.6 (2.0) You are in a valley which may represent the extension zone of the graben bounded by the Johnson Valley fault and the Homestead fault.

94.0 (1.4) Surface offsets on the Johnson Valley and Homestead faults to the right occurred in 1978. It was this activity that led to the first recognition of the Johnson Valley fault.

96.6 (2.6) TURN LEFT on New Dixie Mine Road (graded dirt) at a sign for Landers Community Church. Follow road into Ruby Canyon.

97.7 (1.1) From top of terrace overlooking Ruby Canyon Wash, Ruby Peak is

visible to the right at 2:00; inactive thorium-uranium prospects are to the left. Ruby Peak is named because of the reddish staining produced by weathering of the iron-rich basaltic dike at the peak. The Ruby Mountain basalts are slightly more mafic than those of Pioneertown and are host to ultramafic inclusions and megacrysts of kaersutite, clinopyroxene and feldspar. See Neville, 1986.

98.3 (0.6) STOP 7 at base of cliffs. End of Leg 1.

LEG 2

0.0 0.0 STOP 7. You are parked in a wash within the Ruby Mountain basalt field. Erosion into gneissic and granitic basement has exposed basaltic feeder dikes and flow remnants at Ruby Mountain. At Ruby Peak and adjacent to the stream wash are two large instrusive dikes. The basalts at Ruby Mountain are probably late Miocene in age based upon their association with nearby dated basalt outcrops. Compositionally these basalts are basenites and are comparable to other well-known Mojave Desert basalts such as Dish Hill. These basalts are host to a number of inclusions which include ultramafic xenoliths (mostly spinel lhezolite), megacrysts of amphibole, clinopyroxene, and anorthoclase, and xenoliths of granitoid rock (Neville and others, 1985). See Neville, 1986.

RETRACE ROUTE to Old Woman Springs Road, Highway 247, via New Dixie Mine Road.

0.5 (0.5) View from terrace shows inactive thorium-urnaium prospects to the right. Thorium-bearing allanite as well as radioactive zircon and monazite are found in small quantities in biotite-rich inclusions in the gneissic basement rocks (Moxham and others, 1955).

0.9 (0.4) View of Hidalgo Mountain ahead. The Hidalgo fault is on the near side of Hidalgo Mountain; the Calico fault is on the far side. Dark hills on the near side of Hidalgo Mountain are bounded on the north by the Emerson fault.

1.5 (0.6) TURN LEFT onto Old Woman Springs Road, Highway 247. Proceed westerly.

3.8 (2.3) The Johnson Valley fault is to the right on the east side of the quartz monzonite knob.

6.5 (2.7) The erosional ramp of the surrounding surface to left may be similar to that covered by the basalts of the Pioneertown flows. Bedrock granitics are exposed by weathering as resistant fractured knobs.

8.2 (1.7) The Ord Mountains can be seen straight ahead at 12:00 on the horizon. Melville Lake is hidden behind the ridge of quartz monzonite uplifted along the Johnson Valley fault.

9.5 (1.3) Means Lake is visible at 3:00 across the Johnson Valley fault.

10.2 (0.7) The scarp of the Old Woman Springs fault is viewed straight ahead. Fry Mountain is the dark range of hills at 2:00, left of Ord Mountain. The top of Fry Mountain is a cinder cone; the complex also includes two smaller cinder cones, basalt flows, and dissected vents. The Fry Mountain basalts have been dated at 8.9 ma (Oberlander, 1972). They are of basanite composition and host to ultramafic inclusions like those of

Ruby Mountain (Neville, 1983 and 1986; Neville and others, 1985).

12.4 (2.2) The northern front of the San Bernardino Mountain Range below Bighorn Mountain to the left at 10:00 shows dissected alluvial fan surfaces which have been cut by thrust faulting, as evidenced in "steps".

15.2 (2.8) The Partin Limestone Quarry is visible at 11:00. Carbonates including limestone and marble are quarried from the Paleozoic metasediments of the "Furnace Creek Formation" at several operations on the northern face of the San Bernardino Mountains (Brown, 1986; Gantenbein, 1986).

16.4 (1.2) Cross the trace of the Lenwood fault, visible at 1:00 on the northwest side of the small hill on the east side of the highway.

15.2 (0.8) Soggy Lake, to the right at 2:00, is bissected by the Lenwood fault.

16.2 (1.0) Pleistocene alluvium is in fault contact with basalt along the Old Woman Springs fault in the low range of hills to the left at 9:00. Old Woman Springs basalt is chemically similar to the alkaline olivine basalts at Pioneertown (Neville, 1983).

17.6 (1.4) View of limestone quarry in Arrastre Canyon, to the left.

17.9 (0.3) Old Woman Springs, marked by cottonwood trees, is to the left (south).

19.5 (1.6) TURN RIGHT on dirt road and park.
STOP 8. The dirt road trends north, parallel to the trace of the Old Woman Springs fault, which places Pleistocene alluvium on the west against Mesozoic granitics on the east. View northerly shows Negro Butte at 10:00, Fry Mountain at 12:30 and limestone quarries to the south.

RESUME travel westerly on Highway 247, Old Woman Springs Road.

20.6 (1.1) The Silver Reef landslide is to the left behind the gneissic ridge at 9:00; the Blackhawk landslide is at 11:00. The Silver Reef deposits are the older components of the Silver Reef-Blackhawk landslide complex (see Milepost 23.2). The landslide breccia, predominantly carbonates of the Furnace Creek Formation, was mined for gold and silver at least as early as 1881 (Storm, 1892), although the "reef" was not recognized as a massive landslide until 1928 (Fife, 1982a; Woodford and Harriss, 1928). The Silver Reef consists of two major landslides overridden in part by the younger Blackhawk landslide to the west.

22.2 (1.6) Blackhawk Mountain and Blackhawk Canyon are viewed to the

left. The canyon was the site of extensive gold mining activity from 1871 intermittently until 1942, with an estimated $300,000.00 in recovery. The Arlington-Santa Fe Lode and the Blackhawk Lode were the principal producers, each a belt of gold-bearing limestone that have been heavily developed with tunnels, shafts and cuts during the history of mining activity. A ten-stamp mill was constructed at the base of Blackhawk Canyon; in 1890, ore was delivered to the mill simply by throwing it over the steep cliffs. Later, chutes were constructed down canyon to a wagon loading area. Lodging houses, shops, barns and stables developed at the mill site. Silver discovered in the canyon in 1873 never reached the economic importance of the gold ores; it is interesting to ponder the presence of gold-bearing limestone in place in Blackhawk Canyon in contrast to the silver-bearing landslide deposits whose source was Blackhawk Canyon (Fife, 1982a; Storm, 1892; Robinson, 1977).

23.2 (1.0) TURN LEFT off highway onto dirt road leading to sand and gravel operation which has cut directly into the toe of the Blackhawk landslide. The quarry, operative in May 1986, is private property and should not be entered without permission.

The Blackhawk landslide has been dated at 17,400 +/- 550 ybp (Stout, 1982). Its source is precipitous Blackhawk Canyon on the northern face of the San Bernardino Mountains. The landslide is predominantly dolomitic limestone of the "Furnace Creek Formation" which has been crushed by the catastrophic nature of the landslide (Sadler, 1982). The precipitating factors leading to a landslide of such magnitute (370+ million tons)(Fife, 1982a) are not fully understood, but include resistant limestone thrust over relatively uncemented Tertiary arkose of the Old Woman Sandstone (Fife, 1982a); increased rainfall and highly saturated ground during the Tioga glaciation (Stout, 1982); and possible air rafting of a huge rock fall (Shreve, 1968).

RETRACE ROUTE to Highway 247, Old Woman Springs Road.

23.5 (0.3) TURN LEFT onto Old Woman Springs Road, continue west.

27.5 (4.0) TURN LEFT (south) on Camp Rock Road. View ahead shows level summits of San Bernardino Mountain Range. Limestone quarries visible are, from east, the Kaiser Cement and Kaiser Steel Corporation, the Charles Pfizer, and Pluess-Staufer, with haul roads running to the summit (Brown, 1986). Carbonate deposits of the "Furnace Creek Formation" have been thrust over Tertiary sandstone along the northern frontal fault system of the San Bernardino Mountains (Sadler, 1982). See Brown, 1986.

31.4 (3.9) Tilted beds of the central facies (May and Repenning, 1982b) of resistant, south-dipping Old Woman Sandstone are visible to the left at 10:00.

32.4 (1.0) TURN LEFT toward Big Bear and the San Bernardino Mountains at

the junction of Highway 18.

33.1 (0.7) Cross the trace of the Helendale fault as you head up Cushenbury Grade. Cushenbury Canyon takes its name from John Cushenbury, who discovered a "silver" vein on the north slope of the San Bernardino Mountains in 1861 and laid out a short-lived town named Cushenbury City, perhaps near the site of the Kaiser facility. His vein proved to be "argentiferous galena and lead which they know of no way to profitably extract" (Guardian, March 1, 1867). Cushenbury Road was built in 1864 to reach the Morongo Silver Mining Company veins at Henderson Ledge in Lone Valley, three miles east of Baldwin Lake. The road was improved in 1883 to haul cement and supplies during construction of the Bear Valley Dam. It served as the only reliable winter route into the San Bernardino Mountains until the 1930s, although it remained unpaved until 1934-36 (Leadabrand, 1966; Gudde, 1974; Robinson, 1974).

Quarrying by the Kaiser Cement Corporation began at Cushenbury in 1947; large-scale production followed the construction of the Santa Fe railroad spur in 1955 (Fife, 1982b; and see Gantenbein, 1986). The Kaiser facility is located on a series of coalescing alluvial fans in the tectonically active boundary between the Mojave Desert and the San Bernardino Mountains. Strike-slip faults, dominated by the right lateral Helendale fault, are intersected by thrust faults associated with the northern frontal fault system of the San Bernardino Mountains (Rzonca and Clark, 1982, and see Gantenbein, 1986).

33.5 (0.4) Pass one entrance to the Kaiser Cushenbury Grade facility at right.

33.6 (0.1) TURN RIGHT just before tall tanks into main entrance to Kaiser quarry facility. Pull into parking area along headquarters.

STOP 9. Park in Kaiser parking lot if arrangements have been made for tour of facility. If not, turn around and RETRACE ROUTE north on Highway 18.

33.8 (0.2) TURN LEFT from entrance to Kaiser facility onto Highway 18, proceed south. Overview of Lucerne Valley.

34.1 (0.3) The roadcuts between two low hills shows exposures of Old Woman Sandstone. The trace of the Helendale fault is marked by high ground water supporting cottonwoods and grasses to the left.

36.9 (2.8) Proceed northwest of Highway 18 past the junction of Camp Rock road to the Helendale Fault.

38.3 (1.4) Water dammed along the Helendale fault has allowed the growth of trees to the left.

39.0 (0.7) The Helendale fault runs along the base of the hills at 11:00

to the left, then up the V-shaped notch to the other side of the hills.

40.8 (1.8) TURN LEFT onto graded road due south toward new water tank.

41.1 (0.3) The Helendale fault can be observed where white marl and brown Old Woman Sandstone are faulted against calichified arkosic alluvium. The fault contact dips northeast. The sense of movement may be lateral, but places the Old Woman Sandstone on the east above the fanglomerates on the west.

RETRACE ROUTE to Highway 18.

41.4 (0.3) TURN LEFT onto Highway 18 and continue west.

43.0 (1.6) TURN LEFT onto Meridian Road and head south toward the mountains marked with Pluess-Staufer haul roads. Straight ahead, behind the mountain crest, is Holcomb Valley. William Holcomb discovered placer gold in the valley in 1860, initiating a major southern California "rush" to the San Bernardino Mountains. To the west of Holcomb Valley, at 1:00, gold mines associated with the Greenlead mine of 1876 were worked intermittently through the early 1940s (Beattie and Beattie 1951; Leadabrand, 1966; and see Paul, 1986).

43.8 (0.8) STOP 10. Park on shoulder of road at sand and gravel quarry in Old Woman Sandstone. May and Repenning (1982b) report fossil mammals from two facies of the Old Woman Sandstone. The central facies, east of the junction of Highway 18 and Camp Rock Road, has produced Geomys (Neterogeomys) anzensis and Repomys n. sp. (see also May, 1981). We are stopped in the western facies of the Old Woman Sandstone which has produced fossil remains of Hypolagus furlongi, Paraneotoma n. sp., and Equus (Dolichohippus) simplicidens (May and Repenning, 1982b). The age ranges of the morphologic forms of taxa involved suggest deposition of the western facies between 2.5 and 3.0 ma and deposition of the central facies between 2.0 and 3.2 ma. These taxa are indicative of a late Blancan land mammal age of approximately 2 to 3 ma.

The clast suite within these facies of the Old Woman Sandstone is characteristic of the Mojave Desert and predates development of the north flank of the San Bernardino Mountains. At the start of this trip, a discussion of the Mt. Eden Formation (Reynolds and Reeder, 1986) noted the first record of Transverse Range clasts in sediments which contain mammals suggesting an age of 5.0 to 5.4 ma (May and Repenning, 1982a). Clasts from lithologies in the San Bernardino Mountains first appear in the San Timoteo Formation near a point in the sedimentary section that produced the Cozy Dell fauna of approximately 1.2 ma or younger (Repenning, 1983 and p.c. 1981; Reynolds and Reeder, 1986).

44.6 (0.8) TURN LEFT onto Highway 18, proceed west.

46.3 (1.7) TURN LEFT onto Highway 247 at junction of Highway 18 in Lucerne Valley.

46.5 (0.2) Cross the trace of the Helendale fault. Lucerne Lake is visible at 3:00; Rabbit Springs is marked by cottonwood trees.

49.8 (3.3) Cross Rabbit Dry Lake. Chimney Rock, at the northeast margin of the lake, is California State Historical Landmark 737, the site of the terminal Indian "battle" in southern California. Settlers from the San Bernardino Mountains and San Bernardino Valley formed a posse to permanently remove Indians from the mountains following the murders of three cowboys at Las Flores Ranch in Summit Valley in 1866 and a series of Indian raids and fires at mountain settlements and sawmills in 1867. A small band of Indians was driven from the mountains across Rabbit Dry Lake to Chimney Rock in 1867 where they were killed or scattered (Beattie and Beattie, 1951; Quinn 1980).

White Mountain, elevation 7,736 feet, can be seen to the left at 9:00. A syncline axis passes through the summit; a thrust fault at the base is a part of the San Bernardino Mountains northern frontal fault system.

56.9 (7.1) TURN LEFT at Bear Valley Cutoff. The knob on the north edge of the San Bernardino Mountains to the left at 9:00 is Luna Mountain; the Ord Mountains are at 10:00, the San Gabriel Mountains at 11:00, Quartzite Peak at 1:30, Bell Mountain at 2:00, and the Granite Mountains at 3:00.

60.7 (3.8) Navajo Road junction; continue straight. Note the even skyline of the western San Bernardino Mountains to the left, indicative of the relative lack of erosion and thus the relatively short time span since the Miocene surface was uplifted.

62.3 (1.6) Cross Pleistocene river terraces as you enter the Mojave River drainage.

63.5 (1.2) Cross into recent floodplain sediments of the Mojave River at Apple Valley Road.

64.5 (1.0) Emerge from recent floodplain onto Pleistocene terraces. A thin exposure of Pleistocene lacustrine sediments is visible to the right on top of the terrace surface.

65.7 (1.2) Railroad overpass. To the right, Pleistocene sediments have yielded diverse taxa of Rancholabrean and perhaps Irvingtonian land mammal age including horse, camel, mammoth, rabbits and rodents. (Power, 1985; Reynolds, 1985b; Jefferson, 1986; SBCM collections).

66.4 (0.7) Hesperia Road junction. Fossiliferous Pleistocene sediments to the right have yielded Pleistocene chipmunk and rabbit.

69.4 (3.0) ONRAMPS TO INTERSTATE 15. Return to San Bernardino/Riverside

area via Cajon Pass. Continue to San Bernardino County Museum in Redlands via Interstate 10 from Interstate 15 interchange in Colton.

SIDE TRIP #1

CRAFTON HILLS

Normal faults are conspicuously absent in most of the San Bernardino basin and mountain areas with the notable exception of the Crafton Hills-Beaumont region. Readily visible and easily visited normal faults are found along the south side of the Crafton Hills a short distance east of Interstate 10. The Crafton Hills are basically a horst which forms the northern boundary of a structurally complex graben underlying the Yucaipa Valley area to the south. Part of the graben was an artesian basin until extensive groundwater withdrawal in historic times. The basin is the site of occasional ground fissuring.

0.0	(0.0)	EXIT from Interstate 10 at the Yucaipa Road - Crafton Hills College - Oak Glen offramp at road log Milepost 7.4.
0.5	(0.5)	TURN LEFT across Interstate 10 on Yucaipa Boulevard.
1.7	(1.2)	Several low, south-facing scarps to the left of Yucaipa Boulevard may be fault scarps or may be "lateral spreading" landslide scarps. Most of them are arcuate in plan. Ahead in the distance are faceted spurs produced by normal faulting (Western Heights fault) on the southeast side of the Crafton Hills.
2.1	(0.4)	Stop light at 14th Street and Sand Canyon Road. Continue on Yucaipa Boulevard. Two low scarps are just to the north of Yucaipa Boulevard; a dissected normal fault scarp is seen along the base of the Crafton Hills. The low scarps may be the result of "lateral spreading" landslides.
3.4	(1.3)	TURN LEFT at signal onto Oak Glen Road. Ahead to the north is a good view of the faceted spurs.
3.9	(0.5)	Oak Glen Road is along an active wash. Pleistocene alluvium can be seen along the left side of the road.
5.2	(1.3)	STOP at turn-around point on the north side of Oak Glen Road (or proceed 0.1 mile further on Oak Glen Road and turn around at the entrance to Yucaipa Regional Park). The best views of the normal fault faceted scarps are to the north of Yucaipa Regional Park, across the wash. RETRACE ROUTE to Interstate 10 and resume road log at Milepost 7.4. As you turn around, notice again the linear alignment of the faceted spurs to the west along the south side of the Crafton Hills.

SIDE TRIP #2

SAN TIMOTEO BADLANDS

The Badlands consist of sediments of the Mt. Eden Formation, the San Timoteo Formation, and Pleistocene alluvium. The Pliocene Mt. Eden Formation underlies the Plio-Pleistocene age San Timoteo Formation (Frick, 1921; Fraser, 1931; Dibblee, 1981) which is in turn covered by deeply weathered gravels and flat-lying sediments and by terrace deposits referred to Quaternary Old Alluvium (Morton 1978a, 1978b; Dibblee, 1981). The sedimentary record represents at least three depositional events truncated by erosion, in progress today, which has produced the current badlands topography. In the broad sense, the block of sediments is bounded on the south by the San Jacinto fault and on the north by the Banning branch of the San Andreas fault system (Fraser, 1931; English, 1953; Shuler, 1953; Blacet, 1960; Larsen, 1962; Dibblee, 1964 and 1981; Morton, 1978a and 1978b; Reynolds, 1985).

Plio-Pleistocene sediments of the San Timoteo Formation include a lower lacustrine siltstone facies and an upper fluviatile facies of sands and gravels which includes local clays and conglomerates (Reynolds and Reeder, 1986). Matti and Morton (1975) recognized three units in the formation. The oldest contains clasts of locally-derived basement rocks of the Peninsular Range; the two overlying units contain clasts derived from the San Bernardino and San Gabriel Mountains to the north. Movement and uplift between the fault zones since deposition have folded the sediments anticlinally (Morton, 1978b; Dibblee, 1981).

Paleontologic sites including floras and vertebrates of Pliocene and Pleistocene age are known from the Mt. Eden Formation and the younger San Timoteo Formation (Frick, 1921 and 1933; Axelrod, 1937, 1966 and 1976; Quimby, 1975; Reynolds, 1979, 1981, 1983, 1985a, and 1986; May, 1981; May and Repenning, 1982). The Pliocene Mt. Eden flora and fauna in the Mt. Eden Formation has been dated from 5.0 to 5.4 ma (Axelrod, 1937; May and Repenning, 1982). Fossil mammals in the San Timoteo Formation suggest that deposition took place from the late Blancan land mammal age, approximately 2.0 ma, through the middle Irvingtonian land mammal age, approximately 1.0 ma (see Reynolds and Reeder, 1986).

0.0	(0.0)	EXIT Interstate 10 at Highway 79, Beaumont Avenue, at road log Milepost 17.8.
0.2	(0.2)	TURN RIGHT onto Beaumont Avenue; proceed south and enter Lamb Canyon.
1.2	(1.0)	Road cut to the right exposes deeply-weathered, well developed soil on the San Timoteo Formation, which is dipping shallowly north.
1.5	(0.3)	The silty lacustrine facies of the San Timoteo Formation can be seen dipping to the north.
2.0	(0.5)	The silty lacustrine facies sits on granitic basement rocks. A basal grus (arkose) is developed at the base of the silty facies on the granodiorite boulder surface.

2.2 (0.2) Reenter silty facies of the San Timoteo Formation.

3.8 (1.6) The red clay of the lower portion of the San Timoteo Formation is visible to the left at 10:00.

4.3 (0.5) Tertiary weathering produced the granodiorite boulder surface to the right. Elsewhere in the San Timoteo Formation, similar granitic boulders are coated with tufa (Reynolds, 1986), indicating lacustrine conditions.

4.5 (0.2) Mesozoic metasedimentary rocks including schist, gneiss and marbles are exposed in the road cuts to the left.

4.8 (0.3) The road winds southerly away from Lamb Canyon.

6.0 (1.2) Enter the red, deeply weathered sediments of the Mt. Eden Formation dipping southerly on the south limb of the anticlinal structure.

6.5 (0.5) TURN RIGHT onto Gilman Springs Road, entering the western San Jacinto Valley. The hills to the right are made up of the Mt. Eden Formation.

7.5 (1.0) Pass the mouth of Lamb Canyon on the right.

8.2 (0.7) Pass the mouth of Laborde Canyon on the right.

8.7 (0.5) Gilman Springs Road curves to the west around low hills and then continues northerly. Movement along the San Jacinto fault zone has placed the Mt. Eden Formation (east) against the Bonsall tonalite (west).

9.0 (0.3) The view to the southwest shows the Lakeview Mountains (Lakeview Mountain tonalite) and Mt. Russel (Bonsall tonalite) (Larsen, 1948; Dibblee, 1981). The Casa Loma fault has been projected along the length of the western San Jacinto Valley, a pull-apart basin bounded on the north by the San Jacinto fault zone. The graben has also been affected by lateral stress resulting in offsets along the San Jacinto and Casa Loma faults (Dibblee, 1981; Rasmussen, 1981).

9.9 (0.9) The Mt. Eden Formation is seen to the right at 2:00.

11.0 (1.1) The San Timoteo Formation can be seen to the right at 3:00 as we pass a chain link gate and auto court sign.

11.6 (0.6) TURN RIGHT onto Jack Rabbit Trail. The turn is marked by a sand and gravel operation in Quaternary old alluvium on the corner of Jack Rabbit Trail and Highway 79.

12.1 (0.5) The southwest dipping San Timoteo Formation sediments exposed in the roadcut on the right overlie the Mt. Eden Formation.

12.2 (0.1) Leave bedded greenish gray San Timoteo Formation sediments and

enter the massive reddish brown clays of the Mt. Eden Formation.

12.3 (0.1) Cross the axis of the anticlinal structure in the Mt. Eden Formation. Beds now dip northeasterly. The contact of the northeast dipping Mt. Eden Formation (greenish gray and red massive silts and sands) under the light-colored arkosic sands and gravel stringers of the San Timoteo Formation is exposed in the road cut to the left.

12.4 (0.1) The north-dipping bedded silty sands on the north limb of the anticlinal structure are part of the fine grained facies of the San Timoteo Formation.

12.9 (0.5) View northwest at 10:00 of concordant summits on ridge tops which remain as part of a late Pleistocene erosional surface. The badlands topography evolved as dendritic drainage developed on this surface.

14.1 (1.2) The transition between the silty and sandy facies of the San Timoteo Formation to the coarse gravel facies is exposed in road cuts.

15.4 (1.3) View over San Timoteo Canyon which now drains the Yucaipa basin.

15.9 (0.5) ENTER Highway 60 to right; proceed east through late Pleistocene nonmarine sediments.

18.4 (2.5) Highway 60 merges into Interstate 10 east. Continue on Interstate 10.

19.1 (0.7) Beaumont Avenue offramp. End of side trip; resume field trip log at Milepoint 16.6.

SIDE TRIP #3

WHITEWATER CANYON

Topography in Whitewater Canyon is influenced by the Banning branch of the San Andreas fault system and the Whitewater fault; farther up canyon, erosional features are influenced by branches of the San Andreas and Pinto Mountain faults (fig. 5). In addition to affording views of rock units thrust and offset by these fault systems, the canyon's high water table supports scenic riparian habitats and wildlife. Most of the seemingly accessible land along the side trip route is privately owned.

0.0	(0.0)	EXIT Interstate 10 at Whitewater Road, road log Milepost 44.8.
0.3	(0.3)	TURN LEFT at stop sign, crossing north over freeway, and bear right.
0.7	(0.4)	TURN LEFT onto Whitewater Canyon Road, entering wildlife refuge. Note paleosol at 2:00 under coarse gray gravels which dip upward approaching the Banning fault.
0.9	(0.2)	Cross the scarp of the Garnet Hill fault. To the left of the road, elevated Pleistocene Whitewater gravels are offset right laterally by the Banning fault.
1.3	(0.4)	Cross the MWD Colorado River Aqueduct at the hydroelectric plant to the right. After powering the turbines, water is released here to recharge the Palm Springs basin.
2.3	(1.0)	Enter Bonnie Bell, an area of high water table along the Banning fault. To the right across the canyon, the Banning fault forms a high angle contact between Whitewater River gravels to the south and gravel-capped basement to the north. The north-northwest striking and norhteast dipping Whitewater fault cuts the perched gravels. To the left (west), a canyon has developed along the Banning fault which here dips 60 to 65 degrees north and juxtaposed Whitewater river gravels.
2.6	(0.3)	Up canyon to the right, across the river, is the orange-colored Coachella Fanglomerate. The color change stratigraphically upward reflects the increase in the volcanic component of the fanglomerate. On the north side of this canyon, older deformed Whitewater River gravels rest on basement and are cut off to the east by the Whitewater fault. Younger, undeformed Whitewater River gravels rest unconformably on both the basement and the deformed gravels.
3.2	(0.6)	At 10:00 the deformed Whitewater River gravels are in fault contact with the Coachella Fanglomerate.
4.2	(1.0)	The northern end of the deformed Whitewater River gravels and the Whitewater fault are on the east side of the canyon.

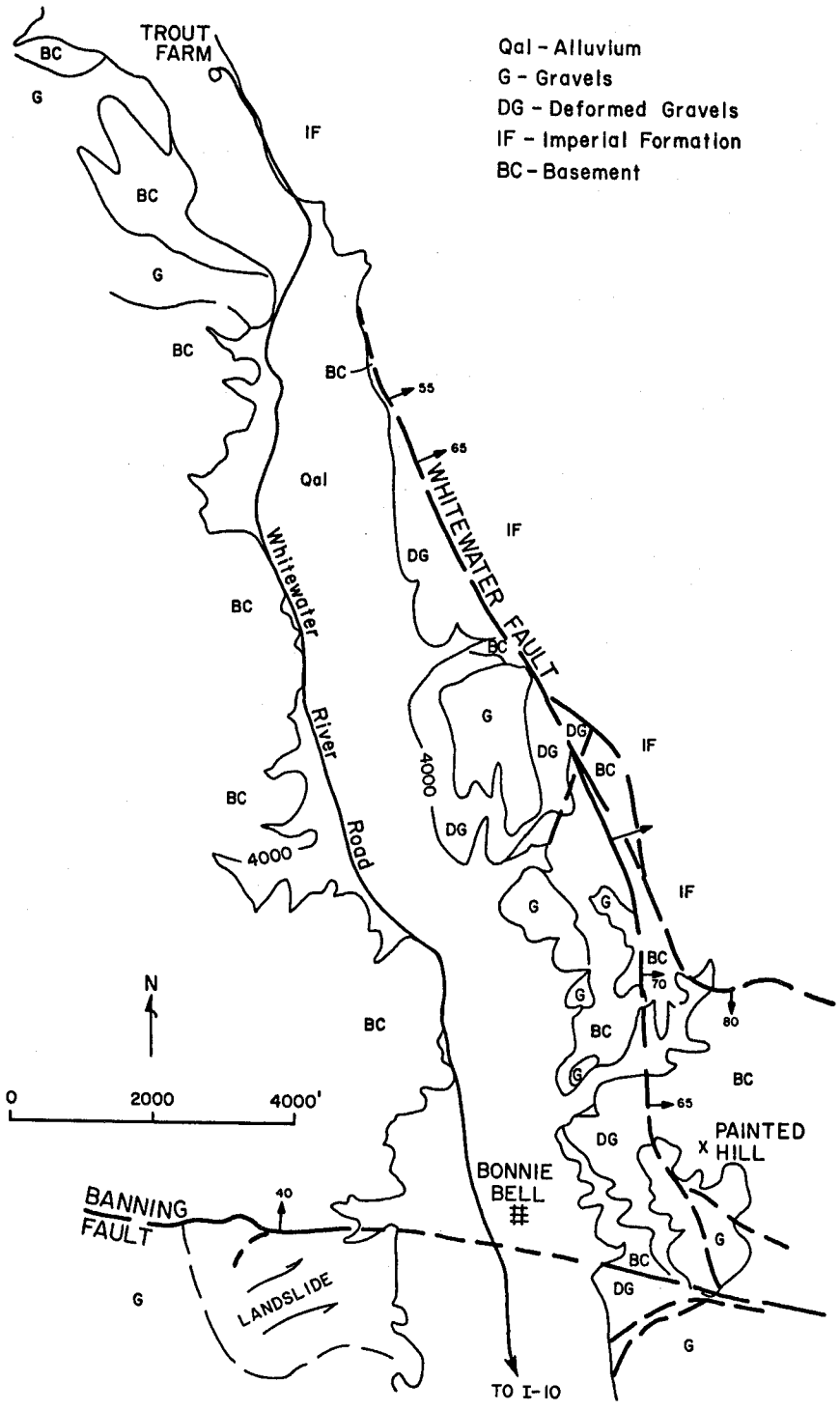

Figure 5. Whitewater River Canyon, showing relationships of rock units and faults. See Side Trip #3.

4.8 (0.6) Junction of the Pacific Crest Trail as it comes down Whitewter Canyon heading to the San Jacinto Mountains via the Snow Creek fan. Cross the Whitewater River.

5.0 (0.2) The basal Coachella Fanglomerate, to the immediate right on the north side of the creative parking area, consists of locally derived material. Most notable here is the abundance of pisiticitic to iron-poor epidote transitional to the commonly occurring piemontite. The piemontite is in a different setting than the better-known piemontite occurrence near Stubbe Canyon, west of Cottonwood Canyon, which we viewed from Milepost 30.7.

5.4 (0.4) TURN AROUND at the Trout Farm and RETRACE ROUTE to Interstate 10.

6.4 (1.0) To the right, the Banning fault juxtaposes Whitewater River gravels against bedrock.

10.2 (3.8) TURN RIGHT from Whitewater Canyon Road onto frontage road, curve over overpass.

10.7 (0.5) TURN RIGHT onto Interstate 10 onramp toward Indio. An excellent overview to the west of San Gorgonio Pass. Resume road log at Milepost 44.8.

SIDE TRIP #4

COPPER BASIN AND CAMPBELL HILL

This side trip skirts the northern boundary of Joshua Tree National Monument following the Pinto Mountain fault as it passes through Copper Basin and offsets lacustrine sediments. The trip continues to Campbell Hill, where Pleistocene sediments have been uplifted along the Mesquite Lake fault, and near the site of geothermal resources.The side trip can be incorporated into your route to campgrounds in the National Monument before continuing on to Leg 2 of the field trip road log.

0.0	(0.0)	TURN RIGHT from Pipes Canyon Road onto Highway 247, Old Woman Springs Road at road log Milepost 90.6 and proceed toward Yucca Valley.
1.0	(1.0)	Magnetic anomalies indicate extensions of the Homestead fault and the Johnson Valley fault to the left. The topography does not reflect the presence of a graben in which the tank (left) sits.
2.8	(1.8)	You are passing through low granitic hills which are transitional between the Sawtooths, near Pioneertown, and Yucca Mesa, to the northeast. Concretionary sands of Tertiary (?) age are exposed in gullies along the road.
5.3	(2.5)	Straight ahead, across the intersection with Highway 62, the fanglomerate does not contain the distinctive basalt or quartzite clasts which are found in similar deposits in this area, suggesting very recent or very localized deposition. "Burnt Mountain" is a volcanic exposure which may be a neck for acidic kaersutite volcanics.
5.4	(0.1)	TURN LEFT (east) at intersection onto Highway 62. Proceeding straight ahead on Highway 247 will lead to Black Rock Canyon Campground, five miles distant.
8.5	(3.1)	The Institute of Mentalphysics is to the left.
11.3	(2.8)	Park Boulevard intersection; entrance to Joshua Tree National Monument. Granitic boulders from the batholith intrusions and metamorphic country rocks in the monument are exposed to the right along Highway 62 as you proceed to Twentynine Palms. The metamorphic rocks were separated into the San Gabriel terrain and the Joshua terrain prior to the intrusion of the granitic batholith by the pre-Cretaceous Red Cloud thrust (more than 665 ma, less than 1.2 ga). The San Gabriel terrain is in part correlated with rocks in the San Gabriel Mountains (Powell, 1982).
15.2	(3.9)	Intersection of Sunfair Road. Continue on Highway 62; prepare to turn left.

16.2 (1.0) TURN LEFT from left turn lane onto Cascade Road; proceed north to second pole line road (Sunnyslope Road).

17.0 (0.8) TURN RIGHT (east) onto Sunnyslope Road, marked in 1986 by a sign reading "Obney's German Shephards". Copper Basin, ahead to the left, evidences significant cracking on its surface. The Regional Parks Department excavated below the natural alluvial surface to create an artificial lake designated for water sports in the basin. The reservoir was 3 meters deep, lined with clay, and had a water capacity of 50 to 60 acre feet. As the lake was being filled, a catastrophic and total water loss occurred on the evening of July 29, 1972. The loss is attributed to the reactivation of desiccation polygons and playa fissures through which the reservoir drained into the groundwater table (Fife, 1980). A northwest/southeast strike-slip fault east of the reservoir (Dibblee, 1968) may have been a contributing factor for the drainage. Lakeside homesites are available.

17.4 (0.4) Enter lacustrine sediments capped with tufa layers at the top of the Copper Mountain lacustrine section. Travel east, down section from the lacustrine sediments, into the fluviatile sediments toward the base of the section.

17.8 (0.4) Sediments dip southwesterly away from the trace of the Pinto Mountain fault. The sedimentary section, from lowest, consists of (1) fluviatile sands and gravels with indurated channel sands; (2) sands with silts and expansive clays; (3) gray lacustrine silt and silty sandstone; (4) columnar and massive tufa that overlies the lacustrine sediments. The coarser lenses of the upper part of the section appear to contain kaersutite in basalt, vesicular basalt, and felsite dike rock. The two volcanic lithologies occur in outcrops between Pioneertown and Ruby Peak (discussed herein and see Neville, 1986); the dike rock occurs in sections 21, 22, and 27, Township 1 North, Range 6 East, east of Highway 247 and west of the town of Joshua Tree, north of the Mentalphysics Institute (Dibblee, 1968). The presence of these clasts as detritus at Copper Mountain is consistent with left lateral displacement on the Pinto Mountain fault. Further mapping and recovery of datable materials in these lacustrine sediments might produce time and rates of offset.

To the left, Copper Mountain has been explored for mineral values since the early 1900s (see Reynolds and Jenkins, 1986).

18.3 (0.5) TURN RIGHT at intersection.

18.4 (0.1) TURN RIGHT at fork onto Gianelli Street, a graded dirt road, heading west.

18.8 (0.4) TURN LEFT at pavement onto Copper Mesa Road (also called Rotary Way); pass Copper Mountain College on the right, and proceed to Highway 62.

20.4 (0.6) TURN LEFT onto Highway 62; proceed east toward Twentynine Palms along Highway 62 approximately parallel the Pinto Mountain fault.

23.5 (3.1) Indian Cove Road leads south to campgrounds in Joshua Tree National Monument. This area is popular with rock climbers.

28.0 (4.5) 49 Palms Avenue. At this point, the Pinto Mountain fault bifurcates. The northern branch, if present, is to the left; the southern branch passes alongside or through Donnell Hill, on the right.

28.4 (0.4) Mesquite Spring Road. Continue along Highway 62.

29.4 (1.0) Stop light at Adobe Road. Proceed straight (east) on 29 Palms Highway. A left turn at the crossroads leads eventually to Amboy and old Route 66 via Wonder Valley and Dale Dry Lake.

30.4 (1.0) Utah Trail junction. Proceed straight on 29 Palms Highway.

31.5 (1.1) Wilshire Avenue. Campbell Hill is to the left (north); the Mesquite Lake fault is on the southwest side of Campbell Hill. Prepare to turn left.

31.7 (0.2) TURN LEFT into Singing Sands Road.
STOP. Late Pleistocene sediments at Campbell Hill have been uplifted along the northeast side of the Mesquite Lake fault (Dibblee, 1968). Vertebrate remains are typical of the Rancholabrean land mammal age and include ground sloths, dwarf pronghorn, sabertooth, mammoth, horse, camel, and bison. Bachellor (1978) tentatively identified the Bishop Tuff in the section, which is dated at .73 ma. See Jefferson, 1986.

Gecthermal resources occur north of Campbell Hill along an extension of the West Bullion Mountains fault (Dibblee, 1967c). See Martin and Elders, 1986.

TURN AROUND and retrace route west along Highway 62.

33.0 (1.3) Utah Trail junction. Proceed west on Highway 62. The scarp of the south branch of the Pinto Mountain fault is marked by more than 29 palm trees to the left at the Oasis of Mara (from the Chemehuevi "Mar-rah", land of little water). Twentynine Palms was named in 1852 by Col. Henry Washington, the surveyor of the San Bernardino baseline, who recorded 29 "cabbage trees" at the oasis. Although the community of Twentynine Palms was not developed by homesteading until the 1920s, a way station existed at the oasis by 1890 (Gudde, 1974; Bagley, 1978; Quinn, 1980).

34.0 (1.0) Adobe Road junction. Proceed on Highway 62.

35.0 (1.0) Mesquite Spring Road. Proceed on Highway 62.

35.4 (0.4) 49 Palms Avenue and Donnell Hill.

39.8 (4.4) Indian Cove Avenue. Widely-spaced fractures of the granitic White Tank intrusion weather to spectacular boulder topography in this area.

43.1 (3.3) Rotary Way/Copper Mesa Road to Copper Basin is on right. Continue on Highway 62.

44.1 (1.0) Cascade Road to right turns off to Copper Basin. Continue on Highway 62.

55.0 (10.9) TURN RIGHT from Highway 62 onto Old Woman Springs Road, Highway 247. Proceed to Pipes Canyon Road junction through granitic hills and along the edge of the Pioneertown basalt flows.

60.4 (5.4) Junction of Highway 247 and Pipes Canyon Road. Go northerly on Highway 247 and resume Leg #1 of road log at Milepost 90.6.

REFERENCES CITED

Allen, C.A., 1957, San Andreas fault zone in San Gorgonio Pass, southern California: Geological Society of America Bulletin, v. 68, p. 315-350.

Archer, M.G., 1976, Yucaipa Valley, California: Yucaipa, Archer, p. 13-48.

Aksoy, R., Sadler, P.M., and Biehler, S., 1986, Gravity anomalies over sedimentary basins on the Helendale fault trend: this volume.

Axelrod, D.I., 1937, A Pliocene flora from the Mount Eden beds, southern California: Carnegie Inst. Wash. Publ. 476, p. 125-183.

_____, 1950, Further studies of the Mount Eden flora, southern California: Carnegie Inst. Wash. Publ. 590, p. 73-117.

_____, 1966, The Pleistocene Soboba flora of southern California: University of California Publications in Geological Sciences 60, 79 p.

_____, 1976, Fossil floras of the California Desert Conservation Area: Riverside, Bureau of Land Management, p. 17-18.

_____, 1985, personal communication to Reynolds re Mill Creek floral localities: University of California, Davis.

Bachellor, J. III, 1978, Quaternary geology of the Mojave Desert - eastern Transverse Ranges boundary in the vicinity of Twentynine Palms, California: MS thesis, Department of Geology, University of California, Los Angeles.

Bagley, H., 1978, Sand in my shoes: Twentynine Palms, Homestead Press, 268 p.

Beattie, G.W. and H.P. Beattie, 1951, Heritage of the Valley: Oakland, Biobooks, 459 p.

Blacet, P.M., 1960, Geology of the Lamb Canyon area north of San Jacinto, California, 1:12,000: University of California, Riverside, unpubl. senior thesis.

Brown, H.J., 1986, Stratigraphy and paleogeographic setting of Paleozoic rocks in the northern San Bernardino Mountains, California: this volume.

Clark, M.M., 1984, Map showing recently active breaks along the San Andreas fault and associated faults between Salton Sea and Whitewater River - Mission Creek, California: U.S. Geological Survey Miscellaneous Investigations series, Map I-1483, scale 1:24,000.

Demirer, A., 1985, The Mill Creek Formation--a strike-slip basin filling in the San Andreas fault zone, San Bernardino County, California (M.S. thesis): University of California, Riverside, Department of Earth Sciences, 108 p.

Dibblee, T.W. Jr., 1964, Geologic map of the San Gorgonio Mountain quadrangle, San Bernardino County, California: U.S. Geological Survey Misc. Geological Investigations Map I-431, scale 1:62,500..

_____, 1967a, Geologic map of the Morongo Valley quadrangle, San Bernardino County, California: U.S. Geological Survey Misc. Geological Investigations Map I-517, scale 1:62,500.

_____, 1967b, Geologic map of the Old Woman Springs quadrangle, San Bernardino County, California: U.S. Geological Survey Misc. Geological Investigations Map I-518, scale 1:62,500.

_____, 1967c, Geologic map of the Joshua Tree quadrangle, San Bernardino and Riverside counties, California: U.S. Geological Survey Misc. Geological Investigations Map I-516, scale 1:62,500.

_____, 1968, Geologic map of the Twentynine Palms quadrangle, San Bernardino and Riverside counties, California: U.S. Geological Survey Intestigations Map I-561, scale 1:62,500.

_____, 1981, Geology of the San Jacinto Mountains and adjacent areas, in Brown, A.R. and Ruff, R.W., eds, Geology of the San Jacinto Mountains: South Coast Geological Society Annual Field Trip Guidebook No. 9, p.1-47.

_____, 1982, Geologic map of the Banning (15-minute) quadrangle, California: South Coast Geological Society Geologic Map SCGS-2, scale 1:62,500.

Dutcher, L.C. and Burnham, W.L., 1959, Geology and ground water hydrology of the Redlands-Beaumont area, California, with special reference to ground water outflow. U.S. Geological Survey Open File Report, scale 1:24,000.

English, H.D., 1953, The geology of the San Timoteo Badlands, Riverside County, scale 1:24,000: MA thesis, Pomona College.

Fife, D.L., 1980, Giant dessication polygons and playa fissures, in Fife, D.L. and Minch, J.A., eds, Geology and mineral wealth of the California desert: South Coast Geological Society, p. 414-429.

_____, 1982a, Mineral potential of the Silver Reef-Blackhawk landslide complex, Lucerne Valley, California, in Fife, D.L. and Minch, J.A., eds, Geology and mineral wealth of the California Transerve Ranges: South Coast Geological Society, p 477-484.

_____, 1982b, White Mountain carbonate resources, Lucerne Valley Limestone district, San Bernardino Mountains, California, in Fife, D.L. and Minch, J.A., eds, Geology and mineral wealth of the California desert: South Coast Geological Society, p. 550-560.

Fraser, D.M., 1931, Geology of the San Jacinto quadrangle south of San Gorgonio Pass, California: California Division of Mines, Mining in California, vol. 27, no. 4, p. 494-540.

Frick, C., 1921, Extinct vertebrate faunas of the Badlands of Bautista Creek and San Timoteo Canyon, southern California: University of California Publications in Geology, vol. 12 no. 5, p. 277-424.

_____, 1933, New remains of Trilophodont-Tetrabelodont mastodons: American Museum of Natural History Bulletin 59, p. 505-652.

Gantenbein, M.E., 1986, Geology of the Cushenbury Quarry, Kaiser Cement Corporation, Lucerne Valley, California: this volume.

Gibson, R.C., 1971, Non-marine turbidites and the San Andreas fault, San Bernardino Mountains, California, in Elders, W.A., ed., Geological excursions in southern California: University of California Riverside Campus Museum Contributions No. 1, p. 167-181.

Grimes, G., 1986, Sediments adjacent to a portion of the Pinto Mountain fault in the Yucca Valley area of San Bernardino County, California: this volume.

Gudde, E.G., 1974, California place names: Berkeley, University of California Press, 416 p.

Harden, J.W., Matti, J.C. and Terhune, C., 1986, Late Quaternary slip rates along the San Andreas fault near Yucaipa, California, derived from soil development on fluvial terraces: Geological Society of America, Cordilleran Section, Abstracts with Programs, vol. 18 no. 2, p. 113.

Jefferson, G.T., 1986, Fossil vertebrates from late Pleistocene sedimentary deposits in the San Bernardino and Little San Bernardino Mountains region: this volume.

Larsen, N.R., 1962, Geology of the Lamb Canyon area, Beaumont, California (M.A. thesis): Pomona College, scale 1:12,000.

Leadabrand, R., 1966, A guidebook to the San Bernardino Mountains of California: Los Angeles, Ward Ritchie Press, 118 p.

Martin, J.J. and Elders, W.A., 1986, Geothermal resource investigation at Twentynine Palms, California: this volume.

Matti, J.C., Cox, B.F. and Iverson, S.R., 1983, Mineral resource potential map of the Raywood Flat roadless areas, San Bernardino and Riverside counties, California: U.S. Geological Survey Miscellaneous Field Studies Map MF-1563-A.

_____, Obi, C.M., Powell, R.E., Hinkle, M.E. and Griscom, A., 1985, Mineral resource potential of the Whitewater Wilderness study area, Riverside and San Bernardino counties, California: U.S. Geological Survey Miscellaneous Field Studies Map MF-1478-A.

_____ and Morton, D.M., 1975, Geologic history of the San Timoteo Badlands, southern California: Geological Society of America Abstracts with Programs, vol. 7 no. 3, p. 344.

May, S.R., 1981, Repomys (Mammalia: Rodentia gen. nov.) from the late Neogene

of California and Nevada: Journal of Vertebrate Paleontology, vol. 1 no. 2, p. 219-230.

_____ and Repenning, C.A., 1982a, New evidence for the age of the Mount Eden fauna, southern California: Journal of Vertebrate Paleontology, vol. 2, no. 1, p. 109-113.

_____, 1982b, New evidence for the age of the Old Woman Sandstone, Mojave Desert, California, in Cooper, J.D., compiler, Guidebook for the Geological Society of America Cordilleran Section Meeting, Anaheim, California, 1982, p. 93-96.

Meisling, K.E. and Weldon, R.J., 1986, Cenozoic uplift of the San Bernardino Mountains - possible thrusting across the San Andreas fault: Geological Society of America, Cordilleran Section, Abstracts with Programs vol. 18 no. 2, p. 157.

Morton, D.M., 1978a, Geologic map of the Redlands 7.5 minute quadrangle, San Bernardino and Riverside counties, California: U.S. Geological Survey Open File Report 78-21.

_____, 1978b, Geologic map of the Sunnymead 7.5 minute quadrangle, Riverside County, California: U.S. Geological Survey Open File Report 78-22.

_____, Matti, J.C. and Cox, B.F., 1980a, Geologic map of the San Jacinto wilderness, Riverside County, California: U.S. Geological Survey Map MF-1159-A, scale 1:62,500.

_____, Cox, B.F. and Matti, J.C., 1980b, Geologic map of the San Gorgonio Wilderness, San Bernardino County, California: U.S. Geological Survey Miscellaneous Field Studies Map MF-1161-A.

Moxham, R.M., Walker, G.W. and Boumgardner, L.H., 1955, Geologic and airborn radioactivity studies in the Rock Corral area, San Bernardino County, California: U.S. Geological Survey Bulletin 1021-C, p. 109-125, pl. 15, 16.

Murphy, M.A., 1986, The Imperial Formation at Painted Hill, near Whitewater, California: this volume.

Neville, S.L., 1983, Late Miocene alkaline volcanism, south-central Mojave Desert and northeast San Bernardino Mountains, California (M.S. thesis): University of California, Riverside, 156 p.

_____, 1986, Late Miocene alkaline volcanism, Ruby Mountain, San Bernardino County, California: this volume.

_____, Schiffman, P. and Sadler, P., 1985, Ultramafic inclusions in late Miocene alkaline basalts from Fry and Ruby Mountains, San Bernardino County, California: American Mineralogist, vol. 70, p. 668-677.

Oberlander, T.M., 1972, Morphogenesis of granitic boulder slopes in the Mojave Desert, California: Journal of Geology, vol. 80, p. 1-19.

Paul, T.A., 1986, Minerals of the Desert View mine: this volume.

Peterson, D., 1976, Patterns of Quaternary denudation and deposition at Pipes Wash, Mojave Desert, California: Ph.D. dissertation, University of California, Riverside, 179 p.

Peterson, M.S., 1975, Geology of the Coachella Fanglomerate, in Crowell, J.C., ed., San Andreas fault in southern California: California Division of Mines and Geology Special Report 118, p. 119-126.

Powell, R.E., 1982, Crystaline basement terranes in the southern eastern Transverse Ranges: Geological Society of America, Cordilleran Section, Field Trip Guidebook 11, p. 109-151.

Power, J.D., 1985, Geologic map of the Bear Valley Road redevelopment area: City of Victorville, ms, 6 p.

Prentice, C.S., 1986, Distribution of slip between the San Andreas and San Jacinto faults near San Bernardino, southern California: Geological Society of America, Cordilleran Section, Abstracts with Programs, vol. 18, no. 2, p. 172.

Proctor, R.J., 1968, Geology of the Desert Hot Springs - Upper Coachella Valley area, California: California Division of Mines Special Report 94, 50 p.

Quimby, G.M., 1975, History of the Potrero Ranch and its neighbors: San Bernardino County Museum Association Quarterly vol. XXII no. 2, p. 24-26.

Quinn, A., 1980, Historical landmarks of San Bernardino County: San Bernardino County Museum Association Quarterly vol. XXVIII nos. 1,2, p. 86 p.

Rasmussen, G.S., 1981, Nature of surface rupture and recurrence interval, Casa Loma fault, in Brown, A.R. and Ruff, R.W., eds, Geology of the San Jacinto Mountains: South Coast Geological Society Annual Field Trip Guidebook No. 9, pp 48-54.

_____ and Reeder, W.A., 1986, What happens to the real San Andreas fault at Cottonwood Canyon, San Gorgonio Pass, California?: this volume.

Reeder, W.A. and Rasmussen, G.S., 1986, Character and Holocene activity of the Mission Creek fault in the vicinity of Desert Hot Springs, Riverside County, California: this volume.

Repenning, C.A., 1983, Pitymys meadensis Hibbard from the Valley of Mexico and the classification of North American species of Pitymys (Rodentia: Cricetidae): Journal of Vertebrate Paleontology, vol. 2, no. 4, p. 471-482.

_____, 1979 - 1986, personal communications to Reynolds re San Timoteo Formation faunad: Menlo Park and Denver, U.S. Geological Survey.

Reynolds, R.E., 1979, Paleontologic, archaeologic, historic and biologic resources assessment, Tract 10272, San Timoteo Canyon area, San Bernardino County, California: Redlands, San Bernardino County Museum Association, 48 p.

_____, 1981, Cultural resources survey, De Anza Cycle Park expansion, San Timoteo Badlands, Riverside County, California: Redlands, San Bernardino County Museum Association, draft ms 24 p.

_____, 1983, Paleontologic resources survey, Haskell Ranch, San Timoteo Badlands area, Riverside County, California: Redlands, San Bernardino County Museum Association, 10 p.

_____, 1985a, Paleontologic resource assessment, Santa Ana River upstream alternatives study, Beaumont/San Timoteo borrow site, for ECOS Management Criteria, Cypress, 17 p.

_____, 1985b. Road log, in Reynolds, R.E., compiler, Geologic excursions along Interstate 15, Cajon Pass to Manix Lake: Redlands, San Bernardino County Museum, p. 5-42.

_____, 1986, Paleontologic resource assessment, Futura Valley Farms, San Timoteo Canyon, Riverside County, California: Redlands, San Bernardino County Museum, for Lerch and Associates, Riverside, 19 p.

_____ and Jenkins, J.E., 1986, Secondary mineral assemblage at the Copper Consolidated Lode, Copper Basin, San Bernardino County, California: this volume.

_____ and Reeder, W.A., 1986, Age and fossil assemblages of the San Timoteo Formation, Riverside County, California: this volume.

Robinson, J.W., 1977, Mines of the San Bernardinos: Glendale, La Siesta Press, 71 p.

Rogers, T.H., 1967, Geologic map of California, San Bernardino sheet, 1:250,000: California Division of Mines and Geology.

Rzonca, G.F. and Clark, D.W., 1982, Local geology, Kaiser Cement Corporation, Cushenbury Facility, Lucerne Valley, California, in Fife, D.L. and Minch, J.A., eds, Geology and mineral wealth of the California Transverse Ranges: South Coast Geological Society, pp 676-678.

Sadler, P.M., 1982, Provenance and structure of late Cenozoic sediments in the northeastern San Bernardino Mountains, in Cooper, J.D., compiler, Geologic excursions in the Transverse Ranges, southern California: Geological Society of America Cordilleran Section Meeting, Guidebook, pp 82-91.

_____ and Demirer, A., 1986, Pelona Schist clasts in the Cenozoic of the San Bernardino MOuntains, southern California, in Ehlig, P.L., compiler, Neotectonics and faulting in southern California: Geological Society of America, Cordilleran Section, 82nd Annual Meeting, guidebook and volume, p. 129-146.

Savage, D.E. and Russell, D.E., 1983, Mammalian paleofaunas of the world: Reading, Addison-Wesley, 432 p.

Shreve, R.L., 1968, The Blackhawk landslide: Geological Society of America Special Paper 108, 47 p.

Shuler, E.H., 1953, Geology of a portion of the San Timoteo Badlands near Beaumont, California (MA thesis): University of Southern California, scale 1:48,000..

Stocker, V.M., 1973, The Whitewater story: San Bernardino County Museum Association Quarterly, vol. XX, nos. 3,4, p. 1-15.

Storm, W.H., 1892, The Blackhawk and Silver Reef districts: California State Bureau of Mines, Eleventh Report of the State Mineralogist, p. 364-366.

Stout, M.L., 1982, Age and engineering geologic observations of the Blackhawk landslide, southern California, in Fife, D.L. and Minch, J.A., eds, Geology and Mineral Wealth of the California Transverse Ranges: South Coast Geological Society, pp 630-631.

Vaughan, F.E., 1922, Geology of the San Bernardino Mountains north of San Gorgonio Pass: University of California Publications in Geological Sciences, vol. 13, p. 319-411.

Woodford, A.O. and Harriss, T.F., 1928, Geology of Blackhawk Canyon, San Bernardino Mountains, California: University of California Publications Geological Sciences, vol. 17, p. 365-304.

AGE AND FOSSIL ASSEMBLAGES OF THE SAN TIMOTEO FORMATION, RIVERSIDE COUNTY, CALIFORNIA

Robert E. Reynolds, Curator, Earth Sciences
San Bernardino County Museum
Redlands, California 92373

Wessly A. Reeder
Gary S. Rasmussen and Associates
San Bernardino, California 92408

INTRODUCTION

The San Timoteo formation is a sedimentary unit of lacustrine and fluviatile sandstones, siltstones, and gravels that lies within the Peninsular Ranges province south of the San Andreas fault and north of the San Jacinto fault in southern California. Fossil floral and faunal assemblages and stratigraphic relationships suggest deposition through Pleistocene times.

The mechanics of deposition of the San Timoteo formation relate to Pliocene and Pleistocene subsidence of the depositional basin, uplift of the San Bernardino Mountains and San Jacinto Mountains, and movement within the San Andreas and San Jacinto fault systems. Establishment of more precise temporal constraints upon the deposition of this formation would provide data for evaluation of the structural, tectonic, and paleoenvironmental history of the region.

Preliminary paleontologic investigations near Calimesa and near Highland Springs Road south of Banning indicate that these localities will provide more information regarding age and fossil assemblages within the San Timoteo formation.

BACKGROUND AND EXTENT

Western exposures of the San Timoteo formation appear near Loma Linda in Reche Canyon. The formation extends easterly south of Interstate 10, running through Yucaipa and as far east as Banning. The San Timoteo Badlands are exposed north and east of Moreno and San Jacinto. Southeast of San Jacinto to Anza, the sediments have been referred to as the Bautista formation (Frick, 1921).

Late Tertiary to early Quaternary sediments in the basin west of the San Jacinto Mountains were divided by Frick (1921) into the Eden, San Timoteo, and Bautista beds. The Eden beds were later redescribed as the Mt. Eden formation (or beds) by Fraser (1931). In the western San Jacinto Mountains, the San Timoteo formation rests conformably on the Mt. Eden formation, but to the southeast and north it laps onto granitic basement (Shuler, 1953; Dibblee, 1981). Based on paleontologic and lithologic similarities, Dibblee (1981) suggests that the Bautista and the San Timoteo formations may be contemporaneous and their differences may merely represent a facies change.

LITHOLOGIC DESCRIPTIONS

Underlying Sediments

Geologic mapping of surface exposures (Fraser, 1931; Morton, 1978a,b,c; Dibblee, 1981, 1982a,b) indicates that the San Timoteo formation was in part deposited on an erosional surface developed on Mesozoic granitic rocks and earlier metasedimentary rocks. The San Timoteo formation apparently rests conformably on the Mt. Eden formation along Laborde Canyon, Lamb Canyon and Massacre Canyon/Potrero Creek (Fraser, 1931).

An oil well located on Shutt Ranch, within the southwest quarter of section 16, Township 2 South, Range 2 West, San Bernardino Base and Meridian, was drilled by the Beaumont Midway Oil Company in 1922. The well was abandoned in 1926 after reaching a total depth of 5,358 feet. No crystalline bedrock was encountered within the well. Records on file with the California Division of Oil and Gas indicate that the well encountered some oil-bearing sands at a depth of 5,187 feet. The well log also indicates that 28 feet of "marine sands" were encountered at a depth of 4,872 feet. Conceivably, marine sediments could exist at depth underlying Tertiary continental deposits (Mt. Eden formation?) as a westward extension of the Imperial formation, which is exposed to the east in Lion Canyon near the community of Cabazon. The San Timoteo formation is distinguishable from the Imperial formation on the basis of the contained marine invertebrates in the latter as well as by sorting and appearance (see Murphy, 1986).

The Mt. Eden formation is described as being primarily reddish sandstone and dark green and brown clay with local reddish fanglomerate and conglomerate (Fraser, 1931; Dibblee, 1981). The age of the fossils (below) and the dark reddish brown coloration distinguish the Mt. Eden formation from the younger, green to gray, tan, and red-weathering San Timoteo formation.

San Timoteo Formation

The sediments of the San Timoteo formation contain a lower silty lacustrine facies and an upper fluviatile facies of sands and gravels. Red clay and conglomerate occur locally.

Morton (1978a) recognizes three units of the San Timoteo formation between Reche Canyon and San Timoteo Canyon. These are, from lower to upper:

Ts_1 -- greenish gray, finely bedded sandstone and siltstone

Ts_2 -- light gray conglomerate containing quartzite clasts

Ts -- grayish to tannish poorly bedded coarse grained sandstone, pebbly sandstone, and conglomerate.

Dibblee (1982) maps two extensive members of the San Timoteo formation in the Laborde Canyon/Lamb Canyon/Massacre Canyon area. A lower silty member similar in description to the Ts_1 of Morton (1978a) contains a red clay unit and conglomerates which differ lithologically from Ts_2 of Morton. The silty member is overlain by a coarse member similar to the Ts of Morton (1978a).

To the east along Highland Springs Road, south of Banning, the lower San Timoteo formation consists of tufa coatings on granitic boulders which in turn are covered by reworked gruss, reworked tufa and arkosic sandstone. The section consists of two facies, from lower to upper:

1. Silty facies -- green and gray lacustrine silts and sands with occasional laterally consistent tufa beds that coat branches, water reeds, and pebbles. Fossils include camel, proboscidean, fish, terrestrial leaves, and water reeds. The top of this silty facies is relatively well-sorted buff to tan sands. A poorly-developed paleosol contains root casts and terrestrial mammal fossils.

2. Coarse facies -- poorly bedded gray to tan sands and gravels with occasional laterally consistent marl beds suggesting ponding during a dominantly fluviatile depositional regime. Mammals including deer are present as fossils.

At Haskell Ranch in eastern San Timoteo Canyon and at Shutt Ranch west of Calimesa, distinctive, well sorted and relatively well bedded tan sands and silts are exposed. These were previously mapped as the upper member of the San Timoteo formation (= Ts of Morton, 1978a, and QTs of Dibblee, 1982). These sediments contain the Shutt Ranch local fauna which Repenning (p.c. 1985) suggests is similar in age to the El Casco local fauna. The finely-bedded sediments are distinct from the underlying coarse facies (Morton, 1978a; Dibblee, 1981; and herein) and may represent a local facies change of the San Timoteo formation or a post-San Timoteo formation depositional unit.

Overlying Sediments

Fine-grained fluviatile sediments and older alluvium of suspected Pleistocene but post-San Timoteo formation age have been mapped on the geomorphic surface in the Calimesa area by several previous workers (Shuler, 1953; Dutcher and Burnham, 1960; Dibblee, 1968, 1982; and Morton, 1978a). Previous workers may have differentiated older alluvium from the underlying San Timoteo formation on the basis of geomorphology and weathering characteristics. Although not extensively field checked, much of what has been previously mapped as undifferentiated older alluvium in the area may actually represent deeply weathered upper San Timoteo formation. This may include the "old red gravels" of Dutcher and Burnham (1960) exposed in Sand Canyon southwest of the Crafton Hills and much of the older alluvium found southeast of Redlands and east to Calimesa. No distinct unconformity was observed on the Shutt Ranch near Calimesa between what has been mapped as older alluvium and the San Timoteo formation.

DEPOSITIONAL ENVIRONMENTS

In general, the San Timoteo formation coarsens upward, probably in response to the uplift of the San Bernardino Mountains and the San Jacinto Mountains during Pleistocene and/or late Pliocene time. Dibblee (1981) suggests that much of the San Timoteo formation and Bautista formation were derived from rocks of the San Bernardino Mountains, the San Jacinto Mountains and the Peninsular Ranges. However, clast lithologies observed within the upper San Timoteo formation in the vicinity of Calimesa are similar to basement materials found in the Transverse Ranges. Also included within the suite are clasts of Pelona Schist which are locally found within the San Gabriel Mountains, the San Bernardino Mountains north of Banning, the Crafton Hills, and at scattered locations in the northern margins of the San Bernardino Valley.

Dibblee (1981) indicates that the San Timoteo formation was probably deposited in a northwest-trending depositional basin which extended from the San Bernardino plain into the San Jacinto Valley, and eastward through San Gorgonio Pass and into the Salton Trough. The upper Pliocene basin in which the San Timoteo formation was deposited was probably partially coincident with the former Mio-Pliocene marine embayment responsible for the deposition of the Imperial formation. Subsequent right lateral movements along the San Andreas fault and the San Jacinto fault in conjunction with uplift of the San Bernardino and San Jacinto Mountains have greatly modified the former depositional environments.

The Mt. Eden formation may have been deposited on the south flank of the same trough and its reddish coloration may be due to deep weathering profiles developed during a period of basin stability prior to renewed basin formation and the deposition of the San Timoteo formation.

Initial deposition of the San Timoteo formation is marked by local gruss and arkose over granitic boul-

ders at the base of the silty facies. The silty facies of the San Timoteo formation suggests lacustrine deposition in a shallow, continually wet basin. The tufa suggests ponding of clear water at the eastern (Potrero) margins of the formation. The coarse facies of the San Timoteo formation suggests that basin filling accelerated and larger clasts were perhaps derived from rising topographic source areas. The basin was better drained and ponding was intermittent and localized.

Paleosols (fossil soil horizons) occur in both facies of the San Timoteo formation and are generally redder (Dibblee, 1981) than similar brown and green horizons in the Bautista sediments. This suggests that between fluviatile events there were locally stable areas susceptible to deep weathering. The difference in paleosol coloration from red in the west to brown and green in the east may suggest that soils weathered under different moisture conditions. Further studies of paleosols and lacustrine deposits may provide information on regional slope, drainage, and impediments to drainage during Pleistocene times.

Refining the ages of basin formation, basin filling, and terrace formation in the San Timoteo formation will help describe the timing of the structural and tectonic events in this portion of southern California.

STRUCTURE

The San Timoteo formation has been folded into a shallow anticline between the San Jacinto fault zone and the San Andreas fault zone. This can be seen while driving along Highway 60 between Moreno and San Timoteo Canyon, from Eden Springs through Laborde Canyon, and along Jack Rabbit Trail between the western San Jacinto Valley and San Timoteo Canyon. The axis of the anticline is parallel to and just northeast of the San Jacinto fault in the Moreno Valley. In the San Jacinto to Bautista area, San Timoteo formation sediments are folded into an anticlinal/synclinal pair. Near Loma Linda, sediments of the San Timoteo formation lie on the southwest as well as the northeast sides of the San Jacinto fault zone. An anticlinal structure persists on the northeast side of the fault. The beds on the southwest side of the San Jacinto fault dip shallowly toward the fault and are overturned very near the fault (Morton, 1978c).

North and east of San Timoteo Creek, the sediments on the north limb of the anticline dip shallowly toward the Banning branch of the San Andreas fault. A change in attitude of the sediments is observed in only a few localities along the Banning fault (Dibblee, 1982).

A very distinctive and slightly tilted geomorphic surface which is prevalent in the vicinity of Calimesa has been developed on the San Timoteo formation. This surface is characterized by uniform and gently rolling topography and by well developed pedological profiles. It may have been developed at the same time as surfaces near Grand Terrace and in Cajon Pass (Prentice and others, 1986). Shlemon (1978) has dated such a surface in the Riverside/Grand Terrace area at 100,000 ybp. The geomorphic surface is nearly continuous in the Calimesa area broken only where it is incised by late Pleistocene and/or Holocene drainages. Similar groups of surfaces which may be nearly time equivalent are found southwest of the Crafton Hills; in the Redlands area; between San Timoteo Canyon and the San Jacinto fault; southwest of the San Jacinto fault in Reche Canyon; along the southwest margin of the San Bernardino Mountains; in the Beaumont-Banning area; and in the Yucaipa area, extending from Yucaipa to the northeast as erosional remnants perhaps as far as Oak Glen and Wildwood Canyon. These groups of geomorphic surfaces and associated alluvial materials have been uplifted, deformed and incised to differing degrees but may have been a nearly continuous surface in the past.

The existence of paleosols coincident with the geomorphic surfaces together with the degree of weathering of specific clast lithologies, current depositional environments, topographic positions, and degree of incision suggest that all of these geomorphic surfaces are at least late Pleistocene in age. In the Calimesa area, the strong development of argillic and calcic soil horizons within the relict paleosols suggest that the geomorphic surface may have a minimum age of late but not latest Pleistocene.

The surface may be temporally related to the terraces along Wilson Creek (Harden and others, 1986) and to the extensive geomorphic surface in the Grand Terrace area (Prentice and others, 1986). The age of the geomorphic surface is important in that it establishes constraints on cessation of the deposition of the San Timoteo formation in this area and on the last movement of the Banning fault. The trace of the Banning fault can be followed as far west as Calimesa where it is lost beneath the Pleistocene surface. The last significant movements on the Banning fault in this area probably date prior to the late Pleistocene since no geomorphic expression of faulting is evident across the Calimesa surface.

AGE CONSTRAINTS OF THE SAN TIMOTEO FORMATION

Determining the age of the San Timoteo formation will help establish the age of basin formation and rates of basin filling as well as timing of subsequent deformation and development of erosional surfaces.

The age of the lower portion of the San Timoteo formation is poorly restricted due to a paucity of localities producing datable fossils. Underlying sedimentary units help to constrain age parameters of basin formation and deposition.

The Imperial formation contains a marine invertebrate fauna similar to those from the Gulf of California. Murphy (1986) lists taxa from this formation which includes oysters, scallops, corals, foraminifera, and shrimp. Murphy (1986) and Krummenacher (in Dibblee, 1981) suggest an age in the Miocene between six and ten million years based on radiometric dates of basalts that bracket the Imperial formation.

The continental Mt. Eden formation underlies the San Timoteo formation in the Potrero Ranch area. Frick (1921) first described a vertebrate fauna which includes (p. 340) rabbit, cat, sabertooth, dog, bear, two sloths, two peccaries; three camelids, deer,

Figure 1
SAN TIMOTEO FORMATION FAUNAS

	El Casco 1.5 +/- 0.3 ma Frick 1921 Repenning p.c. 199, 1981, 1984	Shutt Ranch 1.3 +/- 0.5 ma Repenning pc 1985 Reynolds	Olive Dell 1.5 +/- 0.3 ma Repenning p.c. 1979, 1986; Repenning 1983
Leporidae	present	Sylvilagus sp. Lepus sp.	present
Edentata	Megalonyx	present	
Ursidae	Arctodus		
Mustellidae	present	present	
Canidae	Canis edwardii	Canis sp. cf? edwardi	
Soricidae		Sorex sp.	
Camelidae	Camelops sp. cf. hesternus		
Cervidae	Odocoileus casciensis	present?	Odocoileus sp.
Equidae	Equus (Equus) sp. E. (Hemionus) sp.		
Tapiridae	Tapirus cf. copei		
Proboscidea		Gomphotheriidae	
Sciuridae		Eutamias sp. (?)	
Geomyidae		Thomomys sp.	Thomomys sp. cf. gidleyi
Heteromyidae		Perognathus sp. Dipodomys sp.	Prodipodomys cf. idahoensis
Cricetidae	Neotoma (Teanopus) "prealbigula" N. (Teanoma) "prelepida" N. (Teanopus) "prefucipes" Ondatra annectens Synaptomys kansasensis	Peromyscus sp. Neotoma sp. N. (Teanoma) "prelepida" N. (Teanopus) "prefucipes" Microtus californicus	Peromyscus cf. truei Neotoma (Teanopus) "prefucipes" Allophaiomys sp. (lg)
Erethizontidae	Erethizon cascoensis		

antelope, two horses, and mastodon. Re-evaluation of this fauna by May and Repenning (1982) places emphasis on the geomagnetic polarity of the Mt. Eden sediments and on three vertebrate taxa: Repomys maxsumi, a hypsodont cricetid rodent; "Pliohippus" osborni, a dinohippine horse, and Cuvieronius edensis, a mastodon. The known age range of these mammals together with the reversed polarity of the sediments suggest depositional "...constraint on the interpreted age of the Mt. Eden Fauna at between 5.0 and 5.4 my." (May and Repenning, 1982). This indicates a late Miocene to early Pliocene Hemphillian land mammal age.

The Pliocene Mt. Eden flora is represented by 47 species dominated by woodland vegetation. Some of the species, such as avocado, require mild, frost-free winters and now occur much further south. The flora also includes precursors of chaparral scrub and semi-desert scrub and thorn. The flora is considered to be Pliocene, and equivalent to Hemphillian land mammal age faunas (Axelrod 1937, 1950, 1976).

The lower San Timoteo formation has produced abundant localities for fossil vertebrates (Frick, 1921; SBCM); most are isolated articulated or disarticulated vertebrate remains. Localities along the axis of the anticline reportedly contain Equus (Dolichohippus) sp. which would suggest an age between 4.2 ma and 1.8 ma in the middle to late Blancan land mammal age (Repenning, 1982; Savage and Russell, 1983).

Axelrod has studied two floras in the San Timoteo formation: the Soboba and the Bautista. The Soboba is the largest pre-Wisconsin flora known in North America, with 41 plant species representing five plant communities: yellow pine forest with species of fir, sugar and yellow pine, cedar, aspen, oracle oak, currant, service berry, deer brush, and snowberry; the bigcone spruce forest with Coulter pine, spruce, cypress, false indigo, madrone, canyon and live oaks, and barberry; the oak woodland with live, Palmer and scrub oaks, lilacs, mountain mahogany, buck brush, sugar bush, holly-leaf cherry, and silk-tassel bush; the riparian stream and lake edge community of box elder, dogwood, ash, sycamore, poplar, cottonwood and willow; and two aquatic species. Maple and magnolia indicate summer rain. The assemblage in general suggests greater moisture and lower temperatures than today (Axelrod, 1966 and 1976). The flora was collected in the "Bautista formation" (= San Timoteo formation, see Dibblee, 1981) in fine-grained lacustrine sandstone, shale and limy siltstone above granitic basement rocks. Its age is estimated at 2.2 ma (Axelrod, 1966).

The Bautista flora was collected in a silty sandstone interbedded with coarse sandstone and conglomerate stratigraphically close to the Bautista fauna of Frick (1921) which contains Equus bautistensis (= E. (Dolichohippus). The sample includes nine plant species: Coulter pine, bigcone spruce, cottonwood, willow, alder, mountain mahogany, false indigo, lilac and madrone. The association is typical of riparian and dry-slope bigcone spruce forest. Significantly, no plants of the yellowpine forest community, so well represented in the Soboba flora, are present. The climate at the time of deposition of the Bautista flora was drier and warmer than that of the Soboba, although depression of floral zones is clearly evident. The age of the Bautista flora is estimated to be 2.0 ma (Axelrod, 1966).

Fossil remains recently collected from the Highland Springs Road site south of Banning contain gastropods, fossil fish skeletal elements and scales, and many leaf and plant fragments including willow, oak, water reeds, and magnolia. The locality occurs in silt and shale beds in the silty facies of the San Timoteo formation. The presence of Magnolia suggests possible temporal and paleoclimatic affinities with the Soboba flora (2.2 ma); further collection and study of vertebrates at the Highland Springs Road locality could provide significant temporal data about this facies.

On the north limb of the anticline north of San Timoteo Canyon are sediments that should be stratigraphically high in the section and younger than those along the anticline axis. Several of these localities have produced occurrences of multiple taxa that allow determination of land mammal ages. Three faunas occur in the upper member of the San Timoteo formation and apparently reflect the age of the upper half to the uppermost portion of the San Timoteo formation. These are the El Casco Fauna, located one mile north of El Casco; the Shutt Ranch fauna, located one mile west of Calimesa; and the Olive Dell Fauna, located between Reche Canyon and San Timoteo Canyon. Figure 1 lists the taxa reported by Repenning (1983, and p.c. 1979 through 1986) and Frick (1921),and known from recent studies by the authors and the San Bernardino County Museum.

SUMMARY

The silty facies of the San Timoteo formation, which rests on granitic bedrock, contains the Soboba Flora dated at 2.2 ma; the Highland Springs Road assemblage which may be correlative with the Soboba Flora; and the Bautista flora, dated at 2.0 ma in part due to its apparent association with the Bautista fauna, which contains Equus (Dolichohippus) bautistensis. The floral ages suggested by Axelrod and the limited fauna suggest that the silty facies of the formation near the axis of the anticline may have been deposited in middle Blancan land mammal age in late Pliocene or early Pleistocene times.

Three faunas in the upper facies of the San Timoteo formation are, from oldest to youngest, the El Casco (1.5 ma); the Olive Dell (1.5 ma); and the Shutt Ranch (1.3 ma). These faunas suggest deposition of this portion of the San Timoteo formation in the middle Pleistocene Irvingtonian land mammal age. The Shutt Ranch site is located high in the section, and further study of the Shutt Ranch fauna, in particular the Soricidae, Heteromyidae, and Cricetidae, may substantiate a slightly younger age than the El Casco fauna.

It should be noted that the Shutt Ranch locality is situated in sediments atypical of the coarse facies of the San Timoteo formation. However, in a line south from Calimesa, the otherwise upward-coarsening San Timoteo formation contains silt and angular to subrounded quartz and fieldspar in low energy, near-source sheet flood deposits. At Haskell Ranch these sediments are well-sorted and structurally complex. These facies changes may reflect localized depositional conditions within the San Timoteo formation. Or, they may instead represent a change in depositional

regime from the Irvingtonian upper San Timoteo formation to a post-San Timoteo Pleistocene time.

The Shutt Ranch fauna is important because it can provide minimum dates on deposition of the San Timoteo formation, time constraints on development of the late but not latest Pleistocene terraces, and consequently parameters for the most recent surface rupture of the Banning branch of the San Andreas fault.

REFERENCES CITED

Axelrod, D.L., 1937, A Pliocene flora from the Mount Eden beds, southern California: Carnegie Inst. Wash. Publ. 476, p. 125-183.

___, 1950, Further studies of the Mount Eden flora, southern California: Carnegie Inst. Wash. Publ. 590, p. 73-117.

___, 1966, The Pleistocene Soboba flora of southern California: University of California Publications in Geological Sciences 60, 79 p.

___, 1976, Fossil floras of the California Desert Conservation Area: Riverside, Bureau of Land Management, p. 17-18.

Dibblee, T.W., Jr., 1968, Displacements on the San Andreas fault system in the San Gabriel, San Bernardino and San Jacinto Mountains, southern California, in Dickinson, W.R., and Grant, A.G., eds, Proceedings of conference of geologic problems of San Andreas fault system: Stanford Univesity Publications in Geological Science, vol. 11, p. 260-278.

___, 1981, Geology of the San Jacinto Mountains and adjacent areas, in Brown, A.R. and Ruff, R.W., eds, Geology of the San Jacinto Mountains: South Coast Geological Society Annual Field Trip Guidebook No. 9, p. 1-47.

___, 1982, Geologic map of the Banning (15-minute) quadrangle, California: South Coast Geological Society, Geologic Map SCGS-2, scale 1:62,500.

Dutcher, L.C. and Burnham, W.L., 1960, Geology and ground water hydrology of the Redlands-Beaumont area, California, with special reference to ground water outflow: U.S. Geological Survey Open File Report, scale 1:24,000.

Fraser, D.M., 1931, Geology of the San Jacinto quadrangle south of San Gorgonio Pass, California: California Division of Mines, Mining in California, vol. 17, no. 4, p. 494-560.

Frick, C., 1921, Extinct vertebrate faunas of the Badlands of Bautista Creek and San Timoteo Canyon, southern California: University of California Publications in Geology, vol. 12, no. 5, p. 505-652.

Harden, J.W., Matti, J.C. and Terhune, C., 1986, Late Quaternary slip rates along the San Andreas fault near Yucaipa, California, derived from soil development on fluvial terraces: Geological Society of America, Cordilleran Section, Abstracts with Programs, vol. 18, no. 1, p. 113.

May, S.R. and Repenning, C.A., 1982, New evidence for the age of the Mount Eden fauna, southern California: Journal of Vertebrate Paleontology, vol. 2, no. 1, p. 109-113.

Morton, D.M., 1978a, Geologic map of the Redlands 7.5 minute quadrangle, San Bernardino and Riverside counties, California: U.S. Geological Survey Open File Report 78-21.

___, 1978b, Geologic map of the Sunnymead 7.5 minute quadrangle, Riverside County, California: U.S. Geological Survey Open File Report 78-22.

___, 1978c, Geologic map of the San Bernardino South 7.5 minute quadrangle, San Bernardino and Riverside counties, California: U.S. Geological Survey Open File Report 78-20.

Prentice, C.S., 1986, Distribution of slip between the San Andreas and San Jacinto faults near San Bernardino, southern California: Geological Society of America, Cordilleran Section, Abstracts with Programs, vol. 18, no. 2, p. 172.

Repenning, C.A., 1983. Pitymys meadensis Hibbard from the Valley of Mexico and the classification of North American species of Pitymys (Rodentia: Cricetidae): Journal of Vertebrate Paleontology, vol. 2, no. 4, p. 471-482.

___, 1979 - 1986, personal communications to Reynolds re San Timoteo formation faunas: Menlo Park and Denver, U.S. Geological Survey.

Savage, D.E. and Russell, D.E., 1983, Mammalian paleofaunas of the world: Reading Mass., Addison-Wesley, 432 p.

Shlemon, R.J., 1978, Buried calcic paleosols near Riverside, California, in French, J., ed., Geologic guidegook to the Santa Ana River basin: South Coast Geological Society.

Shuler, E.H., 1953, Geology of a portion of the San Timoteo Badlands near Beaumont, California, scale 1:48,000: MA thesis, University of Southern California.

WHAT HAPPENS TO THE REAL SAN ANDREAS FAULT AT COTTONWOOD CANYON, SAN GORGONIO PASS, CALIFORNIA?

Gary S. Rasmussen
Gary S. Rasmussen & Associates, Inc.
1811 Commercenter W.
San Bernardino, CA 92408

Wessly A. Reeder
Gary S. Rasmussen & Associates, Inc.
1811 Commercenter W.
San Bernardino, CA 92408

INTRODUCTION

The San Andreas fault has been difficult to trace through the San Gorgonio Pass, despite numerous efforts to precisely define its location and style of movement. In this paper we have attempted to provide an alternate explanation for the fault through the San Gorgonio Pass. At this time, our field work has been primarily confined to the terrain between Millard Canyon and Cottonwood Canyon, the easternmost portion of the area where the fault is most elusive. In describing the geologic features of the San Andreas fault from Burro Flats to Cottonwood Canyon, the convention of describing the fault from north to south has been followed. The fault itself and most of the structural features associated with it, however, were created by forces imposed from south to north as the oceanic plate collided with the continental plate.

This paper is the result of several years of observations of the fault in this area. It is based on time and effort unrelated to any outside funding. The increasing pressure of development in the upper Coachella Valley is resulting in many more site specific geologic studies that rely on the published literature. The interaction of man with geologic forces makes it mandatory that we more completely understand the geologic facts prior to modifying or building on the natural terrain.

The purpose of this paper is to offer a possible explanation for most, if not all of the puzzling aspects related to where and what is the real San Andreas fault between Burro Flats and Cottonwood Canyon.

HISTORICAL PERSPECTIVE

The existence, location, type of movement, amount of movement, degree of activity, and terminology of the San Andreas fault through the San Gorgonio Pass has been controversial since it was first mapped by Fairbanks in 1908. The main reason geologists working in the area cannot agree on what actually constitutes the San Andreas fault in this area is its lack of well defined geomorphic expression. Fairbanks, in describing the fault from the northwest as it enters San Gorgonio Pass states that Potato Canyon, northwest of San Gorgonio Pass was "the last of the longitudinal depressions of any size marking the line of the rift" (in Lawson, and others, 1908). He indicated the lack of rift topography in the pass area was due to rapid erosion caused by "recent disturbances".

Vaughn (1922) succeeded in tracing the San Andreas fault intermittently through San Gorgonio Pass. He states "The physiographic expression can be readily followed along Potato Canon to Oak Glen and thence a mile east of Pine Bench. Here the trace of the fault is lost from sight for nearly two miles, but is again seen on the north side of the valley at the heads of Hathaway and Potrero Canons and along the West Branch of Millard Canon. Crossing Millard Canon, it is again lost until about two miles west of Stubby Canon, where definite displacement can be seen. From Stubby Canon eastward to Cottonwood Canon the position of the San Andreas fault cannot be exactly determined."

Allen (1957) has probably conducted the most extensive mapping in the area with the specific purpose of documenting the fault location and character. He concluded that "the surface break that has been called the San Andreas fault is dying out in the vicinity of Burro Flat. This conclusion implies, of course, that displacement on the fault in this area has not been large." Allen favors the hypothesis that the nature of the fault changes from a strike-slip fault to one of major thrusting along the Banning fault from east of Potrero Canyon to west of Cottonwood Canyon. His main reasons for this seem to be an apparent change in strike of the San Andreas fault through Burro Flats together with fault plane solutions indicating that first motion along historic earthquakes east of Potrero Canyon have been predominately thrusting.

Most workers since Allen's 1957 paper have accepted his hypothesis that the San Andreas fault is characterized primarily by thrusting between Potrero Canyon and Cottonwood Canyon. The most recent mapping in the area was that of Matti and others (1985). One of the most important contributions of their mapping with respect to faulting in the area was their recognition of large and abundant landslides.

CONTROVERSY

Most geologists working in the area have agreed that the San Andreas fault is not well defined in San Gorgonio Pass. The major factors contributing to the lack of recognition of a single, through-going San Andreas fault in this area seem to be: 1) lack of rift topography from Burro Flats to Cottonwood Canyon; 2) lack of streams exhibiting right-

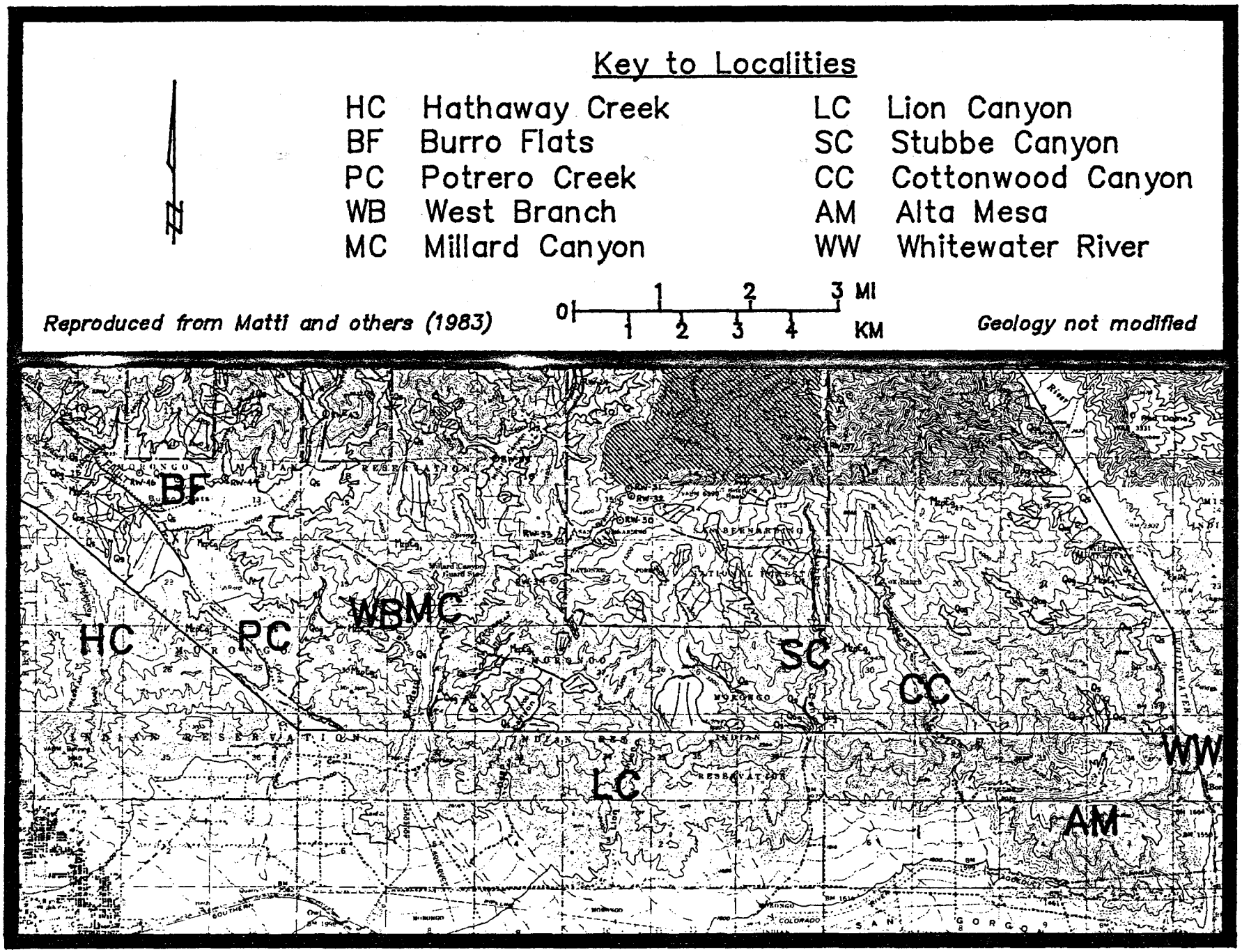

Figure 1. Location Map.

lateral offset; 3) apparent change in strike of the fault in the general area; 4) first motion indicators of historic earthquakes that suggest thrust motion rather than strike-slip motion; 5) the fact that no great earthquakes are known to have occurred along this reach of the fault; and 6) a general lack of geomorphic fault expression in young materials between Burro Flats and Cottonwood Canyon.

FAULT SETTING

San Andreas Fault

Any discussion of the San Andreas fault through San Gorgonio Pass becomes difficult to follow because of the fault's history of sequential evolution and abandonment (Matti and others, 1985). The various old and new strands have been referred to in different names by different papers. For our discussion, the San Andreas fault will be considered to be the fault as expressed to Burro Flats, then continuing along nearly the same strike to the southeast and exposed intermittently as described by Vaughn (1922) to Cottonwood Canyon, then southeast to where it merges with the Mission Creek fault. Most other work refers to the San Andreas fault in this area as that portion of the fault shown as buried from Burro Flats to its juncture with the Banning fault at Potrero Canyon, considerably farther south than where the San Andreas fault is suggested in this paper.

The fault which is considered by us to be the Banning fault includes others (Allen, 1957; Dibblee, 1964, 1982; Matti and others, 1982, 1985) Banning fault from Potrero Canyon to Cottonwood Canyon. Most geologic maps of the Banning fault in this reach show it as a thrust fault. Fault segments are usually characterized by consistent geometries and styles of motion (Rasmussen, 1981). Therefore, the term Banning fault should only refer to that fault segment from near Redlands Heights east to Cottonwood Canyon. Along this reach it is consistently a high angle reverse fault, except immediately west of Cottonwood Canyon. Immediately west of Cottonwood Canyon it appears to be completely covered by massive landslides, whose toes are currently exposed in dissected drainages. From Cottonwood Canyon to the southeast, the Banning fault of others is the same as that described as the San Andreas fault in this paper. Dibblee (1964) refers to this segment as the south branch of the San Andreas fault.

The main trace of the San Andreas fault can be easily observed in both the field and on stereoscopic aerial photographs from Point Arena (north of San Francisco) to Burro Flats (western San Gorgonio Pass area). There are only a few places over this long distance where the fault is not distinct, and these places are relatively short; usually less than 1/2 mile. However, no one has successfully traced the San Andreas fault from Burro Flats to Alta Mesa (hill east of Cottonwood Canyon and west of Whitewater Canyon, referred to as Whitewater Hill by Allen).

Vaughn (1922) noted several locations where he thought the fault existed in this reach, as described earlier. Most others have tended to change the fault strike at Burro Flats and bend it sharply to the south, where it must once again bend sharply to the east and merge with the Banning fault. However, what Allen shows as the main fault scarp through Burro Flats may actually be erosional in origin. Offset drainages, together with changes in drainage gradients and a weak lineament on aerial photographs evident across part of Potrero Canyon suggest that the fault may not change strike at Burro Flats. In addition, the landslide-debris flow deposit (Burnt Canyon Breccia of Allen, 1957) crosses the fault and tends to obscure the geomorphic expression of faulting that existed prior to the latest debris flow. Observation of the aerial photographs suggests that there have been multiple episodes of debris flows at Burro Flats. Southeast of Cottonwood Canyon the fault, commonly referred to as the Banning fault, is again obvious from the north side of Alta Mesa to the north end of the Salton Sea. Near Indio, the San Andreas fault (Banning fault of others) merges with the Mission Creek fault.

Based on recent work by Reeder and Rasmussen (1986) and that of Clark (1984), the term San Andreas fault will be used to describe the Banning fault from Cottonwood Canyon to Indio. The Banning fault should be used to describe the Banning fault (south of the San Andreas fault) from the Redlands Heights-Calimesa area to Cottonwood Canyon, where it is either offset by the San Andreas fault or merges with it. The San Andreas fault system in this area can simplistically be considered to consist of the Mill Creek fault, the Mission Creek fault, the San Andreas fault and the Banning fault. Based on detailed observations of these faults in San Gorgonio Pass, it is apparent that the major motion on the San Andreas fault has transferred between these major fault traces at different times. Matti and others (1985) provide an excellent discussion of modern and ancestral branches of the San Andreas fault in this region. The interaction of the east-west trending Pinto Mountain fault and its parallel, less well known faults has probably had a major influence on which of the three strands of the San Andreas fault system has been the "master" fault for any given time period. For purposes of this paper, the term San Andreas fault is used to refer to the fault trace that exhibits the most evidence for Holocene movement that is relatively continuous, either as a continuous fault or an en echelon feature.

The San Andreas fault (Banning fault of others) from Alta Mesa to the Indio Hills can be easily followed by the abundant vegetation growing along the fault, numerous fault scarps, springs, deflected drainages, and offset sedimentary surfaces. The fault is exposed in the canyon wall of Whitewater River and is dipping steeply to the north. Along the north side of Alta Mesa, the fault is partially obscured by landslides that have failed towards the north. However, the fault maintains a relatively consistent strike obliquely to the northwest along the north side of the nearly east-west trending drainage of Alta Mesa, to the spring and dense vegetation in the bottom of Cottonwood Canyon. Most previous workers have tried to curve the fault more to the south along the drainage bounding the north side of Alta Mesa (Allen, 1957; Dibblee, 1964, 1975; and Matti and others, 1982, 1985). However, there is evidence in the form of offset drainages, offset ridges, a strong lineament on the aerial photographs, and aligned saddles that the fault continues in a straight line to the spring in Cottonwood Canyon. The real problem of continuing the fault along this strike is that there suddenly is no evidence of the fault's existence on the west side of Cottonwood Canyon.

Banning Fault

The Banning fault is an ancestral trace of the San Andreas fault from at least the Redlands Heights area east to Potrero Canyon (Allen, 1957, Morton, 1978, Matti and others 1982, 1985). In nearly all areas west of Potrero Canyon where it is exposed, the Banning fault dips steeply to the north and is characterized by reverse movement. Allen suggested that the Banning fault continues to the west from the Redlands Heights area to the San Jacinto fault and may be an offset trace of one of the Transverse Range faults in

the San Gabriel Mountains. From San Gorgonio Canyon east to Cottonwood Canyon, Allen (1957) and most workers since then consider the Banning fault to be the modern trace of the San Andreas fault. Between Potrero Canyon and Cottonwood Canyon it has been mapped as a major thrust fault as opposed to a strike-slip fault. It merges with or is truncated by the San Andreas fault in the vicinity of Cottonwood Canyon.

Mission Creek Fault

The most recent work along the Mission Creek fault suggests that it merges with the Pinto Mountain fault west of the south fork of Whitewater River and is a major east-west fault south of the Mill Creek fault (Ehlig, 1977; Farley, 1979; Matti and others, 1985). Southeast from Whitewater River, the fault intermittently forms the southern margin of the mountain front of the Little San Bernardino Mountains and forms conspicuous scarps east of State Highway 62. From the base of the Little San Bernardino Mountains northwest of Desert Hot Springs to its merging with the San Andreas fault north of Indio, it is well defined by fault scarps and vegetational lineaments (Reeder and Rasmussen, 1986). Based on detailed trenching near Whitewater River and observation of aerial photographs, it appears that this fault has not been active since Late Pleistocene time from the Whitewater River to State Highway No. 62 (Rasmussen, 1977). It is obvious in the area immediately east of Whitewater River that at one time a great amount of movement took place along the Mission Creek fault, well into mid-Pleistocene time.

The strike of the Mission Creek fault takes a 10 degree bend just northwest of Desert Hot Springs and then continues along a relatively consistent strike through Desert Hot Springs to its merging with the San Andreas fault north of Indio. Recent trenching indicates the fault may not be active (at least in the past 6000 years) north of Mission Lakes Boulevard (Reeder and Rasmussen, 1986). Trenching approximately 3 kilometers to the southeast of that location however, found abundant evidence of recent activity (Rasmussen, 1977). Therefore, the Mission Creek fault is only active for a short distance and appears to be the dying out expression of the San Andreas fault as the Holocene trace curves to the west toward Alta Mesa.

SAN ANDREAS FAULT AT COTTONWOOD CANYON

The San Andreas fault along the north side of Alta Mesa forms a nearly continuous, straight line. It is buried in places by small landslides failing off the north face of Alta Mesa. However, its trace is indicative of a high angle fault, as evidenced by its straight path across irregular topography. It continues this straight trace northwest to the spring in Cottonwood Canyon as previously discussed. Many geologists show a buried trace of the fault within the slightly arcuate drainage north of Alta Mesa (Allen, 1957; Dibblee, 1970, 1975; Matti and others 1982, 1985). The only apparent reason for doing this is that it makes it easier to merge it with the Banning fault west of Cottonwood Canyon, south of the spring. Connecting these faults by dotted lines tends to reinforce the idea that the nearly vertical strike-slip San Andreas fault suddenly becomes a flat thrust fault within less than 1 mile.

A trench was recently excavated immediately west of Cottonwood Canyon, south of the spring. This trench was placed across the projection of the flat-lying plane of what has been mapped as the Banning fault based on exposures along the south and east flank of the hill. A nearly horizontal slip surface was encountered at a depth of 1.2 meters below the alluvial surface. This plane is the same plane described as the Banning fault just south of the trench. However, observation of this plane, together with the continuation of this plane exposed within incised drainages immediately to the south and southwest, revealed tensional features commonly associated with landslides. In fact, this plane dips to the south in some exposures (Allen, 1957).

The continuation of this flat-lying plane north of the dotted trace of the fault mapped by others north of Alta Mesa suggests that if it merges with the San Andreas fault, it would have to do so at Cottonwood Springs. However, the geomorphic expression of the San Andreas fault at Cottonwood Springs suggests that it is still a high angle fault with strike-slip indicators of movement. Therefore, in order for the Banning thrust fault, as mapped by others, to merge with the San Andreas fault, it would have to change from a flat thrust fault to a high angle strike-slip fault within 400 meters. Considering the amount of strain and amount of movement that has to take place along this fault, such an abrupt change in character over this short of a distance is unlikely given the mechanics of the materials involved.

Normally, a sudden change in strike or character of a fault is related to an intersecting fault. There are no intersecting faults in the vicinity of Cottonwood Canyon that would cause such a drastic change in fault character.

The Banning fault west of the area of controversy is a steeply dipping reverse fault and is exposed in many places with this type of geometry. West of Potrero Canyon it is an inactive fault, described as an ancestral San Andreas fault (Allen, 1957; Matti and others, 1982, 1985). It does not offset Late Pleistocene sediments to the west. It does not seem reasonable that the high angle, strike-slip fault characteristic of the San Andreas fault southeast of Cottonwood Canyon and northwest of Burro Flats, would abruptly change to a nearly flat thrust for such a short distance along the older Banning fault. Right-lateral strike-slip movement is evident at both Burro Flats and at Cottonwood Canyon. Given the forces involved with plate tectonics and the inconsistency and high degree of fracturing of the rocks within the segment between Burro Flats and Cottonwood Canyon, it is much more reasonable to continue the fault beneath the massive landslides than to change the character of the San Andreas fault. Even where the Pinto Mountain fault intersects the San Andreas fault near Pine Bench, it does not significantly change the San Andreas fault except to affect the strike.

Detailed observation of the terrain between Stubbe Canyon and Cottonwood Canyon, in the field, in trenches, and on stereoscopic aerial photographs revealed abundant evidence of very recent and on-going landsliding. At Cottonwood Springs, numerous landslides were observed on the aerial photographs and in the field. A small landslide (more than one hundred meters by approximately 300 meters) has failed to the east into Cottonwood Canyon. At least two larger landslides have failed north into Cottonwood Canyon north of the springs. In fact, the abrupt bend in Cottonwood Canyon north of the springs, from a north-south flowing drainage to an east-west flowing drainage, may have been caused by a massive landslide that failed to the northeast.

A geologic reconnaissance along the projected trace of the San Andreas fault from Stubbe Canyon to Cottonwood Canyon failed to find any in-place material that was not part of a landslide. Within this small area, the landslides numbered within the hundreds. In nearly all cases where similar landslide terrain has been observed, there has been at least one or more megalandslides which underlie and delimit the landslide terrain. Subsequently many smaller landslides develop due to the fracturing and increased infiltration of water. The larger slides can move as relatively intact blocks, which may have continuity of structure above the slide plane.

At least two megalandslides with dimensions of the order of 1.5 kilometers by 1.6 kilometers have been identified within massive granitic rocks within the Rim Forest and Running Springs area of the San Bernardino Mountains (Rasmussen, 1978, 1982). The metamorphic and igneous rocks between Millard Canyon and Cottonwood Canyon are less massive than those in the Rim Forest and Running Springs area. Nearly continuous, massive landslides were observed on the aerial photographs between these canyons and abundant, very active landslides between Millard Canyon and Cottonwood Canyon were evident in the field. The "Dry Lake" west of Stubbe Canyon described by Allen is a combination of a large landslide and faulting along the true trace of the San Andreas fault (Rasmussen, personal observation; Matti and others, 1982, 1985).

Numerous closed depressions and basins, on both a small and large scale, exist within this area. Some of the landslides have dammed drainages and have resulted in deposition of more than 30 meters of sediments west of Cottonwood Canyon. Drainage patterns between Millard Canyon and Cottonwood Canyon are characteristic of landsliding on both a normal and mega-scale.

Based on the abundant evidence for large-scale landsliding in the area where the San Andreas fault would project from Millard Canyon to Cottonwood Canyon, the windows of fault exposed within a few deeply incised drainages (Vaughn 1922; Allen 1957; and Matti and others, 1985), what appear to be fault related landslide scarps, a few offset drainages and ridges within the deeper incised drainages, and the fact that the San Andreas fault is very difficult to see where it has been overridden by landsliding (Yucaipa Ridge east of Mill Creek); it appears that the San Andreas fault may indeed continue in a nearly straight line between Burro Flats and Cottonwood Springs in a consistent high-angle strike-slip configuration. The lack of distinct geomorphic expression of faulting can be attributed to the existence of large landslides with literally thousands of smaller landslides, which have overridden the fault. The large degree of void spaces in landslides resulting from fracturing during initial movement allows a much greater amount of fault movement beneath the slide and therefore results in much less geomorphic expression than that which would be observed in a normally deposited, intact sediment or rock. Large landslides crossing the San Andreas fault between Mill Creek and Oak Glen attest to the ability of landslides to obscure surficial expressions of faulting. The recognition of pervasive landsliding in an area where active faulting is being sought is considered to be critical when attempting to delineate faulting.

CONCLUSIONS

Based on observation of fault features within landslides in similar terrain, it appears that much of the real San Andreas fault between Millard Canyon and Cottonwood Canyon may be obscured by landsliding on both a small and extremely large scale.

Landslides are very effective in obscuring rapidly moving faults and many landslides evident where one would expect the San Andreas fault to be in San Gorgonio Pass exhibited evidence of very recent movement. Good examples of other areas where the fault has been obscured or partially obscured exist along the south flank of Yucaipa Ridge, between Mill Creek and Pine Bench.

The alignment of the Kitching Peak earthquake swarm (Richter, and others, 1958) parallels the "projected trace" of the true San Andreas fault and not that of the Banning fault. This suggests a through going tectonic feature at the location indicated in this paper for the San Andreas fault. Fault plane solutions from small earthquakes can usually be interpreted for more than one type of fault geometry. If the earthquake motion records are precise enough in this area, a reevaluation of them should be made to see if a high-angle, strike-slip motion parallel to our suggested San Andreas fault might not make a suitable fault plane solution.

There appears to be little change in strike of the San Andreas fault through San Gorgonio Pass, other than at Pine Bench where it is intersected by the Pinto Mountain fault. The main trace of the San Andreas fault at Burro Flats does not appear to follow the southwesterly most ridge as suggested by Allen (1957), and Matti and others (1985), but based on small scarps, offset drainages, and drainage gradient changes continues along its trend across the ridge formed by the Burnt Canyon Breccia and across Potrero Canyon.

The San Andreas fault between Burro Flats and Cottonwood Canyon is obscured in most places by massive landsliding, but is marked by a few offset drainages, offset ridges, and in some windows incised deeply into the landslides.

We suggest that some of the mapped traces of the Banning fault between Stubbe and Cottonwood Canyons, which exhibit unusually shallow dips, may in many cases be the toe of megalandslides that have been exposed by uplift and erosion. In some of these, the source of the megalandslide may have been displaced significantly by movement along the San Andreas fault. Allen maps one of these large landslide remnants along the front of the mountains. The true Banning fault is likely to have a dip of 60 degrees or greater as is characteristic of it throughout the remainder of its reach.

Although field work to this date is limited, the evidence stated in this paper strongly suggests that the San Andreas fault through San Gorgonio Pass is a continuous feature located north of the "Banning thrust fault" and that it is not drastically different with respect to geometry or components of movement than from the San Andreas fault to the southeast or northwest.

REFERENCES CITED

Allen, C.R., 1957, San Andreas fault zone in San Gorgonio Pass,southern California: Geological Society of America Bulletin, v.68, no. 3, p. 315-350.

Clark, M. M., 1984, Map showing recently active breaks along the San Andreas fault and associated faults between Salton Sea and Whitewater River-Mission Creek, California: U.S. Geological Survey Miscellaneous Investigations Map I-1483, scale 1:24,000.

Cox, B.F., Matti, J.C., Oliver, H.W., and Zilka, N.T., 1983, Mineral resource potential map of the San Gorgonio Wilderness, San Bernardino County, California: U.S. Geological Survey Miscellaneous Field Studies Map MF-1161-C, scale 1:62,500.

Dibblee, T.W., Jr., 1964, Geologic map of the San Gorgonio Mountain quadrangle, San Bernardino and Riverside Counties, California: U.S. Geological Survey Miscellaneous Geologic Investigations Map I-431, scale 1:62,500.

Dibblee, T.W., Jr., 1975, Late Quaternary uplift of the San Bernardino Mountains on the San Andreas and related faults, in Crowell, J.C., ed., San Andreas fault in southern California, a guide to San Andreas fault from Mexico to Carrizo Plain: California Division of Mines and Geology Special Report 118, p. 127-135.

Dibblee, T.W., Jr., 1982, Geology of the San Bernardino Mountains, southern California, in Fife, D.L., and Minch, J.A., eds., Geology and mineral wealth of the California Transverse Ranges: South Coast Geological Society, Annual Symposium and Guidebook Number 10 (Mason Hill volume), p. 148-169.

Ehlig, P.L., 1977, Structure of the San Andreas fault zone in San Gorgonio Pass, southern California: Geological Society of America Abstracts with Programs, v. 9, no. 4, p. 516.

Farley, Thomas, 1979, Geology of a part of northern San Gorgonio Pass, California: California State University, Los Angeles unpublished M.S. thesis, 159 p.

Lawson, A.C., and others, 1908, The California earthquake of April 18, 1906: Carnegie Institute Publication 87, v. 1, 451p.

Matti, J.C., and Morton, D.M., 1982, Geologic history of the Banning fault zone, southern California: Geological Society of America Abstracts with Programs, v. 14, no. 4, p. 184.

Matti, J.C., Cox, B.F., Obi, C.M., Powell, R.E., Hinkle, M.E., Griscom, Andrew, and McHugh, E.L., 1982, Mineral resource potential map of the Whitewater Wilderness Study Area, Riverside and San Bernardino Counties, California: U.S. Geological Survey Miscellaneous Field Studies Map MF-1478, scale 1:24,000.

Matti, J.C., Cox, B.F., and Iverson, S.R., 1983, Mineral resource potential map of the Raywood Flat Roadless Area, San Bernardino and Riverside Counties, California: U.S. Geological Survey Miscellaneous Field Studies Map MF 1563-A, scale 1:62,500.

Matti, J.C., Morton, D.M., and Cox, B.F., 1985, Distribution and geologic relations of fault systems in the vicinity of the Central Transverse Ranges, southern California: U.S. Geological Survey Open File Report 85-365, 27 p., scale 1:24,000.

Morton, D.M., 1978, Geologic map of the Redlands 7.5' quadrangle, San Bernardino and Riverside Counties, California: U.S. Geological Survey Open-File report 78-21, scale 1:24,000.

Morton, D.M., Cox, B.F., and Matti, J.C., 1980, Geologic map of the San Gorgonio Mountain Wilderness: U.S. Geological Survey Miscellaneous Field Studies Map MF-1164-A, scale 1:62,500.

Rasmussen, G.S., 1981, San Andreas fault geometry and maximum probable earthquakes in southern California: Geological Society of America Abstracts with Programs, v. 13, no. 2, p. 102.

Rasmussen, G.S., 1982, Geologic features and rate of movement along the south branch of the San Andreas fault, San Bernardino, California, in Rasmussen, G.S., ed., Geologic hazards along the San Andreas fault system, San Bernardino-Hemet-Chino, California, field trip no. 4 of Cooper, J.D., compiler, Neotectonics in southern California: Geological Society of America, Cordilleran Section, 78th Annual Meeting, Volume and Guidebook, p. 109-114.

Rasmussen, G.S. and Associates, Inc., August 16, 1977, Engineering Geology Investigation, Lots 14-17, Pierson Boulevard, West of Palm Drive, Desert Hot Springs, California, Project No. 1230.

Rasmussen, G.S. and Associates, Inc., August 9, 1977, Engineering geology investigation of Alquist-Priolo Special Studies Zones portions of Parcel Maps 3303 and 3304, Portions of Sections 31 and 33, T1S, R3E, SBB&M, san Bernardino County, California, Project Number 1136, 30 p.

Rasmussen, G.S. and Associates, Inc., June 29, 1978, Landslide affecting sewage lift station, south of Apache Trail and Blackfoot Trail West, Rimforest, California, Project Number 1323, 13 p.

Rasmussen, G.S. and Associates, Inc., September 30, 1982, Preliminary engineering geology evaluation of slope instability, John Duckworth residence, Running Springs, California, Project Number 1475.

Reeder, W.A. and Rasmussen, G.S., 1986, Character and Holocene activity of the Mission Creek fault in the vicinity of Desert Hot Springs, Riverside County, California (this volume).

Richter, C.F., 1958, Elementary Seismology: W.H. Freeman and Company, 768 p.

Vaughn, F.E., 1922, Geology of the San Bernardino Mountains north of San Gorgonio Pass: California University Publications in Geological Sciences, v. 13, p. 319-411.

THE IMPERIAL FORMATION AT PAINTED HILL, NEAR WHITEWATER, CALIFORNIA

MICHAEL A. MURPHY
Department of Earth Sciences
University of California
Riverside, California, 92521

INTRODUCTION

In pursuit of my duties as a faculty member at the University of California, Riverside, I have used the Painted Hill area (Fig. 1) in a training exercise in field geology since the early sixties. The present contribution summarizes some of the things my collegues, students and I have learned about the area during this time. These observations are not the result of a planned or completed research program and should not be treated as such.

The rocks that I will discuss have been assigned to the Imperial Formation by most authors. Whether or not this is justified is a moot point, but there is faunal and lithologic similarity to the type Imperial, so that practice will be continued here.

The Imperial Formation in the Painted Hill area rests unconformably on the San Gorgonio igneous and metamorphic basement complex in the southern exposures and on the Coachella Fanglomerate in the northern exposures (Allen, 1957). Only the southern exposures just north of the Banning Fault are discussed here (Fig. 2). In this small area, a number of critical structural and stratigraphic relationships may be observed. These permit us to say that the formation may be divided into two members, which are present in isolated remnants of a formerly more continuous marine sandstone and breccia unit (Fig. 2). An unconformity separates a second marine sandstone and conglomerate unit from the Imperial Formation (Figs. 2 and 3). This is, in turn, overlain by non-marine conglomerates. The units above the unconformity were included in the Painted Hill Formation by Allen (1957). Significant deformation and erosion occurred between the deposition of the Imperial and the Painted Hill Formations. This is manifest in strongly angular relations between the two units and the discontinuous outcrop pattern of the Imperial.

STRATIGRAPHY

The Imperial Formation

The earliest deposits of the Imperial Formation fill the channels and low spots of the pre-Imperial surface. They are characteristically basal breccias composed almost entirely of fragments derived from the immediately underlying rock (Figs. 4 and 5). In some places, they so closely resemble the weathered basement that it is difficult to locate the contact. One such outcrop may be visited where the breccia outcrop is cut by the stream channel in area A (Figs. 2 and 3). Part of the evidence of their sedimentary origin is the shell fragments that can be found in the breccia under careful scrutiny.

The basal breccia beds are highly lenticular, very poorly sorted, cobble-sized rudites with lenses of fine and medium sandstone. Articulated mollusks

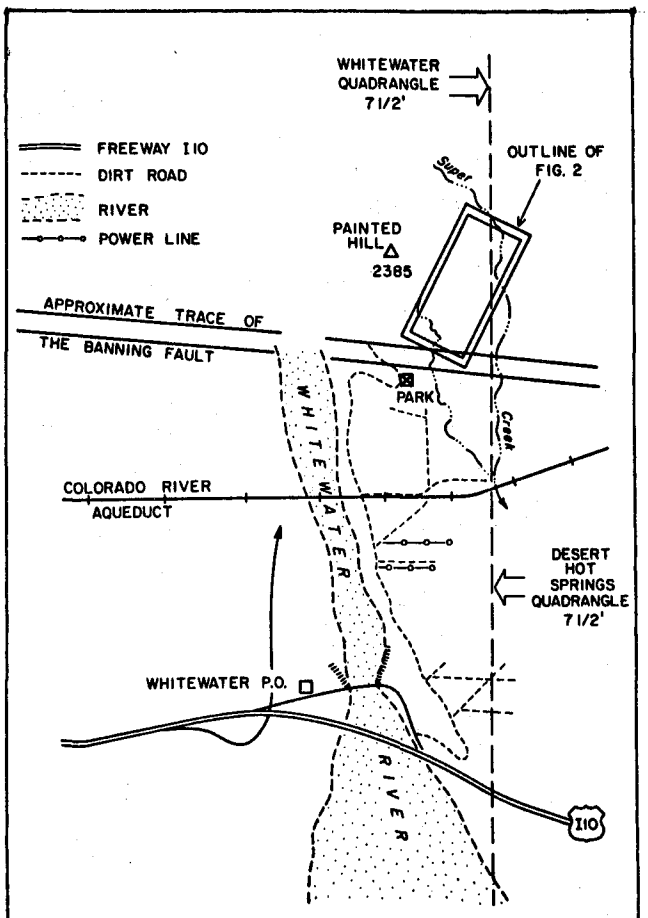

Fig. 1. Locality map.

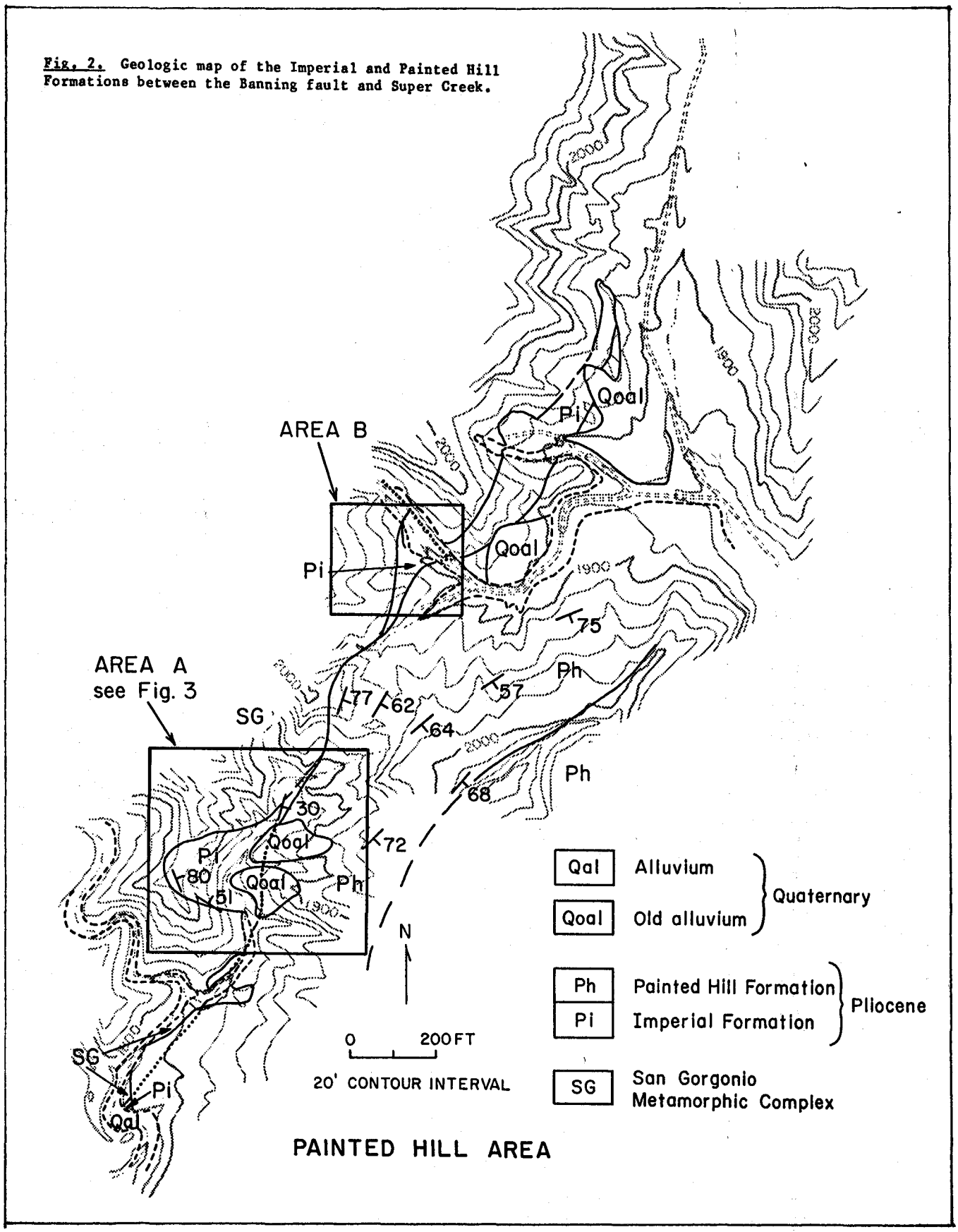

Fig. 2. Geologic map of the Imperial and Painted Hill Formations between the Banning fault and Super Creek.

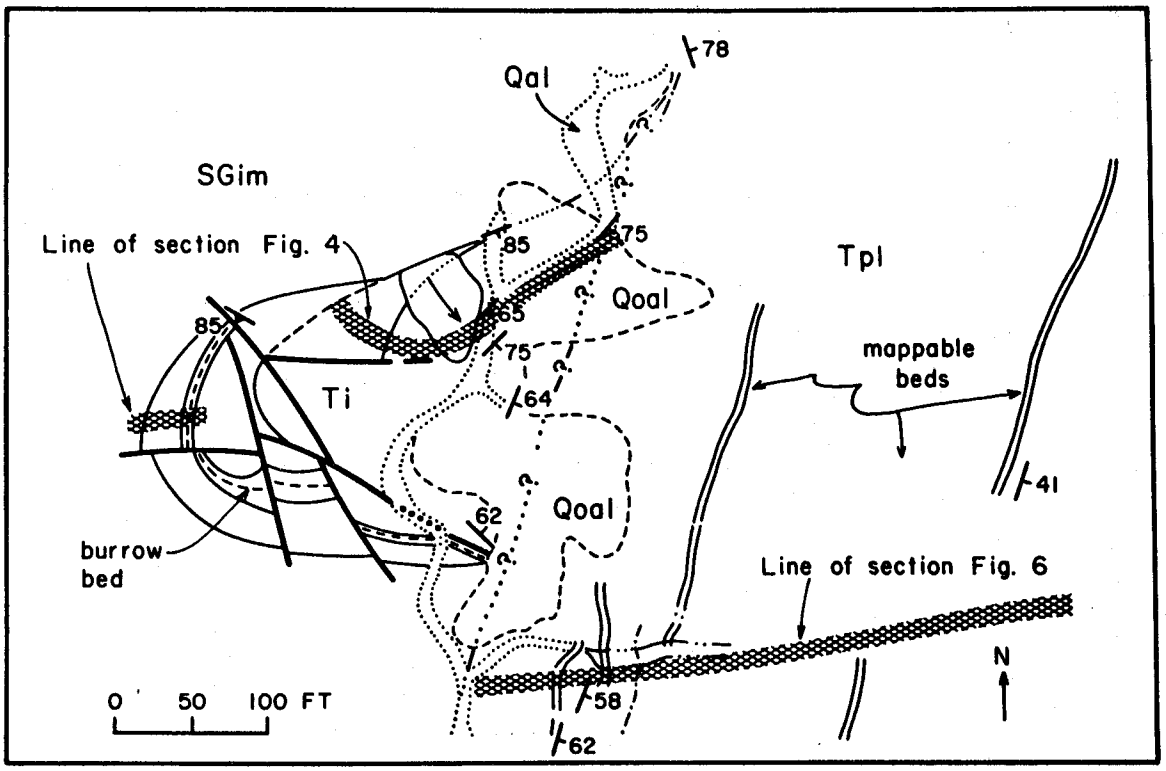

Fig. 3. Detail of structures and mappable beds in the Imperial and Painted Hill Formations in area A of Fig. 2. See Fig. 2 for legend.

are common, particularly the genera Ostrea, Pecten, Aequipecten, and Spondylus. The hermatypic coral genus, Solenastrea, and a large foram, Amphistigina, are also present, but less conspicuous. Some clypeastroid sand dollars have been seen in cross section. The angular nature of the breccia clasts and the lithologic identity with the underlying basement indicate that the unit is of local origin and the clasts have undergone little transport.

Above the basal breccia beds, a distinctive and extensive, thin, yellowish gray bed composed predominantly of reworked clay or silt burrow casts serves as a marker bed that helps unravel the structure and correlate the different outcrops of the lower member. The burrow casts occur as fragments with both ends sharply truncated, with one end rounded, free in the sediment or enclosed in claystone clasts. Their orientation is commonly parallel to the bedding although other orientations are frequent. That they are reworked is clear from their preferred orientation, broken ends and inclusion in clay clasts. They are doubtless also local in origin, perhaps representing deposits of large storms, which eroded and redeposited the material of shallow mud flats practically in situ. The burrow casts are interpreted as remnants of the burrows of the intertidal shrimp, Callianassa, as a few of them show clay pads on the walls of the burrow or their impressions on the casts. A few specimens of the barnacles Balanus concava and Boscia also came from this bed.

Above the burrow bed is a second lenticular gneiss-bearing breccia with shell fragments that is present in both areas A and B (Figs. 2, 4, and 5). This bed weathers with a pot-hole surface and is much better cemented than the adjacent beds and, therefore, topographically high. This bed is followed by a yellowish gray (5Y 7/2) micaceous silt with abundant specimens of Atrina in living position and with the most diverse fauna in the formation. Many other mollusks, barnacles, forams, ostracodes, and a large mammal have been observed. The unit is present in both areas A and B, but poorly exposed. In both areas the upper contact is normally covered, but some years, when the runoff has cleaned out the stream bed, it can be seen in contact with the upper member which consists of very light gray pebbly sandstones that grade upward through tens of feet into sandstone and lenticular conglomerate. The contact is abrupt and juxtaposes two distinctly different lithologies and the sedimentary structures are different. It may indicate a change from marine to non-marine conditions of sedimentation, but similar looking sandstones close by have yielded marine mollusks, so this interpretation is not certain. In area B, these sands and conglomerates of the upper unit also have some yellowish brown siltstone intercalations that are lithologically similar to the marine Atrina-bearing bed below.

The upper member of the Imperial contains pebbly and conglomeratic sandstone with rounded clasts of a variety of metamorphic and igneous lithologies. The rocks appear to be more closely related to the beds of the overlying Painted Hill Formation, but these beds belong to the Imperial structurally because, especially in area B, they strike at high angles to the bedding in the Painted Hill.

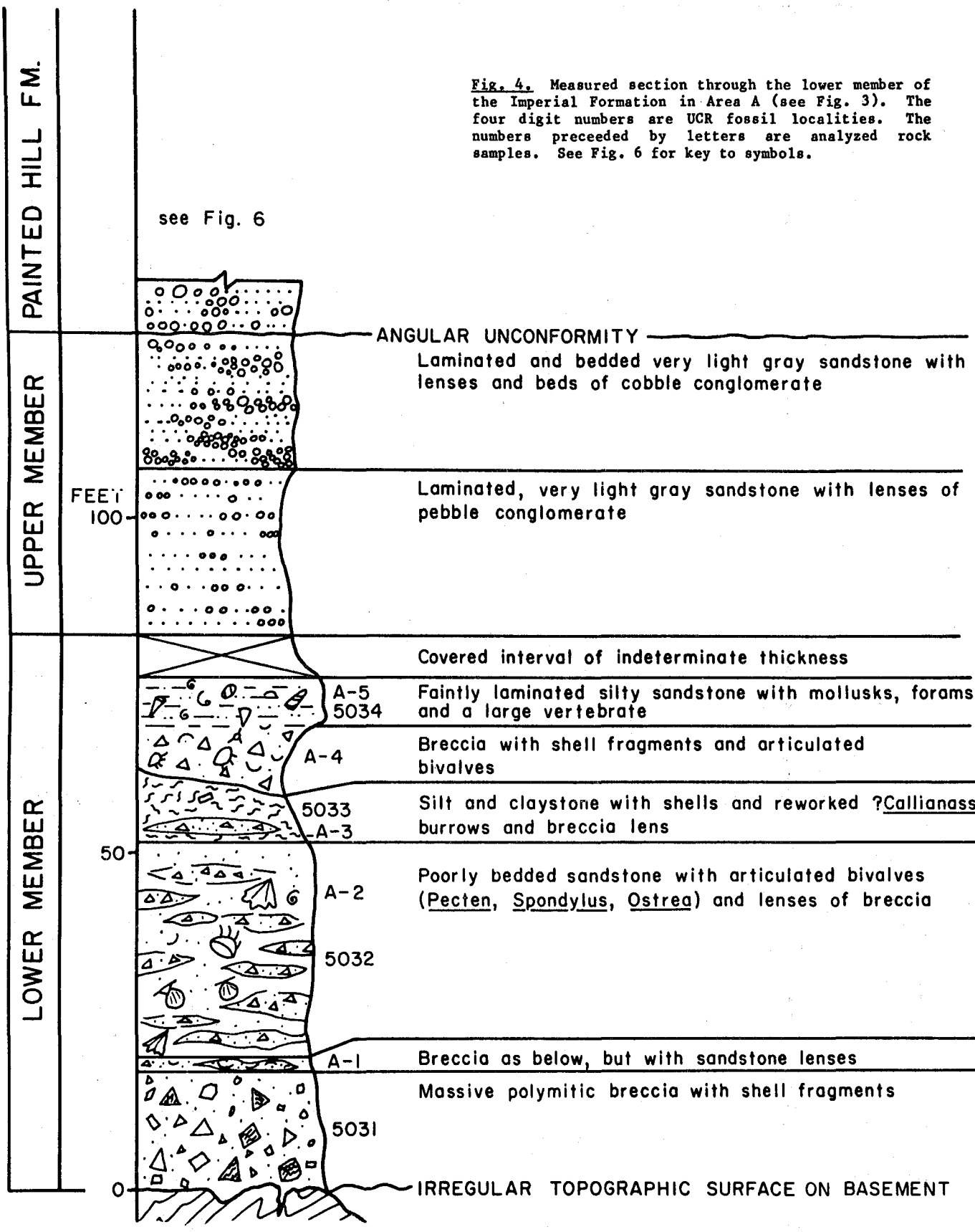

Fig. 4. Measured section through the lower member of the Imperial Formation in Area A (see Fig. 3). The four digit numbers are UCR fossil localities. The numbers preceeded by letters are analyzed rock samples. See Fig. 6 for key to symbols.

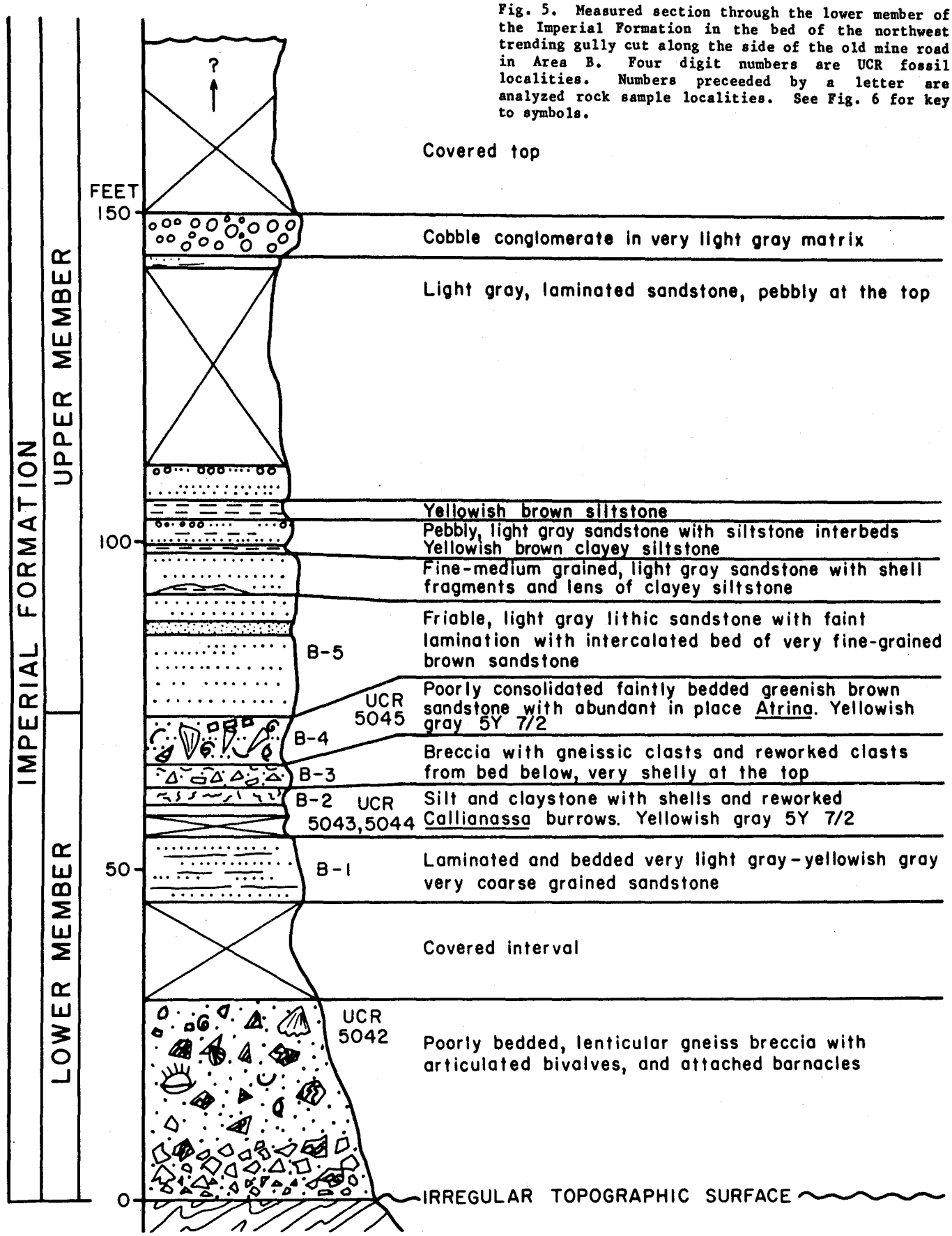

Fig. 5. Measured section through the lower member of the Imperial Formation in the bed of the northwest trending gully cut along the side of the old mine road in Area B. Four digit numbers are UCR fossil localities. Numbers preceeded by a letter are analyzed rock sample localities. See Fig. 6 for key to symbols.

The Painted Hill Formation

The Painted Hill Formation rests unconformably on the San Gorgonio complex or the Imperial Formation. However, the contact is normally hidden under old alluvial deposits and the relationship between the formations is largely inferred from the marked differences in the attitudes of the beds in the two units.

The lithology of the Painted Hill Formation contrasts strongly with that found in the lower member (up through the Atrina-bearing bed) of the Imperial, but is similar to that in the upper member (Fig. 6). The fauna in the Painted Hill is similar to that of the Imperial , but much less diverse. The rocks are predominantly very light gray, very coarse grained sandstone with lenses and beds of pebble, cobble, and boulder conglomerate. The clasts are mostly rounded and are composed of a variety of volcanic, gneissic and granitic rocks. Some of these light gray beds contain fragments of marine shells. Sandy clays and silts of yellowish brown color that pinch out northward are intercalated between the light gray beds. These beds are irregular in thickness because of an irregular substrate and from subsequent channeling of their upper parts, but they are easily traced across the area because of their yellowish brown color. Marine fossils have been found in some of them and are abundant in some of the stratigraphically lower ones.

STRUCTURE

The Painted Hill area lies at the southeastern end of the San Gorgonio igneous and metamorphic complex. It is bordered to the south by the Banning Fault, which drags the Imperial beds adjacent to the fault strongly westward along the fault. The formation strikes almost due north from the Banning Fault and dips at high angles to the east or with overturned dips to the west in the lower member. The upper member generally dips east at from 55 to 80 degrees and the dip shallows progressively eastward at higher levels in the section.

It is clear from the basal contacts of both the Imperial and the Painted Hill Formations on the San Gorgonio igneous and metamorphic complex and the structural relations between them that two unconformities are present in the sequence, one at its base and one between the Formations. It is suspected

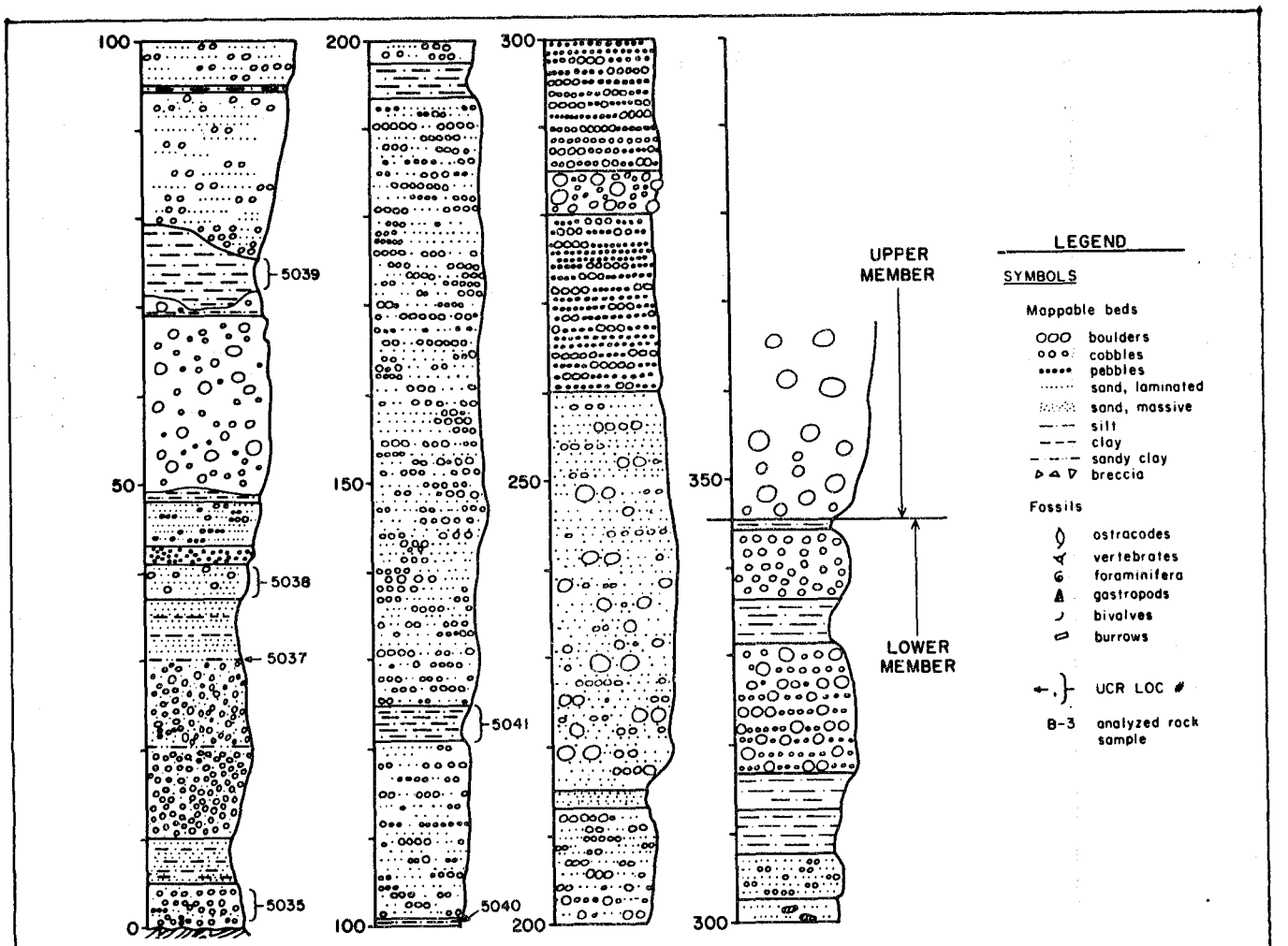

Fig. 6. Stratigraphic section of the lower member of the Painted Hill Formation in area A of Fig. 2.

that several minor discontinuities exist between most of the units in the lower member of the Imperial as well. For example, I believe that the burrow bed rests on an erosion surface because it rests directly on gneiss in places, it is discontinuous along the strike as though it were filling in the low spots in the topography, and its lithology is markedly different from that of the breccia beds below.

The Painted Hill Formation contains evidence of channeling of the marine silt and fine sand units (Fig. 6) and there is much channeling within the sand and conglomerate units. These discontinuities are not mappable for more than a few tens of feet and cannot, at present, be further evaluated.

The contact of the lower Painted Hill with a grayer, cliff-forming boulder unit, here called the upper member of the Painted Hill Formation (Tpu in Fig. 2), may also represent an unconformity, but it could as well be a progradation of the fans originating along the front of the San Bernardino Mountains.

There are minor faults in the lower member of the Imperial Formation, which are probably the result of the strong folding it has undergone. Also in area B, it is clear that the Imperial Formation is cut off by a fault extending up from the basement. There is, however, no evidence that this fault cuts the upper member (Fig. 2).

The overturning of the Imperial Formation along the contact with the San Gorgonio igneous and metamorphic complex suggests eastward thrusting somewhere just to the west within the complex. If this deformation also involved the Banning Fault, the drag of the Imperial along it could have happened at the same time. This period of deformation was apparently responsible for the folding of the lower member in area A.

AGE AND FOSSILS

Previous workers have related the faunas of the Imperial Formation to the Panamanian province and the Gulf of California faunas (Durham, 1950). If the Gulf of California opened up approximately four million years ago, as some say, then the Imperial Formation with its Gulf of California fauna should be less than four million years old. However, a basalt flow that overlies the Imperial Formation has been dated as approximately six million years old (Matti and others, 1985).

Its maximum age is constrained by a flow in the Coachella Fanglomerate that has been dated as approximately 10 million years of age (Peterson, 1975).

The fossils of the Imperial Formation have been studied by a number of different workers (Bramkamp, 1935; Durham, 1950; Hanna, 1926; Vaughn, 1917, 1922; Woodring, 1931, 1942). Several unpublished student reports are on file in the Department of Earth Sciences at the University of California, Riverside (Jefferson, 1966; Nichols, 1968).

REFERENCES

Allen, C. R. 1957, The San Andreas Fault Zone in San Gorgonio Pass, Southern California: Geological Society of America Bulletin, v. 68, p. 315-349.

Bramkamp, R. A., 1935, Stratigraphy and molluscan fauna of the Imperial Formation of San Gorgonio Pass, California (PhD Dissertation): University of California, Berkeley, 312 p.

Durham, J. W., 1950, Megascopic paleontology and marine stratigraphy: in Anderson, C. A., and others, eds., E. W. Scripps Cruise to the Gulf of California, Part II, Megascopic paleontology and marine stratigraphy, Geological Society of America Memoir 43, p. 1-216.

Hanna, G. D., 1926, Paleontology of Coyote Mountain, Imperial County, California: Proceedings of the California Academy of Sciences, Series 4, v. 14, p. 427-503.

Jefferson, G. T., 1966, The paleoecology of a "burrow horizon" in the base of the Imperial Formation at Whitewater, California (class report): University of California, Riverside, Department of Earth Sciences, 14 p.

Matti, J. C., Morton, D. M., and Cox, B. F., 1985, Distribution and geologic relations of fault systems in the vicinity of the central Transverse Ranges, southern California: U.S. Geological Survey Open File Report 85-365, 23 p.

Nichols, K. M., 1968, Structural and stratigraphic relations of the Imperial (?) and Painted Hill Formations at Whitewater, Riverside County, California (Senior Thesis): University of California, Riverside, Department of Earth Sciences, 69 p.

Peterson, M. S., 1975, Geology of the Coachella Fanglomerate: in Crowell, J. C., ed., San Andreas Fault in southern California, California Division of Mines and Geology Special Report 118, p. 119-126.

Vaughn, T. W., 1917, The reef coral fauna of Carrizo Creek, Imperial County, California and its significance: U.S. Geological Survey Professional Paper 98-T, p. 355-395.

___, 1922, Geology of the San Bernardino Mountains north of San Gorgonio Pass: University of California Publications, Bulletin of the Department of Geological Sciences, v. 13, No. 9, p. 319-411.

Woodring, W. P., 1931, Distribution and age of the marine Tertiary deposits of the Colorado Desert: Carnegie Institution of Washington, Publication 418, p. 1-25.

___, 1942, Marine mollusks from Cajon Pass, California: Journal of Paleontology, v. 16, p. 78-83.

CHARACTER AND HOLOCENE ACTIVITY OF THE MISSION CREEK FAULT IN THE VICINITY OF DESERT HOT SPRINGS, RIVERSIDE COUNTY, CALIFORNIA

Wessly A. Reeder
Gary S. Rasmussen & Associates, Inc.
1811 Commercenter W.
San Bernardino, CA 92408

Gary S. Rasmussen
Gary S. Rasmussen & Associates, Inc.
1811 Commercenter W.
San Bernardino, CA 92408

INTRODUCTION

The Mission Creek fault is a major branch of the San Andreas fault that obliquely traverses a series of coalescing Quaternary alluvial fans through the community of Desert Hot Springs in the Coachella Valley. The near surface trace of the Mission Creek fault is readily apparent as a distinct vegetational lineament, accented by modified fault scarps visible on aerial photographs flown prior to major development of Desert Hot Springs. The Mission Creek fault is generally referred to as the north branch of the San Andreas fault in the Coachella Valley and the Banning fault is referred to as the south branch. The Mission Creek and Banning faults apparently merge southeast of Desert Hot Springs in the Indio Hills.

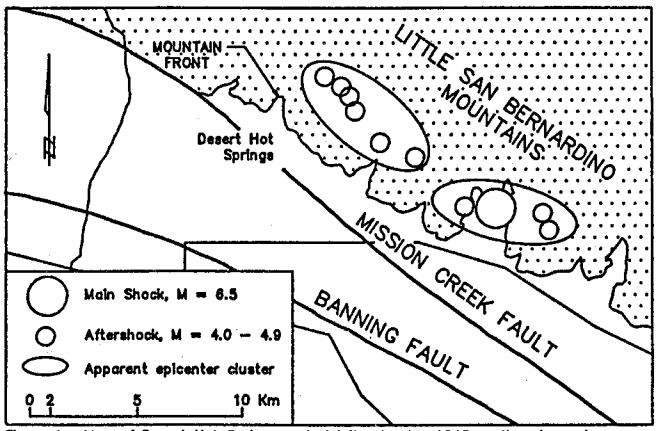

Figure 1. Map of Desert Hot Springs and vicinity showing 1948 earthquake and its aftershocks recorded between Dec. 1, 1948 and Dec. 1, 1957, modified from Richter and others (1958).

1948 DESERT HOT SPRINGS EARTHQUAKE

On December 4, 1948, a moderately large earthquake, estimated at Richter magnitude 6.5, occurred in the foothills of the Little San Bernardino Mountains, just east-southeast of Desert Hot Springs. The epicenter of this earthquake was located approximately 5 kilometers northeast of the Mission Creek fault as mapped by Proctor (1968), Dibblee (1982) and Clark (1984). Following the main shock, numerous aftershocks occurred (up to Richter magnitude 4.9) which continued for a period of approximately 10 years. Nearly all of these aftershocks were also located northeast of the mapped fault trace (Fig. 1). No evidence for any surface fault rupture was observed following the earthquake.

Richter and others (1958, page 332) attribute the apparent "displacement" of epicenters from the mapped fault trace to a northeast dipping fault plane which they calculated could be no steeper than 65 degrees. Based on an analysis of first motion data, they indicate that movement on the Mission Creek fault was oblique, being a combination of thrust slip and right-lateral slip.

A principal reason why Richter and others (1958) assumed that the 1948 earthquake occurred on the Mission Creek fault was the fact that aftershock epicenters were apparently aligned parallel to the trend of the Mission Creek fault. However, a plot of the earthquake epicenters greater than Richter magnitude 4.0 reveals two epicenter clusters: a northwestern cluster located northeast of Desert Hot Springs and a southeastern cluster located east-southeast of Desert Hot Springs. The southeast cluster includes the main shock. The alignment of the northwest cluster of events trends approximately N50°W and the alignment of the southeast cluster trends approximately N75-80°W. The alignments of both of these seismic clusters reflects the general change in trend of the mountain front. The mapped trace of the Mission Creek fault exhibits no corresponding change in strike.

Subsequent to the Richter and others (1958) analysis of the character of the Mission Creek fault, numerous trenching investigations across the Mission Creek fault have been completed in the Desert Hot Springs area in conformance with Alquist-Priolo Special Studies Zone requirements and are on file with the City of Desert Hot Springs and the County of Riverside. Typically, these investigations have revealed high-angle faulting with a relatively consistent strike. Review of trench logs indicates that the main fault is often bounded on the northeast and southwest by lower angle, apparent normal faulting with minor offsets which is often typical of strike-slip faulting as observed in trench walls. No evidence for reverse movement is evident on the trench logs. The Mission Creek fault, as indicated by the numerous trenches across its trace in the vicinity of Desert Hot Springs, seems to be characterized by strike-slip movement with very little reverse or oblique movement. It is structurally unlikely that the Mission Creek fault becomes a lower angle oblique fault at depth without any expression of reverse movement at the surface.

Apparent fault "scarps" occur in the Desert Hot Springs area which suggest a vertical component of movement. However, many of these scarps can be explained by topographically low areas right-laterally displaced along the Mission Creek fault and juxtaposed against topographically high areas. In addition, apparent fault scarps that are coincident with vegetation lineaments are often the result of denudation by both wind and water along the non-vegetated margin and aeolian deposition of sands and silts along the vegetated margin.

Rather than readily assuming that the 1948 Desert Hot Springs earthquake occurred along the Mission Creek fault at depth, it is just as reasonable to assume that it occurred along any one of the many potentially active faults in the foothills of the Little San Bernardino Mountains including the Morongo Reverse fault, Dillion Shear Zone or other related faults. Detailed geologic mapping and evaluation of fault activity is needed to better assess the role that these faults play in the neotectonic setting of the region.

HOLOCENE SEISMICITY

Trench logs documenting numerous subsurface investigations across the Mission Creek fault in the Desert Hot Springs area indicate fault rupture to within a few feet of the ground surface (Rasmussen, August 16, 1977; November 21, 1977; January 30, 1978; January 15, 1979; January 18, 1979; April 17, 1979; September 28, 1984). Most of the upper sediments observed in the trenches were considered to be less than 2,000 years in age, primarily based on surface geomorphology (current depositional environments) and soil development. Although recurrence intervals have not, as yet, been established for the Mission Creek fault in Desert Hot Springs, fault rupture to within a few feet of the ground surface, together with the young geomorphic expression of faulting, suggests that recurrence intervals are probably less than 500 years.

The Mission Creek fault can be observed on early aerial photographs as a semi-continuous lineament through Desert Hot Springs to a point just northwest of Desert Hot Springs. Northwest of this point to the mountain front of the Little San Bernardino Mountains near the mouth of White House Canyon, the Mission Creek fault is mapped as a buried fault trace (Proctor, 1968; Dibblee, 1982).

A recent subsurface investigation across the projection of the lineament did not encounter faulting within 6 meters of the original ground surface (Rasmussen, January 23, 1986). A zone of abundant near vertical, calcium carbonate-filled fractures and possible slight warping of the sediments was observed in the deep trench. This zone occurs along the northwest projection of the aerial photograph lineament. Most of the filled fractures were found to trend parallel to the trend of the Mission Creek fault. The coincidence of increasingly closely spaced, calcium carbonate-filled fractures together with their well defined alignment with the known fault location to the southeast is strong evidence that the buried trace of the Mission Creek fault exists at this location.

The age of the unruptured alluvial materials at a depth of 6 meters was not known with certainty. However, based on weathering of specific clast lithologies, induration, abundance of secondary calcium carbonate and the presence of three buried paleosols, we estimate the age of these materials to be at least 6,000 years and perhaps as old as 9,000 years.

If the state of activity of the Mission Creek fault were uniform along the fault, primary fault rupture should have been encountered, in at least one of the recently excavated trenches northwest of Desert Hot Springs (Rasmussen, January 23, 1986; Leighton, June 29, 1978; Southern California Soil & Testing, December 2, 1985). Due to the fact that the sediments are probably much older than 2,000 years and may be as old as 9,000 years in the deepest trench, the fault should have been obvious. Since fault rupture was not encountered and the surface expression of faulting appears to become less and less distinct northwest of Desert Hot Springs, it appears that Holocene activity along the Mission Creek fault decreases towards the northwest.

A subsurface investigation conducted near the juncture of the Mission Creek and Pinto Mountain fault zones (Rasmussen, August 9, 1977) revealed no evidence of Holocene activity of the Mission Creek fault at that location. This suggests that the Mission Creek fault may be inactive (not having experienced surface fault rupture during Holocene time) northwest of Desert Hot Springs.

The Mission Creek fault exhibits a relatively consistent strike (approximately N45°W) through Desert Hot Springs to White House Canyon. Northwest of White House Canyon the fault is coincident with the mountain front of the Little San Bernardino Mountains and exhibits a different strike, which varies from that to the southeast by approximately 10 degrees.

A bend in the surface trace of the Mission Creek fault apparently occurs in order to accommodate the change in strike, if the fault represents a continuous structure. The change in strike of the Mission Creek fault suggests that at least two distinct fault segments exist in this area. Each segment is probably characterized by a separate fault geometry and separate earthquake history (Rasmussen, 1981).

SUMMARY

Subsurface investigations across the trace of the Mission Creek fault in Desert Hot Springs during the past 10 years suggest that the Mission Creek fault is characterized by strike-slip movement. No evidence of significant reverse movement has been documented. These studies reveal that the Mission Creek fault is relatively steeply inclined at the surface, which is in contrast to the maximum dip of 65° as proposed by Richter and others (1958, page 332). Based on this, we suggest that the 1948 Desert Hot Springs earthquake may not necessarily have occurred on the Mission Creek fault but may have occurred on any one of several, possibly related faults, within the Little San Bernardino Mountains.

The San Andreas fault is characterized along portions of its reach by fault segments which may exhibit different fault geometries and have different earthquake histories (Rasmussen, 1981). Preliminary data suggest that two such segments exist in the Desert Hot Springs area and a third along the Banning fault. The junction or boundary of the two fault segments in the Desert Hot Springs area occurs just northwest of Desert Hot Springs in the vicinity of White House Canyon.

The evidence further suggests that the Mission Creek fault is not an active feature northwest of White House Canyon. The Mission Creek fault northwest of Desert Hot Springs apparently no longer represents the main trace of the San Andreas fault in this region. Its abandonment may have

been the result of left-lateral movement along the Morongo and Pinto Mountain faults and right-lateral movement along the south branch of the San Andreas fault in San Gorgonio Pass (Rasmussen and Reeder, 1986).

REFERENCES CITED

Clark, M.M., 1984, Map showing recently active breaks along the San Andreas fault and associated faults between Salton Sea and Whitewater River-Mission Creek, California: U.S. Geological Survey Miscellaneous Investigations Series, Map I-1483, Scale 1:24,000.

Dibblee, T.W., Jr., 1982, Geologic Map of the Palm Springs (15-minute) Quadrangle, California: South Coast Geological Society, Scale: 1:62,500.

Leighton & Associates, Incorporated, June 29, 1978, Geologic and Seismic Investigation of 160-Acre Parcel (NW 1/4, Section 25, T2S, R4E), Southeast of the Intersection of Mission Lakes Boulevard and Little Morongo Road, Desert Hot Springs, County of Riverside, California, Project No. 678031-02.

Proctor, R.J., 1968, Geology of the Desert Hot Springs, Upper Coachella Valley area, California: California Division of Mines and Geology Special Report 94.

Rasmussen, Gary S., April 1981, San Andreas fault geometry and maximum probable earthquakes in southern California: in Abstracts with programs, Cordilleran Section, Geological Society of America, 77th Annual Meeting, v. 13, no. 2, p. 102.

Rasmussen, Gary S. & Associates, Inc., August 9, 1977, Engineering Geology Investigation, Portions of Parcel Maps 3303 and 3304, Sections 31 and 33, T1S, R3E, San Bernardino County, California, Project No. 1136.

Rasmussen, Gary S. & Associates, Inc., August 16, 1977, Engineerinng Geology Investigation, Lots 14-17, Pierson Boulevard, West of Palm Drive, Desert Hot Springs, California, Project No. 1230.

Rasmussen, Gary S. & Associates, Inc., November 21, 1977, Engineering Geology Investigation, 40-Acre Parcel, NW Corner, 19th Avenue and Palm View, Desert Hot Springs, California, Project No. 1255.

Rasmussen, Gary S. & Associates, Inc., January 30, 1978, Enginneering Geology Investigation, 190-Acre Parcel, Two Bunch Palms, Desert Hot Springs, California, Project No. 1256-2.

Rasmussen, Gary S. & Associates, Inc., January 15, 1979, Subsurface Engineering Geology Investigation, 2 1/2-Acre Site South of Dillon Road and West of Corkhill Road, Desert Hot Springs, California, Project No. 1412-2.

Rasmussen, Gary S. & Associates, Inc., January 18, 1979, Engineering Geology Investigation, 100-Acre Parcel, North of Dillon Road, East of Long Canyon Road, Desert Hot Springs, California, Project No. 1430.

Rasmussen, Gary S. & Associates, Inc., April 17, 1979, Engineering Geology Investigation, 30-Acre Parcel, Dillon Road, 1,341 Feet West of Corkhill Road, Desert Hot Springs, California, Project No. 1473.

Rasmussen, Gary S. & Associates, Inc., September 28, 1984, Engineering Geology Investigation of Lots 1, 2, 48 and 49, Block D, Tract 3, Immediately Southwest of the Intersection of Palm Drive and Acoma Avenue, Desert Hot Springs, California, Project No. 2066.

Rasmussen, Gary S. & Associates, Inc., January 23, 1986, Subsurface Engineering Geology Investigation of Tract 21107, NW 1/4 of Section 25, T2S, R4E, SBB&M, Desert Hot Springs, California, Project No. 2222.1.

Rasmussen, G.S., and Reeder, W.A., 1986, What Happens to the Real San Andreas Fault at Cottonwood Canyon: San Gorgonio Pass, California? (This Volume).

Richter, C.F., Allen, C.R., and Nordquist, J.M., 1958, The Desert Hot Springs earthquakes and their tectonic environment: Seismological Society of America Bulletin, v. 48, p. 315-337.

Southern California Soil & Testing, Incorporated, December 2, 1985, Report of Alquist-Priolo Geotechnical Study for Tract 21107, Northwest 1/4, Section 25, T2S, R4E, SBB&M, Riverside County, California, Project No. 8531095, Report No. 2.

SEDIMENTS ADJACENT TO A PORTION OF THE PINTO MOUNTAIN FAULT IN THE YUCCA VALLEY AREA OF SAN BERNARDINO COUNTY, CALIFORNIA

Gerald Grimes
John R. Byerly, Inc.
2230 South Riverside Avenue
Bloomington, California 92316

ABSTRACT

Three late Cenozoic sedimentary units exposed between Morongo Valley and Yucca Valley record the transition from a depositional regime dominated by low energy arkosic sedimentation to one characterized by high energy fanglomerates. It is probable that activity along the Pinto Mcuntain fault zone initiated the orogenesis which resulted in the tilting of coarse fanglomerates. The changes in the characteristic clast assemblages of the fanglomerate units suggest that source areas changed during fault development, most likely due to strike-slip fault movements.

INTRODUCTION

In the vicinity of the Pinto Mountain fault zone at the top of the grade between Morongo Valley and Yucca Valley, California, well exposed pre-Holocene sediments can be differentiated into three units. These three units were studied in order to ascertain their possible relationship with activity of the Pinto Mountain fault.

TECTONIC SETTING

Yucca Valley is located along the central portion of the Pinto Mountain fault. This fault is the northernmost of a set of west-trending, left-lateral faults which are characteristic of the eastern transverse ranges (Sonoran tectonic block of Miller and others, 1982). Within this set of west-trending faults, the more northern faults demonstrate greater displacements (Dibblee, 1968; Hope, 1969) together with more recent activity as evidenced by "faulted young alluvium and recorded seismicity" (Powell, 1982, p. 134). North of the Pinto Mountain fault, the Mojave Desert block has been deformed by late Cenozoic right-lateral strike-slip displacements (Dokka, 1983).

BASEMENT ROCKS

Within the study area, crystalline basement rocks exposed south of the Pinto Mountain fault zone are characterized by migmatitic gneiss, schist, augen gneiss, and granitic gneiss (Joshua Tree Terrane of Powell, 1982), while batholithic granitic rocks are exposed north of the fault. The granitic rocks contain varying amounts of muscovite (estimated 0-2%) and appear to be part of the two-mica Cretaceous peraluminus batholithic belt of the western Cordillera (Miller, 1981).

LATE CENOZOIC SEDIMENTS

Late Cenozoic sediments exposed south of 29 Palms Highway can be separated into three distinct units on the basis of lithology, structure, and distinctive clasts. The oldest unit is a silty arkosic sand unconformably overlain by a fanglomerate characterized by quartzite clasts, which is in fault contact with a fanglomerate characterized by basalt clasts.

Arkose

The arkose is a 700 foot thick section of well-sorted sands and minor silts (approximately 5%). Sand grains are predominantly subangular quartz with lesser amounts of both weathered and fresh feldspar grains. The majority of the unit is poorly bedded with the exception of a carbonate horizon (marl bed?) near the top of the exposed section.

Exposures of the arkose are bounded by high angle faults, which caused the wedge thus produced to dip steeply to the north. An angular unconformity between the arkose and the overlying Quartzite Clast Fanglomerate indicates tilting of the arkose occurred prior to the deposition of the fanglomerate.

Quartzite Clast Fanglomerate

The quartzite clast fanglomerate contains a wide range of grain sizes (clay to boulders), which are sorted into well-defined beds (boulders in a sand matrix, mixed sand and silt, sand, or mixed silt and clay). Although characterized by quartzite clasts, granitic and metamorphic cobbles and boulders predominate. The quartzite clasts are concentrated atop a relatively flat geomorphic surface which is marked by a three-foot thick reddish soil horizon. The quartzite has been recrystallized and many of the boulders include intrusive granitic contacts. The stratigraphic thickness of the unit is estimated to be 300 feet.

Basalt Clast Fanglomerate

The dominant clast types are granitic and metamorphic rocks, but basalt clasts distinguish this unit. The unit is moderately- to well-bedded with the

cobble-sized clasts supported by sand, silt, and clay. The characteristic clasts are a distinctive assemblage of both olivine basalt and basalt containing euhedral amphibole megacrysts up to 12 mm in length. The age of the extrusive source areas for the basalt clasts are 6 to 9 my (Neville and others, 1983). The unit is only 30 to 40 feet thick.

CONCLUSIONS

The arkose unit is interpreted to be from a mature source area of granitic and metamorphic terrain. The severe angular unconformity between the arkose and the quartzite fanglomerate plus the coarser nature of the younger units suggests that the depositional regime was rapidly altered by orogenesis.

The lack of nearby source areas for the quartzite and basalt clasts and the differences in clast assemblages between the two fanglomerates suggest that the orogenesis involved strike-slip faulting. The immediate proximity of the Pinto Mountain fault suggests that it may be responsible for a change in the nature of sedimentation and the displacement of source areas. If so, a better knowledge of the age of these sedimentary units and their source areas may aid in establishing the age of initiation of movement or renewed activity and magnitude of offsets on the Pinto Mountain fault.

REFERENCES CITED

Dokka, R.K., 1983, Displacements on late Cenozoic strike-slip faults of the central Mojave Desert: California Geology, vol. 11, p. 305-308.

Dibblee, T.W., Jr., 1968, Evidence of major lateral displacements on the Pinto Mountain fault, southeastern California (abs): Geological Society of America, Cordilleran Section, 63rd Annual Meeting, p. 322.

Hope, R.A., 1969, The Blue Cut fault, southeastern California: U.S. Geological Survey Professional Paper 650-D, p. D116-D121.

Miller, C.F., 1981, Cordilleran peraluminous granites: an ancient quartzofeldspathic source, in Howard, K.A., Carr, M.D., and Miller, D.M., Tectonic framework of the Mojave and Sonoran deserts, California and Arizona: U.S. Geological Survey Open File Report 81-503.

Neville, S.L., Schiffman, P., and Sadler, P.M., 1983, New discoveries of spinel lherzolite and garnet websterite nodules in alkaline basalts from the south-central Mojave Desert and northeast Transverse Ranges, California. Geological Society of America, Cordilleran Section (abs).

Powell, R.E., 1982, Crystalline basement terranes in the southern eastern Transverse Ranges: Geological Society of America, Cordilleran section, Field Trip Guidebook 11, p. 109-151.

FOSSIL VERTEBRATES FROM LATE PLEISTOCENE SEDIMENTARY DEPOSITS IN THE SAN BERNARDINO AND LITTLE SAN BERNARDINO MOUNTAINS REGION

George T. Jefferson
George C. Page Museum
Natural History Museum of Los Angeles County
5801 Wilshire Boulevard
Los Angeles, California 90036

ABSTRACT

The Irvingtonian/Rancholabrean Land Mammal Age boundary is a significant biochronologic marker in deposits formed during the uplift of the San Bernardino and Little San Bernardino Mountains. In conjunction with other dating techniques, late Pleistocene terrestrial vertebrate assemblages may help defing the timing of regional tectonic events. The Rancholabrean age began about 500,000 years ago with the arrival of Bison in temperate North America. Fossil vertebrate remains of this period have been recovered from four, widely separated areas wihin the region. These are the lacustrine facies of the Pinto Formation in Joshua Tree National Monument, the fluvial deposits north and east of the city of Twentynine Palms, the fluvio-lacustrine facies of the Shoemaker Gravels and fluvial deposits of Nobel's Old Alluvium in the Victorville area, and fluvio-lacustrine and alluvial deposits near Beaumont, California.

INTRODUCTION

In conjunction with other dating techniques, the age of terrestrial fossil vertebrate assemblages may provide information that will allow a better understanding of the timing of regional tectonic events. The Irvingtonian/Rancholabrean Land Mammal Age boundary is a significant biochronologic marker in deposits formed during the uplift of the San Bernardino and Little San Bernardino Mountains. Middle and early Pleistocene vertebrate fossils define the Irvingtonian Land Mammal Age (Savage, 1951) which is based on an assemblage from Irvington, California. This period began about 1.85 million years ago, within the Olduvai event of the Matuyama geomagnetic polarity epoch (Lindsay et al., 1975), and is recognized by the first appearance of Mammuthus (mammoth) in North America (exclusive of Alaska). The period ends about 500,000 years ago with the arrival of Bison (American buffalo) from Asia. The late Pleistocene, Rancholabrean Land Mammal Age (Savage, 1951) is typified by the presence of extinct species of Bison. Although the type locality in Los Angeles, California has produced radiometric dates no older than about 39,000 years (Marcus and Berger, 1984), assemblages that contain Bison and other taxa found at Rancho La Brea approach 500,000 years in age.

Fossil vertebrate remains have been recovered from four, widely separated areas of Pleistocene sedimentary deposits in the San Bernardino and Little San Bernardino Mountains region. These are (1) the lacustrine facies of the Pinto Formation in Joshua Tree National Monument, (2) the fluvial deposits north and east of the city of Twentynine Palms, (3) the fluvio-lacustrine facies of the Shoemaker Gravels and fluvial deposits of Nobel's Old Alluvium in the Victorville area, and (4) fluvio-lacustrine and alluvial deposits near Beaumont.

DISCUSSION

Pinto Basin

The late Pleistocene vertebrate remains from Pinto Basin (Table 1) were first described by Campbell and Campbell (1935). Close proximity of these fossils with a wide assortment of flaked and ground stone artifacts (Amsden, 1935), and partially permineralized archaeologic faunal debris, initially led to the assumption that the artifacts were very old. However, the fossils are now known to have weathered from the lacustrine sediments of the Pinto Formation of Scharf (1935). These sediments are locally, comformably overlain by mid-Holocene alluvial deposits that yield the artifacts and archaeologic faunal materials (Jefferson, 1973).

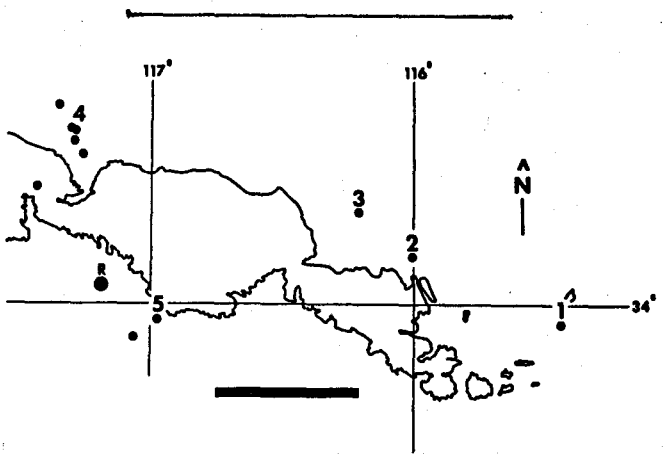

Figure 1. Rancholabrean Land Mammal Age Vertebrate Localities in the San Bernardino and Little San Bernardino Mountains Region. Explanation: 1, Pinto Basin; 2, Twentynine Palms; 3, Suprise Spring; 4, Victorville Localities; 5, Beaumont Localities; R, Redlands; solid heavy line, 1000 meter elevation contour; scale bar is 50 kilometers.

The Pinto Formation crops out in low bluffs exposed along Pinto Wash in the eastern third of Pinto Basin (Figure 1, number 1). In this area of the basin, 6 meters (m) of flat-lying lacustrine silts and sands overlie and interfinger with basalt flows to the south. Aproximately 17 m of lacustrine deposits overlain by 9 m of basalt are exposed to the east toward the base of the Coxcomb Mountains where the formation has been gently tilted and dips to the east. A thick section of cobble to boulder-sized conglomerate composed of granitic clasts which average 1 to 2 m in diameter overlies these exposures.

During deposition of the Pinto Formation, both the Coxcomb Mountains to the east and the Eagle Mountains to the south of Pinto Basin were relatively low. Little, coarse sedimentary debris is found in lake margin deposits. Subsequent, rapid uplift of these ranges which resulted in the deposition of the conglomerate that overlies the Pinto Formation is estimated at between 250 and 300 m (Scharf, 1935).

The precise age of the vertebrate fossils is not known. However, the presence of a large and small species of Equus (extinct horse), Camelops (large extinct camel) and Hemiauchenia (extinct llama) is typical of Rancholabrean age assemblages from other Mojave Desert sites (Jefferson in prep.).

Table 1. Faunal Lists for Rancholabrean Land Mammal Age Vertebrate Localities in the San Bernardino and Little San Bernardino Mountains Region. Numbers in parentheses refer to Figure 1. Institutional locality acronyms: AMNH = American Museum of Natural History, LACM(CIT) = Los Angeles County Museum California Institute of Technology, LACM = Los Angeles County Museum of Natural History, SBCM = San Bernardino County Museum.

Beaumont (5): AMNH
- Bison antiquus

Campbell Hill and Twentynine Palms Gravel Pit Localities (2): LACM 4281-83; SBCM 1.86.4, 1.86.9
- Gopherus sp.
- Megalonyx sp.
- Nothrotheriops sp.
- Thomomys sp.
- Taxidea taxus
- Smilodon cf. S. californicus
- Felis concolor
- Mammuthus sp.
- Equus sp.
- Camelops sp.
- Hemiauchenia sp.
- Odocoileus cf. O. virginianus
- Capromeryx sp.
- Bison cf. B. antiquus
- Ovis cf. O. canadensis

Hesperia North, Dean Avenue and Dean Place (4): LACM 1224
- cf. Camelops

Hesperia North, Big Bear Cutoff at Mojave River (4): LACM (field notes, T. Downs pers. comm.)
- Mammuthus sp. (specimen not in collection)

Jack Rabbit Trail Gravel Pit (5): LACM 4540
- Equus sp.

Oro Grande/George Air Force Base (4): LACM (no locality number assigned); SBCM 1.114.1 (locality number only)
- Mammut sp.

Pinto Basin (1): Department of Anthropology Univ. Calif., Riverside CaRiv 521-22; LACM(CIT) 208; LACM 3414
- Equus sp. (large)
- E. sp. (small)
- Camelops sp. (large)
- Hemiauchenia sp.

Summit Safety Rest Area (4): SBCM 1.103.80
- Plantae
- Reptilia
- Spermophilus sp. (small)
- Eutamias cf. E. merriami
- Dipodomys cf. D. merriami
- Neotoma cf. N. lepida
- N. sp.

Suprise Springs, Deadman Lake (3): LACM 3350
- Equus sp.
- Camelops sp.
- Hemiauchenia sp.
- Bison sp.

Victorville (4): LACM 3352-3353, 3498
- Equus sp. (large)

Victorville East (4): LACM 3512
- Equus sp. (large)

Victorville, El Evado Edison Road (4): SBCM 1.114.29
- Gopherus sp.
- Rodentia
- Equus sp.
- Camelidae

Victorville, Eureka Street (4): SBCM 1.114.7
- Mammuthus sp.

Victorville, Leon (4): SBCM 1.114.3
- Equus sp.

Victorville, Thorn (4): SBCM 1.114.6-.114.24
- Dipodomys sp.
- Mammuthus sp.
- Equus sp.
- Camelops sp.
- Hemiauchenia sp.

Victorville, Turner Springs (4): SBCM 1.114.24-.114.26
- Freshwater invertebrate (not listed)
- Lepus sp.

Victorville, Village Drive (4): SBCM 1.114.27-.114.28
- Mammuthus sp.
- Equus sp.
- Camelidae

Victorville West (4): LACM(CIT) 209
- Mammuthus sp.
- Equus sp. (large)

Twentynine Palms Localities

Three localities near Twentynine Palms have produced late Pleistocene fossil vertebrates. Two, Campbell Hill and the Twentynine Palms Gravel Pit (Figure 1, number 2) occur in sediments that have been uplifted along the northeast side of the Mesquite Lake Fault east of the city (Dibblee, 1968). The deposits have been gently tilted and dip an average of 30 degrees to the northeast. Here, the fossils were recovered from an approximately 300-400 m thick stratigraphic section of dissected fluviatile sands and gravels. These sediments were presumably shed off the north slope of the Little San Bernardino Mountains as the range was uplifted. The Bishop Tuff, dated at 730,000 years, has been tentatively identified in the stratigraphic section (Bacheller, 1978). It and several other volcanic ashes were ejected from the Long Valley caldera east of the central Sierra Nevada Mountains between 660,000 to 770,000 years ago (Sarna-Wocicki et al., 1980). The potential of recovering early Rancholabrean or Irvingtonian age fossils that may help refine the ages of uplift along this portion of the transverse ranges warrants further investigation.

The vertebrate remains include one of only two records in the desert region of Megalonyx (medium-sized ground sloth) as well as Capromeryx (dwarf pronghorn) (Jefferson in prep.). Many other typical Rancholabrean age taxa have been reported (Reynolds pers. comm.) including Nothrotheriops (small ground sloth), Smilodon (sabercat), Mammuthus, Equus, Camelops and Bison (Table 1).

The vertebrate fossils from the third locality near Suprise Spring (Figure 1, number 3) are also Rancholabrean in age based on the presence of Bison (Table 1). This site is located 24 kilometers northwest of Twentynine Palms in sediments uplifted along a northwest/southeast trending fault parallel to the Mesquite Lake and Bullion Faults (Dibblee, 1967).

Victorville Localities

A dozen separate vertebrate fossil localities are scattered along the west side of the Mojave River from north and west of Hesperia, through Victorville, to north of Oro Grande (Figure 1, number 4). North of Victorville, the sites occur in a 40 m thick stratigraphic section composed of interfingered lacustrine clays and silts, and fluviatile sands and gravels. South of Victorville and north of Hesperia, the exposed stratigraphic section is thinner and mainly composed of fluviatile materials. These flat-lying sediments are exposed where the Mojave River and local tributaries have dissected the eastern margin of the Victorville Fan (Weldon, 1985).

The upper portion of the Victorville Fan is separable into two formations, the older Shoemaker Gravels and the younger Nobel's Old Alluvium. Dates based on the position of the boundary between the younger Brunhes and older Matuyama geomagnetic polarity epochs (730,000 years) within the western exposures of these formations in Cajon Pass suggest a minimum age of about 600,000 years for the Shoemaker Gravels and slightly less than 500,000 years for Nobel's Old Alluvium (Weldon, 1985). These units may be younger in exposures along the Mojave River, northeast of Cajon Pass and away from the source area of the fan. However, because Bison has not been recovered from any of the Victorville area localities, their Land Mammal Age is not precisely known, and may be earliest Rancholabrean and/or late Irvingtonian.

The vertebrate taxa recovered from these deposits (Table 1) are similar to other Rancholabrean age assemblages within the desert region (Jefferson in prep.). They include Mammut (mastodon), Mammuthus, a large species of Equus, Hemiauchenia, and Camelops. A small species of Equus, typically present regionally in late Pleistocene assemblages, has not been reported.

Beaumont Localities

The early Pleistocene Baustista Beds which crop out in The Badlands south and west of Beaumont in Baustita Creek and San Timoteo Canyon have produced a vertebrate fauna of Irvingtonian age (Frick, 1921; Savage, 1951). These uplifted, tilted and locally folded fluvial and lacustrine deposits crop out in dissected exposures north and east of the San Jacinto and Claremont faults.

McDonald (1981) reports an occurrence of Bison remains from Beaumont. This single specimen was presumably recovered from alluvial deposits, possibly the Heights fanglomerate which flanks the southern margin of the San Bernardino Mountains (Allen, 1957) between Beaumont and Banning (Figure 1, number 5). A single specimen of Equus was recovered from alluvium in a gravel pit near the west end of Jack Rabbit Trail. Unfortunately, these isolated occurrences add little to an understanding of the timing of local tectonic events.

ACKNOWLEDGEMENTS

The assistance of R. E. Reynolds in the examination of records and collections of the San Bernardino County Museum is greatly appreciated. Associates at the George C. Page and Natural History Museums are kindly thanked for their comments on the manuscript.

REFERENCES CITED

Allen, C. R., 1957, San Andreas fault zone in San Gorgonio Pass, southern California. Geological Society of America Bulletin 68(3):315-350.

Amsden, C. A., 1935, The Pinto Basin artifacts. Southwest Museum Papers no. 9, p. 33-50.

Bacheller, III, J., 1978, Quaternary geology of the Mojave Desert - eastern Transverse Ranges boundary in the vicinity of Twentynine Palms, California. Thesis manuscript on file Department of Geology, University of California, Los Angeles.

Campbell, E. W. C. and W. H. Campbell, 1935, The Pinto Basin Site. Southwest Museum Papers no. 9, p. 21-31.

Dibblee, T. W. Jr., 1967, Geologic map of the Deadman Lake quadrangle San Bernardino County, California. United States Geological Survey, Miscellaneous Geologic Investigations Map I-488.

---1968, Geologic map of the Twentynine Palms quadrangle San Bernardino and Riverside Counties, California. United States Geological Survey, Miscellaneous Geologic Investigations Map I-561.

Frick, C., 1921, Extinct vertebrate faunas of the badlands of Baustita Creek and San Timoteo Can(y)on, southern California. University of California Publications Bulletin Department of Geological Sciences v. 12, p. 277-424.

Jefferson, G. T., 1973, Re-examination of the Pinto Basin Site, Joshua Tree National Monument. Society

for American Archaeology, Abstracts submitted for the meetings in San Francisco, and unpublished manuscript on file Department of Anthropology, University of California, Riverside.

---in prep., Late Pleistocene large mammalian herbivores in southern California and southern Nevada. in Whitley, D. ed., Early man in the southwest, interdisciplinary approaches (title not confirmed): University of Utah Press.

Lindsay, E. H., N. M. Johnson and N. D. Opdyke, 1975, Preliminary correlation of North American Land Mammal Ages and geomagnetic chronology. Studies on Cenozoic Paleontology and Stratigraphy in Honor of Claude W. Hibbard, University of Michigan Papers on Paleontology v. 12, p. 111-119.

Marcus, L. F. and R. Berger, 1984, The significance of radiocarbon dates for Rancho La Brea. in Martin, P. S., and Kline, R. G., eds., Quaternary extinctions, a prehistoric revolution: University of Arizona Press, Tucson, p. 159-183.

McDonald, J. N., 1981, North American bison, their classification and evolution. University of California Press, Berkeley, 316 p.

Sarna-Wojcicki, A. M., H. R. Bowman, C. E. Meyer, P. C. Russell, F. Asaro, H. Michael, J. J. Rowe, P. A. Baedecker and G. McCoy, 1980, Chemical analyses, correlations, and ages of late Cenozoic tephra units of east-central and southern California. United States Geological Survey Open File Report no. 80-231, 50 p.

Savage, D. E., 1951, Late Cenezoic vertebrates of the San Francisco Bay region. University of California Publications Bulletin Department of Geological Sciences v. 28, no. 10, p. 215-314.

Scharf, D., 1935, The Quaternary history of the Pinto Basin. Southwest Museum Papers no. 9, p. 11-19.

Weldon, R., 1985, Implications of the age and distribution of the late Cenozoic stratigraphy in Cajon Pass, southern California. in Reynolds, R. E., ed., Cajon Pass to Manix Lake, geological investigations along interstate 15: San Bernardino County Museum, Redlands, p. 59-68.

SECONDARY MINERAL ASSEMBLAGE, COPPER CONSOLIDATED LODE COPPER BASIN, SAN BERNARDINO COUNTY, CALIFORNIA

Robert E. Reynolds
Curator of Earth Sciences
San Bernardino County Museum
Redlands, California 92374

John E. Jenkins, Research Associate
Department of Earth Sciences
San Bernardino County Museum
Redlands, California 92374

INTRODUCTION

The Copper Consolidated Lode is a group of workings located in the north end of the Copper Mountains, north of Highway 62, east of Yucca Valley and west of Twentynine Palms, in San Bernardino County, California. The property consists of patented land and one unpatented claim. The property was developed to exploit copper ore and is presently held in anticipation of eventual identification and extraction of economic ore minerals.

The mineral assemblage at the mine consists of sulfides, oxides, carbonates, silicates, sulfates, a halide, a molybdate and a vanadate. The association is locally unique, and as such has academic and research interest.

BACKGROUND

The Copper Consolidated Lode is located in sections 1 and 12, Township 1 North, Range 7 East, San Bernardino Base and Meridian, as shown on the Twentynine Palms 15-minute topographic quadrangle map.

A patent survey of the workings was filed in 1913 based upon field survey performed on July 15 - 30, 1912 by Louis D. Rasor, U.S. Mineral Surveyor. Rasor described the mining claim, which then was held by J. S. Hudspeth, as the Copper Consolidated Lode, encompassing the 96 Copper; No. 2, 97 Copper; Black Quartz; Blue Quartz; Red Quartz; No. 1, 97 Copper; Copper Jack; Gray Quartz; White Quartz; and Iron lodes. At that time, improvements were described as 12 tunnels, 4 drifts, 3 shafts, 5 cuts and 1 trench, with a total property value of $9,261.00 (Office of the Surveyor General for California, 2/18/1913).

An undated reference in the offices of the Bureau of Land Management filed as Mineral Survey 5025 is probably approximately contemporary with the 1912 survey. It names the owner as H.R. Hudspeth of Los Angeles, and describes the development as shafts, drifts, cuts, and a tunnel 105 feet in length. This document states that the mineralized deposit is "between lime and porphyry" in a zone about 250 feet wide.

Today, the tunnel is approximately 200 feet in length, ending in a fracture zone of boulders. Minor mineralization can be seen in the tunnel, and no production records are known for the property. It is currently owned outright and, in part, claimed by Mark Baker of Yucca Valley. Permission of the landowner must be obtained before the property can be entered.

GEOLOGY

Mapping by Dibblee (1968) shows Copper Mountain consisting in part of plagioclase quartz gneiss with foliated biotite laminae suggestive of Prepaleozoic metasedimentary rocks. This has been intruded by Dibblee's "Older Granitic Rocks", primarily quartz monzonite, as well as diorites and gabbros. A younger suite of quartz monzonite intrudes the older plutonic rocks. Dikes of a variety of composition--quartz, simple pegmatite, felsite, and diorite--trend northwesterly through the igneous and metamorphic rocks and parallel to the trace and shear zone of the Emerson Fault (Dibblee, 1967a,b). Foliation of gneiss in northern Copper Mountain near the Copper Consolidated Lode is north to northwesterly. The claims of the Copper Consolidated Lode are laid out along a bearing of North 50° W. Elsewhere, in the southern Copper Mountains, foliation of gneiss is northeasterly.

MINERALOGY

Ore mineralization at the Copper Consolidated Lode appears to be controlled along northwest trending fractures and shear zones in the metasediments. Emplacement may have occurred during or after the suite of dike rocks or as late as the early development of the Mojave Desert province, of which the Emerson fault is a tensional structure.

The primary suite of hydrothermal ore minerals includes chalcopyrite, covellite, chalcocite, galena, sphalerite, magnetite and, present as pseudomorphs, pyrite. Gold is present in minor amounts and silver is reported (Baker, p.c. 1985), although silver halides have not been identified. Cuprite, reported to have been a primary copper source (BLM Mineral Survey 5025) is not abundant, but cuprite, tenorite, and chrysocolla are present, as are the carbonates of lead, copper and zinc.

The presence of sulfates and the carbonate/sulfate

mineral caledonite suggest limited availability of a carbonate source or carbonic acid in groundwater (Crowley, 1977; Maynard, 1984). The molybdate and vanadate radicals may have been transported from relatively distant porphyrys to react with galena and form wulfenite and vanadinite (Maynard, 1984). Late-stage silicates such as hemimorphite and quartz were deposited by groundwater under near-surface conditions. Ito (1970) also reported a translucent, almost clear coating which fluoresces greenish-yellow under shortwave ultraviolet light; he tentatively identified the occurrence as hyalite.

The minerals listed below were identified by John Jenkins, a Research Associate of the Earth Sciences Department, using visual and chemical tests. In general, the mineralization of the specimens was limited and crystals were microscopic.

Mineral Assemblage

Native Elements

Gold	Au (elemental)

Sulfides

Pyrite (pseud)	FeS_2
Chalcopyrite	$CuFeS_2$
Covellite	CuS
Chalcocite	Cu_2S
Galena	PbS
Sphalerite	$(Zn,Fe)S$

Halides

Fluorite	CaF_2

Oxides

Magnetite	$FeFe_2O_4$
Goethite	$FeO(OH)$
Hematite	Fe_2O_3
Cuprite	Cu_2O
Tenorite	CuO

Carbonates

Aragonite	$CaCO_3$
Cerussite	$PbCO_3$
Malachite	$Cu_2(CO_3)(OH)_2$
Aurichalcite	$(Zn,Cu)_5(CO_3)_2(OH)_6$

Silicates

Chrysocolla	$(Cu,Al)_2H_2Si_2O_5(OH)_4.nH_2O$
Hemimorphite	$Zn_4Si_2O_7(OH)_2 \cdot H_2O$
Quartz	SiO_2
Opal var. hyalite	$SiO_2.nH_2O$

Sulfates

Anglesite	$PbSO_4$
Brochantite	$Cu_4(SO_4)(OH)_2$
Caledonite	$Pb_5Cu_2(CO_3)(SO_4)_3(OH)_6$
Linarite	$PbCu(SO_4)(OH)_2$

Molybdates

Wulfenite	$PbMo_4$

Vanadates

Vanadinite	$Pb_5(VO_4)_3Cl$

Mineral A	unidentified

non-metallic black, dense mineral

DISCUSSION

The mineral assemblage at the Copper Consolidated Lode is similar to, but more limited than, that found in the Blue Bell (Hard Luck) mines near Baker, San Bernardino County (Crowley, 1977; Maynard, 1984). The Blue Bell and the Copper Consolidated assemblages contain a similar suite of sulfide minerals and lead/copper sulfates deposited under similar EH-pH conditions (Crowley, 1977). The Blue Bell suite, however, includes two silver halides, chlorargyrite and embolite, which have not been reported from the Copper Consolidated. Both contain wulfenite, a lead molybdate.

The vanadate radical is present at the Copper Consolidated, in contrast to the Blue Bell mines which contains the phosphate radical. The occurrence of vanadinite without pyromorphite may reflect regional distribution. Such occurrences are known from the El Dorado mine, Hexie Mountains; the Black Eagle mine, Eagle Mountains; and the War Eagle mine in the Bullion Mountains (Wright and others, 1953; Goodwin, 1957; Murdoch and Webb, 1966; Pemberton 1983).

SUMMARY

The mineral assemblage found at the Copper Consolidated Lode at Copper Mountain is generally typical of secondary enrichment minerals of copper and lead. The locality is notable for the occurrence of copper/lead sulfates, wulfenite and vanadinite in an otherwise undistinguished assemblage. The mineral specimens themselves are small to microscopic. At the present time, the locality is of most interest for the acquisition of locality suites and to species collectors and micromounters.

Through the courtesy of Mark Baker, the property owner, a representative suite of minerals from the Copper Consolidated Lode is available for study in the locality collections of the Earth Science Department of the San Bernardino County Museum in Redlands, California.

REFERENCES CITED

Crowley, J.A., 1977, Minerals of the Blue Bell mine, San Bernardino County, California: Mineralogical Record, vol. 8, no. 6, p. 494-496, 518.

Dibblee, T.W., Jr., 1967a, Geologic map of the Joshua Tree quadrangle, San Bernardino and Riverside counties, California: U.S. Geological Survey Miscellaneous Geologic Investigations Map I-516.

___, 1967b, Geologic map of the Emerson Lake quadrangle, San Bernardino County, California: U.S. Geological Survey Miscellaneous Geologic Investigations Map I-490.

___, 1968, Geologic map of the Twentynine Palms quadrangle, San Bernardino and Riverside counties, California: U.S. Geological Survey Miscellaneous Geologic Investigations Map I-561.

Goodwin, J.G., 1957, Lead and zinc in California: California Journal of Mines and Geology, vol. 53, p. 353-724.

Ito, T., 1970, written communication to J.A. Baker: Redondo Beach, February 21, 3 p.

Maynard, M., ed., 1984, The Blue Bell claims, San Bernardino County, California: Redlands, San Bernardino County Museum, 61 p.

Murdoch, J., and Webb, R.W., 1966, Minerals of California: California Division of Mines and Geology, Bulletin 189, 559 p.

Pemberton, H.E., 1983, Minerals of California: New York, Van Nostrand Reinhold Company, 591 p.

Wright, L.A., Stewart, R.M., Gay, T.E. Jr., and Hazenbush, G.C., 1953, Mines and mineral deposits of San Bernardino County, California: California Journal of Mines and Geology, vol. 49, p. 49-192.

GEOTHERMAL RESOURCE INVESTIGATIONS AT TWENTYNINE PALMS, CALIFORNIA

Jay J. Martin[1]
URS Corporation
412 W. Hospitality Ln.
San Bernardino, CA 92408

Wilfred A. Elders[2]
URS Corporation
412 W. Hospitality Ln.
San Bernardino, CA 92408

The purpose of this report is to document the use of an inexpensive exploration methodology applied to a low temperature geothermal resource in the Mojave desert. Data from numerous shallow domestic water wells were compiled and thermally anomalous zones delimited using geothermometry from water analyses. Identification of the thermal anomalies was followed by temperature gradient measurements in existing wells.

The existence of a low-temperature geothermal resource at Twentynine Palms was first suggested by the data of Bader and Moyle (1960), who reported temperatures of up to 60C in two domestic water wells. Since that time, very little information regarding the resource has appeared in the literature. Although the resource is known to many local residents the only economic application of it to date has been insignificant, limited to use in residential heat pumps (Leivas and others, 1981) and brief use as a mineral bath. In fact, many residents who rely on domestic wells tapping the geothermal water regard it as a nuisance because of the scalding wellhead temperatures and the marginal potability of the highly mineralized water.

Severe housing shortages, expansion plans of the Marine Base, and block housing grants to the County of San Bernardino are creating a favorable climate for construction of low- to moderate-income housing in the Twentynine Palms area. Apprehension about reliance on fossil fuels and costs of these fuels has kindled interest in the use of geothermal resources for space heating and cooling, an application particularly well suited to the extreme climate of the Twentynine Palms area. Interest has also developed in cascading the waste water for greenhouse and aquaculture use.

Potential applications of the geothermal resource were first discussed by Moyle (1974), who reported three water wells with temperatures up to 54C. Leivas and others (1981) discussed five wells with temperatures of up to 63C and made a preliminary delineation of the boundary of the thermal zone based on these wells. Geothermal drilling on the Marine Corps base to the north (Trexler and others, 1984) was largely unsuccessful. Although more than 2,000m of drilling was done in 7 holes, only two of these holes encountered even a marginally useful resource (54C and 68C) and these holes were greater than 286m deep. The other five holes bottomed at greater than 243m and showed disappointing temperatures of less than 35C. One of these five holes encountered a thermal gradient (1.3C/100m) that was less than the 2.5 to 3.0C/100m cited by Trexler and others (1984) as the regional geothermal gradient.

This paper describes the geologic results of an investigation conducted to ascertain the occurrence and extent of the geothermal resource and its feasibility for economic applications, particularly space heating and cooling of single and/or multiple family residences. The economic and efficiency aspects are not discussed in detail here; readers interested in the complete investigation are directed to the report by URS Corporation (1985) on file with the County of San Bernardino Department of Housing and Community Development. The geochemical database used herein appears in that report.

The initial phase of this study was a reconnaissance assessment of the geothermal potential of an area greater than 100 square miles. The primary exploration tool used in the reconnaissance phase was geochemical geothermometry, which, under certain assumptions, uses concentrations of various phases in solution to estimate the temperature at which that solution equilibrated with reservoir rocks. Ternary plots of ion ratios and maps of chemical species concentrations were also used to identify, define and characterize the geothermal resource. Most of the geochemical data used in this study was obtained from the extensive, though fragmented, water chemistry and temperature database that is available in the public domain as a result of extensive interest in potable water supplies in desert communities. This published information was supplemented with chemical, temperature and well construction data (depths, perforations, etc.) solicited from local well owners and drillers or obtained by direct sampling.

After preliminary identification of potential geothermal resource areas, a more detailed investigation of these areas involved downhole temperature logging of five existing wells. Bottom

1.Current address: Gary S. Rasmussen and Associates, 1811 Commercenter W., San Bernardino, CA 92408
2.Current address: I.G.P.P., University of California, Riverside, CA 92521

hole temperatures of 71C, sufficient for direct use applications such as space heating and cooling, were encountered in two wells less than 125m deep. Downhole temperature logs of several wells in which chemical data were available allowed calibration of the geothermometers. The results of this study and geophysical data (Biehler and Gilpin, 1983; Moyle, 1984) permit an interpretation of the origin of some of the geothermal fluids in the Twentynine Palms area.

GEOHYDROLOGIC SETTING

The Twentynine Palms area lies in the southern Mojave Desert immediately north of the Little San Bernardino Mountains. Basement rocks exposed to the northeast in the Bullion Mountains and in the Little San Bernardino Mountains consist of granitoids ranging in composition from quartz monzonite to diorite (Dibblee, 1968, figure 1). Between the basement exposures is a basin filled with Quaternary to possibly Late Tertiary-age continental deposits, chiefly alluvium, windblown sand and lacustrine sediments (Dibblee, 1968). These sediments reach a maximum thickness of perhaps 1,200m beneath Mesquite Lake (Biehler and Gilpin, 1983). Gravity data (Biehler and Gilpin, 1983; Moyle, 1984) and westerly exposures of basement rock indicate the basement/sediment interface slopes upward to the west from beneath Mesquite Lake at a relatively shallow angle.

Deformation of the basin is occurring along two distinct active fault systems. The east-west trending Pinto Mountain fault, south of Twentynine Palms, is an active fault that crosses the alluvial fans emanating from the Little San Bernardino Mountains. The northwesterly trending Mesquite Lake and West Bullion Mountain faults northeast of Twentynine Palms are part of a larger system of similarly oriented active and potentially active faults that characterize the Mojave Desert region. The Mesquite Lake fault appears as a prominent lineament on aerial photographs in very young sediments and is thought to be active. Sense of motion on this fault appears to be oblique-slip; the minor vertical component is opposite in different parts of the basin (John Foster, pers. comm., 1985). The West Bullion Mountain fault has little or no expression in older alluvium and is probably an older, inactive fault. The West Bullion Mountain fault has been shown on the basis of seismic refraction to have a significant dip-slip component with the upthrown block to the east (Biehler and Gilpin,1983).

The Pinto Mountain and Mesquite Lake faults are effective barriers to groundwater movement (Department of Water Resources, 1984; Moyle, 1984) and divide the basin into three hydrologic subbasins. The highest groundwater elevations occur south of the Pinto Mountain fault in the alluvial fans draining the Little San Bernardino Mountains. Runoff from these mountains appears to be a significant source of recharge to the area due to the much greater precipitation reaching the mountains compared with the amount that reaches the desert floor. This basin has the highest quality groundwater in the area and is the major source of municipal water. North of the Pinto Mountain fault water quality decreases abruptly for several reasons, including longer groundwater residence time and evaporation in the discharge area at Mesquite Lake. Data from Department of Water Resources (1984) indicate that groundwater north of the Pinto Mountain fault increases in total dissolved solids and progresses from a bicarbonate-type to an acid-sulfate-type water from south to north.

Groundwater is about 73m lower on the northeast side of Mesquite Lake fault, reflecting the barrier effect of this fault. Waters here are high in dissolved solids and are considered to have the longest residence time of groundwaters in the basin. The area northeast of the Mesquite Lake fault is thus potentially the best for geothermal prospecting.

GEOTHERMOMETRY

Concentrations of specific ions can be used to calculate the temperature at which the solution equilibrated with reservoir rocks. The method uses published formulas that relate experimental solubilities to temperatures. The geothermometers used in this study are the silica and alkali (Na-Ca-K ± Mg) geothermometers. The relevant formulas can be found in Fournier (1981). Although the two geothermometers often yield different calculated temperatures when applied to the same water, the differences can be useful in interpreting the thermal history of the sample.

The silica geothermometer uses the absolute concentration of silica in a sample to estimate the equilibrium temperature. It assumes that sufficient silica exists in the reservoir rocks. Silica can exist in at least four different phases, each with a different solubility-temperature relationship. Extremely slow silica precipitation rates allow hot silica-rich waters to retain their elevated silica content and thus their geothermal signature, even after the hot waters have moved into colder rocks. But because the silica geothermometer is dependent on absolute silica concentration, it is affected by such processes as steam loss due to boiling, polymerization or precipitation of silica before or after sampling, changes in pH, and dilution by cold, low silica groundwater (Fournier, 1981). Of the five silica geothermometers applied in this study, two that yielded frequent negative temperatures were discarded. Another, quartz with maximum steam loss, yielded results considered to be invalid when applied to this low temperature resource.

The quartz with no steam loss geothermometer (Qnsl) is theoretically the most appropriate silica geothermometer in this study given the presence of the low-temperature resource (no boiling) and the probable abundance of quartz in the (granitoid) reservoir rocks. A plot of Qnsl, figure 2, shows anomalously high values ranging from about 80C to 148C in several parts of the study area. There appears to be a somewhat non-systematic or random component to the data which implies dilution or chemical problems, or alternatively, reservoir temperatures that vary widely over relatively small distances. Clearly invalid, near-freezing temperatures are obtained in the southern and central portions of the study area.

The chalcedony geothermometer (Schal) is considered to be potentially valid in this study. Calculated temperatures are uniformly lower than for Qnsl, and many invalid negative temperatures are shown in fig. 3. However, as will be shown later, Schal is

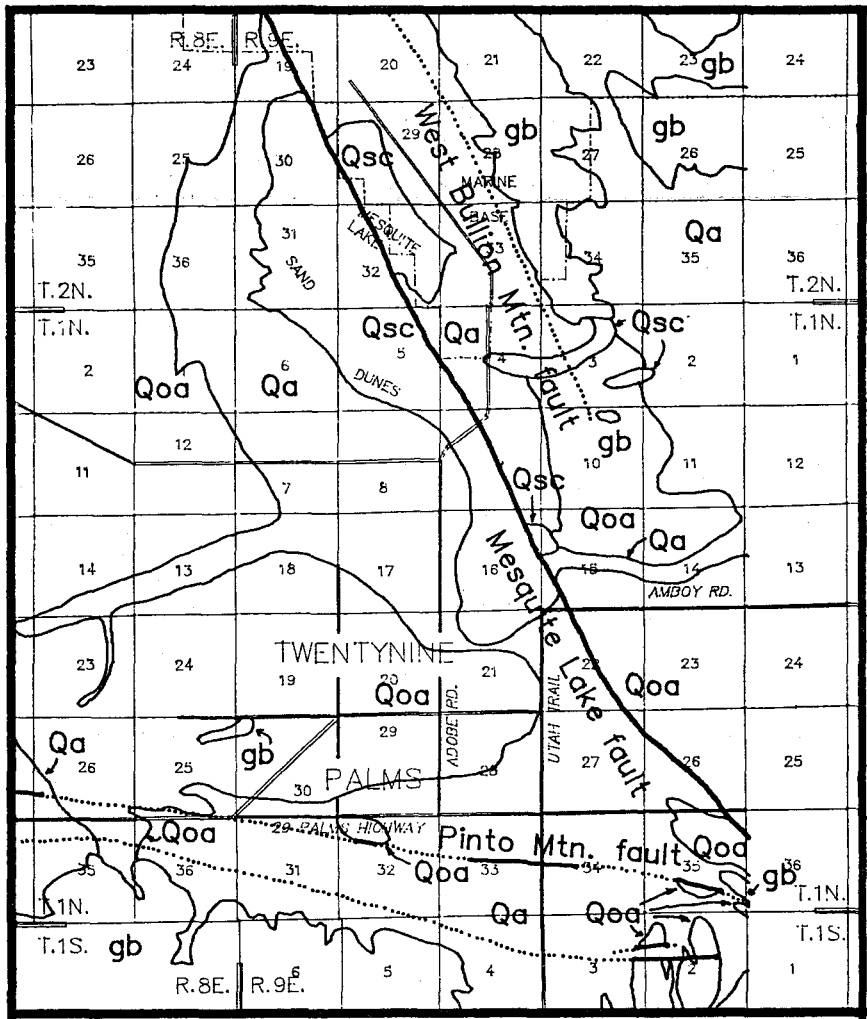

figure 1

GEOLOGIC MAP

Qsc *dune sand and clay*
Qa *younger alluvium*
Qoa *older alluvium and gravels*
gb *basement, dominantly granitoid*

Quaternary
pre-Tertiary

contact
fault, *dotted where buried or inferred*

0 1 2 KM
0 1 2 MI

generalized from Dibblee (1968)

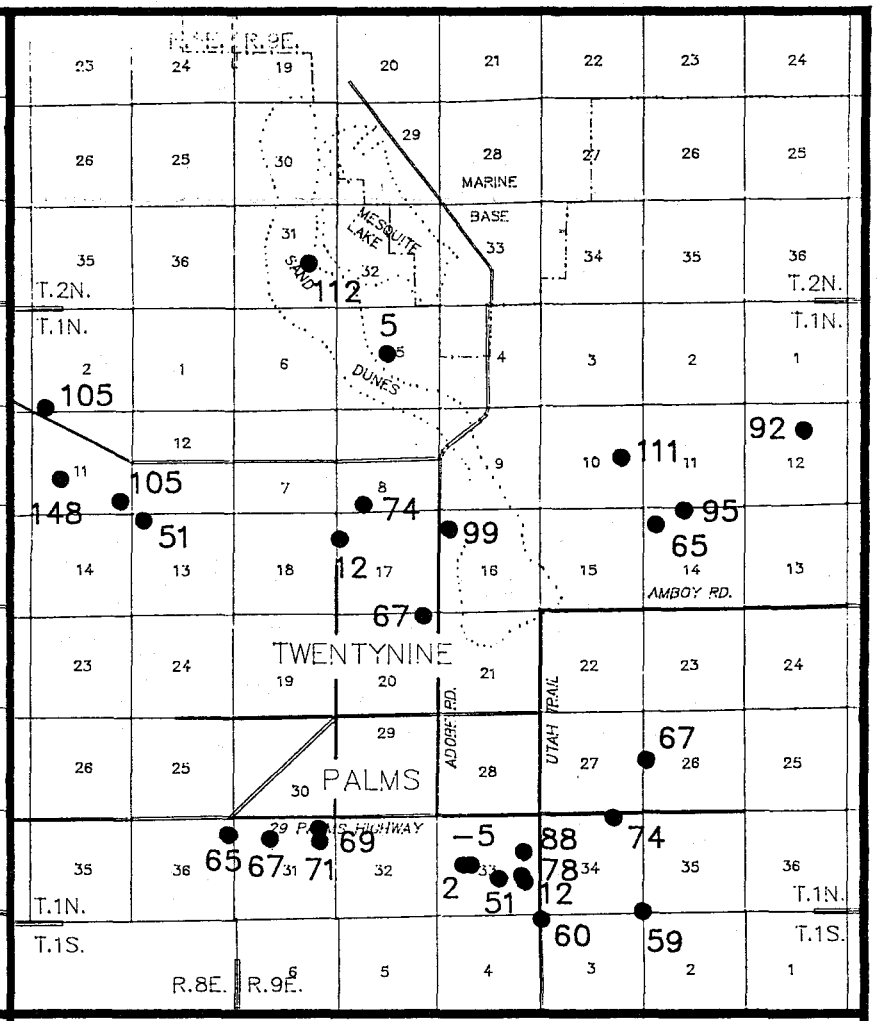

figure 2

QUARTZ WITH NO STEAM LOSS GEOTHERMOMETRY (Qnsl) (°C)

0 1 2 KM
0 1 2 MI

the best predictor of maximum wellhead temperatures in domestic water wells.

The alkali geothermometer (Fournier and Truesdell, 1973) uses ratios of Na, K, and Ca concentrations in solution determined by experiment to provide an estimate of equilibrium temperature. The method assumes sufficient feldspar in reservoir rocks, a reasonable assumption considering the granitoids underlying the area. In contrast with the silica geothermometer, the alkali geothermometer depends on ratios of ions that are not significantly affected by mixing with cold, dilute groundwaters. But the alkali geothermometer must be used with caution, especially where evaporites are suspected to exist in the reservoir. Gross geochemistry can also significantly affect temperatures yielded by the alkali geothermometer. Its use should be avoided in bicarbonate-rich waters, where pH exerts strong control on bicarbonate solubility and consequently Ca concentration.

Anomalously high alkali geothermometry values occur in several parts of the study area (fig. 4). Anomalies of 87 to 135C occur in an area of about 7 square miles in the east-central part of the study area (sections 10, 11 and 14, T1N, R9E). Anomalies of 70 to 127C occur in a small zone in the extreme west-central portion of the study area (sec. 2, 11 and 13, T1N, R8E). Isolated anomalies occur at single wells in the central (87C) and south-central (108C) portions of the study area (sec. 8 and 23, respectively, T1N, R9E).

Anomalously high geothermometry is often obtained when applying the alkali geothermometer to waters rich in magnesium (Fournier and Potter, 1979). A Mg correction to the alkali geothermometer was provided by Fournier and Potter (1979). Only seven wells in the study area show Mg concentrations high enough to meet published criteria (Fournier, 1981) for applying the Mg correction to the alkali geothermometer. Suspiciously low Mg-corrected temperatures were obtained for several of the wells in the study area, and it appears that application of the Mg correction is unnecessary in this study.

MAXIMUM MEASURED TEMPERATURES

A plot of maximum measured temperatures compiled from the literature, from measurements made during this study, and from data solicited from drillers and well owners appears in figure 5. Anomalously high temperatures of 71C, sufficient for space heating, occur in the east-central (sec. 14, T1N, R9E) and west-central (sec. 11, T1N, R8E) portions of the study area. Significant but less intense anomalies occur associated with the 71C anomalies, suggesting relatively large areas are underlain by a potentially useful resource. There is no evidence in the temperature data that the two areas underlain by the 71C resource are connected at depth, although most of the wells for which temperature data are available are less than 125m deep. The temperature data alone suggest that even relatively shallow wells could produce water hotter than 71C, as those two wells are less than 125m deep.

A third anomaly (48C) occurs in the south-central (sec. 29, T1N, R9E) portion of the study area. None of the available evidence indicates a potentially useful resource exists there, as a second well drilled within a few hundred feet of the 48C well was cold.

CALIBRATION OF GEOTHERMOMETRY WITH MEASURED TEMPERATURES

Both chemical and temperature data are available in several wells in the study area, allowing calibration of the geothermometers. Although the geothermometers are frequently inaccurate predictors of wellhead temperature, correlations between anomalous geothermometry and anomalous measured temperatures demonstrate the usefulness of the method for exploration. Qnsl and alkali geothermometry data plotted against maximum measured temperature in individual wells appear in figure 6.

The alkali geothermometer generally overestimates maximum temperatures in wells in the study area, in some cases by as much as 80C. Overestimation should be expected as the alkali geothermometer is relatively unaffected by dilution or cooling of the sample. The overestimation may be the result of cooling prior to sampling and may reflect actual reservoir temperatures at depth. It could also be the result of inaccuracy in the method. However, the wells with anomalously high alkali geothermometry generally show anomalously high measured temperatures.

Qnsl also overestimates measured temperatures. As with the alkali geothermometer, this may indicate higher reservoir temperatures at depth. The overestimation is not a result of dilution of the sample by cold, low silica groundwaters because dilution results in lowering the calculated temperature.

Based on available measured temperature-geothermometry data it appears that Schal is the best, although frequently unreliable, predictor of wellhead temperatures in shallow wells in the study area. Chalcedony is the phase that controls aqueous silica at and below temperatures near 100C in some granitic terrains (Fournier, 1981) and in basaltic terrain in Iceland (Anorsson and others, 1976). It is unlikely that significant chalcedony exists in reservoir rocks in the area. Based on available data, the alkali and Qnsl geothermometers are considered to be generally valid in this study; the high calculated temperatures probably reflect reservoir temperatures that are significantly higher than the maximum 71C measured temperatures encountered in shallow wells.

TERNARY DIAGRAMS

Ternary diagrams of molal ratios of Cl-B-HCO3 and Cl-B-SO4 can be used to characterize water geochemistry and identify the relative degree of mixing of shallow groundwater and geothermal water. The geochemical "fingerprint" can also be used to identify different populations of waters. However, ternary Cl-B-HCO3 and Cl-B-SO4 diagrams of wells in the study area did not reveal any evidence of different populations of geothermal waters. Waters from the geothermal resource areas at sec. 14 (T1N,

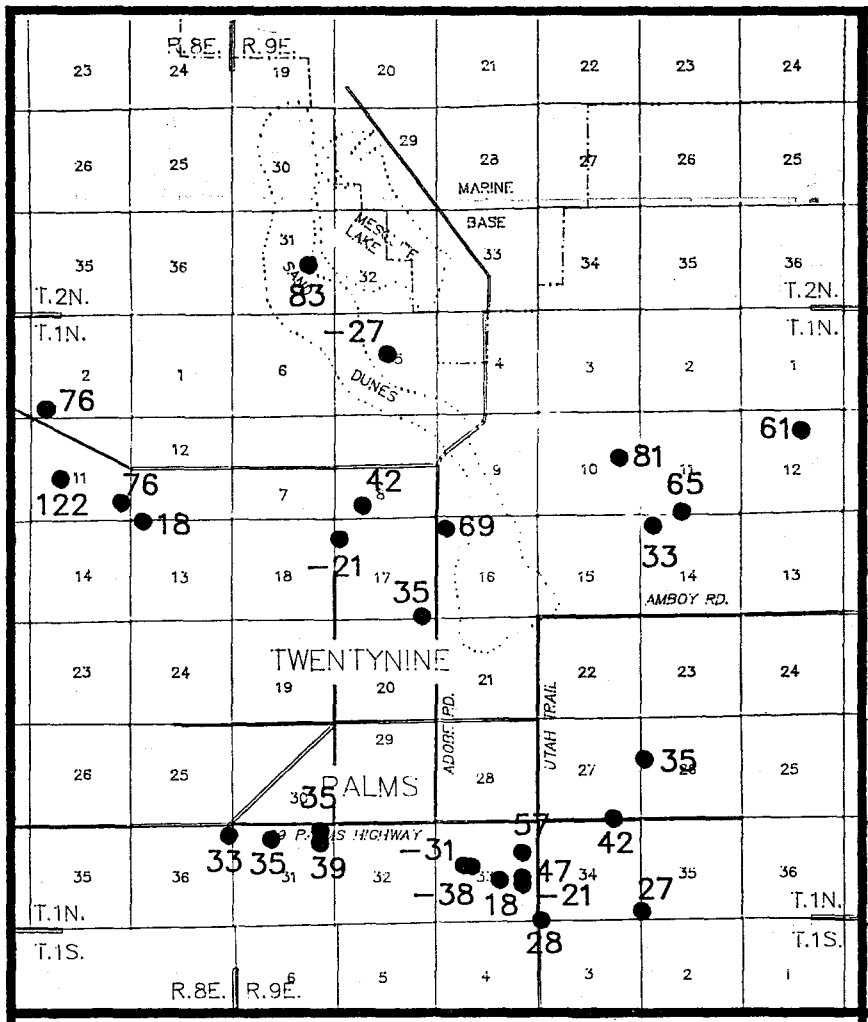

figure 3

CHALCEDONY GEOTHERMOMETRY (Schal) (°C)

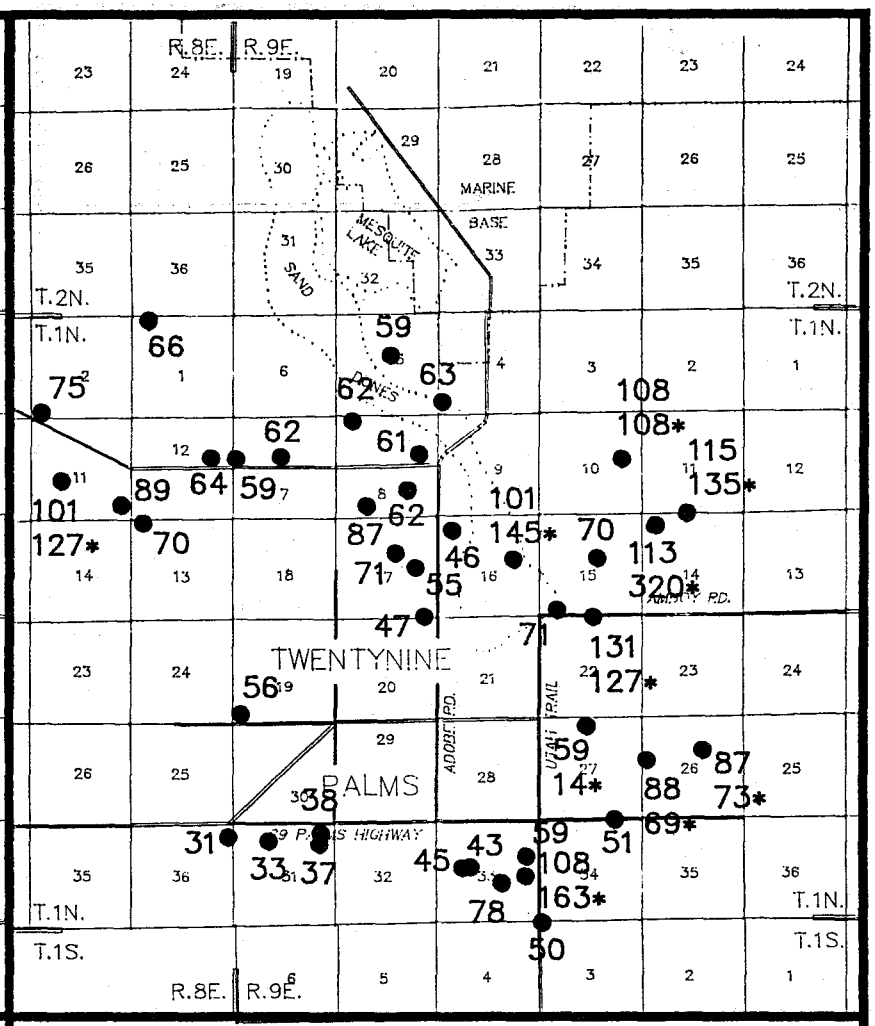

figure 4

ALKALI GEOTHERMOMETRY (°C, β = 4/3)

135* β = 1/3 (where valid)

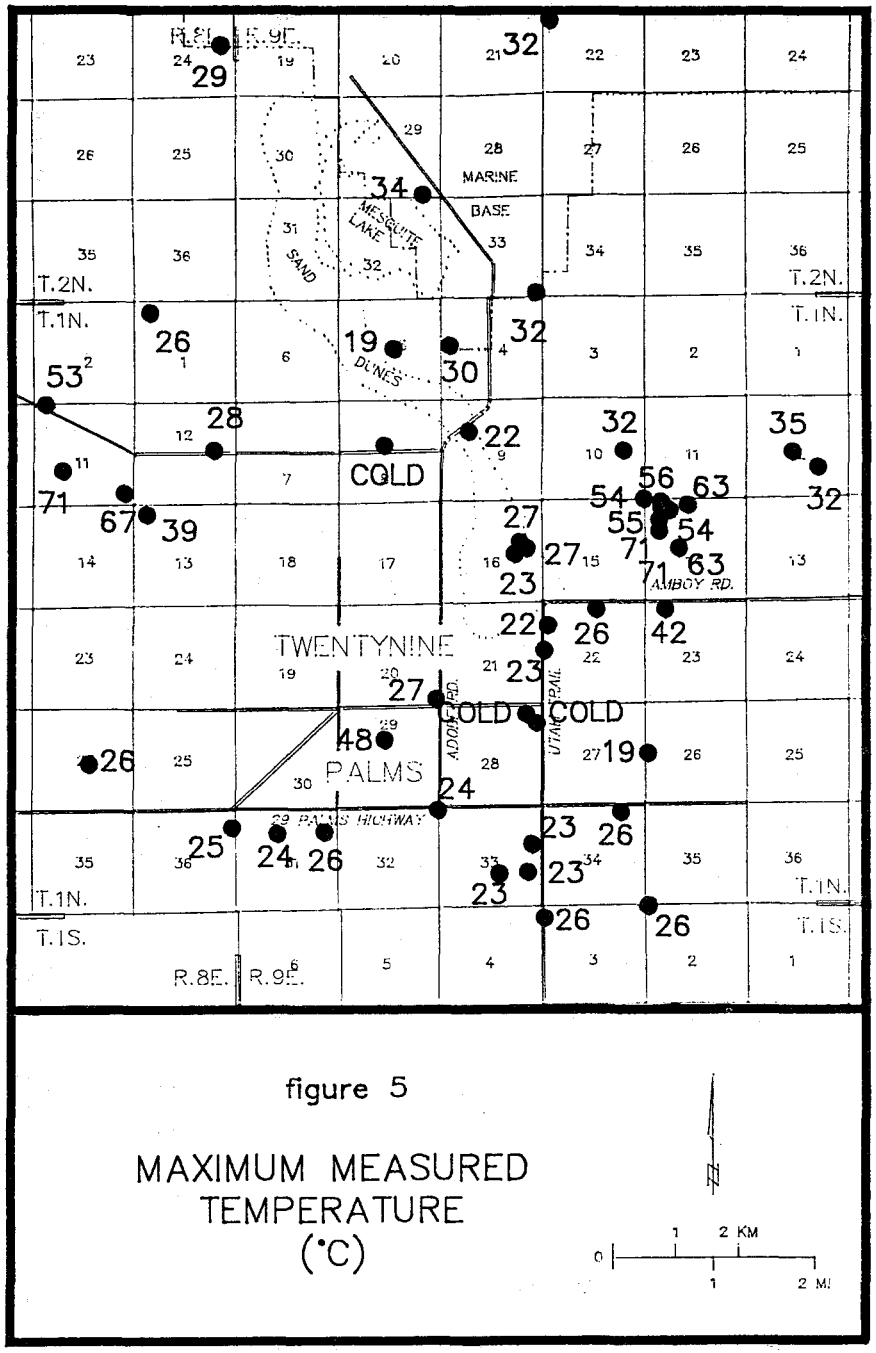

figure 5

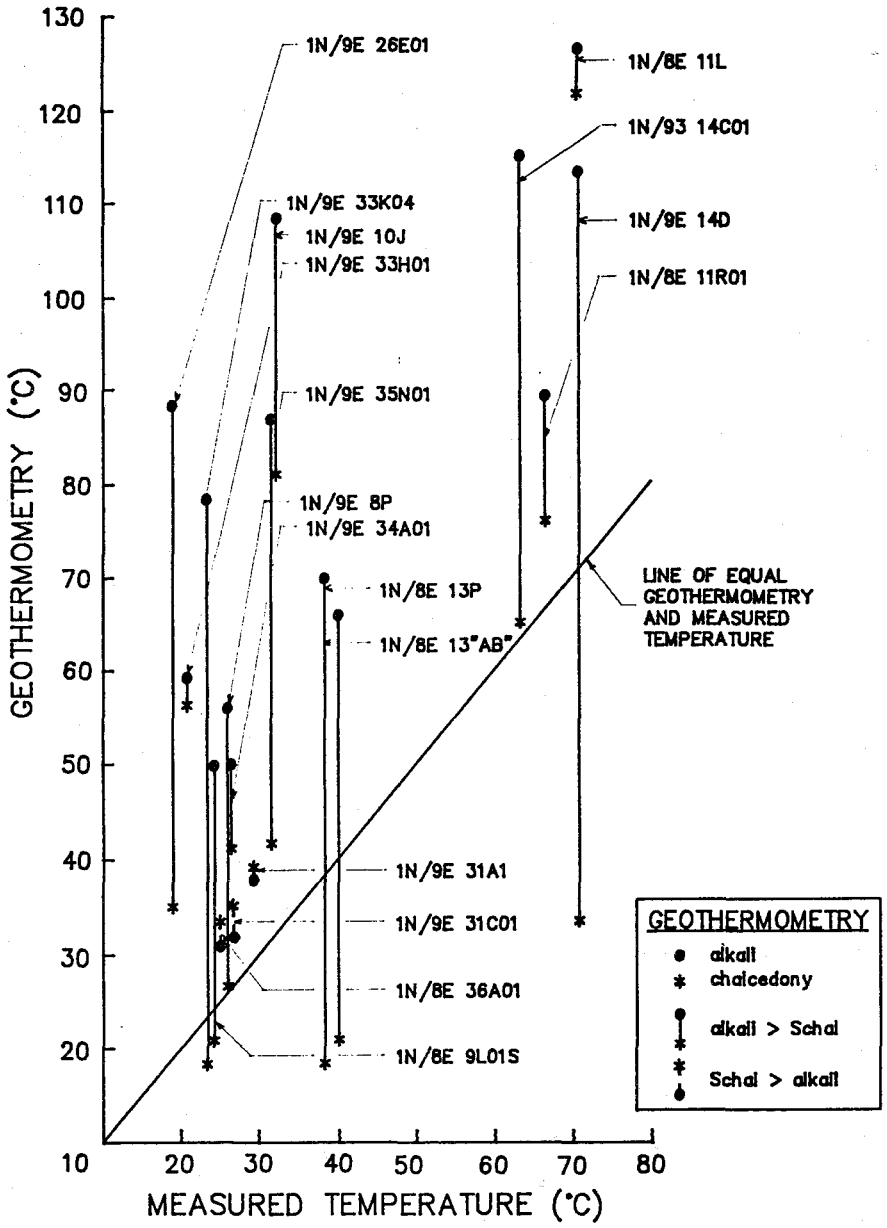

Figure 6. Calibration of geothermometry with measured temperatures.

R9E) and sec. 11 (T1N, R8E) show no consistent trends on the ternary diagrams. Some of the scatter in the ternary diagrams is due to widely varying and non-systematic Cl-B ratios, discussed briefly in the following section.

CHEMICAL CONCENTRATION MAPS

Maps of concentrations of chemical species can be useful in identifying and characterizing anomalies in geothermal reservoirs (Ellis and Mahon,1977). Most of the common groundwater constituents show increased solubilities at higher temperatures. The conservative chloride, boron and fluoride ions resist interaction with reservoir rocks and so record elevated temperatures, reflected in elevated concentrations, as a thermal water cools.

As expected, groundwaters near the Pinto Mountain fault show uniformly low concentrations of chloride, boron, and fluoride associated with a high groundwater flux in that area. Cl, B, and F increase to the north, which can be attributed to longer groundwater residence time and evaporative discharge at Mesquite Lake where groundwater is at or near the ground surface. As a result, the three constituents fail to indicate clearly defined zones where elevated species concentrations are likely to be the result of geothermal activity. However, clearly elevated Cl is associated with the section 14 (T1N, R9E) resource area.

Contrary to expectations the section 14 (T1N, R9E) resource area shows anomalously low fluoride concentrations. Three wells near the center of the high-temperature area show fluoride concentrations of 1-4 ppm in contrast with surrounding wells of 7-12 ppm. This could be due to the presence of low F reservoir rocks or unexpected relations between F solubility and temperature.

Chloride concentrations are significantly different between the section 14 (T1N, R9E) and section 8 (T1N, R8E) resource areas. The section 8 resource area has moderate to low Cl, while the section 14 resource area has distinctly high Cl. It is possible that the contrast is a result of lower groundwater residence times in the section 8 resource area due to east-flowing recharge waters originating west of the study area. It may indicate the existence of two geothermal resources of distinctly different character, one low in Cl and one high in Cl. Cl-B ratios are constant in many geothermal reservoirs. However, Cl/B plotted for wells in the study area show no general trends that would indicate the presence of two distinct reservoirs in the study area. Cl/B shows significant and sometimes extreme variability. Some of the variability may be due to elevated Cl associated with the Mesquite Lake discharge area.

DOWNHOLE TEMPERATURE LOGS

Temperature logs of five existing water wells in the east central portion of the study area were made with a custom-built thermistor-based probe and appear in fig. 7. These wells were chosen for logging due to their location within and near the section 14 resource area as identified by geochemistry and maximum measured temperatures. Four of the logged wells occur east of the Mesquite Lake fault associated with the geothermal resource at section 14. A fifth well (well #12) located immediately west of the Mesquite Lake fault was chosen for probing based on an alkali geothermometry anomaly and its location on a different structural block.

The four wells located in the identified thermal area at section 14 showed bottom-hole temperatures exceeding 54C. Two of the wells had bottom-hole temperatures of 71C (#8 and 10), and two had temperatures of 54 to 55C (#9 and 14C01). These temperatures were obtained at depths of less than 110m and suggest a significant potential for direct use geothermal applications such as space heating and cooling.

A large horizontal temperature gradient at the depth of the water table (about 79m) in the vicinity of section 14 is evident from the downhole logs. The horizontal temperature gradient between well #9 and well #8 at that depth is about 7C/100m. This suggests the source of geothermal fluids is localized and/or horizontal flow in the aquifer is restricted.

Large vertical temperature gradients suggest vertical movement of geothermal fluids is restricted. Average vertical gradients in wells #8, #10 and 14C01 are about 13C/100m, far in excess of the 1.3 to 2.7C/100m gradient for the region cited by Trexler and others (1984). The fourth well (#9) has a much smaller gradient of 6C/100m.

No significant temperature reversals are evident in the wells that were shut-in prior to logging. Well 14C01 was flowing immediately prior to logging and shows a significant reversal at the bottom of the well. This reversal is probably the result of pumping, with thermal waters drawn horizontally along primary or fracture permeability at the depth of the perforations.

Well control in the vicinity of the section 14 resource is sufficient to allow contouring of the 60C isotherm at the depth of the water table (figure 8). The area underlain by a minimum 60C resource at that depth is approximately 70 acres and is elongate in a northwest-southeast direction. The 60C isotherm was chosen because this is considered to be the threshold temperature for use in residential space heating applications.

AQUIFER PERMEABILITY AND THICKNESS

Aquifer permeability data are very limited in the vicinity of the section 14 resource. Sustained pump tests are almost never performed on domestic water wells such as those in the general area. Data from well #8 (8 inch diameter casing) indicate a drawdown of 7m at a flow rate of 85 to 100 gpm. The log also indicates that in the driller's opinion the well could supply 200gpm. A sustained flow rate of 200gpm is within the range of flow rates needed for low temperature geothermal exploitation.

Lithologies indicated on driller's logs from the vicinity of the section 14 resource were converted to specific yields (volume percent of recoverable water) with data from Johnson (1967). Average specific yield

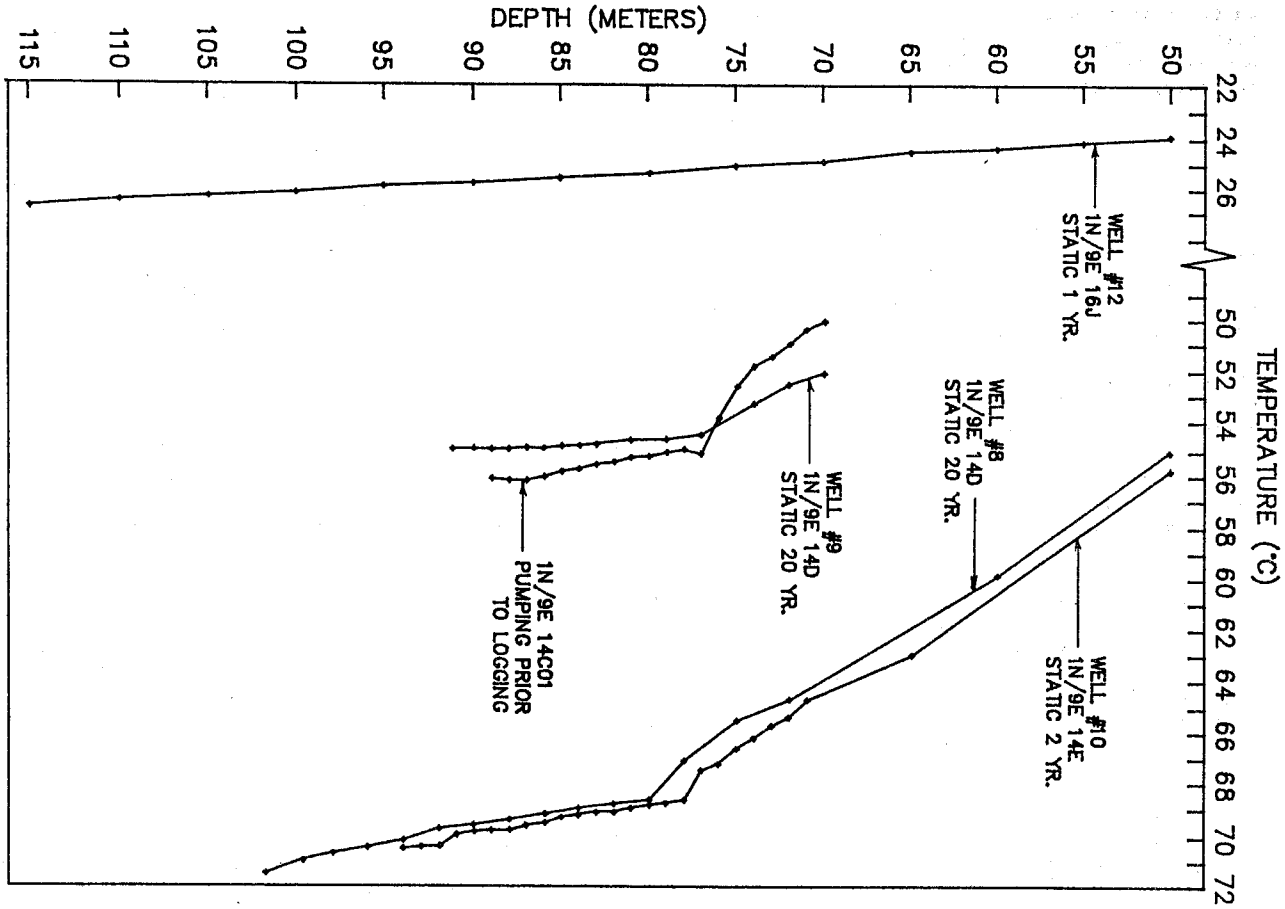

Figure 7. Downhole temperature logs.

inferred from two complete logs and one partial log (well #8) is approximately 9 percent. This value is consistent between the logs and is consistent with the flow rate and drawdown data from well #8. The specific yield of 9 percent and specific capacity of about 5800 gallons per day per foot of drawdown translate to an aquifer of poor to fair permeability.

The partial log of well #8 indicates the well bottomed in 1m of "rock" between a depth of 108 and 109 m. The "rock" is probably not a boulder, as the other well logs do not indicate boulders and the depositional environment suggested by the lithologies militates against "high energy" deposition. Seismic refraction and gravity data (Biehler and Gilpin, 1983; Moyle, 1984) suggest the presence of a bedrock high and relatively shallow bedrock in the vicinity of the section 14 resource. The existence of shallow bedrock is supported by an outcrop of biotite-rich quartz monzonite in the northeast quarter of section 10, T1N, R9E. The depth to the water table in the area is about 76m. If shallow bedrock is pervasive in the vicinity of the section 14 resource and only about 30m of saturated sediments is available, it would severely limit attempting to increase the transmissivity and flow rates by well deepening. A significant decline in the water table due to geothermal extraction could make geothermal wells in the area uneconomic and precipitate other engineering hazards such as ground subsidence.

ORIGIN OF THE GEOTHERMAL FLUIDS AT THE SECTION 14 RESOURCE

Seismic refraction data (Biehler and Gilpin, 1983) and gravity data (Biehler and Gilpin, 1983; Moyle, 1984) suggest the existence of a continuous, west-facing, southeasterly-trending basement scarp beneath sediments in the eastern portion of the study area. At the Marine Base this inferred basement topography is coincident with a buried fault mapped by Dibblee (1968) and referred to as the West Bullion Mountain fault by Biehler and Gilpin (1983). This fault appears to be responsible for the uplift of the west side of the Bullion Mountains. Dibblee (1968) does not continue the buried trace of the fault southeastward along its projection to the section 14 resource; however, the geophysical data, the thermal and geochemical anomalies, and the apparent shallow bedrock as indicated on the log of well #8 justify continuing the fault to the southeast (fig. 8). Deep circulation in the West Bullion Mountain fault is the most likely source of the geothermal fluids in the section 14 resource. Fault control of the resource is supported by the shape of the 60C isotherm on the water table, which is elongate parallel to the postulated fault.

Temperature data from exploratory wells drilled on the Marine Base led Trexler and others (1984) to conclude that, in the area of the Base Administrative Center, the West Bullion Mountain fault was not the controlling structure for the migration of geothermal

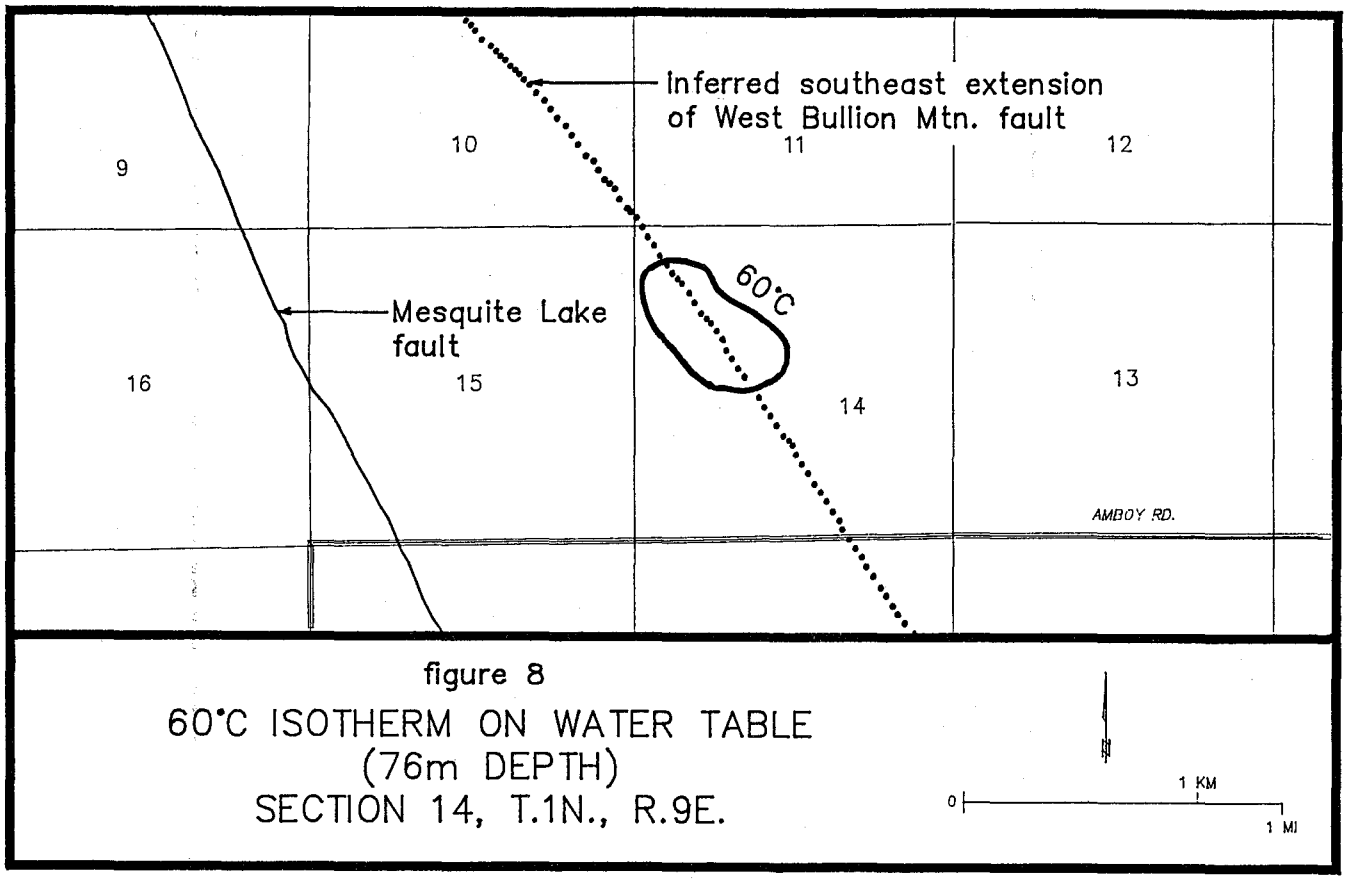

figure 8

60°C ISOTHERM ON WATER TABLE
(76m DEPTH)
SECTION 14, T.1N., R.9E.

fluids. A well drilled to a depth of 268m directly over the mapped trace of the fault in that area encountered maximum temperatures of only 33C (Trexler and others, 1984). Many faults in geothermal systems act as conduits for both recharge and discharge of geothermal fluids. It is likely that the West Bullion Mountain fault is a recharge area near the Marine Base and is a discharge area at the section 14 resource.

The downhole temperature log of well #12 (fig. 7) shows a gradient of approximately 6C/100m with a maximum temperature of 26C. This well is located over the deep portion of Mesquite basin immediately west of the Mesquite Lake fault. Downward extrapolation of the 6C/100m gradient indicates that the 71C isotherm would be reached at a depth of about 1,200m. It may be significant that Biehler and Gilpin (1983) postulate the depth to basement in the deepest part of Mesquite basin to be about 1,200m. This suggests that geothermal fluids may be emanating from the Mesquite Lake fault or West Bullion Mountain fault and flowing westward along the basement/sediment contact to the deepest part of Mesquite basin.

SUMMARY AND CONCLUSIONS

Two geothermal resource areas in the Twentynine Palms area with temperatures of 71C at depths of less than 122m have been identified on the basis of geochemical and temperature data. These areas are located within sec. 11, T1N, R8E and sec. 14, T1N, R9E. The 71C temperatures are considered to be promising for direct use applications such as residential and greenhouse space heating and aquaculture. Deeper wells would undoubtedly encounter higher temperatures. Alkali geothermometry suggests the presence at depth of a reservoir of 100C or greater.

Anomalously high alkali and silica geothermometry values generally correspond to high measured temperatures, although apparently spurious anomalies are common. The alkali and silica geothermometers appear to be useful for exploration in low-temperature geothermal systems if carefully applied and interpreted.

Four downhole temperature logs within the section 14 resource show positive temperature gradients with no significant reversals. The temperature logs indicate large vertical and horizontal temperature gradients exist in the aquifer and suggest movement of fluids is restricted.

Available data on the aquifer characteristics of section 14 are sparse. However, specific yields of approximately 9 percent and poor to fair permeability suggest flow rates of 200gpm or more are possible. This is in the range of flow rates necessary for a modest direct use development. Geophysical data and a well log suggest a relatively shallow depth to basement in the area of this resource.

In order to prove the resource and to obtain the necessary reservoir engineering data, we have

suggested the drilling and testing of three 120m deep wells in section 14. The County of San Bernardino will be funded by the California Energy Commission to carry out this activity.

The low groundwater flux in the area probably necessitates reinjection of the geothermal effluent to avoid significant water table declines. Maintenance of reinjection wells for the geothermal effluent would be costly due to the high dissolved solids content of the water. This water is not considered to be potable.

Geophysical data (Biehler and Gilpin, 1983; Moyle, 1984), a well log, geothermometry and downhole temperature data suggest the controlling structure for geothermal fluids in the section 14 resource is a southeasterly extension of the West Bullion Mountain fault. A potential for fracture permeability in basement rocks may exist associated with faulting and increase production and reinjection capabilities. However, exploration for any fracture permeability in the shallow basement will be difficult beneath the sedimentary cover.

ACKNOWLEDGEMENTS

URS Corporation and the County of San Bernardino Department of Housing and Community Development kindly allowed us use of their data. Access to a CAD system for drafting the figures was provided by Gary Rasmussen. Marilyn Kooser critically reviewed the manuscript.

REFERENCES CITED

Anorsson, S., Bjornsson, A., Gislason, G., and Gudmundsson, G., 1976, Systematic exploration of the Krisuvik high temperature area, Rey Kjanes Peninsula, Iceland: 2nd U.N. Symposium Proceedings (2) 853-864.

Bader, J.S., and Moyle Jr., W.R., 1960, Data on water wells and springs in the Yucca Valley-Twentynine Palms area, San Bernardino and Riverside Counties, California: California Department of Water Resources Bulletin 91-2.

Biehler, S. and Gilpin, B., 1983, Geophysical investigations of the Twentynine Palms area, California: unpublished report prepared for Wahler Associates and the U.S. Navy.

California Department of Water Resources, 1984, Twentynine Palms Groundwater Study.

Dibblee, T.W. Jr., 1968, Geologic map of the Twentynine Palms quadrangle, San Bernardino and Riverside Counties, California: U.S. Geological Survey Miscellaneous Investigations Map I-561. Scale: 1:62,500.

Ellis, A.J., and Mahon, W.A.H., 1977, Geochemistry and Geothermal Systems: Academic Press.

Fournier, R.O., and Truesdell, A.H., 1973, An empirical Na-Ca-K geothermometer for natural waters: Geochimica Cosmochimica Acta (37) 1225-1275.

Fournier, R.O., and Potter, R.W. II, 1979, Magnesium correction for the Na-Ca-K geothermometer: Geochimica Cosmochimica Acta (43) 1255-1275.

Fournier, R.O., 1981, Application of water geochemistry to geothermal exploration and reservoir engineering, in, Ryback, L., and Muffler, J.P., eds., Geothermal Systems: Principles and Case Histories: John Wiley and Sons.

Johnson, A.I., 1967, Specific yield - compilation of specific yields for various materials: U.S. Geological Survey Water Supply Paper 1662-D.

Leivas, E., Martin, R., Higgins, C., and Bezore, S., 1981, Reconnaissance geothermal resource assessment of 40 sites in California: California Division of Mines and Geology Open File Report 82-4 SAC.

Moyle Jr., W.R., 1974, Temperature and chemical data for selected thermal wells and springs in southeastern California: U.S. Geological Survey Water Resources Investigation 33-73.

Moyle Jr., W.R., 1984, Bouguer gravity anomaly map of the Twentynine Palms Marine Corps Base and vicinity, Twentynine Palms, California: U.S. Geological Survey Water Resources Investigation 84-4005. Scale: 1:62,500.

Trexler, D.T., Flynn, T., and Ghusn Jr., G., 1984, Drilling and Thermal Gradient Measurements at U.S. Marine Corps Air Ground Combat Center, Twentynine Palms, California: unpublished report prepared for U.S. Department of Energy.

U.R.S. Corporation, 1985, Geothermal Resource Assessment of Twentynine Palms, California: unpublished report prepared for San Bernardino County Department of Housing and Community Development.

LATE MIOCENE ALKALINE VOLCANISM, RUBY MOUNTAIN, SAN BERNARDINO COUNTY, CALIFORNIA

S.L. Neville
Irvine Consulting Group
15 Mason Street
Irvine, California 92714

INTRODUCTION

Flow remnants and intrusive dikes of alkaline basalt (basanite) of probable late Miocene age are found at Ruby Mountain (34 deg. 16' N, 116 deg. 40' W), San Bernardino County, California. This site of volcanism is one of two prolific ultramafic inclusion localities within an approximately 1000 square kilometer area of predominantly inclusion-free alkaline basaltic volcanism in the south-central Mojave Desert and adjacent San Bernardino Mountains (fig. 1).

These volcanic rocks are, in turn, part of a suite of young alkaline basalts that occur across the northeast and central Mojave Desert, notably: Pisgah Crater, Amboy Crater, Dish Hill, and the Cima volcanic field (fig. 1). In all of these localities relatively small volumes of basalt have been erupted from single, or small fields of, cinder cone vents. Many of these flows and dikes, like the Ruby Mountain Volcanics, contain coarse-grained ultramafic inclusions and megacrysts.

The range of radiometric and stratigraphic ages for these alkaline lavas of the Mojave Desert region is from approximately 10 million years before the present (mybp) to Holocene (330-480 years old) (Dohrenwend and others, 1984; Katz and Boettcher, 1980; Peterson, 1976; Woodburne, 1975; Oberlander, 1972; Wilshire and Trask, 1971; Wise, 1966, 1969; and Parker, 1959).

This entire Mojave group of alkaline basalts has been related to the late Cenozoic alkaline volcanism of the Basin and Range Province (Glazner, 1981; Katz and Boettcher, 1980), a tectonic environment characterized by high heat flow and a thinning crust (Leeman and Rogers, 1970; Best and Brimhall, 1974).

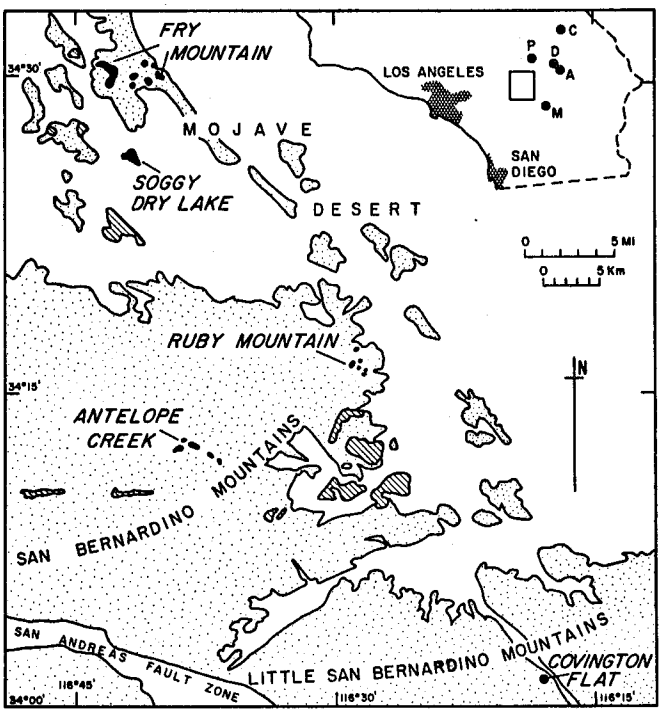

Fig. 1. Ultramafic inclusion localities in the south-central Mojave Desert and adjacent San Bernardino Mountains. The inset map in the upper right shows the location of other major Mojave Desert alkaline basalt localities including: Amboy Crater (A), Cima Dome (C), Dish Hill (D), Malapai Hill (M), and Pisgah Crater (P). Generalized geologic units shown include: pre-Tertiary basement (stippled), late Tertiary ultramafic inclusion-absent alkaline basalts (diagonal rule), late Tertiary ultramafic inclusion-bearing alkaline basalts (solid black), and alluvium (white). Figure from Neville and others (1985).

LOCAL GEOLOGY

Erosion of igneous and metamorphic basement that includes porphyritic quartz monzonite, granite, and biotite gneiss (see Moxham and others, 1955; Dibblee, 1967) has exposed two basaltic feeder dikes in the Ruby Mountain area (fig. 2). One dike is located immediately adjacent to the New Dixie Mine Road; the other is found at the peak of Ruby Mountain. Where exposed, dike-basement contacts are generally sharp and well developed chill margins may be observed (for example, at the northwest end of the dike near the New Dixie Mine Road). Brecciated contact zones and northwest-trending basaltic apophyses may be observed

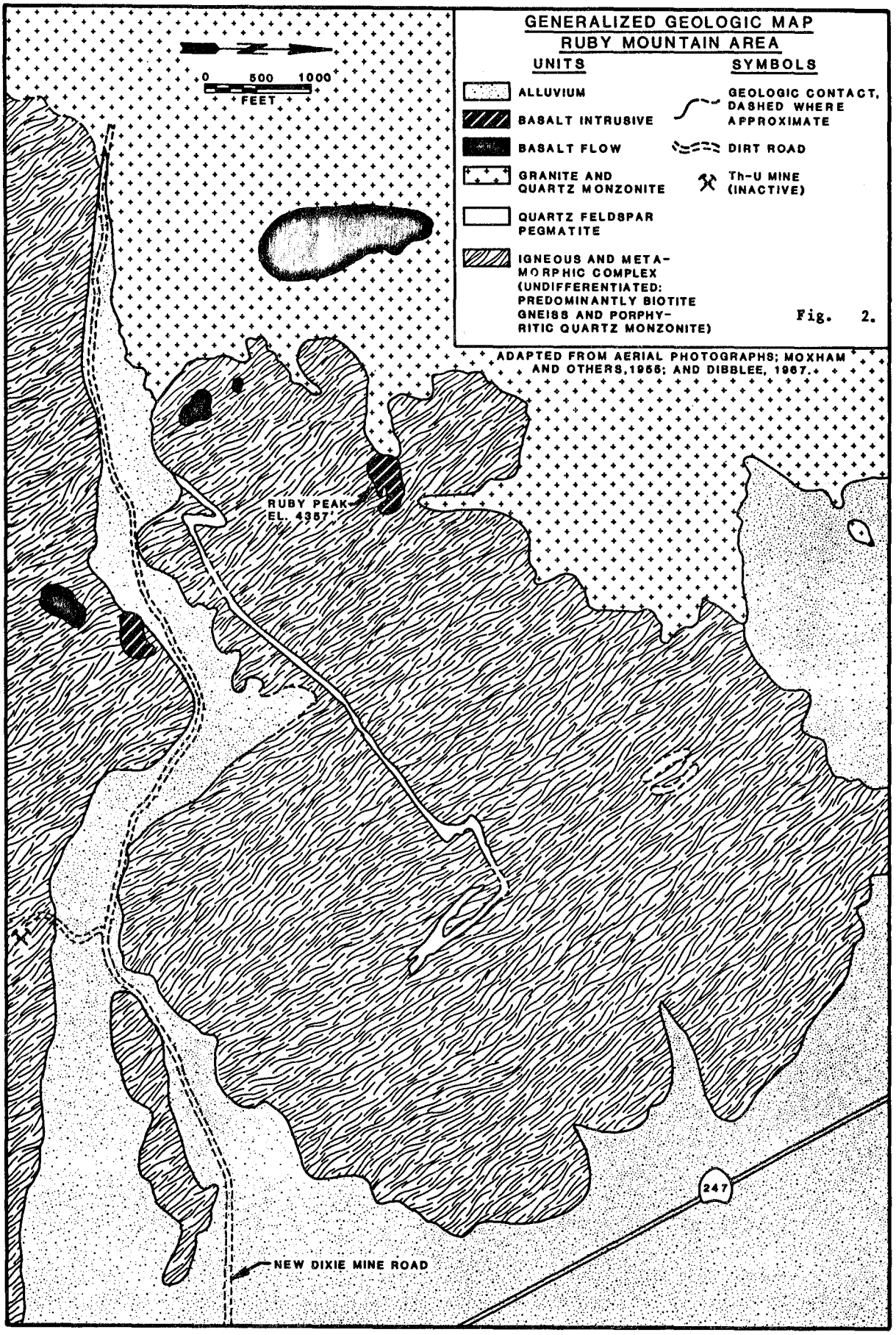
GENERALIZED GEOLOGIC MAP
RUBY MOUNTAIN AREA
UNITS
SYMBOLS
ALLUVIUM
BASALT INTRUSIVE
BASALT FLOW
GRANITE AND QUARTZ MONZONITE
QUARTZ FELDSPAR PEGMATITE
IGNEOUS AND METAMORPHIC COMPLEX (UNDIFFERENTIATED: PREDOMINANTLY BIOTITE GNEISS AND PORPHYRITIC QUARTZ MONZONITE)
GEOLOGIC CONTACT, DASHED WHERE APPROXIMATE
DIRT ROAD
Th-U MINE (INACTIVE)
0 500 1000
FEET
ADAPTED FROM AERIAL PHOTOGRAPHS; MOXHAM AND OTHERS, 1955; AND DIBBLEE, 1967.
RUBY PEAK EL. 4387'
247
NEW DIXIE MINE ROAD

Fig. 2.

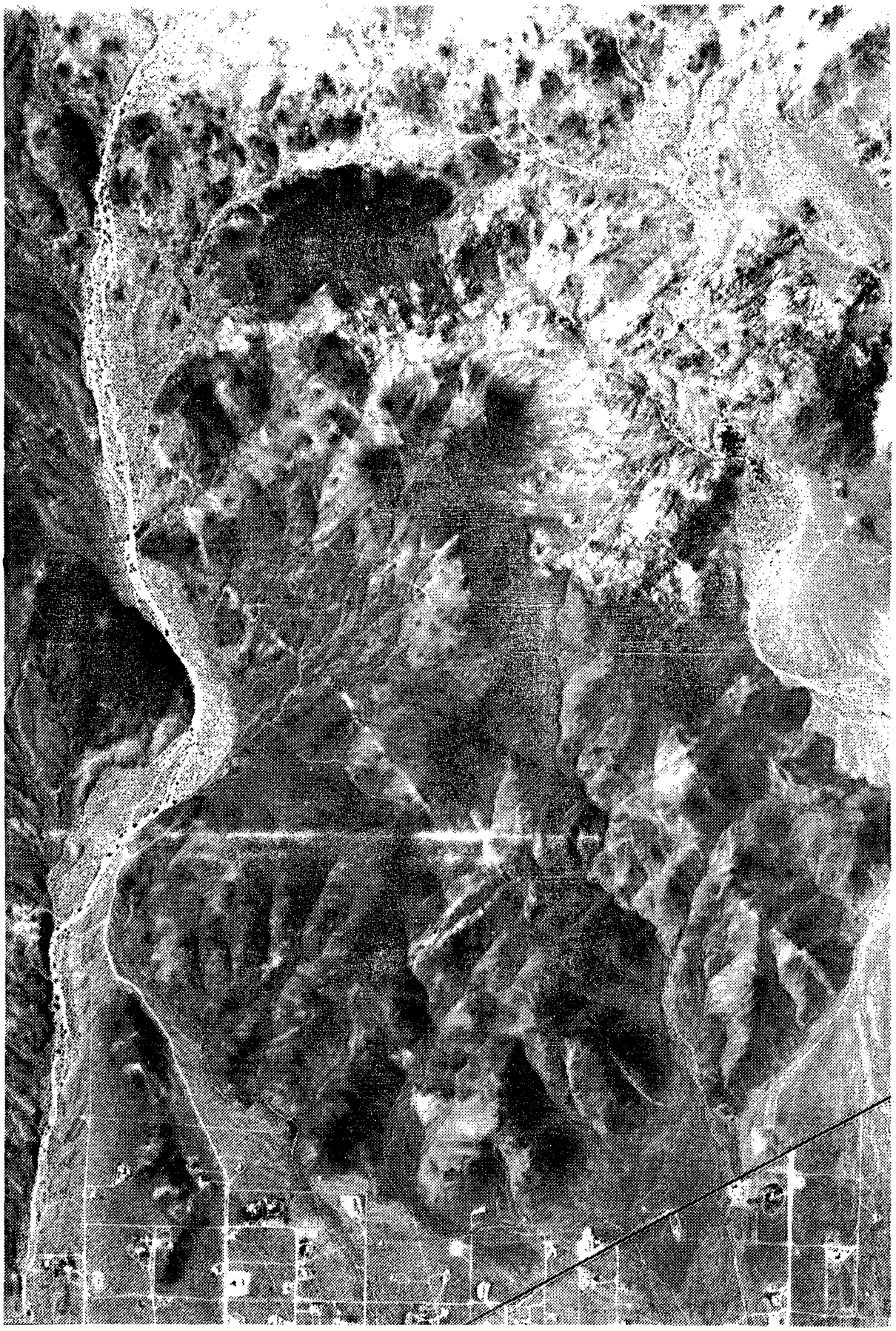

Air photo of Ruby Mountain area shown in Figure 2. Courtesy of the Department of Earth Sciences, University of California, Riverside, and S. Neville.

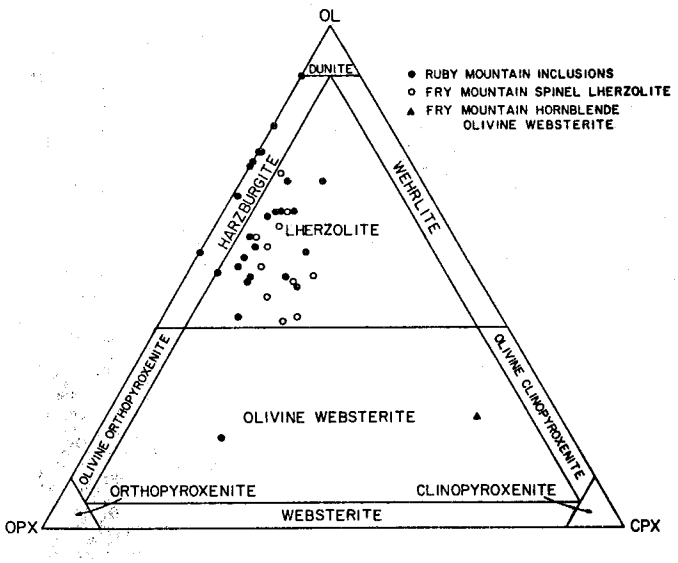

Fig. 3. Mineral modes of ultramafic inclusions from Ruby Mountain. Also included are those inclusions from Fry Mountain. Figure from Neville and others (1985).

at the margins of the funnel-shaped dike at Ruby Mountain Peak. The remaining basalt outcrops are flow remnants of up to 15 meters thick which rest upon basement.

The basalts at Ruby Mountain have not been dated; however, outcrops of basalts at Pioneertown, Old Woman Springs, Fry Mountain and Onyx Peak have been dated radiometrically and are found to be between 10 and 6 mybp in age (Morton, written communication 1980; Peterson, 1976; Woodburne, 1975; Oberlander, 1972). The basalts at Ruby Mountain are probably late Miocene in age.

BASALT AND INCLUSION PETROGRAPHY

The basalts from Ruby Mountain are markedly uniform in their petrographic character. They are fine-grained and sparsely phyric; microphenocrysts generally make up less than 15% of the mode and include olivine and lesser titaniferous augite. Pilotaxitic groundmass minerals include olivine, clinopyroxene, plagioclase, Fe-Ti oxides, and rare apatite. Deuteric zeolites, natrolite and analcite (?), may occur interstitially in the groundmass or in microfractures and microvesicles.

In each basalt outcrop at Ruby Mountain, ultramafic inclusions may be observed. Inclusions display varying stages of weathering ranging from a rusty-brown staining to complete disintegration leaving hollow casts in the basalt host. The inclusions range in size from 1 to 12 centimeters in diameter and are typically elongate to equant and subangular to well rounded. They generally display faceted forms with smooth surfaces and rounded corners and edges.

Ultramafic inclusions are coarse-grained and are composed for the most part of green olivine with lesser dark green to black enstatite, emerald green chrome-diopside and brown to black spinel. Modal analysis (fig. 3) shows the inclusions to be dominantly spinel lherzolite. All inclusions display tectonic fabrics with many strained and bent crystals.

The basalts are also host to large single crystals or "megacrysts" of black, vitreous clinopyroxene and amphibole (kaersutite) and translucent white anorthoclase. Clinopyroxene and amphibole megacrysts may be found as large as 5 centimeters in length while anorthoclase may grow as large as 3 centimeters in length. Both clinopyroxene and amphibole display a conchoidal-type fracture and subhedral to anhedral, elongate crystal forms. Additionally, kaersutites typically exhibit some traces of cleavage whereas clinopyroxene megacrysts do not. Anorthoclase megacrysts generally are tabular and subhedral.

In addition to ultramafic inclusions and megacrysts, granitoid xenoliths of up to 10 centimeters in diameter are commonly found included in these basalts. Presumably these xenoliths represent local Mesozoic plutonic rock entrained during the rise of basaltic magma.

BASALT CHEMISTRY

The basalts at Ruby Mountain are alkaline and may be further classified as basanites using the classification of Wise (1969). According to this classification, basanites typically contain less than 46 wt % SiO_2, greater than 5% normative nephaline, and greater than 1.5 wt % K_2O. The alkali variation diagram (fig. 4) demonstrates the limited SiO_2 compositional variation of the basalts from Ruby Mountain as well as other petrographically similar inclusion-bearing and inclusion-free basalts from localities depicted in figure 1.

ORIGIN OF BASALTS AND INCLUSIONS

As noted in the introduction, the young basalts of the Mojave Desert region are related to late Cenozoic volcanism of the Basin and Range Province, a

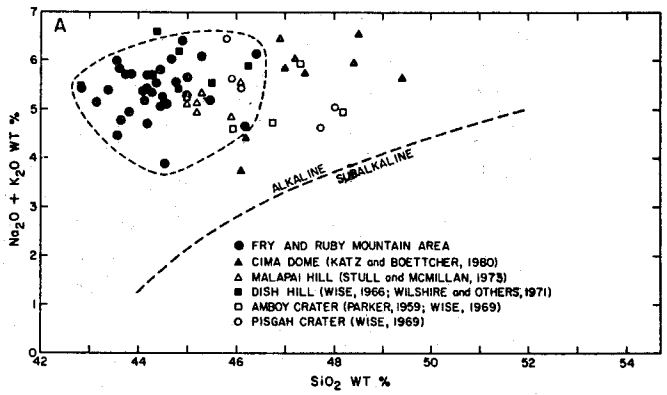

Fig. 4. Alkali variation diagram of alkaline basalts from the Ruby and Fry Mountain areas in comparison to younger, Central Mojave Desert alkaline basalts. The dashed line separates fields of alkaline and subalkaline basalts. Figure from Neville and others (1985).

tectonic setting of extension, thinning of crust and relatively high heat flow. The magmas generated in the Basin and Range Province and Mojave Desert are believed to have been produced by no greater than 20% partial melting of a peridotite mantle at depths ranging from 40 and 60 kilometers (Leeman and Rogers, 1970).

Sometime during the last 6 to 10 million years, basalt lava was generated in the upper mantle and made its way to the surface at Ruby Mountain, bringing with it a suite of inclusions and megacrysts. The ultramafic inclusions at Ruby Mountain display all the characteristics of mantle-derived xenoliths (chrome-diopside group of Wilshire and Shervais, 1975), namely: lherzolite dominant inclusions, tectonite textures, and chrome-rich diopside. In addition, thermobarometric calculations done on Ruby Mountain inclusions (Neville and others, 1985) indicate equilibrium temperatures and pressures of mantle origin. These mantle fragments, therefore, are believed to bave been entrained by the basaltic magma during its ascent from the mantle.

The megacrysts present at Ruby Mountain are generally common in alkaline basalts and because they usually occur as monocrystalline, euhedral-subhedral crystals, these megacrysts have been interpreted to represent high pressure (i.e., 10 to 20 kbar) near-liquidus phases (for example, see Green and Ringwood, 1967; Irving, 1974).

CONCLUSIONS

The Ruby Mountain basalts are part of a 6 to 10 million year old basalt province that is preserved in the eastern San Bernardino Mountains and immediately adjacent basins. Latest age estimates for alkaline basalts in the Central Mojave indicate that volcanism began approximately 6 million years ago and has continued into historic time. The local termination of alkaline basalt volcanism in and near the San Bernardino Mountains appears coincident with estimates of beginning transpressional tectonics for the region (4-6 million years ago; Sadler and Reeder, 1983).

REFERENCES CITED

Best, M.G., and Brimhall, W.H., 1974, Late Cenozoic alkalic basaltic magmas in the western Colorado plateau and the Basin and Range transition zone, U.S.A. and their bearing on mantle dynamics: Geological Society of America Bulletin, v. 85, p. 1677-1690.

Dibblee, T.W., Jr., 1967, Geologic map of the Emerson Lake quadrangle, San Bernardino County, California: U.S. Geological Survey Miscellaneous Geological Investigations Map I-490.

Dohrenwend, J.C., McFadden, L.D., Turrin, B.D., and Wells, S.G., 1984, K-Ar dating of the Cima volcanic field, eastern Mojave Desert, California: Late Cenozoic volcanic history and landscape evolution: Geology, v. 12, p. 163-167.

Glazner, A., 1981, Cenozoic evolution of the Mojave Block and adjacent areas (PhD dissertation): University of California, Los Angeles, 170 p.

Green, D.H., and Ringwood, A.E., 1967, The stability fields of aluminous pyroxene peridotite and garnet peridotite and their relevance in upper mantle structure: Earth Planetary and Science Letters, v. 3, p. 151-160.

Irving, A.J., 1974, Megacrysts from the Newer Basalts and other basaltic rocks of southeastern Australia: Geological Society of America Bulletin, v. 85, p. 1503-1514.

Katz, M.M., and Boettcher, A., 1980, The Cima volcanic field: in Fife, D.L., and Brown, A.R., eds., Geology and mineral wealth of the California Desert: South Coast Geological Society Publication, p. 236-241.

Leeman, W.P., and Rogers, J.J.W., 1970, Late Cenozoic alkali-olivine basalts of the Basin-Range province, U.S.A.: Contributions to Mineralogy and Petrology, v. 25, p. 1-24.

Moxham, R.M., Walker, G.W., and Baumgardner, L.H., 1955, Geologic and airborne radioactivity studies in the Rock Corral area, San Bernardino County, California: U.S. Geological Survey Bulletin 1021-C, p. 109-125, pl. 15, 16.

Neville, S.L., Schiffman, P., and Sadler, P., 1985, Ultramafic inclusions in late Miocene alkaline basalts from Fry and Ruby Mountains, San Bernardino County, California: American Mineralogist, v. 70, p. 668-677.

Oberlander, T.M., 1972, Morphogenesis of granitic boulder slopes in the Mojave Desert, California: Journal of Geology, v. 80, p. 1-19.

Parker, R.B., 1959, Magmatic differentiation of Amboy Crater, California: American Mineralogist, v. 44, p. 656-658.

Peterson, D., 1976, Patterns of Quaternary denudation and deposition at Pipes Wash, Mojave Desert, California (PhD dissertation): University of California, Riverside, 279 p.

Sadler, P.M., and Reeder, W.A., 1983, Upper Cenozoic, quartzite-bearing gravels of the San Bernardino Mountains, Southern California: recycling and mixing as a result of transpressional uplift: in Andersen, D.W., and Rymer, M.J., eds., Tectonics and sedimentation along faults of the San Andreas system, Society of Economic Mineralogists and Paleontologists Pacific Section, Los Angeles, p. 45-57.

Stull, R.J., and McMillan, K., 1973, Origin of lherzolite inclusions in the Malapai Hill basalt, Joshua Tree National Monument, California: Geological Society of America Bulletin, v. 84, p. 2343-2350.

Wilshire, H.G., and Shervais, J.W., 1975, Al-augite and Cr-diopside ultramafic xenoliths in basaltic rocks from the western United States: in Ahrens, L.H., and others, eds., Physics and Chemistry of the Earth, 9, Pergamon, New York, p. 257-272.

Wilshire, H.G., and Trask, N.J., 1971, Structural and textural relationships of amphibole and phlogopite in peridotite inclusions, Dish Hill, Calfiornia: American Mineralogist, v. 56, p. 240-255.

Wilshire, H.G., Calk, L.C., and Schwarzman, E.C., 1971, Kaersutite--a product of reaction between paragasite and basanite at Dish Hill, California: Earth Science and Planetary Letters, v. 10, p. 281-284.

Wise, W.S., 1966, Zeolite basanite from southeastern Calfiornia: Bulletin of Volcanology, v. 29, p. 235-252.

___, 1969, Origin of basaltic magmas in the Mojave Desert area, California: Contributions to Mineralogy and Petrology, v. 23, p. 53-64.

Woodburne, M.O., 1975, Cenozoic stratigraphy of the Transverse Ranges and adjacent areas, southern California: Geological Society of America Special Paper 162, 91 p.

GEOLOGY OF THE CUSHENBURY QUARRY, KAISER CEMENT CORPORATION, LUCERNE VALLEY, CALIFORNIA

Michael E. Gantenbein
Kaiser Cement Corporation
Star Route Box 40
Lucerne Valley, California 92556

INTRODUCTION

Cushenbury quarry is located on the north flank of the San Bernardino Mountains at the mouth of Cushenbury Canyon (fig. 1). The rock mined from the quarry consists of pre-Mesozoic miogeosynclinal strata exposed as a roof pendant that is associated with a quartz monzonite batholith of Mesozoic age.

QUARRY MARBLES

Pre-Mesozoic rock of the Cushenbury quarry consists of limestone that has been influenced by regional and contact metamorphism. The effect of metamorphism upon the limestone has created various metamorphic grades of calcite marble.

Early reconnaissance included the Cushenbury quarry marbles with the Furnace Limestone, in which the upper portion was dated by megafossils as Mississippian and Pennsylvanian or Permian (Hollenbaugh, 1968). Recent workers have correlated the metasediments of the north flank of the San Bernardino mountains with late Precambrian through Permian strata of the Cordilleran miogeosyncline (Stewart and Poole, 1975; Brown, this volume).

Within the limits of the Kaiser quarry pit, the Cushenbury mining staff has distinguished three groups of marbles with varying purity; white marble, light gray marble, and dark gray marble (fig. 2).

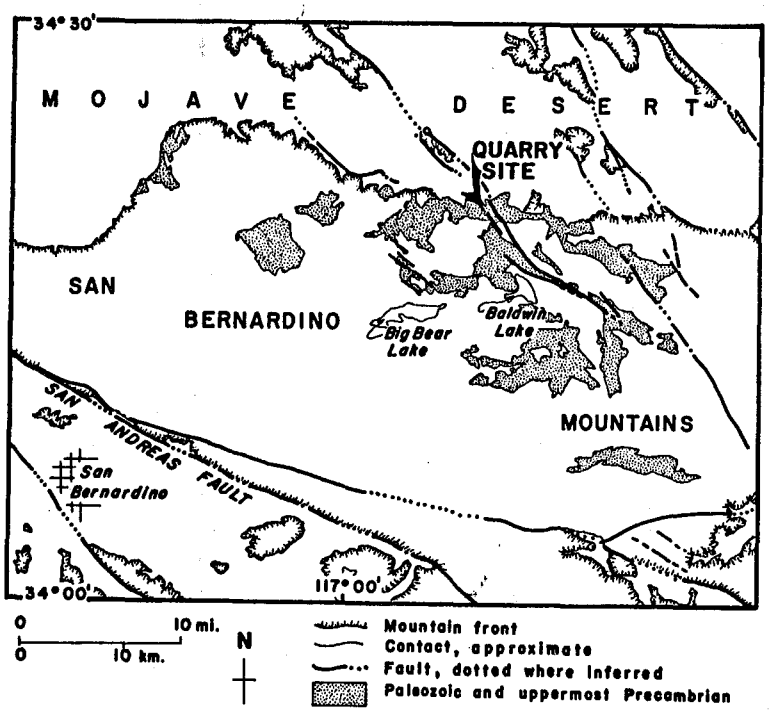

Figure 1. Index map showing the site of Kaiser Cement Corporation's Cushenbury Quarry and outcrop areas of uppermost Precambrian and Paleozoic metasedimentary rocks within the San Bernardino Mountains. (Geology greatly simplified from Rogers, 1967).

ROCK UNIT SEQUENCE
OF
CUSHENBURY QUARRY

ELEV. FT.	ROCK UNITS	DESCRIPTION	MINING GRADE
5200	Dark Gray Marbles	Medium gray, fine crystalline, pale yellowish orange weathering; Hematite and Mica are accessory minerals.	Medium Grade
5100		Dark gray, micro crystalline, moderate reddish orange and grayish orange weathering, slightly fetid.	Low Grade/ Waste
5000		Medium to medium dark gray, fine crystalline with dark gray clay lenses and pods.	Medium Grade
4900		Medium gray, medium crystalline, massive.	Medium Grade
	Hornfels	Medium dark gray to light brown, fine to micro crystalline, laminated very light gray siltstone?	Waste
4800	Thrust Fault Unit	Incorporates Calc-Hornfels and marble between slickensides, contains high amount of graphite.	Low Grade/Wst.
	Light Gray Marbles	Medium gray to light gray, medium to coarse crystalline, slightly fetid. (thickness varies)	Medium Grade
4700	White Marble	White, coarse crystalline, massive,	High Grade
	Calc-silicate	Medium dark to light gray, medium crystalline with bands of white, micro crystalline silica.	Waste
4600	White Marble	White, coarse crystalline, slightly dolomitic, massive.	High Grade

Aplitic Quartz Monzonite dike and sill intrusions are found in all rock units; influencing mining grades.

Figure 2. Geologic section and description of units exposed in the Cushenbury Quarry.

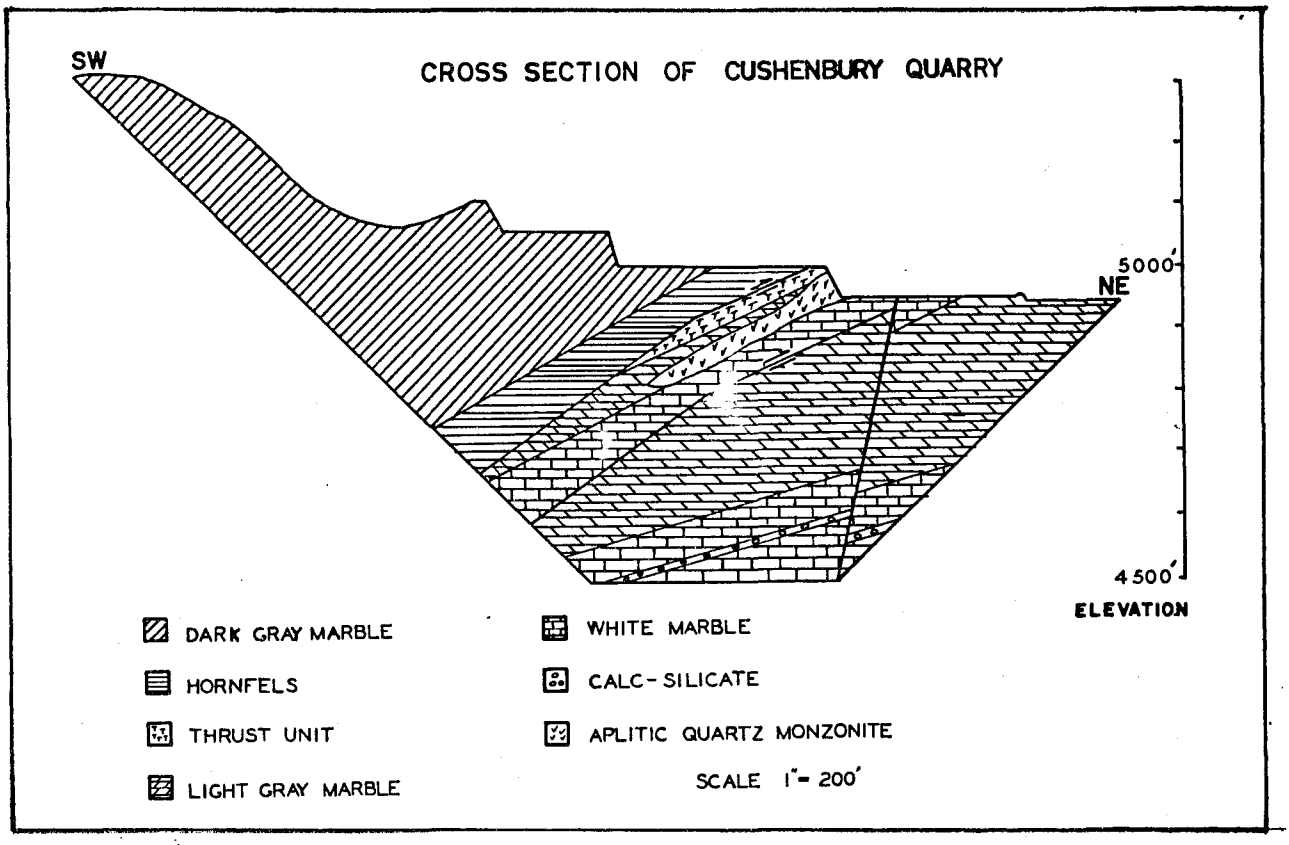

Figure 3. Southwest to northeast cross section of the Cushenbury Quarry.

STRUCTURE

Structure of the north flank of the San Bernardino Mountains is a complex multiphase Mesozoic deformation and is superimposed with late Cenozoic deformation (Sadler, 1982; Brown, this volume). In the quarry, the structure has been influenced by two main events (fig. 3), low angle thrust faulting and high angle strike-slip faulting in a right lateral sense. Strike-slip faulting has an additional element of dip-slip and trends north-by-northwest (Fife, 1982; Sadler, 1982).

REFERENCES CITED

Brown, H.J., 1986, Stratigraphy and paleogeographic setting of Paleozoic rocks in the northern San Bernardino Mountains, California: this volume.

Fife, D.L., 1982, Mineral resources investigation Cushenbury Limestone Quarry area Lucerne Valley, San Bernardino County, California: in-house report, Kaiser Cement Corporation.

Hollenbaugh, K.L., 1968, Geology of a portion of the north flank of the San Bernardino Mountains (PhD dissertation): University of Idaho, 84 p.

Sadler, P.M.,1982, Provenance and structure of late Cenozoic sediment in the northeast San Bernardino Mountains: in Sadler, P.M., and Kooser, M.A., editors, Late Cenozoic stratigraphy and structure of the San Bernardino Mountains; in Cooper, J.D., compiler, Geologic excursions in the Transverse Ranges, volume and guidebook, Geological Soiciety of America Cordilleran Section, 78th annual meeting, Anaheim, California, p. 82-91.

Stewart, J.H., and Poole, F.G., 1975, Extension of the Cordilleran miogeosyncline belt to the San Andreas fault, southern California: Geological Society of America Bulletin, v. 86, p. 205-212.

STRATIGRAPHY AND PALEOGEOGRAPHIC SETTING OF PALEOZOIC ROCKS IN THE NORTHERN SAN BERNARDINO MOUNTAINS, CALIFORNIA

Howard J. Brown
Pluess-Staufer (California) Inc.
P.O. Box 825
Lucerne Valley, California 92356

ABSTRACT

Extensive exposures of pre-Mesozoic metasedimentary rocks are present in the San Bernardino Mountains. Overlying Precambrian basement are thick quartzite dominated sequences previously correlated with late Precambrian and Early Cambrian miogeoclinal strata of the Big Bear Group, Johnie Formation, Stirling Quartzite, Wood Canyon Formation, Zabriskie Quartzite, and Carrara Formation.

Overlying is a thick section of carbonate rocks previously lumped into the Furnace Limestone of Carboniferous age. Recent detailed mapping, chemical and paleontological data indicate that the sequence can be subdivided and correlated with the Cambrian Bonanza King and Nopah Formations, the unconformably overlying Sultan Limestone of Devonian age, Mississippian Monte Cristo Limestone, and theunconformably overlying Bird Spring Formation of Pennsylvanian through Permian age. Ordovician and Silurian strata have not been recognized in the area.

The carbonate strata are identical to transitional-miogeoclinal strata exposed in several ranges in the Mojave Desert region, and were deposited in a shallow marine environment. Regional isopachous and facies trends originally extended southwest across the Mojave, and suggest a westward bulge in the continental margin prior to Mesozoic truncation and compressional tectonics.

INTRODUCTION

The San Bernardino Mountains are one of the major ranges in the east-west trending Transverse Ranges Province of southern California (Fig. 1). The north slope of the range rises abruptly from the desert floor in Lucerne Valley, and elevations along the north range crest reach 8400 feet.

Although the northern range front forms the southern boundary of the Mojave Desert geomorphic province, rocks in the San Bernardino Mountains have close affinity to rocks in the Mojave Desert region, and they have shared an exceedingly complex geologic history. Roof pendants within the extensive Mesozoic batholithic terrane of the southern Cordillera include numerous exposures of deformed and metamorphosed Paleozoic strata (Fig. 1).

Previous studies of lower Paleozoic rocks in the San Bernardino Mountains have suggested they are correlative with miogeoclinal strata exposed in the Mojave Desert region (Stewart and Poole, 1975). The complex deformation and metamorphism however, in many cases hampered identification of specific formations, and therefore correlations were generalized, and based predominantly on reconnaissance examinations.

My own studies in the San Bernardino Mountains and Mojave Desert region (Brown, 1981, 1982a, b, 1984a, b, c, in press) include detailed mapping in many ranges at scales ranging from 1:480 (1" = 40') to 1:12,000 (1" = 1000'). These detailed studies have allowed recognition of complex structural relationships, and have permitted the complex stratigraphic relationships to be determined. Paleontological data and chemical analysis of several hundred samples from various Paleozoic formations in the region (Brown, 1984c) provide additional support.

In this report, the Paleozoic stratigraphy of the northern San Bernardino Mountains will be described, and the rocks correlated with formations of the Cordilleran miogeocline. Depositional environments, paleogeographic setting, and facies relationships in the region will also be discussed. Areas noted in the text are shown on Figure 2.

SAN BERNARDINO MOUNTAINS STRATIGRAPHY

Unconformably overlying basement gneiss are late Precambrian and Paleozoic metasedimentary rocks which are exposed as several large roof pendants (Fig. 3). The rocks are highly deformed and metamorphism ranges from greenschist to granulite facies. On the basis of reconnaissance work, Richmond (1960) and Dibblee (1964) divided the rocks into three formations, the Saragosa and Chicopee Quartzites of pre-Carboniferous age, and the overlying Furnace Limestone of Carboniferous age. More recent detailed studies however, indicate the use of the older nomenclature should be discontinued, as the rocks are now divided into many formations and correlated with late Precambrian through Permain strata of the Cordilleran miogeocline (Stewart and Poole, 1975; Sadler, 1982; Brown, 1984a, b) (Fig. 4).

Late Precambrian and Early Cambrian Strata

In the Big Bear area, a thick section of quartzite, phyllite, and marble unconformably overlying crystalline basement has been named the Big

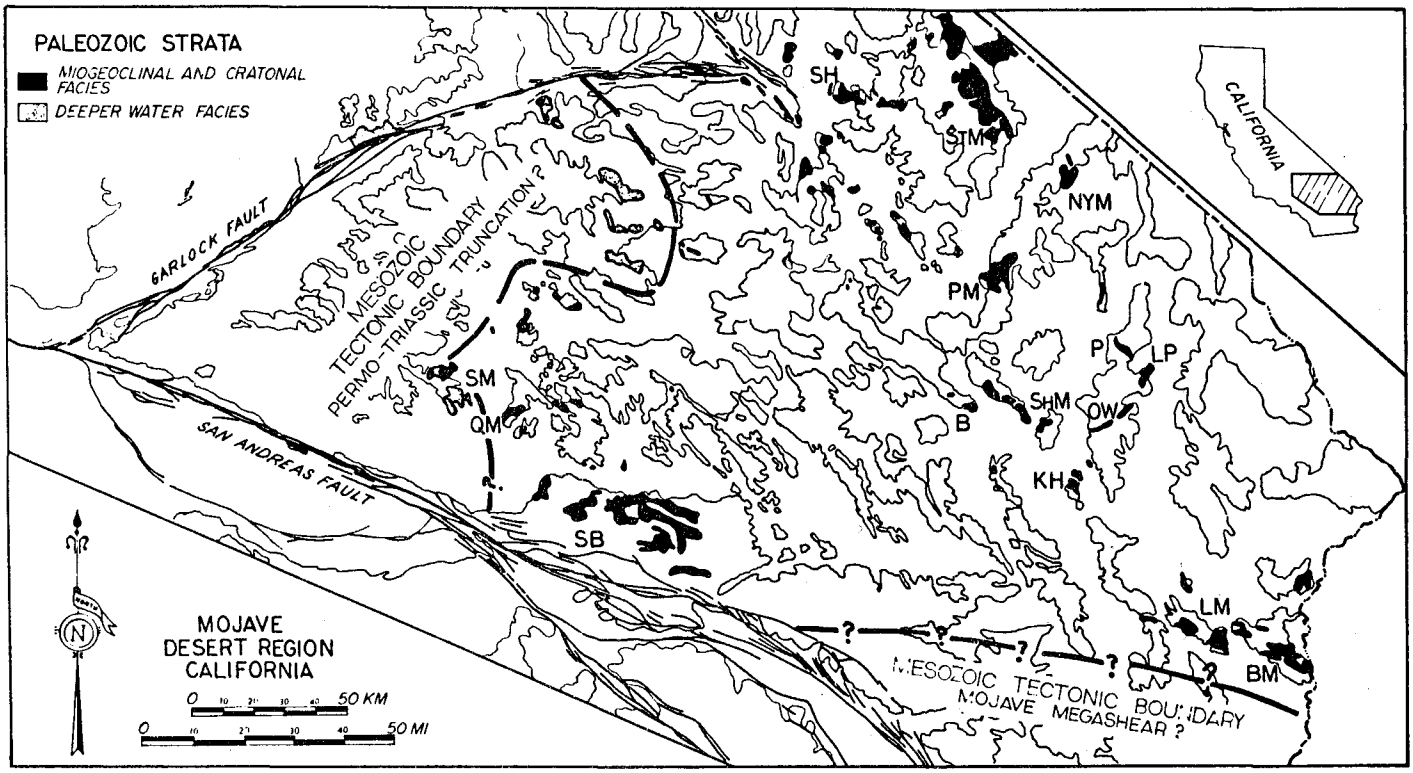

Figure 1. Map showing Paleozoic strata in the Mojave Desert region. SB=San Bernardino Mountains, SM=Shadow Mountains, QM=Quartzite Mountain, B=Bristol Mountains, ShM=Ship Mountains, P=Piute Mountains, LP=Little Piute Mountains, OW=Old Woman Mountains, KH=Kilbeck Hills, LM=Little Maria Mountains, BM=Big Maria Mountains, PM=Providence Mountains, NYM=New York Mountains, STM=Striped Mountain, SH=Silurian Hills.

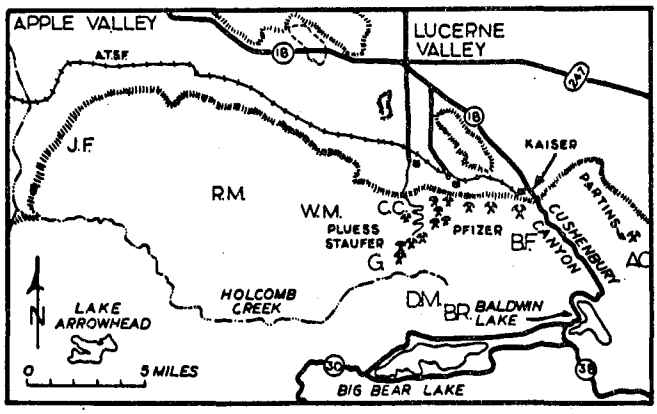

Figure 2. Map of the Lucerne Valley area and northwestern San Bernardino Mountains showing locations of areas mentioned in the text. JF=Juniper Flats, RM=Rattlesnake Mountains, WM=White Mountain, CC=Crystal Creek, G=Greenlead Mine area, BF=Burnt Flat area, DM=Delamar Mountain, BR=Bertha Ridge, AC=Arrastre Creek.

Bear Group, and assigned a late Precambrian age (Cameron, 1982). Buff dolomite, calc-silicate rock and quartzite correlative with the upper Precambrian Johnie Formation and Stirling Quartzite overlie the Big Bear Group (Fig. 4). Younger upper Precambrian and Lower Cambrian metasedimentary rocks include; cross-bedded and pebbly quartzite, phyllite, and dark schist correlative with the Wood Canyon Formation, white vitreous quartzite correlative with the Zabriskie Quartzite, and a heterogenous sequence of red-brown and green calc-silicate rock, schist, hornfels, and dark grey siliceous marble correlative with the Lower and Middle Cambrian Carrara Formation (Fig. 4).

Middle to Upper Cambrian and Devonian Strata

Middle to Upper Cambrian and Devonian strata are widely exposed in the area, and form a distinctive dolomite dominated sequence (Fig. 4). Visually and chemically distinctive (Brown, 1984c), thin-banded to mottled, light to dark grey, slightly dolomitic marble of the Lower Member of the Bonanza King Formation is overlain by a thick sequence of buff, tan, light to dark grey, and white dolomite (Brown, 1982b, 1984c). Recognition of distinctive, regionally persistant hornfels and calc-silicate marker beds (Table 1) allows the thick dolomite dominated sequence to be subdivided into several formations and members including the Cambrian Bonanza King Formation (three members), Cambrian Nopah Formation (Dunderberg Shale Member and Upper Member), and the unconformably

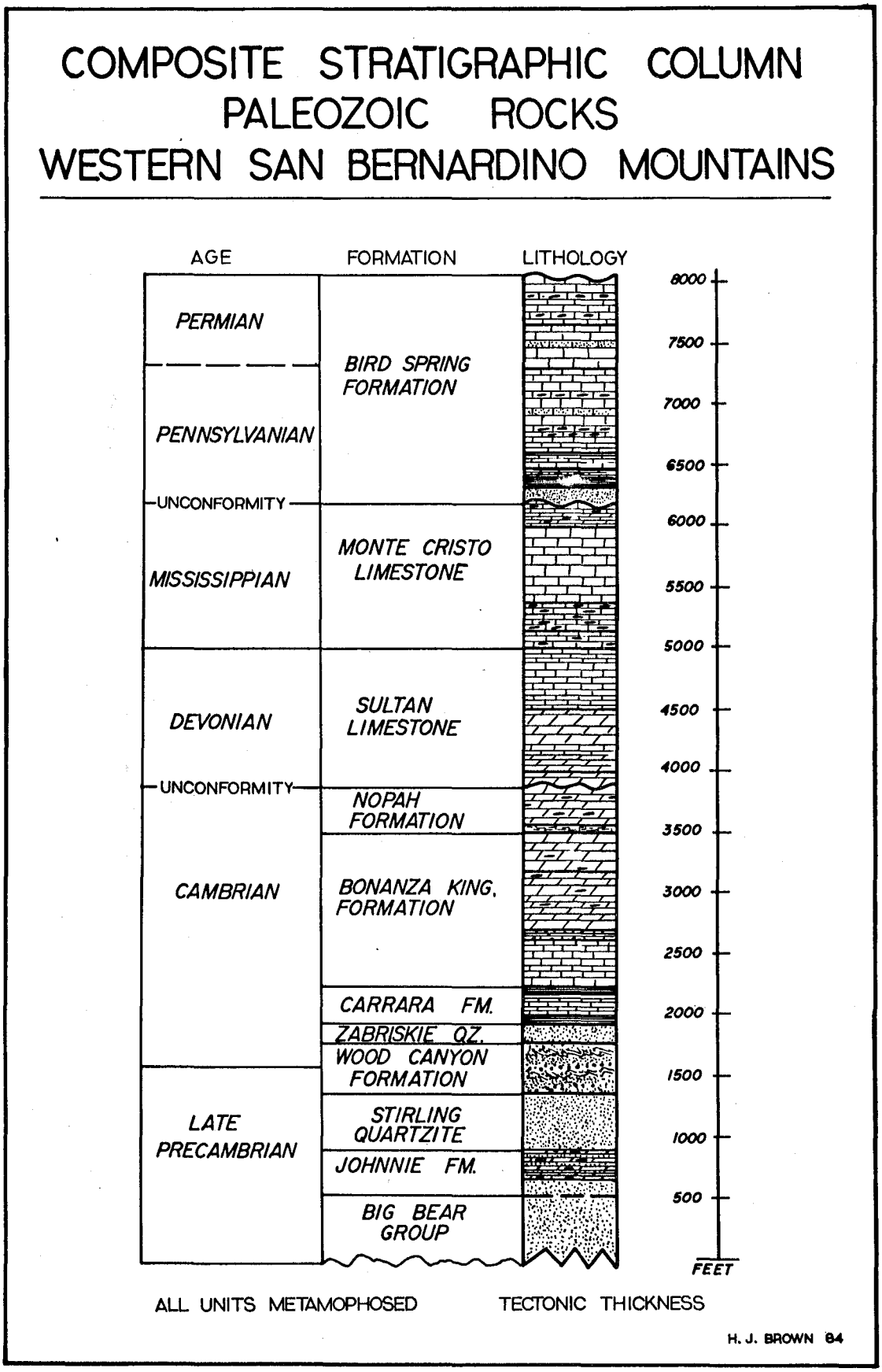

Figure 4. Composite stratigraphic column of Paleozoic rocks in the northwestern San Bernardino Mountains.

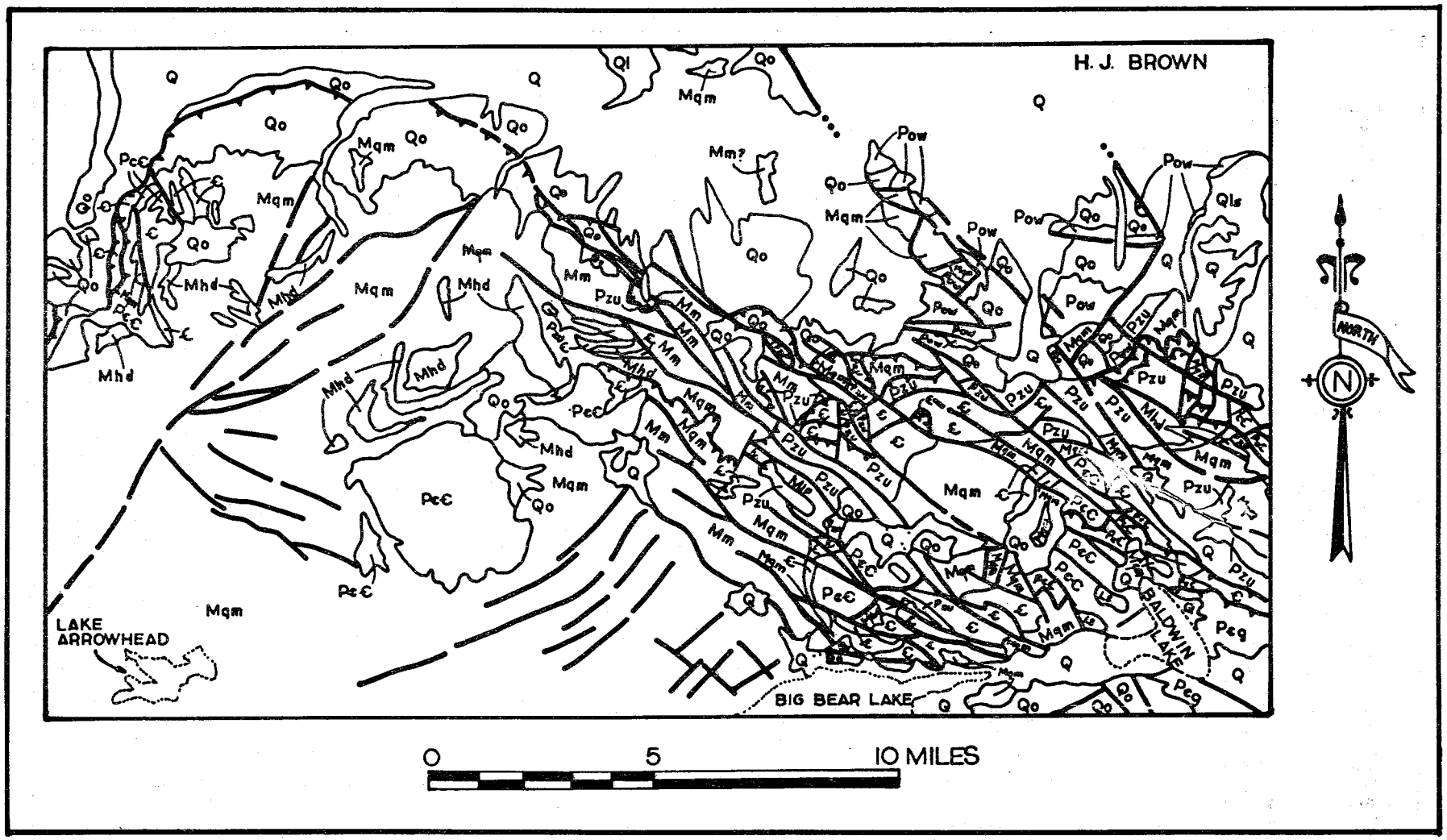

Figure 3. Generalized geologic map of the Lucerne Valley area and northwestern San Bernardino Mountains. Compiled and simplified from unpublished mapping by the author (1979-1985), at scales ranging from 1:480 to 1:12,000, and various published reconnaissance maps cited in the text. Note, area shown on map is the same as Figure 2.

Figure 3.

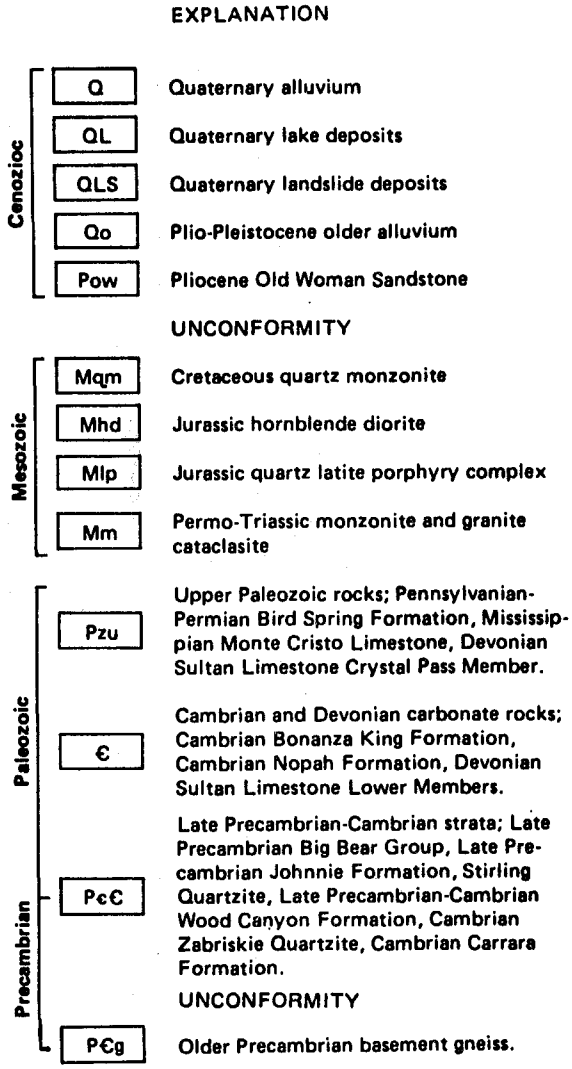

GENERALIZED GEOLOGIC MAP OF THE NORTHWESTERN SAN BERNARDINO MOUNTAINS SAN BERNARDINO COUNTY, CALIFORNIA

overlying Devonian Sultan Limestone (Ironsides Member and Middle Member) (Brown, 1984a). Stromatoporoids have been noted from the lower Sultan Limestone at Bertha Ridge, and in the Crystal Creek area, and are characteristic of the lower part of the formation in many areas of the region (Burchfiel and Davis, 1977, 1981). Rocks of Ordovician and Silurian age have not been recognized in the San Bernardino Mountains, and a major unconformity is present between Upper Cambrian and Devonian rocks in the Mojave Desert and San Bernardino Mountains region (Burchfiel and Davis, 1981).

Upper Paleozoic Strata

Upper Paleozoic rocks are abundantly exposed along the north range front, and comprise shallow water platform carbonate sequences dominated by limestone and calcite marble (Brown, 1984a). In some places metamorphism is weak, and mapping has disclosed several fossil locations. Carboniferous megafossils have been reported (Richmond, 1960), and recent conodont studies (Ozanich, 1982; Bruce Wardlaw, personal communication, 1984) indicate Pennsylvanian (Morrowan) strata are present. Further conodont studies are currently in progress (F. G. Poole, personal communication, 1985).

Detailed mapping has allowed recognition of several distinctive Upper Paleozoic formations and members including; Devonian Sultan Limestone (Crystal Pass Member), Mississippian Monte Cristo Limestone (Dawn, Anchor, Bullion and Yellowpine Members), and the unconformably overlying Pennsylvanian through Permian Bird Spring Formation (including the Indian Springs Member and three overlying informal members) (Fig. 4) (Brown, 1984a). Brief descriptions of these units as they appear in the San Bernardino Mountains (and elsewhere in the Mojave region) are given in Table 1.

REGIONAL STRATIGRAPHIC SETTING

Within the San Bernardino Mountains and Mojave Desert region Paleozoic strata comprise three facies groups. Paleozoic rocks exposed in the south-eastern Mojave Desert area are of cratonal affinity (Fig. 5). The sections are remarkably similar, and can be subdivided into distinctive rock units of consistant lithologic character. The sections are relatively thin, often less than 3500 feet, and several unconformities are present. The sequences lack late Precambrian sediments, and are very similar to the epicontinental and shallow water cratonal section exposed in the Grand Canyon area (Stone, Howard and Hamilton, 1983).

Paleozoic rock sequences in the central and western Mojave Desert region thicken and contain elements of both cratonal and miogeoclinal affinity, depending on which part of the sectin is examined. Upper Precambrian and Lower Cambrian rocks have a different distribution of cratonal and miogeoclinal facies than do Middle Cambrian carbonate rocks. In both cratonal and miogeoclinal sequences of this region, a major unconformity is present between Upper Cambrian rocks and stromatoporoid bearing Devonian strata (Burchfiel and Davis, 1981). Lack of a distinctive lithologic break, extreme deformation, and metamorphism in many areas have obscured contact relationships, and the unconformable contact is not always discernable. Upper Paleozoic rocks of the south-eastern Mojave Desert are of cratonal affinity, while age equivalent exposures in the central Mojave are of inner miogeoclinal affinity (Fig. 6).

In the San Bernardino Mountains late Precambrian and Lower Cambrian rocks are of miogeoclinal affinity, Middle Cambrian strata are of cratonal affinity, and upper Paleozoic rocks are identical to inner miogeoclinal strata of the central and northeastern Mojave Desert region (Fig. 6).

An unconformity is present between Mississippian and Early Pennsylvanian strata throughout the region. The basal Bird Spring Formation (miogeoclinal) and Supai Group (cratonal) is often marked by the presence of conglomerate, quartzite, or terrigenous rocks. In the San Bernardino Mountains the lower Bird Spring

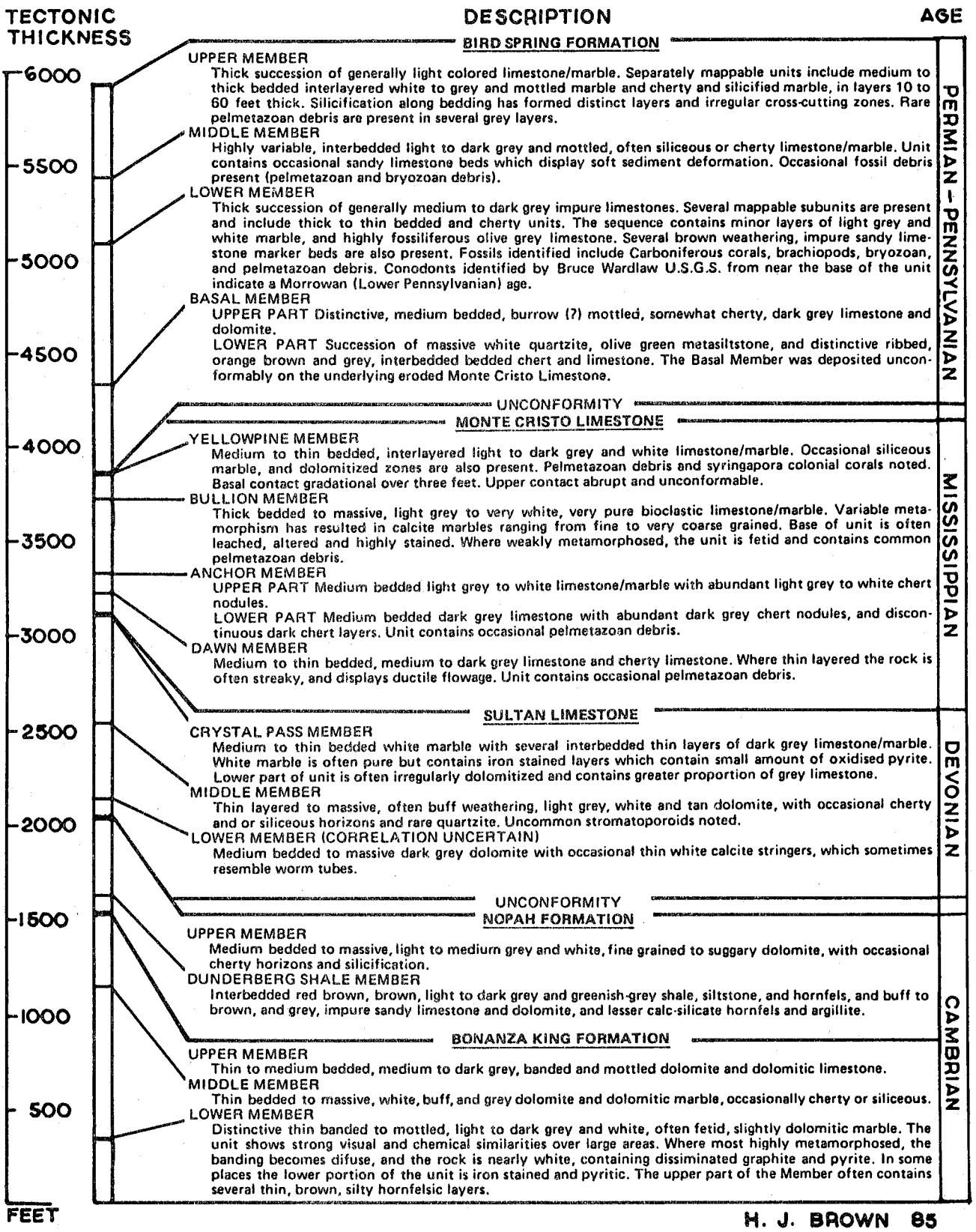

Table 1. Description of Paleozoic carbonate rocks, northwestern San Bernardino Mountains.

Formation (Indian Springs Member) is composed of quartzite, metasiltstone and impure muddy limestone which unconformably overlie the eroded uppermost Monte Cristo Limestone.

In contrast to the shallow water, carbonate dominated cratonal and miogeoclinal strata of the central Mojave Desert and San Bernardino Mountains, are exotic strata of the "Northwestern Mojave Terrane" (Fig. 1). Siliceous clastic and volcanogenic strata are exposed in several ranges, and include deep water continental slope and rise deposits of Cambrian through Permian age (Carr and others, 1984).

Environments of Deposition

Late Precambrian and Paleozoic rocks of the central and western Mojave Desert and San Bernardino Mountains were deposited in a generally shallow marine environment of the Cordilleran miogeocline, which extended at least as far southwest as the present day location of the San Andreas fault (Stewart and Poole, 1975). Stromatolitic and thin-laminated cryptalgal dolomites suggest shallow marine and supratidal conditions at various times during late Precambrian, Cambrian and Early Devonian time. An extensive shallow marine shelf environment during Middle Cambrian time is indicated by the very thin, distinctive, and regionally persistant lower member of the Bonanza King Formation. Rocks of this unit are virtually identical over the entire Mojave Desert region, even though the (tectonic) thickness is often less than 40 feet (Brown, 1982b).

High and low energy shallow marine environments during portions of Devonian and Pennsylvanian time are suggested by variable thin-bedded to massive limestones of variable silt content and purity, which comprise portions of the Crystal Pass Member of the Sultan Limestone, and Bird Spring Formation. Several of the Mississippian and Pennsylvanian rock units are composed of very pure bioclastic limestone, and may represent carbonate bank deposits in a high energy shallow marine environment. The Bullion Member of the Monte Cristo Limestone forms a thick, regionally extensive, shallow water bioclastic limestone deposit (Fig. 6).

Late Paleozoic cratonal rocks of the southeastern Mojave region were deposited in environments which ranged from terrigenous to shallow marine. Supratidal environments are represented by evaporite sequences present in several Upper Paleozoic formations (Fig. 5) exposed in the southeastern Mojave area.

Paleozoic sedimentary rocks of the "Northwestern Mojave Terrane" were deposited in a variety of generally deep water continental slope and rise environments. Foreland basin deposits, turbidites, and flysch deposits are present, as well as minor shallow water limestone (Carr and others, 1984).

Facies and Isopachous Trends

Several facies changes are present in the region, and locations of facies boundaries have changed over time. Paleozoic strata once formed a continuous blanket over the entire Mojave Desert, and facies and isopachous trends generally project southwest across the region, with the exception of Middle Cambrian trends which are more nearly east-west (Fig. 7).

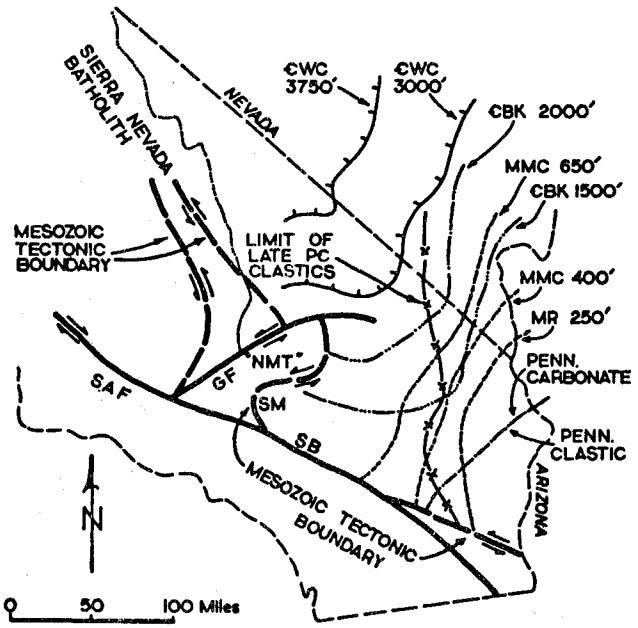

Figure 7. Interpretive map of selected late Precambrian and Paleozoic isopachous trends. CWC=late Precambrian-Cambrian Wood Canyon Formation, CBK=Cambrian Bonanza King Formation, MMC=Mississippian Monte Cristo Limestone (miogeoclinal), MR=Mississippian Redwall Limestone (cratonal), Penn. carbonate=Bird Spring Formation (miogeoclinal), Penn. clastic=Supai Group (cratonal), SAF=San Andreas Fault, GF=Garlock Fault, SM=Shadow Mountains, SB=San Bernardino Mountains, "NMT"=Northwestern Mojave Terrane. Isopachous lines are tectonic thickness. Wood Canyon Formation isopachous, limit of late Precambrian clastics, and location of Mesozoic tectonic boundary north of the Garlock Fault after Burchfiel and Davis (1981).

Cambrian rocks of cratonal affinity extend across the Mojave as far west as the Shadow Mountains (Fig. 7). The remarkable similarities between cratonal facies of the lower member of the Bonanza King Formation in the southeastern Mojave and exposures in the Shadow Mountains and Quartzite Mountain area in the western Mojave, suggest that Cambrian cratonal-miogeoclinal depositional trends may have extended a considerable distance to the west, and that the western Mojave may have been a westward projecting bulge in the North American continent prior to Permo-Triassic truncation and Mesozoic tectonism (Burchfiel and Davis, 1981; Brown, 1982b).

Shallow marine Paleozoic rocks of the southern and central Mojave Desert and San Bernardino Mountains are clearly indigenous to southwestern North America, and even though deformed, appear to be paleogeographically coherent. The regionally persistant and nearly identical rock sequences, and changing facies boundaries suggest original paleogeographic continuity of the Cordilleran miogeocline across the Mojave Desert, at least as far west as the Shadow Mountains (Fig. 7).

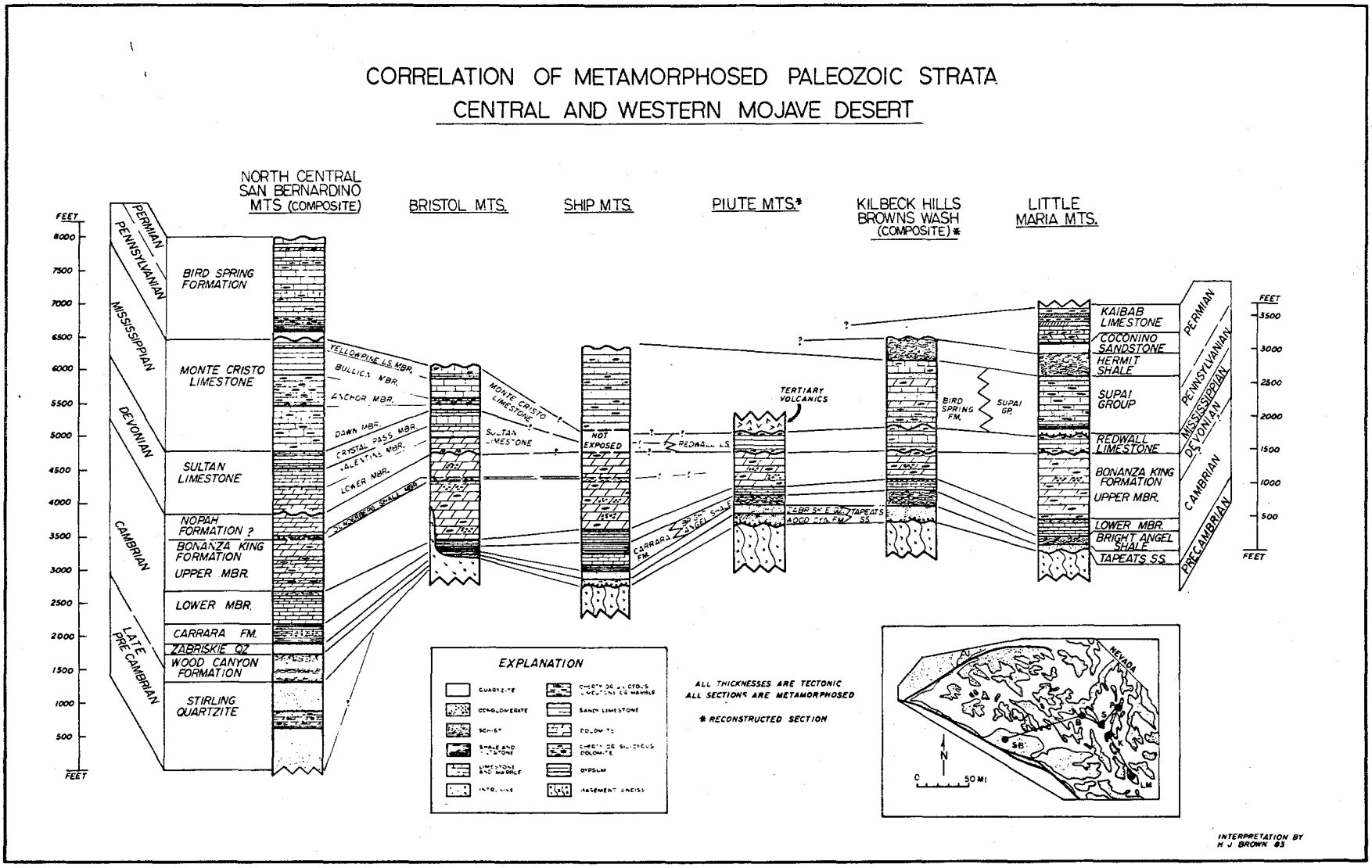

Figure 5. Correlation of metamorphosed Paleozoic strata from the San Bernardino Mountains to the southeastern Mojave Desert region.

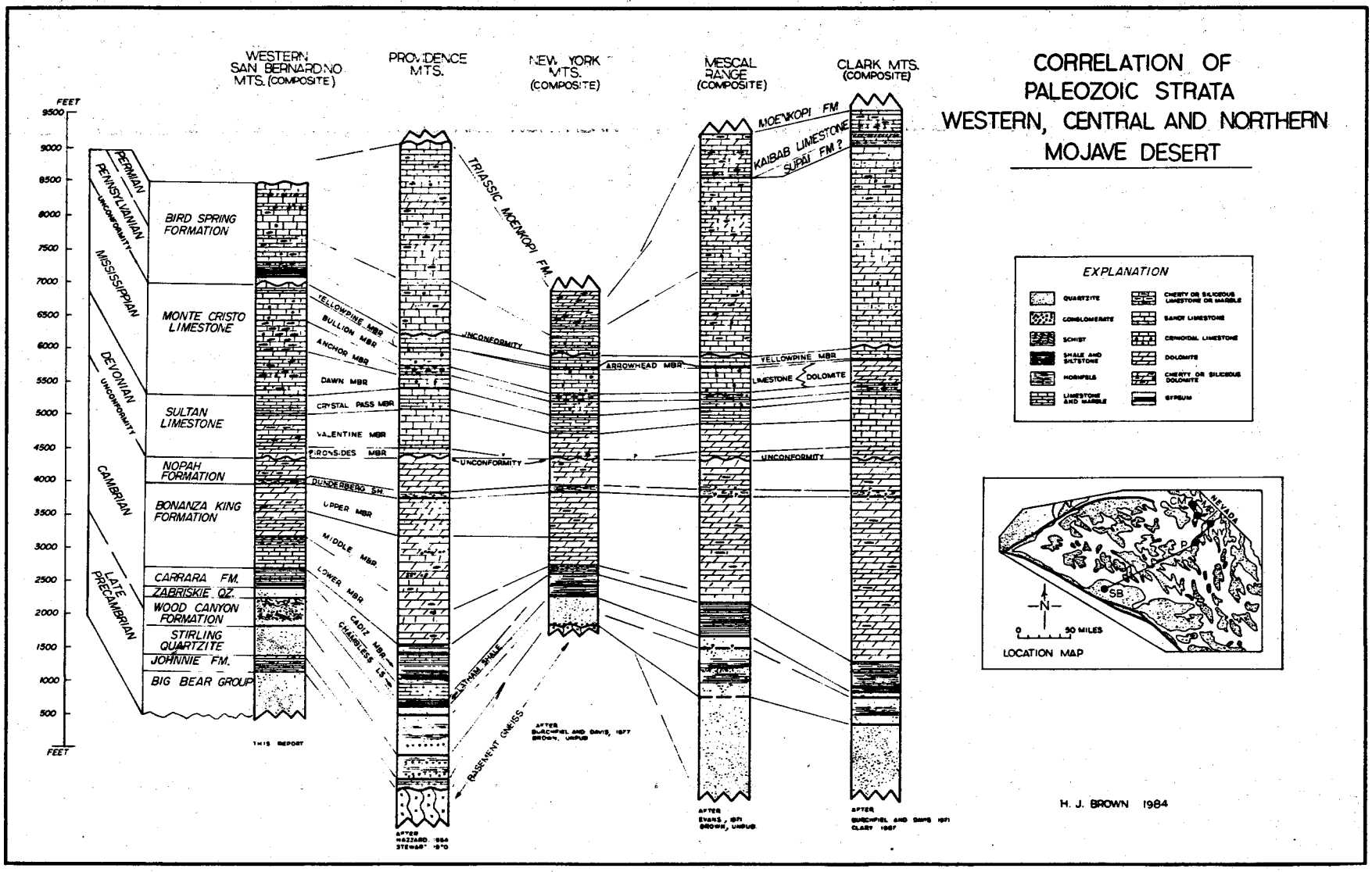

Figure 6. Correlation of Paleozoic strata from the San Bernardino Mountains to the northeasten Mojave Desert region.

Rocks of the "Northwestern Mojave Terrane" which are considered by most workers to be allochthonous, display evidence of a major Paleozoic tectonic event, that Carr and others (1984) interpreted to be related to the Antler orogeny of Mississippian age. Because miogeoclinal-cratonal strata in the Mojave Desert and San Bernardino Mountains show no evidence of Antler age deformation, a major tectonic boundary is thought to separate cratonal-miogeoclinal strata from rocks of the "Northwestern Mojave Terrane" (Fig. 7). Burchfiel and Davis (1972) proposed a major left slip truncation event during Permo-Triassic time to juxtapose the facies. Although nowhere exposed, the contact truncates facies and isopachous trends of the shallow water rocks, and has juxtaposed allochthonous deep water strata against them.

CONCLUSION

Extensive exposures of pre-Mesozoic metasedimentary rocks unconformably overlie Precambrian basement in the San Bernardino Mountains. The lower part of the section is clastic dominated, the middle part is dolomite dominated, and the upper part is limestone dominated. The section is generally of shallow water affinity, and the rocks are identical to and correlative with strata of the Cordilleran miogeocline exposed in many ranges in the Mojave region.

Detailed mapping, chemical and paleontological data demonstrate that Paleozoic formational nomenclature used in the eastern Mojave Desert and southern Basin and Range provinces can be applied to strata in the San Bernardino Mountains, and that use of older nomenclature should be discontinued.

Late Precambrian and Paleozoic isopachous and facies trends originally extended southwest across the Mojave region, and Paleozoic strata in the San Bernardino Mountains are of inner miogeoclinal affinity. Cambrian cratonal isopachous trends however, are nearly east-west, and suggest Cambrian depositional trends may have extended a considerable distance to the west of the San Bernardino Mountains, and that during Cambrian time, the western Mojave may have been a westward protruding bulge in the North American continent.

Shallow marine strata of the central Mojave Desert and San Bernardino Mountains are clearly indigenous to southwestern North America, and regional studies indicate original paleogeographic continuity of the Cordilleran miogeocline across the Mojave Desert region.

Exotic deep water Paleozoic strata of the "Northwestern Mojave Terrane" are juxtaposed against the shallow marine, carbonate dominated miogeoclinal strata. Although the contact between these contrasting terranes is not exposed, Burchfiel and Davis (1972) proposed a major left slip truncation event during Permo-Triassic time to juxtapose the allochthonous deep-water facies against the shallow water facies.

ACKNOWLEDGEMENTS

Thanks are due to Paul Stone, Marilyn Kooser, and Bob Reynolds for helpful reviews, comments and discussions, and to Pluess-Staufer (California) Inc., for permission to publish the data.

REFERENCES CITED

Brown, H.J., 1981, Stratigraphy and structure of a portion of the Bristol Mountains, San Bernardino County California: in Howard, K, Carr, M.D., and Miller, D.M., eds., Tectonic framework of the Mojave and Sonoran Deserts, California and Arizona: U.S. Geological Survey Open File Report 81-503, p. 10-11.

___, 1982a, Stratigraphy and structure of a portion of the Piute Mountains, San Bernardino County, California: Geological Society of America Abstracts with Programs, v. 14, p. 152.

___, 1982b, Possible Cambrian miogeoclinal strata in the Shadow Mountains, western Mojave Desert, California: in Fife, D.L., and Minch, J., eds., Geology and mineral wealth of the California Transverse Ranges: South Coast Geological Society, p. 355-365.

___, 1984a, Summary of the geology of the north range front of the San Bernardino Mountains, Lucerne Valley, California: in Kupfermann, S, McIver, D., and Morton, P., eds., Major limestone producers of the western Mojave Desert, California: Field Trip Guidebook, 112th annual meeting of the American Institute of Mining Engineers, p. 12-29.

___, 1984b, Paleozoic carbonate stratigraphy of the San Bernardino Mountains, southern California: Geological Society of America Abstracts with Programs, v. 16, p. 456.

___, 1984c, Correlation of metamorphosed Paleozoic strata of the southeastern Mojave Desert region, California and Arizona, Discussion and Reply: Geological Society of America Bulletin, v. 95, p. 1482-1486.

___, in press, Geological setting of the Lucerne Valley limestone mining district, and overview of the Pluess-Staufer mining operation, Lucerne Valley, California: in Pierce, W., ed., 21st Annual Industrial Minerals Conference Proceedings: Arizona Bureau of Mines.

Burchfiel, B.C., and Davis, G.A., 1971, Clark Mountain thrust complex in the Cordillera of southeastern California, Geologic summary and Field Trip Guide: University of California, Riverside, Campus Museum Contributions, v. 1, p. 1-28.

___, 1972, Structural framework and evolution of the southern part of the Cordilleran orogen, western United States: American Journal of Science, v. 272, p. 97-118.

___, 1977, Geology of the Sagamore Canyon-Slaughterhouse Spring area, New York Mountains, California: Geological Society of America Bulletin, v. 88, p. 1623-1640.

___, 1981, Mojave Desert and environs: in Ernst, W.G., ed., The Geotectonic Development of California: Rubey Volume 1, Prentice-Hall, Englewood Cliffs, New Jersey, p. 217-252.

Cameron, C.S., 1982, Stratigraphy and significance of the Upper Precambrian Big Bear Group: in Cooper, J., Troxel, B., and Wright, L., eds., Geology of selected areas of the San Bernardino Mountains and western Mojave Desert, and southern Great Basin of California: Field Trip Guidebook, 78th meeting of the Cordilleran Section, Geological Society of America, p. 5-20.

Carr, M.D., Christiansen, R.L., and Poole, F.G., 1984, Pre-Cenozoic geology of the El Paso Mountains, southwestern great basin, California: in Western

geological excursions: Field Trip Guidebook, Geological Society of America, v. 4, p. 84-93.
Clary, M.R., 1967, Geology of the eastern part of the Clark Mountain range, San Bernardino County, California: California Division of Mines and Geology Map Sheet 6.
Dibblee, T.W., 1964, Geologic map of the Lucerne Valley Quadrangle, San Bernardino County, California: U.S. Geological Survey Miscellaneous Investigations Map I-426.
Evans, J.R., 1971, Geology and mineral deposits of the Mescal Range Quadrangle, San Bernardino County, California: California Division of Mines and Geology Map Sheet 17.
Hazzard, J.C., 1954, Rocks and structures of the northern Providence Mountains, San Bernardino County, California: in Jahns, R.H., ed., Geology of southern California: California Division of Mines and Geology Bulletin 170, v. 1, p. 27-35.
Ozanich, G., 1982, New Pennsylvanian conodonts from the Furnace Limestone, San Bernardino Mountains, California (Senior Thesis): Earth Sciences Department, University of California, Riverside, 21 p.
Richmond, J.F., 1960, Geology of the San Bernardino Mountains north of Big Bear Lake, California: California Division of Mines and Geology Special Report 65, 68 p.
Sadler, P.M., 1982, Geology of the Fauwnskin and Big Bear City 7 1/2 ' Quadrangles, California: California Division of Mines and Geology Open File Report 82-18.
Stewart, J.H., 1970, Upper Precambrian and Lower Cambrian strata in the southern Great Basin, California and Nevada: U.S. Geological Survey Professional Paper 620, 206 p.
___, and Poole, F.G., 1975, Extension of the Cordilleran miogeosynclinal belt to the San Andreas fault, southern California: Geological Society of America Bulletin, v. 86, p. 205-212.
Stone, P., Howard, K., and Hamilton, W., 1983, Correlation of metamorphosed Paleozoic strata of the southeastern Mojave Desert region, California and Arizona: Geological Society of America Bulletin, v. 94, p. 1135-1147.

MINERALS OF THE DESERT VIEW MINE

Tracy A. Paul
Department of Geological Sciences
University of California
Santa Barbara, California 93106

INTRODUCTION

The Desert View Mine is located in the San Bernardino Mountains, northwest of Big Bear Lake and the town of Fawnskin, at an elevation of 7,600 feet (fig. 1). It is a relatively small metamorphic-metasomatic deposit at the contact between regionally extensive Paleozoic marbles and a granite porphyry, and is recognized by its unique fluorescent minerals and their similarities to those found at Franklin, New Jersey.

MINERALOGY

The bulk composition of the Desert View deposit is calcium and silica with manganese, iron, zinc, aluminum, and small amounts of magnesium. Hetaerolite is the most abundant metal oxide. It occurs as a well-crystallized brown opaque mass replacing the marble host and contains very small translucent orange zincite crystals and quartz. The zinc silicate willemite, found in brown opaque disseminated manganese oxide in the calcite, is associated with this assemblage. The colorless willemite grains are extremely difficult to identify in the rocks visually. However, small amounts of manganese substituting for zinc in the willemite result in a bright green fluorescense under the short-wave ultra-violet radiation of a black-light.

A second oxide assemblage is present which includes magnetite containing significant amounts of the spinel end-members, jacobsite, and franklinite. This assemblage occurs with andraditic garnet, willemite, epidote, and quartz. The rock itself is very dark, as though it were pure magnetite, yet X-ray and microprobe studies reveal that this is actually a heterogeneous retro-skarn.

The skarn of the deposit is composed of very pure, white crystalline calcite, pale green massive grossular garnet, and white fibrous wollastonite containing an opaque altered magnesium silicate mineral. Microprobe analyses confirm that this is a magnesium silicate but its structure has been altered, possibly due to serpentinization, so that identification by X-ray diffractometry or optical properties is very difficult. Grossular garnet veins cut the wollastonite, and calcite veins cut both the garnet and wollastonite. As in the willemite, small amounts of manganese substituting for calcium in the wollastonite result in a pale orange to bright yellow luminescence.

The marble assemblage includes small yellow-orange andraditic garnets up to 2 mm in size with black, metallic balls of jacobsite. The jacobsite grains grow up to 2 mm in diameter within the calcite host, contain significant amounts of zinc, and often display regular crystal faces. The marble assemblage also includes a late-stage vein containing yellow-green epidote, andraditic garnet, quartz, and translucent blue sphalerite grains. The sphalerite grains have microscopic inclusions of chalcopyrite which may be responsible for their blue color.

ORIGIN

Although the mineralogy of the Desert View Mine is fairly simple, explaining its origin is somewhat more difficult. There are probably a number of valid scenarios that can be used to explain the mineral assemblages present. Regardless of its details, any hypothesis must account for the abundance of manganese in a high oxidation state.

Figure 1. Regional map of a portion of the San Bernardino Mountains, showing location of Desert View Mine.

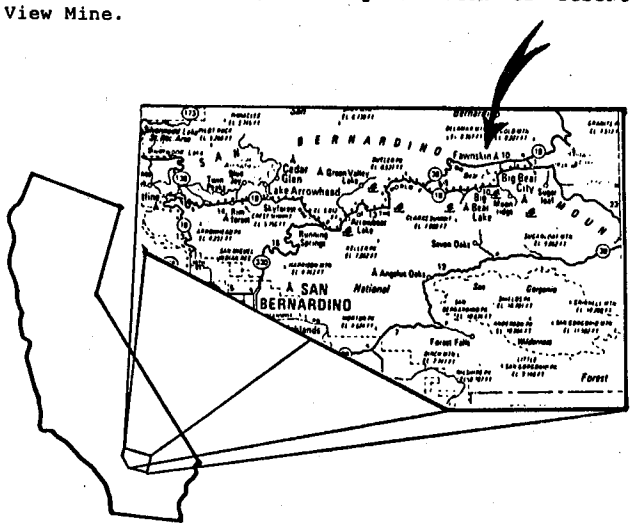

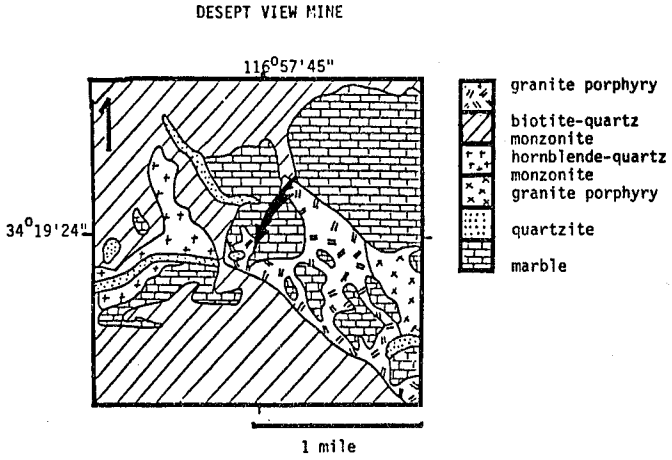

Figure 2. Lithological relationship at the Desert View Mine.

Figure 2 shows the important lithologic relationship present at the deposit: the contact between the Paleozoic marble and younger granitic intrusion at which the Desert View Mine is located. The proposed model considers the marble to be the source of calcium, silica, iron, aluminum, magnesium, and manganese. Although the source of the manganese has not been confirmed by field evidence, several plausible origins may explain its presence in the marble formation. It may have precipitated directly from sea water in an oxygenated near shore environment of a marine basin, or it is possible that manganese was introduced into the host within a silicious sediment, was metamorphosed and weathered, and left a residual manganese oxide deposit. The miogeoclinal shallow water carbonate-shelf environment proposed by Brown (1986) to have formed the extensive Bonanza King marble in which the Desert View Mine is located supports the idea that precipitation of manganese was from sea water.

Considering an igneous origin of the manganese does not adequately explain its abundance or its high oxidation state. In general, even iron-rich igneous bodies contain less than 5% manganese. In the Desert View rocks, manganese is the dominant metal. Also, the +3 oxidation state is most common, especially in hetaerolite which requires a highly oxidizing environment for formation to occur--much higher than can be achieved by introduction from a magma. Late stage circulation of ground water could introduce oxygen into the system to further oxidize earlier formed minerals, but not enough to justify the formation of hetaerolite. At this stage, the temperature would be relatively cool, which contradicts the metamorphic texture observed in hand specimens. There is no evidence in the hand samples of a post-intrusive metamorphic or recrystallization event. This suggests that the hetaerolite formed as a primary mineral with manganese supplied by the host, while the granitic intrusion supplied the silica and some of the metals, especially zinc.

During the initial formation of the deposit, heat emanating from the newly emplaced granite caused the surrounding host marble to recrystallize into wollastonite and the magnesium silicate mineral, followed by grossular garnet (fig. 3a). This succession is suggested by the garnet veins cutting the wollastonite. This metamorphic stage was followed by a metasomatic sequence in which a high temperature zinc sulfide saturated magmatic fluid was introduced into the host marble (fig. 8b). As the sulfide came into contact with the marble, it was oxidized and then reacted with the manganese contained within this formation to form hetaerolite and zincite with quartz. These conditions explain the metamorphic texture of the hetaerolite, while the presence of zincite between the calcite grains also suggests that the fluid was moving through the calcite when it was oxidized to zincite. A decrease in the wall rocks' ability to oxidize the penetrating magmatic fluid resulted in the silicate, willemite, forming rather than the oxide. In later stages when the intrusion had cooled to a solid form, circulating ground waters moved through the pluton and wall rocks, carrying dissolved minerals and promoting retrograde reactions (fig. 3c). This included formation of the marble assemblage in which jacobsite and andradite precipitated in the marble host along with the epidote vein containing sphalerite. The magnetite assemblage is also associated with retrograde formation, as the epidote-garnet constitu-

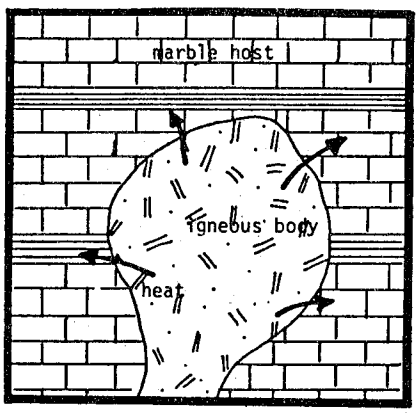

Figure 3A: Igneous intrusion

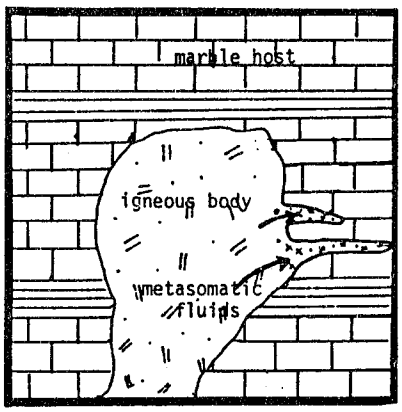

Figure 3b: Magmatic fluid moving into host.

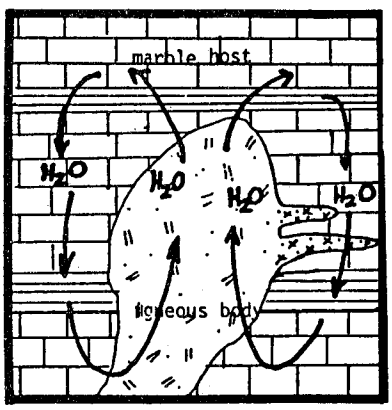

Figure 3c: Late state circulation of ground water

Table 1: Microprobe Analyses of Minerals from the Desert View Mine

HETAEROLITE ASSEMBLAGES	
hetaerolite	$(Zn_{.54}Mn_{.3}Fe_{.15}Mg_{.01})(Mn_{1.94}Al_{.06})O_4$
zincite	$(Zn,Mn)O$
quartz	SiO_2
willemite (fluor green)	$(Zn,Mn)_2SiO_4$
calcite	$CaCO_3$
Mn-Oxide	(?)
MAGNETITE ASSEMBLAGE	
magnetite	$(Fe,Mn,Zn)Fe_2O_4$
andraditic garnet	$Ca_3Fe_2(SiO_4)_3$
willemite (fluor green)	$(Zn,Mn)_2SiO_4$
epidote	$Ca_2(Al,Fe)_3(SiO_4)_3(OH)_3$
quartz	SiO_2
SKARN ASSEMBLAGE	
grossular garnet ($gr_{68}an_{32}$)	$Ca_3(Al_{1.4}Fe_{.6})(SiO_4)_3$
wollastonite (fluor yellow)	$(Ca,Mn)SiO_3$
calcite (sometimes fluor red)	$(Ca,Mn)CO_3$
MARBLE ASSEMBLAGE	
jacobsite	$(Mn_{.58}Fe_{.25}Zn_{.16}Mg_{.01})(Fe_{1.93}Al_{.07})O_4$
andraditic garnet ($an_{85}gr_{15}$)	$Ca_3(Fe_{1.8}Al_{.2})(SiO_4)_3$
epidote	$Ca_2(Al,Fe)_3(SiO_4)_3(OH)_3$
quartz (opal variety fluor light blue)	SiO_2
sphalerite	ZnS
chalcopyrite (inclusions in sphalerite)	$(Cu,Fe)S_2$

ents suggest. Although these assemblages formed at very nearly the same time, the different combinations of zinc within the rocks suggest that the two assemblages formed in different environments. The magnetite assemblage contains zinc as a silicate, while the marble assemblage contains zinc as a sulfide, indicating a somewhat more reducing environment.

COMPARISONS

Franklin, New Jersey

One of the interesting aspects of the Desert View deposit is its similarity to other well known localities, most notably Franklin, New Jersey. The minerals of the Desert View Mine exhibit fluorescent characteristics like those of Franklin, which in both cases can be attributed to the presence of manganese impurities. Like the Desert View, the New Jersey ore body is highly oxidized and located in a marble formation that has been regionally metamorphosed and intruded by igneous rocks. Sphalerite found at Franklin is not associated with other sulfides, but is contained within veins. Although sulfides are abundant at Franklin, they are very rare at the Desert View. The hetaerolite at Franklin is common as a weathering product. It is granular, soft, and lacks the metamorphic texture displayed by the Desert View hetaerolite, suggesting different conditions of formation. The explanation of Franklin's origin is far from settled, but it does require the same essential consideration of an abundance of highly oxidized manganese (Koestler and others, 1983).

Langban, Sweden

The manganese and zinc ores of Langban, Sweden have often been compared to Franklin, and they offer some similarities to the Desert View Mine as well. The common skarn rocks are assemblages of calcite-andradite-epidote; manganese silicates are also very abundant. Spinels in the magnetite-jacobsite series occur in retrograde skarn assemblages of diopside-tremolite-andradite, which seem to correspond to the Desert View's magnetite assemblage. The major difference at Langban is that the iron and manganese ores are differentiated as magnetite and haussmanite, while at Franklin and the Desert View they occur together in such minerals as franklinite, jacobsite, and zincite. Zinc occurs only as a sulfide at Langban. Metamorphosed volcanic flows and tuffs with dolomite serve as the host to Langban's ore body, creating a unique lithologic relationship not present at either Franklin or the Desert View Mine (Moore, 1970).

Broken Hills, Australia

Broken Hill, Australia also offers some analogy to the deposits at Franklin, Langban, and the Desert View

in that it contains abundant manganese and zinc minerals in a high grade metamorphic terrain. However, the zinc occurs predominantly as a sulfide, while zincite, franklinite, and willemite are unknown and jacobsite is not abundant. The skarns of Broken Hill are composed of manganese calc-silicates, spessartine and andraditic garnet, and are associated with abundant rhodonite and other manganese silicates, which are unknown at the Desert View (Mason, 1976).

SUMMARY

In comparison to other skarn deposits of the San Bernardino Mountains, the Desert View Mine is unique. Although mineral assemblages rarely found in the county are abundant at the mine, its primary recognition will always be from its fluorescent minerals and their chemical and physical likeness to the famous Franklin, New Jersey ore body.

REFERENCES CITED

Brown, H., 1986, Stratigraphy and paleogeographic setting of Paleozoic rocks in the northern San Bernardino Mountains: this volume.

Koestler, R., Peters, T.A., Peters, J.J., and Grube, C.H., 1983, Minerals of the Buckwheat Dolomite, Franklin, New Jersey: Mineralogical Record, vol. 14, no. 3, p. 183-194.

Mason, B., 1976, Famous mineral localities: Broken Hill, Australia: Mineralogical Record, vol. 7, no. 1, p. 25-33.

Moore, P.B., 1970, Mineralogy and chemistry of Lang ban-type deposits in Bergslagen, Sweden: Mineralogical Record, vol. 1, no. 4, p. 154-171.

GRAVITY ANOMALIES OVER SEDIMENTARY BASINS ON THE HELENDALE FAULT TREND

Rahmi Aksoy, Peter M. Sadler, and Shawn Biehler
Department of Earth Sciences
University of California
Riverside, CA 92521

INTRODUCTION

The southern Mojave Desert has a crude, northwest trending basin-and-range topography (Fig. 1); but the range margins do not appear to be dominated by simple normal faults. The northwest trending scarps are more usually interpreted in terms of a set of about seven major, right-lateral, strike slip faults (Hewett, 1954; Hill, 1954; Garfunkle, 1974; Cummings, 1976; Dibblee, 1980).

These faults are more persistent than individual ranges and their traces have been drawn to connect linear range fronts and young-looking fault features that traverse the basins (Morton and others, 1980). Historic seismic activity can be attributed to several of these faults. Nevertheless, evidence of large-scale strike slip across these faults is not particularly convincing and their ages are poorly constrained. We may still ask whether strike slip has been superimposed on older basin structures, or whether some basin formation may be attributed to "pull-apart" at steps in the strike slip fault set.

It is appropriate, therefore, to investigate the buried topography of the basin floors. Well data are sparse for the southern Mojave Desert, but, since the basin fillings are less dense than the basement rocks, basin form must to some extent influence the earth's gravitational field. Differences in gravitational attraction across a basin should reflect surface elevation and lateral variations of subsurface density. After correction for the topographic effects, therefore, the gravity anomalies should most strongly reflect changes in basement density and the depth of basin fill. It is also reasonable to suppose that the strong local differences result from shallow crustal effects. Lateral density changes at the depths

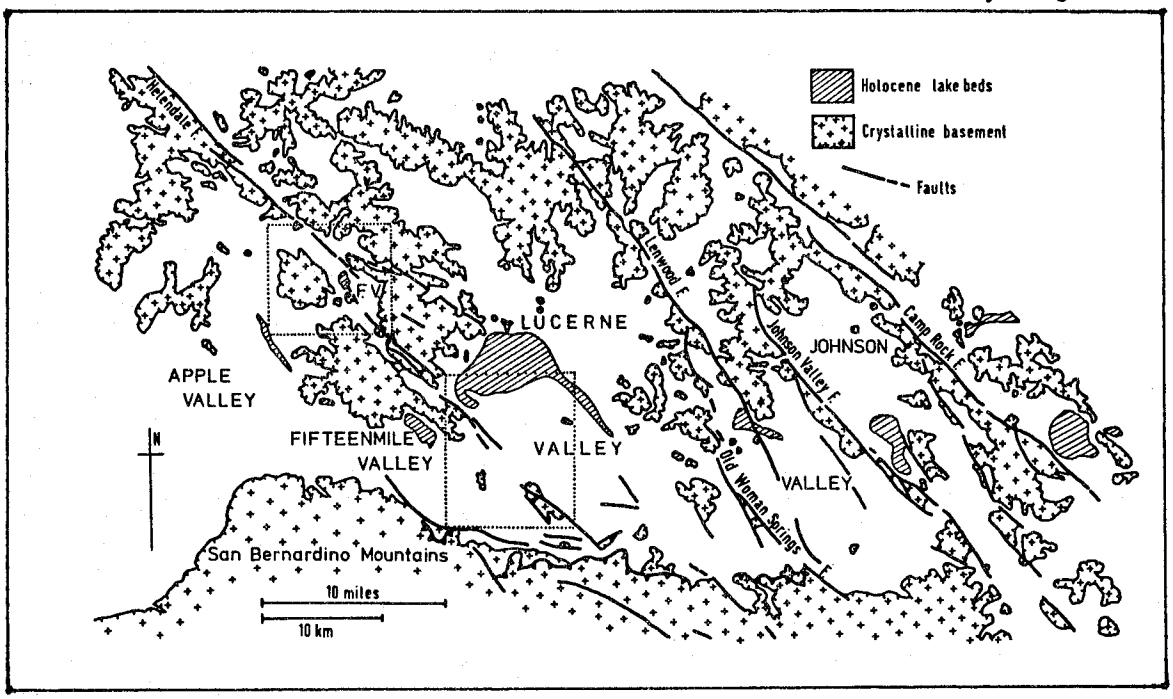

Figure 1. Location of the gravity anomaly surveys (dotted rectangles) and fault zones in the south central Mojave Desert, and the string of playa lakes north of the San Bernardino Mountains. F.V.: Fairview Valley.

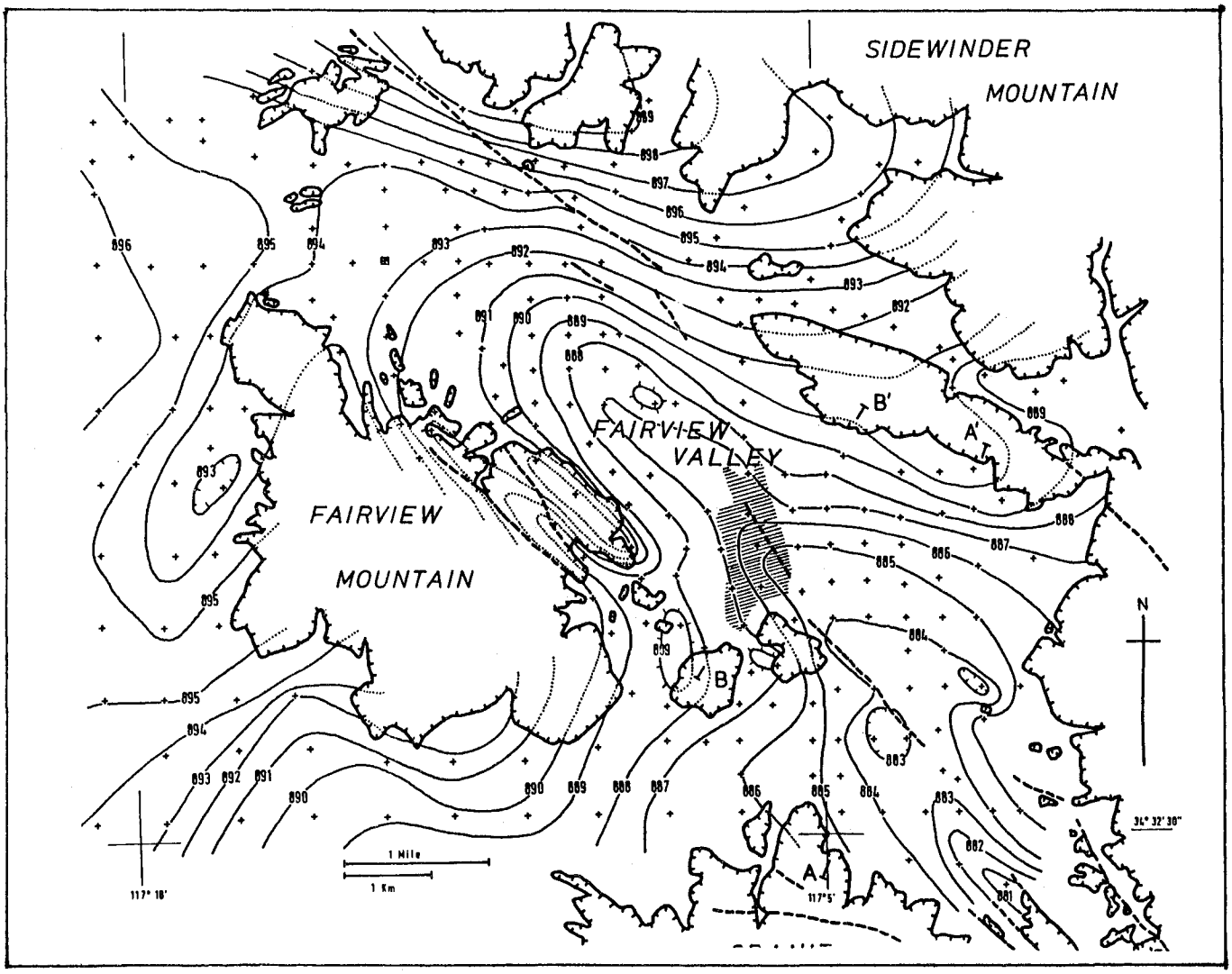

Figure 2. Bouguer gravity anomalies in Fairview Valley. Contours were hand drawn from computer-located stations. The key to symbols is on Figure 4.

of isostatic compensation will be reflected in regional patterns of gravity anomalies.

Mabey (1960) has generated a gravity anomaly map that successfully indicates basin geometry beneath alluvial cover in the western Mojave Desert, where the San Andreas fault marks its southern boundary. The major strike-slip fault traces begin to the east of this part of the desert. Moyle (1984) has used gravity anomalies to model basins near the southeast limit of the fault set, where they approach the Pinto Mountain fault near Twentynine Palms. Between these two areas the southern limit of the Mojave Desert is formed by the north scarp of the San Bernardino Mountains.

Immediately north of the San Bernardino Mountains the Mojave Desert ranges are not prominently expressed (Fig. 1). The Fifteenmile Valley, Lucerne Valley and Johnson Valley basins merge southward into an east-west trending bajada and there is a concentration of playa lakes about 15 km north of the range front. Some of these lakes may have been larger before the influx of sediment from the San Bernardino Mountains encroached onto their southern margin. We surmise that the zone represents a peripheral sink that developed in tandem with the Pliocene uplift of the northern San Bernardino Mountains.

During ground-water investigations of these basins French (1978) and Schaefer (1979) showed that a sparse network of gravity stations could be used to estimate storage volumes. We chose to use much tighter control to investigate the trace of the Helendale fault across Lucerne Valley and into the smaller Fairview Valley to the northwest (Fig. 1).

METHODS

The gravity surveys used the Lacoste-Romberg geodetic gravity meter number G22. This instrument has an accuracy of +/-0.01 milligals over a range of more than seven gals. Oliver (1980, p. 50) gives correction factors relative to other meters in California. Using USGS 7.5 minute topographic maps,

250 stations and their elevations were located in Fairview Valley and 288 stations in western Lucerne Valley (Figs. 2 and 4). Wherever access was easy, readings were made at quarter-mile intervals. Approximately half of the stations in Lucerne Valley were located at benchmarks and spot heights; the elevations of other stations were determined from contours.

The gravity measurements were tied to a local base station in each valley that had been established relative to the State of California gravity base at U.C. Riverside (Chapman, 1966). The Fairview Valley local base station (Fig. 2) is located at the southeast corner of the intersection of Johnson Road and Via Vista (T6N, R2W, sec. 19), which is 2 miles north and 3 miles east of the beacon at Apple Valley county airport. The Lucerne Valley local base station (Fig. 4) is located at a benchmark in the southeast corner of the intersection between State Highway 18 and Highland Road, in the town of Lucerne Valley (T4N, R1W, sec. 14).

The gravity data have been reduced to complete Bouguer anomalies. This means that we are presenting the difference between a corrected, local gravity observation and the theoretical value for sea level at the latitude of each station. The corrected observation is derived from each station measurement by allowing for earth tides, for any residual meter drift, for the actual elevation of the station, for the density of material between the station and sea level, and for the effect of neighbouring hills and valleys. The last factor is termed a terrain correction and is made in two parts. The inner zone terrain correction allows for the topography within 2 km of the station. It was determined manually using Hammer charts (Hammer, 1939; Douglas and Prahl, 1972). The outer zone terrain correction included topography within a 20 km radius, and was accomplished by the same computer procedure that made all the other corrections. The total terrain correction never exceeded 1.5 mgal and was very often zero over the lake beds.

A standard density of 2.67 for near-surface materials was included in the Bouguer corrections. This means that the pattern of final anomalies will reflect lateral differences in crustal density. In order to make all values positive 1,000 has been added to the anomaly values in milligals.

Selected gravity profiles were modelled using the techniques of Talwani and others (1959) and Bott (1960) in two programs developed by Biehler: "TALTDG" (Talwani Two-dimensional Gravity Modelling) and "ATDPOL" (Automatic Two-dimensional Gravity for Polygons). The TALTDG program accepts a structural model built of several subsurface polygons, for which three density contrasts may be specified. It calculates theoretical anomaly profiles and plots them with the observed anomaly. The ATDPOL program operates in the opposite direction accepting the observed anomaly and building a model to fit. The profile must be anchored at exposed basement at both ends. This allows the program to interpolate a simple, linear, regional anomaly between the end values and generate a two-layer structural model to account for the residual anomaly. It accepts a fixed density for the lower layer and three density contrasts across the boundary to the upper layer.

FAIRVIEW VALLEY

Fairview Valley is the much smaller and simpler of the two basins investigated; it is nearly enclosed. Surface lineaments suggest that the youngest trace of the Helendale fault might run diagonally across the basin fill.

The distribution of gravity lows in the Bouguer anomaly map (Fig. 2) approximately replicates the form of the modern topographic basin. Steep gradients characterize the trace of the Helendale fault at the northwest and southeast corners of the basin, but there is no strong gravity signature indicative of a basement step beneath the lineaments that cross the basin linking these corner segments. Steep gravity gradients are more clearly associated with the northeast and southwest flanks of the basin. Older fault traces, now buried, may have generated the whole basin by a right step and "pull-apart".

Since the topography and gravity anomalies are relatively simple in Fairview Valley, the ATDPOL program can generate acceptable models of the basin floor. Figure 3 suggests basement depths that could generate the observed anomalies along two profiles, if the basement density is fixed at 2.67 gm/cc, and the density of the fill is between 2.27 and 2.37 gm/cc. No well data have been found to constrain the modelling.

LUCERNE VALLEY

The Helendale fault zone traverses the southwestern edge of Lucerne Valley between a spur of the Granite Mountains and a northwest trending basement ridge near the San Bernardino range front. Thus, the geologic map conveys the impression that a shallow basement sill separates Lucerne Valley from Fifteenmile Valley. But the gravity anomaly map (Fig.

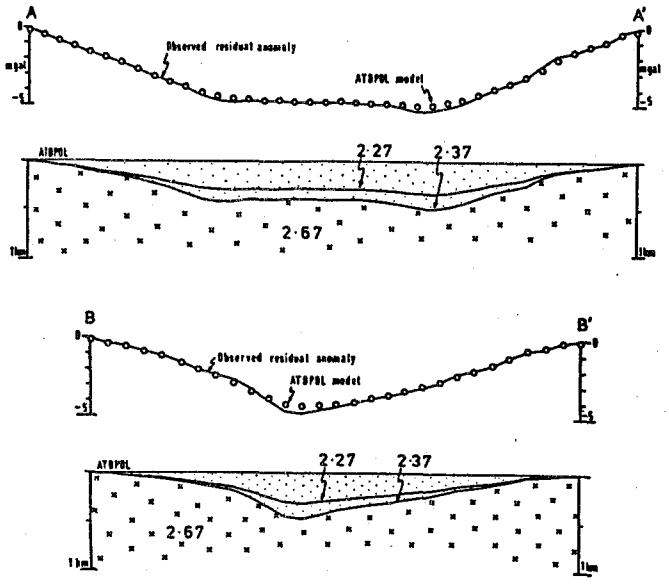

Figure 3. Gravity profiles across Fairview Valley modelled using ATDPOL. Basement density is fixed; a range of basin depth is modelled for sedimentary fill densities between 2.27 and 2.37 gm/cc. Section ends are located on Figure 2.

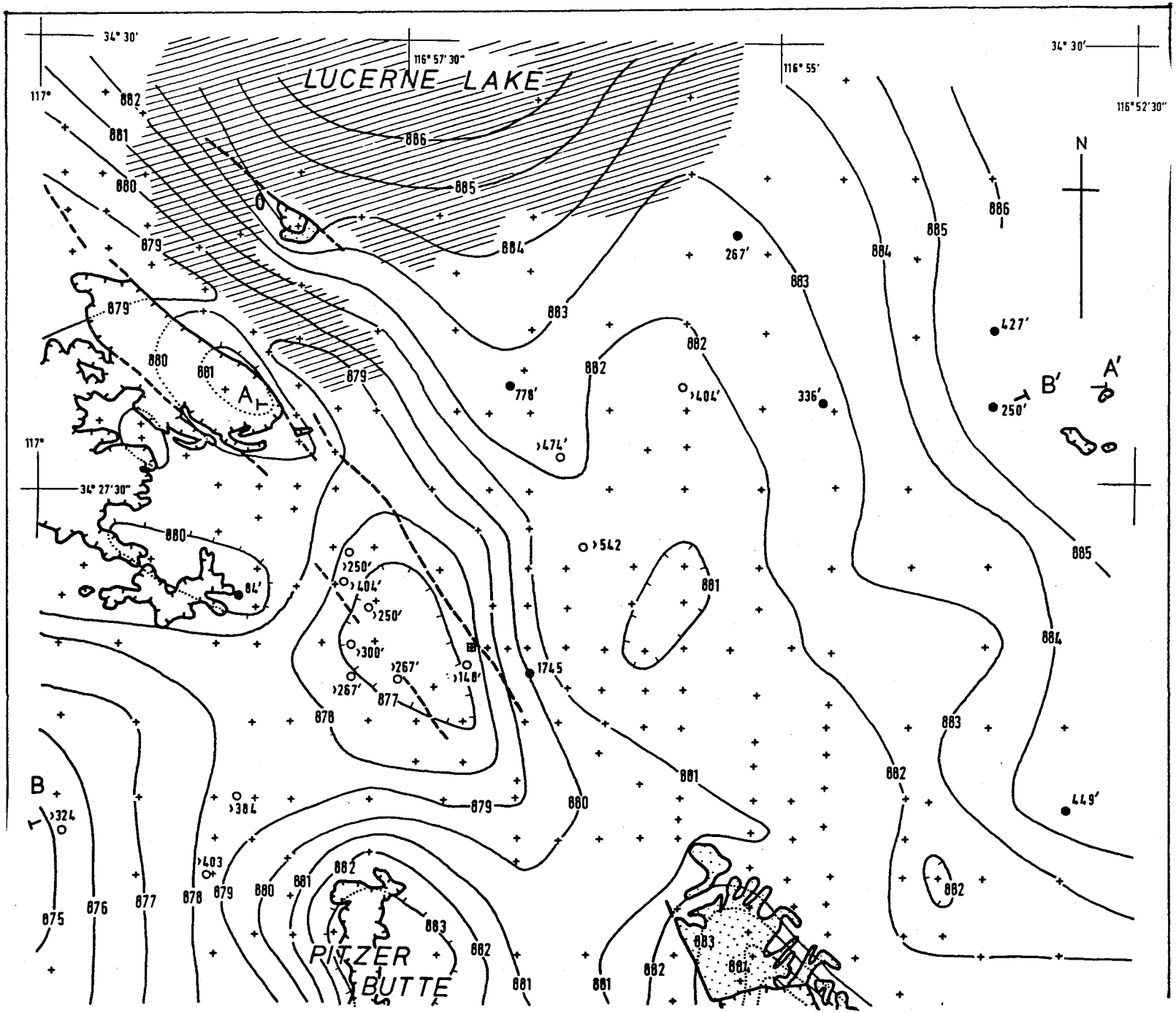
LUCERNE LAKE
PITZER BUTTE
34° 30'
116° 57' 30"
116° 55'
116° 52' 30"
117°
34° 27' 30"
N
A
A'
B
B'
882
881
880
879
886
885
884
883
878
877
876
875
267'
427'
778'
404'
336'
250'
474'
542
1745
300'
148'
324
384
403
449'

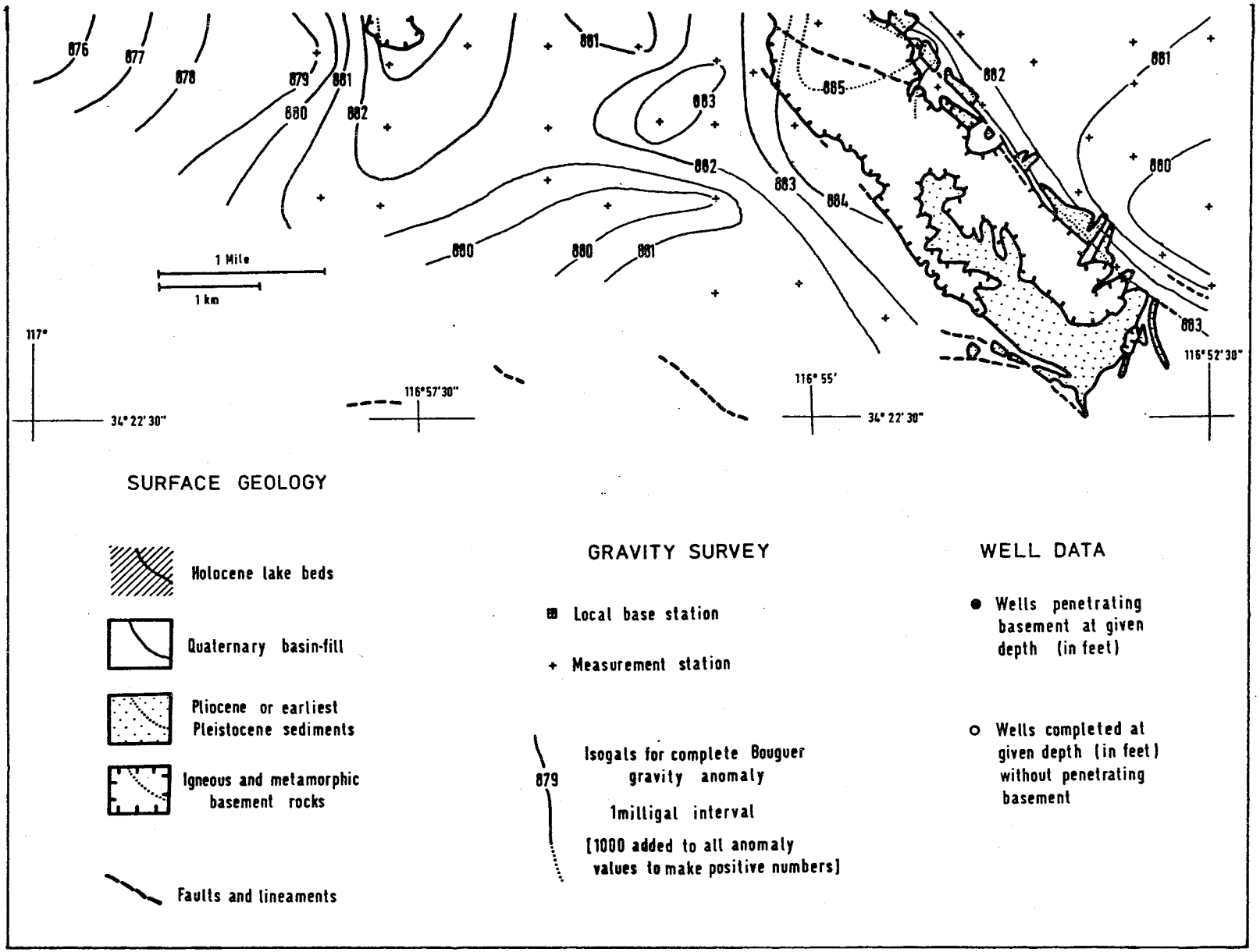

Figure 4. Bouguer gravity anomalies in the Lucerne Valley area. Contours were hand drawn from computer-located stations.

4) indicates otherwise. Although the Bouguer gravity anomalies show the same overall range as found in Fairview Valley, the distribution of gravity lows does not so nearly replicate the modern topographic basin.

The large-scale anomaly pattern over the Lucerne Valley basin is a northwest-striking gradient that descends nine milligals from highs over Lucerne Lake and the northeast edge of the basin to lows near the Helendale fault zone. The gradient steepens near the supposed trace of the Helendale fault on the east side of the basement highs. Nevertheless, the linear zone of steep anomaly gradients is often appreciably east of the surface fault features and includes a pronounced discontinuity northeast of Pitzer Butte. Such a discontinuous signature is not unreasonable for a strike slip fault, since its gravity signature can be generated by contrasts between blocks juxtaposed by slipping past one another, rather than a simple dip-slip step. Where the trace crosses alluvium between basement highs, however, the Bouguer anomalies show the most pronounced gravity low of the basin.

Seven wells that penetrate basement in the surveyed area, and two just beyond it, show a general relationship of increasing basement depth with decreasing Bouguer anomaly values (Fig. 5). The deepest of these wells penetrates basement on the flank of the gravity minimum in the Helendale fault zone. Extrapolation of the loosely constrained depth/Bouguer anomaly regression indicates that the basin floor may locally lie as deep as 2500 feet.

The relationship between anomaly values and basement depth is not altogether simple, however; it breaks down over the spur of the Granite Mountains. Here the Bouguer high is 4-5 milligals weaker than over all other basement outcrops in the survey area (Figs. 4 and 5), including the nearby basement island in Lucerne Lake. The granitoid rocks of this anomalous spur are highly altered relative to the other outcrops. Even moderately fresh biotite and hornblende are quite rare. Extensive hydrothermal alteration may have significantly reduced density at depth.

The ATDPOL program failed to generate models that were consistent with known well depths for any profiles ending in the Granite Mountains. Figure 6b is an example of such a model that underestimates basement depth, and even predicts a non-existent outcrop east of the Granite Mountains. Thus, a simple regional gradient cannot be assumed. We must allow for inhomogeneous basement composition or structure. Furthermore, we must consider the possibility that the anomalous, low basement densities continue southwestward at depth from the Granite Mountains and account for the some of the gravity minimum near the fault zone.

Modelling with the TALTDG program (Figs. 6 and 7) shows that, even if a lighter basement layer that can account for the Granite Mountains anomaly is extended to the gravity minimum, a residual anomaly remains that is suggestive of a deep basin. Figure 6c is for direct comparison with the unsuccessful ATDPOL model. Figure 7 shows a TALTDG model across Lucerne Valley that includes the main gravity low in the Helendale fault zone.

The TALTDG models fit a combination of both less

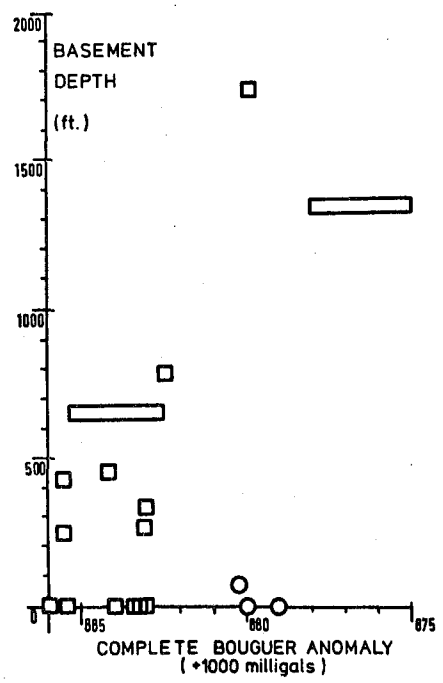

Figure 5. Relationship of Bouguer anomalies to basement depth in southwest Lucerne Valley. Squares and circles: well data (after Riley, 1956) and outcrop limits (zero depth). Circles: Granite Mountains spur. Rectangular boxes: wells just beyond survey area for which gravity value is estimated.

dense basement and a sedimentary basin to the main gravity low. The models make at least two simplifications: firstly, the addition of a shallow layer of low density basement is an entirely arbitrary means of accounting for the Granite Mountains anomaly; secondly, Pliocene Old Woman Sandstone should account for some of the sedimentary basin fill, but was omitted for lack of subsurface control. The modelling exercise, nevertheless, indicates that an arbitrary density reduction in the basement layer that can account for the Granite Mountains anomaly, is not alone adequate to generate the main Bouguer low in the fault zone.

The gravity anomalies can be most closely modelled if the main fault break in the basement is placed east of the surface expressions of the Helendale fault near Lucerne Lake. Schaefer (1979) suggested a major fault even farther east on the basis of water table topography, but his data are not compelling and we found no corresponding gravity signature.

Evidently, in Lucerne Valley there is no simple relationship between the modern lake depression and the depth of the basement below. The Helendale fault does not simply flank a continuous basement sill. It follows a zone characterized by elongate basement highs and a small deep basin. Any sill separating the Lucerne Valley and Fifteenmile Valley basins, should run from the Granite Mountains south through Pitzer Butte.

The coverage of the gravity survey leaves open

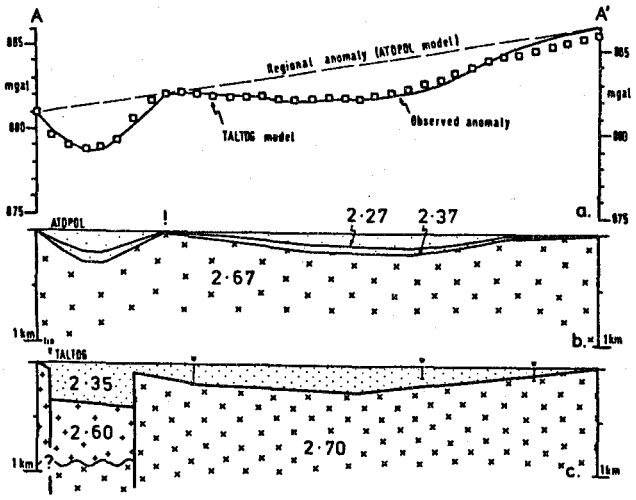

Figure 6. Gravity profile across Lucerne Valley with anomalies modelled by ATDPOL (a) and TALTDG (b). The ATDPOL model assumes uniform basement density and generates a spurious basement sill (!). The TALTDG model attributes much of the regional gradient to density changes in the basement. Section ends are located on Figure 4.

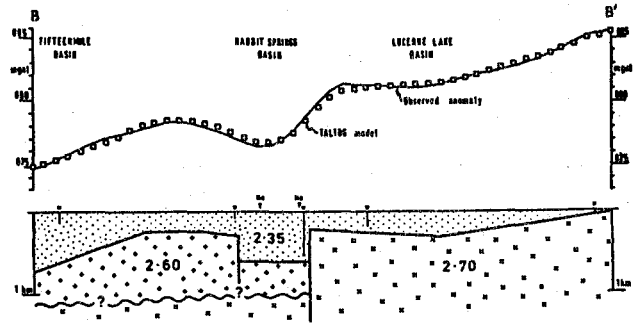

Figure 7. TALTDG gravity model of the Helendale fault zone in Lucerne Valley. Section ends are located on Figure 4.

the possiblilty that an offset portion of the basin in the fault zone exists to the southeast. But there is no clear independent evidence for this. It is also possible that the small basin in the fault zone originated by "pull-apart" at a right step in the active trace. Fault lineaments east of Pitzer Butte permit such an interpretation, but the youngest activity appears to have occurred along a straighter trace. The gravity anomaly gradient over the basement high east of Pitzer Butte is steepest parallel to the east flank where the youngest-looking fault features occur. Trenches opened on this flank by G. Grimes revealed complex fault geometry that included a thrust fault carrying basement rocks over the alluvial fill. It is also probable that a fault controlled the west flank. This older west flank structure could have set up a right step and "pull-apart" geometry to the northwest.

CONCLUSIONS

Steep northwest striking gradients in the gravity anomalies aid in the definition of the Helendale fault zone. The gravity field can be interpreted as support for the notion that the Helendale fault zone has a strike slip character, since it shows no consistent sense of vertical displacement of basement across the zone. Furthermore, small basins in the fault zone, both topographically expressed and buried, may have been generated by "pull-apart" at right steps.

In contrast, the larger, modern Lucerne Valley basin has no simple genetic relationship with the fault. The zone of lake beds and coalesced alluvial valleys at the south central limit of the Mojave Desert is more likely a counterpart of the compressional uplift of the San Bernardino range front, which it parallels. West and east of these mountains, the distribution of playa lakes in the Mojave Desert is rather different. Pliocene sediments indicate that some subsidence occurred in this zone just prior to orogenesis. It is not simply a matter of burial of older relief under coalescing fans after uplift of the San Bernardino Mountains.

REFERENCES CITED

Bott, M. H. P., 1960, The use of rapid digital computing methods for direct gravity interpretation of sedimentary basins: Geophysical Journal, v. 3, p. 63-67.

Chapman, R. H., 1966, Gravity base station network: California Division of Mines and Geology Special Report 90, 49 p.

Cummings, D., 1976, Theory of plasticity applied to faulting, Mojave Desert, southern California: Geological Society of America Bulletin, v. 87, p. 720-724.

Dibblee, T. W., 1980, Geologic structure of the Mojave Desert: in, Fife, D. L. and Brown, A. R. (eds.), Geology and Mineral Wealth of the California Desert, South Coast Geological Society, Santa Ana, p. 69-100.

Douglas, J. K. and Prahl, S. R., 1972, Extended terrain correction tables for gravity reductions: Geophysics, v. 37, p. 377-379.

French, J. J., 1978, Ground-water storage in the Johnson Valley area, San Bernardino County, California: U.S. Geological Survey Water Resources Investigations 77-130.

Garfunkle, Z., 1974, Model for the late Cenozoic tectonic history of the Mojave Desert, California, and its relation to adjacent regions: Geological Society of America Bulletin, v. 85, p. 1931-1944.

Hammer, S., 1939, Terrain corrections for gravimeter stations: Geophysics, v. 4, p. 184-194.

Hewett, D. F., 1954, A fault map of the Mojave Desert region, in, Jahns, R. H. (ed.), Geology of Southern California: California Division of Mines and Geology Bulletin 170, p. 15-18.

Hill, M. L., 1954, Tectonics of faulting in southern California, in Jahns, R. H. (ed.), Geology of Southern California: California Division of Mines and Geology Bulletin 170, p. 5-15.

Mabey, D. R., 1960, Gravity Survey of the Western Mojave Desert, California: U.S. Geological Survey Professional Paper 316-D, p. 51-73.

Morton, D. M., Miller, F. K. and Smith, C. C., 1980, Photoreconnaissance maps showing young-looking

fault features in the southern Mojave Desert, California: U.S. Geological Survey Miscellaneous Field Studies Map MF-1051.

Moyle, W. R., 1984, Bouguer gravity anomaly map of the Twentynine Palms marine corps base and vicinity, California: U.S. Geological Survey Water Resources Investigations Rept. 84-4005.

Oliver, H. W., 1980, Interpretation of the Gravity map of California and its continental margin: California Division of Mines and Geology Bulletin 205, 52 p.

Riley, F. S., 1956, Data on water wells in Lucerne, Johnson and Fry valleys, San Bernardino County, California: U.S. Geological Survey Open File Report, 126 p.

Schaefer, D. H., 1979, Ground-water conditions and potential for artificial recharge in Lucerne Valley, San Bernardino County, California: U.S. Geological Survey Water Resources Investigations 78-118.

Talwani, M., Worzel, J. L., and Landisman, M., 1959, Rapid gravity computations for two dimensional bodies with applications to the Mendocino submarine fracture zone: Journal of Geophysical Research, v. 64, p. 49-59.

Rear Cover:
The Blackhawk landslide.
After P.M. Sadler, 1983, Geology of a portion of the Cougar Buttes quadrangle: California Division of Mines and Geology.


BM 3101
BM 30
al
ol
as
ol
al
20
as
af
ol
ol
aa
aa
rls
af
rls
bbg
al
rls
ol
aa
29
gl
rls
ig
al
al
rls
al
ol
aa
aa